Field-Scale Evaluation of Enhanced Agricultural Management Practices Using a Novel Unsaturated Zone Nitrate Mass Load Approach

by

Loren Bekeris

A thesis
presented to the University of Waterloo
in fulfillment of the
thesis requirement for the degree of
Master of Science
in
Earth Sciences

Waterloo, Ontario, Canada, 2007

Author's Declaration

I hereby declare that I am the sole author of this thesis. This is a true copy of the thesis, including any required final revisions, as accepted by my examiners.

I understand that my thesis may be made electronically available to the public.

Abstract

Rising groundwater nitrate concentrations associated with the increased use of synthetic and organic agricultural fertilizers in recent decades have prompted the adoption of agricultural best management practices (BMPs), which may include a targeted reduction in nutrient application. This study was prompted by the lack of published research about the effectiveness of these agricultural BMPs, particularly in cases where the thickness and geologic composition of the unsaturated zone prevent short-term effects from being observed in the groundwater quality. The monitoring of nitrate mass load through the unsaturated zone below agricultural land was therefore proposed as a novel technique to assess the effect of agricultural BMPs. The objectives of the study were to: develop field techniques and apply computational models for the quantification of nitrate mass flux below active agricultural land operating under a BMP; scale the point mass flux results to a nitrate mass load across the agricultural parcel; and assess the resulting nitrate mass load measurements as indicators to evaluate the effect of the BMP. The study was conducted in the vicinity of the Thornton Well Field in the County of Oxford, where the nitrogen application rate on a 73-hectare parcel of land was reduced by 20 to 50% relative to historical rates in an effort to curb increasing groundwater nitrate concentrations in the municipal supply wells.

At eight topographically and geologically diverse locations across the study site, soil water content profiles, soil temperature profiles and groundwater quality were regularly monitored, and several rounds of geologic cores were collected for analysis of bulk soil nitrate and an applied bromide tracer. Meteorological parameters were also continuously measured on-site. The field data were applied in several analytical techniques for estimating recharge, including the calculation of unsaturated zone tracer movement, an unsaturated zone water balance, and an overall water balance based on an empirical equation for evapotranspiration. Two numerical models designed to simulate flow in the unsaturated zone (Simultaneous Heat and Water, SHAW, and Hydrologic Evaluation of Landfill Performance, HELP) were also used in order to refine the recharge estimates. The recharge rate at each measurement location was then combined with unsaturated zone nitrate data to quantify nitrate mass flux. Upscaling of the flux values to field-scale mass load was based mainly on topography, geology and field observations such as occasional surface water ponding.

The calculation of stored nitrate mass in the shallow subsurface (i.e., the upper two to three metres) showed some correlation to changes in surface nitrogen application, with the greatest decreases in stored mass (up to 80%) observed at locations underlain by sand where there was a switch from a corn-soybean-wheat rotation to a grass crop. In contrast, the calculation of nitrate mass load suggested that the post-BMP value (4.1 t NO_3-N/yr below the area on which BMPs were implemented) was greater than the pre-BMP value (2.2 t NO_3-N/yr). However, the calculation of nitrate mass load was limited by several factors, including a lack of nitrate concentration data from the deep unsaturated zone and an above-average (by 30%) annual precipitation rate; as a result, the findings suggesting an increase in nitrate mass load in response to decreasing nutrient inputs should be interpreted with caution. Across the study site, the nitrate mass flux through the portion of the unsaturated zone assumed to have been affected by the BMPs ranged from 3.4 to 13.2 g/yr/m^2, indicating that some areas of the study site are more critical than others in terms of their contribution to groundwater nitrate.

Continued monitoring of nitrate mass load and stored nitrate mass in the unsaturated zone is recommended to determine whether further benefits from the BMPs are observed as the measurement period lengthens and the unsaturated zone is progressively flushed. It is anticipated that the factors that affected the accuracy of the nitrate mass load measurements in this study will be mitigated by a longer measurement period and refinements to the method.

Acknowledgements

I gratefully acknowledge the financial support of the following agencies: the Natural Sciences and Engineering Research Council of Canada, the Canadian Water Network, the County of Oxford, Ontario Pork, and the Canadian Foundation for Innovation.

I extend my thanks to my supervisors Dr. David Rudolph and Dr. Neil Thomson, for the opportunity to pursue a challenging and relevant field project, for providing human, technical and financial resources, conceptual and editorial guidance, encouragement and good humour, and (in Dave's case) for the Winnipeg reminiscences. I am also indebted to my committee members Dr. Brewster Conant Jr., for the invaluable technical support at the onset of the study, and further guidance and encouragement along the way, and Dr. Gary Parkin, for providing modelling support and unsaturated zone expertise.

Thank you to Rob Walton, Marg Misek-Evans, John Braam and Garry Martin of the County of Oxford, for access to the project and the site. David Start offered remarkable flexibility and forgiveness in the coordination of field work, many detailed agricultural explanations, and an inspiring commitment to making agriculture more efficient and environmentally sound. John McIntyre provided access to an interesting study location.

My degree might have taken ten years had Claus Haslauer not passed on a wealth of site experience and data and provided a sympathetic ear during coffee break. Thanks to Odum Idika for learning the Woodstock ropes with me and enduring all kinds of field conditions to obtain data, and to Bob Ingleton, Paul Johnson and Scott Piggott for innovative technical approaches to dealing with the challenges of the site. The following summer, co-op and visiting students also contributed to data collection and analysis: Kate Critchley, Jason Cole, Stephan Wendt, Thore Linke, Andrew Wiebe, Marilla Murray, Colby Steelman and Jamie Koch. Thank you to David Fallow for assistance with the SHAW model.

Finally, thank you to my friends in Waterloo and all points (mostly) west, for support and diversion; to my family, for endlessly encouraging me despite never really understanding what I was studying; and to Stefano, for always having confidence in me, even when I didn't.

Table of Contents

List of Tables

List of Figures

1. Introduction

1.1. Best Management Practices in Agriculture

Changes in North American agricultural practices during the last four decades have included a marked increase in synthetic fertilizer application (Burkart and Stoner, 2002), and a spatial intensification of manure land application (Agriculture and Agri-Food Canada, 1997). Among the essential nutrients within these fertilizers, nitrogen poses the greatest threat to groundwater quality due its high leaching potential (Foth, 1984). Because of increased nutrient inputs, a soil nutrient surplus has become common in the non-prairie agricultural regions of Canada, resulting in nitrogen losses to the hydrologic system (AAFC, 1997). Groundwater concentrations of nitrate (the most highly oxidized form of nitrogen) have exhibited an increasing trend since the 1970s and in some instances exceed the drinking water limit of 10 mg NO_3-N/L (AAFC, 1997). Nitrate is, in fact, the most common groundwater contaminant, and agriculture its most significant source (Burkart and Stoner, 2002). In addition to its prevalence, groundwater contamination from excess agricultural nitrogen inputs is characterized by its diffuse nature and variability in space and time.

Faced with an increasing threat to drinking water supply aquifers from elevated nitrate concentrations, regulators and water resources managers have introduced both mandatory and voluntary standards for agricultural practice to reduce nitrate losses. Nutrient management regulations in many jurisdictions, including the Province of Ontario, contain criteria for the land application of nutrients, such as set-backs from groundwater wells and restrictions on winter application (Nutrient Management Act, 2002). In addition to meeting these requirements, farmers are encouraged to further enhance soil and water protection by implementing other best management practices (BMPs) which may include improved estimates of crops' fertilizer needs, spatially adjusted and properly timed fertilizer application, and the use of cover crops when commercial crops are not being grown (OMAF, 1994).

The BMPs recommended for nutrient land application are based on a well-established understanding of nitrate fate and transport, and an intuitive sense of how to minimize nitrate losses. What has not yet been scientifically determined is the effect of BMPs on groundwater

quality, particularly the maximum attainable benefit from implementing the BMPs in settings where the impacts from excess nutrient application are present and on-going. Although the increase in groundwater nitrate concentration below fertilized fields over time has been well documented (Almasri and Kaluarachchi, 2004; Rodvang et al., 2004; Burkart and Stoner, 2002), the anticipated abatement or reversal of the trend due to the adoption of BMPs has been less often reported. Most published studies have attempted to measure the effect of BMPs on surface water rather than groundwater quality (Lombardo et al., 2000). Where groundwater nitrate trends have been monitored, results have been equivocal or delayed. Beneficial effects of BMPs on groundwater nitrate levels were observed in The Netherlands under a shallow sandy unsaturated zone by Boumans et al. (1999) and in Pennsylvania with a time lag of 4 to 19 months by Hall et al. (1997). In Germany, the effect of reducing fertilizer input by 50% was found to have a measurable effect on nutrient leaching through the unsaturated zone, but not until 13 years after implementation (Meissner et al., 2002). A study of BMP implementation at several farms in Southern Ontario reported a decrease in leachable soil nitrogen but trends in groundwater quality were not monitored (Burr and Goss, 2003). A more recent study showed that groundwater nitrate concentrations in the Abbotsford-Sumas aquifer that straddles the Western Canada-United States border have not significantly changed even after a decade of voluntary agricultural BMPs (Wassenaar et al., 2006).

1.2. Measuring Nitrate Mass Load

The mitigating effect of reducing nutrient inputs or implementing other BMPs may be delayed or attenuated by the time required for nitrogen already present in the unsaturated zone to be transported to the water table (Rudolph et al., 2002). Estimating the effect of BMPs during this time lag between their implementation and their impact on the saturated groundwater system may be aided by the quantification of the unsaturated zone nitrate mass load. The unsaturated zone nitrate mass load is defined here as the rate (mass/time) at which nitrate migrates through a specified vertical interval of the unsaturated zone. The mass load may be determined by multiplying a plan area by the unsaturated zone nitrate mass flux (a mass/time/area contaminant migration rate through the unsaturated zone) below that area. The nitrate mass flux is itself derived by multiplying the groundwater recharge rate by the average aqueous nitrate concentration within the specified unsaturated zone interval.

The unsaturated zone nitrate mass load may be monitored over time to observe an early indication of the effect of BMPs and to estimate the potential effect on underlying groundwater quality. In order to properly apply this approach, it is important to evaluate the spatial variation of these measurements. Spatial variability of historical land application practices and subsurface characteristics such as hydraulic conductivity will lead to a heterogeneous nitrate mass flux distribution. Due to this spatial variability it may be inappropriate to assign to an entire site an average mass flux value estimated from only a limited number of measurement points. Mass load estimates may also be used to represent the surficial contaminant source term for transport modelling efforts focusing on predictive scenario analyses.

Several field methods exist for estimating groundwater recharge, a parameter used in the calculation of mass flux at a point. Techniques include measurement of tracer movement (Rice et al., 1986), unsaturated zone water balance (Schuh et al., 1993; Wellings, 1984), water table fluctuation analysis (Healy and Cook, 2002), and water balance (Román et al., 1996). Studies comparing the results and suitability of several methods to particular field conditions often identify significant variation between techniques (Delin et al., 2000; Grismer et al., 2000). Analysis of the spatial variability of recharge may be based on the comparison of a small number of point measurements (Delin et al., 2000; Schuh et al., 1993), or the use of geostatistics applied to a large sample volume (Nolan et al., 2003; Vieira et al., 1981).

There are a limited number of site-specific studies of nitrate mass load under agricultural land and its spatial variability. Kraft and Stites (2003) used shallow groundwater chloride profiles to delineate annual recharge contributions, and groundwater nitrate concentrations to determine a mass load. Onsoy et al. (2005) determined an unsaturated zone nitrate mass based on statistical and geostatistical analyses of nitrate content, and compared the result to an estimate based on water and nitrogen mass balances. Although they did not calculate nitrate mass load directly, McMahon et al. (2006) concluded that spatial variability of groundwater recharge and the development of unsaturated zone nitrate reservoirs in a semi-arid setting were likely to cause spatially variable groundwater nitrate concentrations. Overall, published reports of field-measured nitrate mass load under agricultural fields are limited, and there are few available studies connecting load measurements to BMP evaluation.

1.3. Predictive Modelling

Modelling is a common tool for predicting the effect of BMPs and may incorporate or replace field-based estimates of nitrate load. One-dimensional models simulating crop growth and unsaturated water flow are often employed to estimate nutrient leaching under various nutrient management approaches (Azevedo et al., 1997) and are in some cases validated with small-scale laboratory or field experiments (Nakamura et al., 2004; Follett, 1995). Regional three-dimensional groundwater models are also used to evaluate large-scale response to nutrient loads and their reduction as a result of BMPs. For the use of such models to be computationally feasible, the spatial resolution may be such that several agricultural fields are represented by one computational node which is assigned a single groundwater recharge or mass flux value (Koo and O'Connell, 2006; French et al., 2006). This value is often determined using a one-dimensional model with input parameters assumed to be average or representative of the area associated with the computational node. In some cases a uniform recharge value is applied across the site (Molénat and Gascuel-Odoux, 2002). As with field methods, in modelling studies there is limited consideration of the spatial variability of mass flux at the agricultural field scale and its effect on the accuracy of watershed-scale models.

1.4. Objectives

Although there is a lack of certain data related to nitrate mass load (its measurement, spatial variability and upscaling) and agricultural BMPs (their short- and long-term effectiveness), analysis of the former may prove useful in evaluation of the latter. To this end, the objectives of this study are to:

- Develop and implement field techniques to quantify the unsaturated zone nitrate mass flux (g NO_3-N/m^2/yr) at multiple locations within an agricultural land parcel operating under BMPs.

- Assess the potential contribution of different modelling approaches to the quantification of nitrate mass flux.

- Establish an approach for upscaling the point-scale nitrate mass flux estimates to a nitrate mass load estimate (t NO_3-N/yr) at the field scale.

- Assess the utility of unsaturated zone nitrate mass load measurements in the evaluation of BMPs, both to indicate at an early stage their effectiveness and to predict their long-term impact.

1.5. Evaluating BMPs at the Field Scale: Woodstock, Ontario

It is proposed in this study that measurements of unsaturated zone nitrate mass load, in some cases coupled with local- and regional-scale numerical models, can be used to evaluate and predict the effectiveness of BMPs. The County of Oxford in southwestern Ontario is one of an increasing number of municipalities requiring this type of BMP evaluation. Faced with rising nitrate concentrations in its municipal supply wells including in some instances values above the drinking water limit, the County purchased 111 hectares of farmland in the well capture zone in 2003 in a pro-active mitigation effort. The land is now rented to farmers who are required to apply reduced nutrient quantities in order to minimize the potential for leaching. The questions now posed by the County are whether this BMP (reduced nutrient application) has affected the field conditions, when improvements to groundwater quality may be anticipated, and how significant these improvements may be. With an unsaturated zone varying in depth from 3 to 30 m and comprised of a layered aquifer-aquitard system, the benefits of the BMP may not be immediately observed in the groundwater quality. It may, however, be possible to detect early changes in the nitrate mass load in the unsaturated zone. If so, these changes could be used to directly evaluate the impact of the decreased surface inputs, and also as part of a predictive modelling exercise to estimate the impact of this BMP on the nitrate concentrations in water extracted by the municipal supply wells.

1.6. Study Approach

As discussed in Section 1.2, there is a lack of published data related to the field measurement of nitrate mass load through the unsaturated zone, particularly as an indicator of BMP effectiveness. Therefore, a novel approach was necessary to satisfy the study objectives. Eight field study locations, chosen to represent various topographic and geologic conditions, were established across the study site comprised of agricultural fields within the capture zone of the impacted well field. The principal field data regularly collected at these locations included soil water content profiles using a neutron moisture probe, soil temperature profiles and groundwater quality. A bromide tracer was applied at surface, and several rounds of geologic

core sampling provided soil profiles of both bromide and nitrate. Meteorological parameters were also continuously measured on-site.

The field data were used in conjunction with several analytical techniques for estimating recharge, including an unsaturated zone water balance, the calculation of unsaturated zone tracer movement, and an overall water balance based on an empirical equation for evapotranspiration. In order to refine the recharge estimates, the field data were also used to constrain and calibrate two unsaturated zone models: Simultaneous Heat and Water model (SHAW, version 2.4; Flerchinger, 2000) and the Hydrologic Evaluation of Landfill Performance (HELP, version 3; Schroeder et al., 1994).

Recharge estimates across the fields were then combined with unsaturated zone nitrate data to quantify nitrate mass flux. Upscaling of the flux values to determine a total field-scale mass load was based mainly on topography, geology and field observations. Finally, trends in nitrate mass load across the site and over time were evaluated to assess the effect of agricultural BMPs.

Chapter 2 provides background on the field site and land use practices. Chapter 3 describes the study methods while Chapter 4 presents field and modelling results. Chapter 5 provides interpretation and discussion of the results, and Chapter 6 contains conclusions and recommendations relative to the study objectives.

2. Background

2.1. The Nitrogen Cycle

Nitrogen is essential for plant growth and is subject to a complex cycle of processes within soil and plants (Foth, 1984). In the context of this study, which focuses on nitrate transport in the subsurface toward the water table, it is important to understand the processes by which nitrogen is initially added to or removed from the soil. As will be further described, however, the scope of the mass load calculations does not include elements of the nitrogen cycle. The focus, rather, is in on mass load below the zone of root growth and biological activity in which most processes of the nitrogen cycle are likely to occur (Foth, 1984). The nitrogen cycle may be considered to control the input of nitrate to the deeper unsaturated zone.

One process by which nitrogen is added to the soil is fixation, wherein microbes convert atmospheric nitrogen gas (N_2) into forms of nitrogen that are usable by plants. Certain nitrogen-fixing bacteria form a symbiotic relationship with a host plant, commonly a legume, whereas other bacteria fix nitrogen independently of plants (Donahue et al., 1983).

Mineralization is the conversion of nitrogen in soil organic matter to the ammonium ion (NH_4^+). The ammonium is then commonly oxidized to nitrate (NO_3^-) by *Nitrosomonas* and *Nitrobacter* bacteria, a process called nitrification. Nitrite (NO_2^-) is an intermediate and toxic product of this process but rarely accumulates in soil (Addiscott, 2004). Ammonium and nitrate return to an organic nitrogen form during the process of immobilization. Nitrogen may be cycled repeatedly through the cycle of mineralization, nitrification and immobilization (Foth, 1984).

In order to maximize crop growth, farmers supplement the nitrogen additions from fixation and mineralization with the addition of organic (manure) or inorganic nitrogen fertilizers. Inorganic fertilizers are widely used and, with the exception of urea, contain ammonia or nitrate or both. Ammonia and urea through different processes are ultimately converted to ammonium and then to nitrate by nitrification (Addiscott, 2004).

Losses of nitrogen from the soil may occur in the form of denitrification or leaching. Denitrification is the reduction of nitrate to nitrogen gas by facultative anaerobic organisms using nitrate in place of oxygen for respiration (Foth, 1984). The gaseous nitrogen subsequently escapes to the atmosphere. Denitrification requires certain conditions including an anaerobic environment and the presence of sufficient electron donors such as organic carbon. Nitrate reduction may also occur in the presence of reduced iron or sulphur (Appelo and Postma, 1999).

Nitrogen leaching is an important aspect of the cycle from an environmental perspective and is the process of interest in this study. Nitrate and ammonium are both highly soluble in water, but the ammonium ion's positive charge results in sorption to cation exchange sites. Nitrate is readily leached through the soil to groundwater (Donahue et al., 1983). The time required for the nitrate-bearing water leaching out of the root zone to reach the water table depends on the unsaturated flow parameters, including the soil water content, unsaturated hydraulic conductivity and the groundwater recharge.

2.2. Health and Environmental Consequences of Nitrate

The critical nature of nitrate inputs to groundwater is related to the potential impacts to drinking water sources and subsequent health risks. Limits on nitrate concentrations in drinking water are related to two main health concerns: methaemoglobinaemia and cancer. Nitric oxide, whose production mechanisms include nitrate reduction, converts haemoglobin in the blood to methaemoglobin, an abnormal oxidized form that does not bind oxygen properly. Nitrite produced from nitrate reduction may also react in the stomach to form N-nitroso compounds, some of which are carcinogenic (Addiscott, 2004). A link between elevated nitrate concentrations and adverse reproductive effects has also been suggested (Manassaram et al., 2006). Additional studies have been recommended to better identify the relative contributions of nitrate from drinking water sources and other cofactors in causing these health effects (Ward et al., 2005) but in light of the potential adverse consequences, Health Canada has established a Maximum Acceptable Concentration (MAC) of 10 mg NO_3-N/L for nitrate in drinking water (Health Canada, 2006). Nitrogen also contributes to eutrophication in surface water, and nitrous oxide produced during nitrification or incomplete denitrification contributes to the greenhouse effect and the destruction of ozone in the atmosphere (Addiscott, 2004). These environmental effects provide additional support for limiting excess nitrogen inputs to the agricultural system.

2.3. Site Location and Topography

The study site is an area of agricultural land located in south-western Ontario, just north of the Thornton Well Field in the County of Oxford (Figure 2.1). The well field, consisting of Wells 1, 3, 5, 8 and 11, provides the majority of the municipal water supply for the City of Woodstock, which has a population of 33,600 and lies approximately two kilometres north-east of the well field. The study site is primarily composed of a land parcel owned by the County of Oxford which is bounded by Curry Road to the northwest and the well field's woodlot to the east. The northwest corner of the study site includes a triangular section of privately-owned agricultural land located south of Old Stage Road and north of Curry Road.

The topography at the study site is gently rolling, with ground elevations ranging from 300 to 330 metres above sea level (masl) (Figure 2.2). Surface water within the study site drains into Cedar Creek, a tributary of the Thames River (Haslauer, 2005). The groundwater flow direction n the shallow supply aquifer is regionally from southwest to northeast (Haslauer, 2005) and locally from west to east (Padusenko, 2001).

2.4. Previous Site Studies

Hydrogeological investigations in the vicinity of the study site were first initiated in response to rising nitrate groundwater concentrations in municipal supply wells within the Thornton Well Field. These concentrations have exhibited an increasing trend since the 1970s (Figure 2.3) and first exceeded the MAC of 10 mg NO_3-N/L in the mid-1990s. Oxford County's current groundwater management scheme (i.e., controlling the pumping rate, alternating between supply wells and blending with water from another well field) maintains a nitrate concentration below the MAC.

The dominant land-use beyond the Woodstock city limits, and within the study site, is agriculture. The most commonly cultivated crops in the region include corn, soybeans, wheat and grass (Fertilizer Institute of Ontario Foundation, 2001). Agricultural inputs such as inorganic fertilizers, manure and crop residue are a widely recognized source of nitrate contamination to groundwater (Addiscott, 2004). The temporal correlation between the three-fold increase in the total fertilizer use in Oxford County from 1955 to 1985 (Fertilizer Institute

of Ontario Foundation, 2001) and the subsequent increase in the Thornton Well Field's groundwater nitrate concentrations suggests that agricultural land use upgradient of the well field is likely a major contributor to the rising nitrate levels.

Padusenko (2001) undertook a regional hydrogeologic evaluation in the vicinity of the Thornton Well Field in order to better define the factors controlling agricultural impacts on groundwater quality. This study was complemented by a detailed geochemical investigation (Heagle, 2000) and groundwater age dating (Sebol, 2000; Sebol, 2004), and revealed a nitrate plume migrating from the west toward the well field, as shown in Figure 2.4. Haslauer (2005) subsequently conducted additional site investigations to refine the conceptual hydrogeological model and estimate the quantity of nitrate stored in the unsaturated zone, as further described in Section 2.8.

In an effort to reduce the potential for nitrate leaching to groundwater in the vicinity of the well field, the County of Oxford purchased two parcels of farmland (Parcels A and B) totaling 111 ha in 2003. The parcels are part of the 2-year time of travel capture zone for the well field, as determined by Golder Associates (2001) (Figure 2.4). The land is now rented to farmers, who farm it under nutrient application restrictions. The study site defined in Section 2.3 coincides almost exactly with Parcel B, a 73-hectare parcel on which minimum nutrient inputs are now determined from extensive soil testing and applied with the assistance of equipment controlled by a global positioning system (GPS). The agricultural BMP under evaluation in this study is the overall reduction in nitrogen fertilizer application.

2.5. Current and Historical Site Agricultural Practices

Parcel B is divided into 7 agricultural fields (Fields 1 through 7) (Figure 2.5). Table 2.1 summarizes crops planted and average nitrogen application for each of these fields since the purchase of Parcels A and B by the County in 2003, and includes available data for the field located northwest of Curry Road adjacent to Old Stage Road ("Old Stage Road field"). The Old Stage Road field is not within Parcel B and is therefore not subject to the nutrient reductions associated with Fields 1 through 7. The nitrogen application rate varies significantly with crop type: corn is generally supplied with starter fertilizer at planting and sidedress nitrogen in late spring, while nitrogen-fixing soybeans are not fertilized with nitrogen.

There are no detailed records available of the land use and applied nitrogen mass at the study site prior to 2003. Anecdotal information indicates that historical cropping practices on Fields 1 through 4 included grass and the wheat-corn-soybean rotation common to the area (David Start, pers. comm.). It should be noted that before 2003, the wheat in the rotation was hard red winter wheat, a high protein grain that requires high nitrogen input. In 2003 this crop was changed to soft red winter wheat, the nitrogen requirement for which is almost 50% lower than for the hard wheat.

Fields 5 through 7 were previously part of a livestock farm. It is probable that manure was applied to these fields during the farm's operation (David Start, pers. comm.). Concentrated manure application may also have occurred at the site of the former barnyard and pasture, located in Field 6 (Figure 2.5). The locally high phosphorus and excessive potassium levels previously measured in the soil at that location indicated that cattle manure had been stored or cattle had been confined for a long period of time (Soil Resource Group, 2006). Finally, the Old Stage Road field has also been cropped both under rotation and in alfalfa for several years in the last decade. Because alfalfa is grown continuously for more than one year, a field in alfalfa may receive several nitrogen applications without the planting of an additional crop to take up excess nutrients. This may lead in some cases to a high residual nitrogen value in the soil.

For all fields within the study site, historical nitrogen application rates may be approximated from recommended and commonly used rates in agriculture (David Start, pers. comm.). These values are provided in Table 2.2. A comparison of Tables 2.1 and 2.2 indicates that nitrogen is being applied at a lower rate within Parcel B than is generally used in agriculture. The average nitrogen application rate on corn in Fields 1 through 7 from 2003 to 2005 was approximately 40% lower than the regular rate. On the soft winter wheat, the average application was 20% lower than the regular rate for that crop, and 50% of the rate for hard winter wheat. Overall, for the years 2003 to 2005, the average nitrogen balance across Parcel B (calculated as the nitrogen fertilizer input minus the nitrogen within crops removed from the field at harvest) was approximately -38 kg N/ha (-34 lb N/ac), compared to an estimated +26 kg N/ac (+23 lb N/ac) historically (Don King, pers. comm.). Despite the reduction in nitrogen application, the

harvested yields for wheat and corn in 2004 and 2005 met or exceeded the long-term average for the region (Soil Resource Group, 2006).

2.6. Geology

The bedrock geology of the greater Woodstock area consists of Silurian dolostone and shale, as well as Devonian limestone, with a bedrock surface that generally slopes to the south and is flat or gently rolling (Cowan, 1975). During installation of a monitoring well at the western corner of the study site, the bedrock was encountered approximately 69 m below ground and identified as limestone of the Detroit River Formation (Haslauer, 2005).

Quaternary geology is shown in Figure 2.6. The greater Woodstock area is part of an interlobate zone characterized by the invasion of several distinct ice lobes over time which resulted in an overall mixing of sediments and the production of lithologically similar tills. Within the smaller site of this study, the surficial Quaternary geology is dominated by the Zorra Till, a stiff, stony silt till. Older, deeper formations include the Catfish Creek Till and possibly the Port Stanley Till (Cowan, 1975). As a result of its complex glacial history, the Woodstock area has a variable geomorphology. Much of the terrain mapped as Zorra Till and Port Stanley Till consists of ground moraine. The study site includes the Woodstock drumlin field and may be described as drumlinized ground moraine. The Ingersoll Moraine is located to the east of the site (Cowan, 1975). Glaciofluvial outwash sand and gravel are also present on the eastern side of the study site.

As shown on Figure 2.7, the most prevalent soil type at the study site is the Honeywood-Guelph complex, consisting of mixed silty alluvial deposits over loam till. The complex consists of mixed profiles incorporating the Honeywood silt loam soils having few stones and the stonier loam-textured Guelph soils. Other soils across the study site include the Fox sandy loam overlying the glaciofluvial outwash deposits described above, and the Embro silt loam which is similar to the Honeywood series but has a lacustrian basin origin and has imperfect drainage (Wicklund and Richards, 1961). The geology of the study site is further described by Padusenko (2001) and Haslauer (2005).

2.7. Hydrogeology

Hydrogeological investigations by Padusenko (2001) and Haslauer (2005) in the Thornton Well Field and the 2 km^2 area northwest of the well field have increased the understanding of the complex groundwater flow system. The conceptual model of the hydrogeological system presented by Haslauer (2005) includes a layered overburden system of four aquitards and four aquifers, each of which ranges across the site from zero to tens of metres in thickness, as well as the underlying bedrock aquifer. Figure 2.8 is a stratigraphic cross-section along Curry Road on the northwest edge of the study site, showing the layered sequence. Of the five aquifers, the units named Aquifers 3, 4 and 5 are identified as water supply aquifers. The Thornton supply wells are located in Aquifer 3. Aquifer 2 appears to be unsaturated across most of the site, except toward the east where the saturated glaciofluvial outwash channel is part of the aquifer. Aquitard 2 is locally discontinuous and consists of a hard, dry mixture of particle sizes ranging from clay to fine gravel. It is overlain by either Aquitard 1 (silt and clay) or Aquifer 1, which may support a perched water table above Aquitard 2.

Haslauer (2005) also noted the potential for rapid water infiltration in the vicinity of the outwash channel shown in Figure 2.6, as suggested by the rapid response of the water table to the spring melt, and drill logs and geophysical surveys that indicate that Aquitards 1 and 2 are absent or discontinuous in the area. This area is consequently considered a likely rapid pathway for nitrate migration from surface to groundwater.

An extensive array of groundwater monitoring wells including multilevel nests exists between the Thornton Well Field and the outer limit of the study site (Figure 2.9). Most of these monitoring wells are screened within Aquifer 3 and Aquifer 2 where it is saturated.

Oxford County lies within the Great Lakes climatic region, and experiences relatively uniform precipitation during the year totaling 950 mm annually on average. Mean monthly temperatures range from -6.3ºC in January to 20.4ºC in July, with an annual average of 7.5ºC (Environment Canada 2006).

2.8. Previous Recharge and Nitrate Mass Load Estimates

In an initial assessment of agricultural impacts on the Thornton Well Field, Padusenko (2001) used the storage-routing model HELP to estimate groundwater recharge within a model domain encompassing this study's site. Using topographic and soils maps, and a meteorological preprocessor to generate input data, he estimated an annual recharge rate for each of eleven surficial regions defined by soil type, vegetation and ground slope. For the study site defined in Section 2.3, Padusenko's (2001) recharge estimates were 11 cm/year for sandy silt till with agricultural crop cover and 23 cm/year for glaciofluvial outwash sand with agricultural crop cover.

Padusenko (2001) also estimated the timeframe and magnitude of the impact on supply well nitrate concentrations from the nitrogen input restrictions, with refinements to these estimates completed by Haslauer (2005). These authors recognized the legacy of nitrogen stored in the unsaturated zone that must be flushed by clean infiltrating water before the full effect of the land-use change can be observed. Haslauer (2005) estimated the nitrate mass load to the groundwater table below Parcel B as 1.1 to 2.5 t NO_3-N/yr, by using an average nitrate concentration in the unsaturated zone and Padusenko's (2001) recharge estimates. He compared the average nitrate mass load below Parcel B (1.8 t NO_3-N/yr) to the nitrate mass extracted annually from the Thornton supply wells (14 to 36 t NO_3-N/yr), and determined that if nitrogen input were reduced to zero on Parcel B, the associated potential decrease in supply well nitrate concentration would range from 6 to 17% and would require approximately 15 years to be fully realized. This analysis assumed advective transport only and did not account for dispersion. It furthermore required the assumption of a uniform groundwater recharge rate across the site based on Padusenko's (2001) estimates, which may not be representative given the heterogeneous hydrogeologic system.

Table 2.1. Recent crop and nitrogen application history in the study area. Note: n/a = data not available

Field	2002		2003		2004		2005		2006	
	Crop	Applied nitrogen, kg N/ha (month)	Crop	Applied nitrogen, kg N/ha (month)	Crop	Applied nitrogen, kg N/ha (month)	Crop	Applied nitrogen, kg N/ha (month)	Crop	Applied nitrogen, kg N/ha (month)
1	Corn	n/a	Soybean	0	Corn	13 (May) 108 (Jun.)	Soybean	0	W.wheat	n/a
2	Corn	n/a	Corn	22 (May) 128 (Jun.)	Romano beans	21 (May) 5.6 (July)	W.wheat	92 (April)	Corn	n/a
					W.wheat	4.0 (Oct.)				
3a	Corn	n/a	Grass						Corn	n/a
3b	Corn	n/a	Soybean	0	W.wheat	73 (May)	Oats/grass	11 (April)	Grass	n/a
			W.wheat	6.2 (Oct.)						
4	Corn	n/a	Soybean	0	W.wheat / clover	73 (May)	Corn	30 (May) 70 (June)	Romano beans	n/a
			W.wheat	6.2 (Oct.)						
5	Corn	n/a	Soybean	0	W.wheat/ clover	73 (May)	Corn	30 (May) 59 (June)	Soybean	n/a
			W.wheat	6.2 (Oct.)						
6	Corn	n/a	Soybean	0	W.wheat/ clover	73 (May)	Corn	30 (May)	Soybean	n/a
			W.wheat	6.2 (Oct.)						
7	Corn	n/a	Soybean	0	W.wheat/ clover	73 (May)	Oats/grass	11 (April)	Grass	n/a
			W.wheat	6.2 (Oct.)						
Old Stage Rd.	Alfalfa	n/a	Alfalfa	n/a	Corn	n/a	Soybean	n/a	Wheat	n/a
							Wheat			

Table 2.2. Recommended and assumed historical nitrogen application rates

Crop	Regular Nitrogen Application (kg N/ha)	Notes
Corn	157 -190 annual total	May be reduced by planting red clover with wheat in the preceding year
Hard red winter wheat	157 - 168 134 minimum	Crop's value dependent on protein content
Soft red winter wheat	100	Low protein content is desirable
Soybean	0	Nitrogen fixer

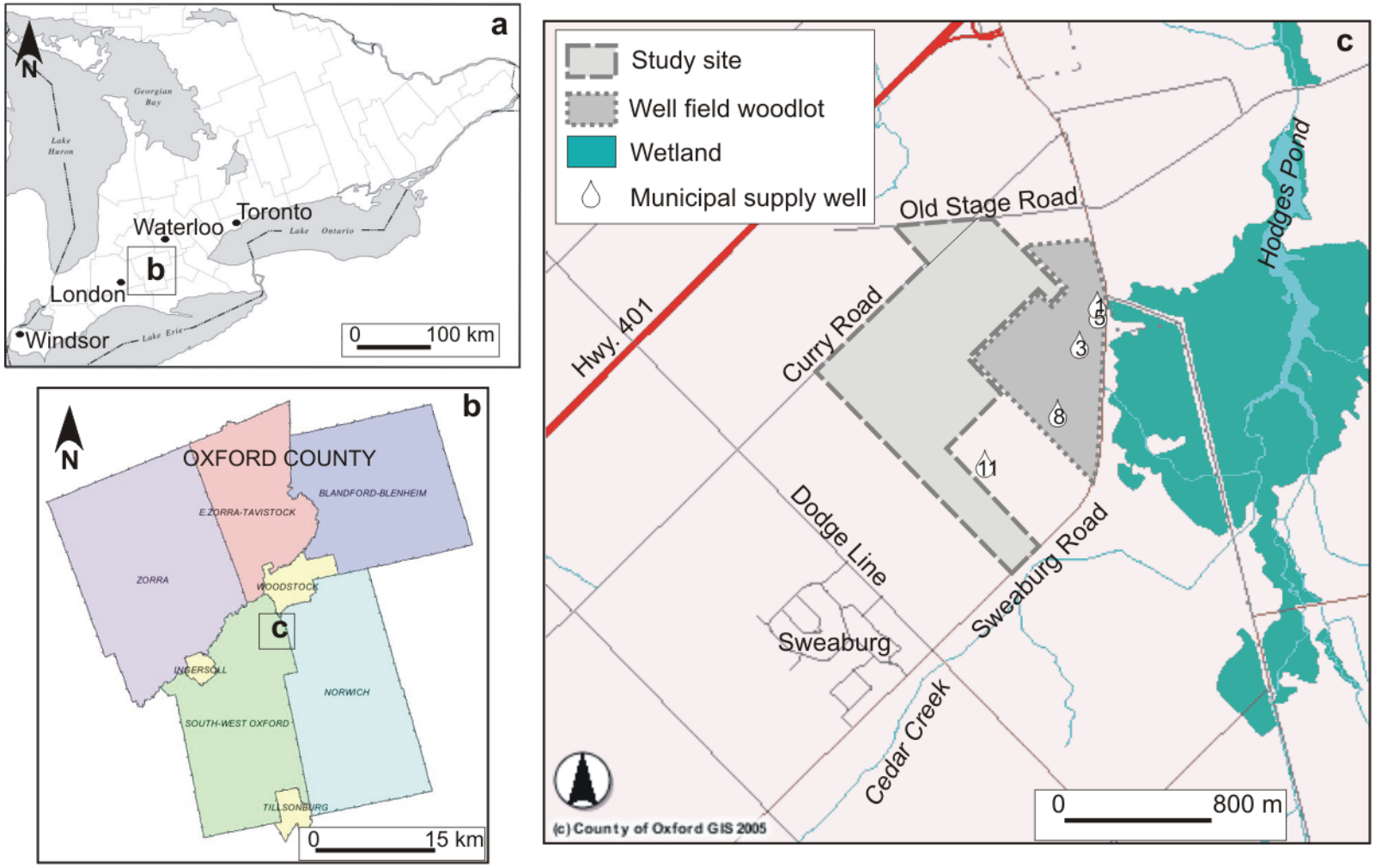

Figure 2.1. a) Location of Oxford County within Southern Ontario. Contains data from Brock University Map Library (n.d.). b) Location of study site within Oxford County. Contains data from The Corporation of the County of Oxford (1990). c) Study site limits, municipal well locations and surface water features. Contains data from The Corporation of the County of Oxford (1990, 2003a, 2003b, 2003c, 2003d, 2003e).

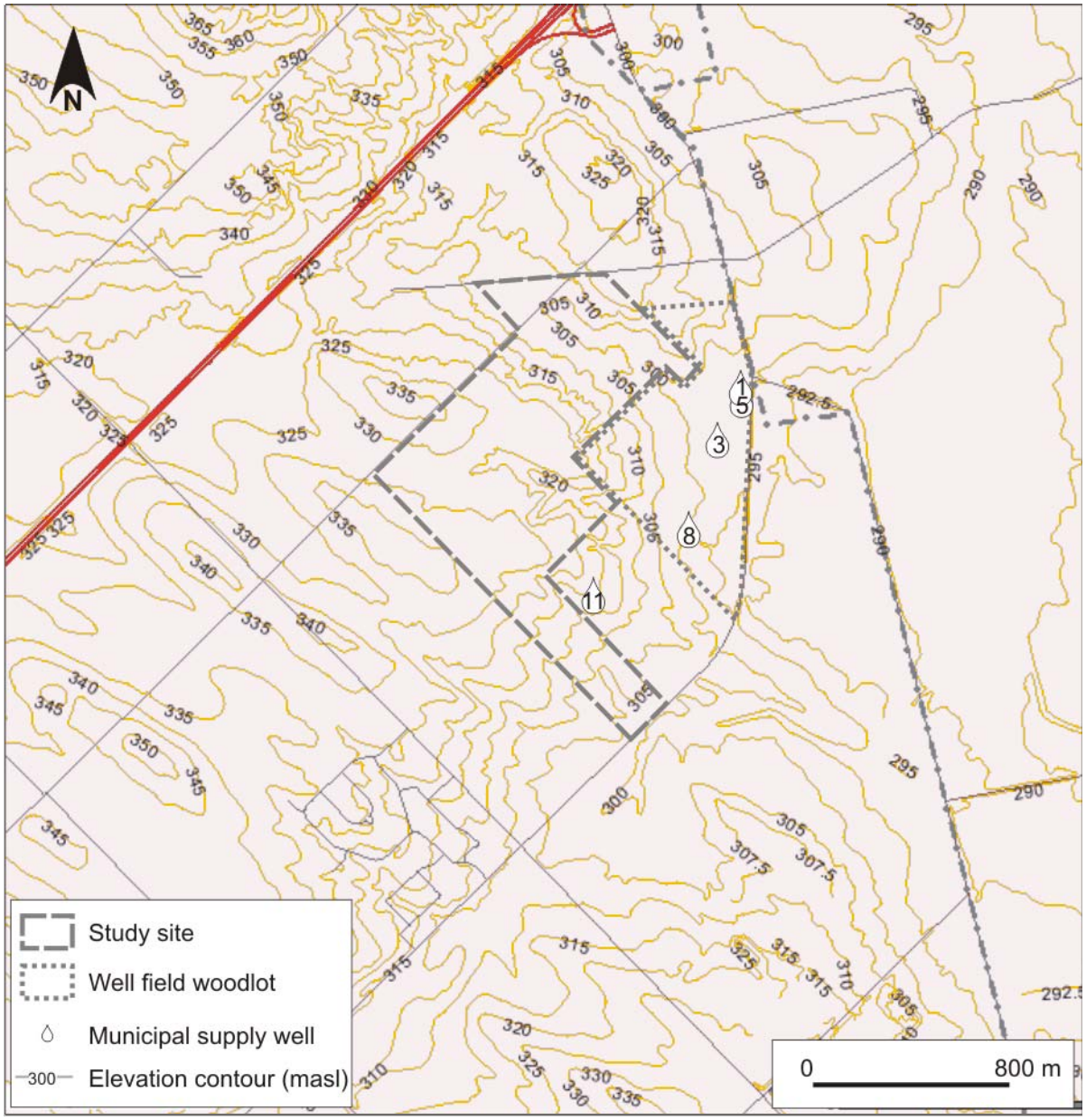

Figure 2.2. Topography of study site and surrounding area. Contains data from The Corporation of the County of Oxford (1990, 2003b, 2003c, 2003e).

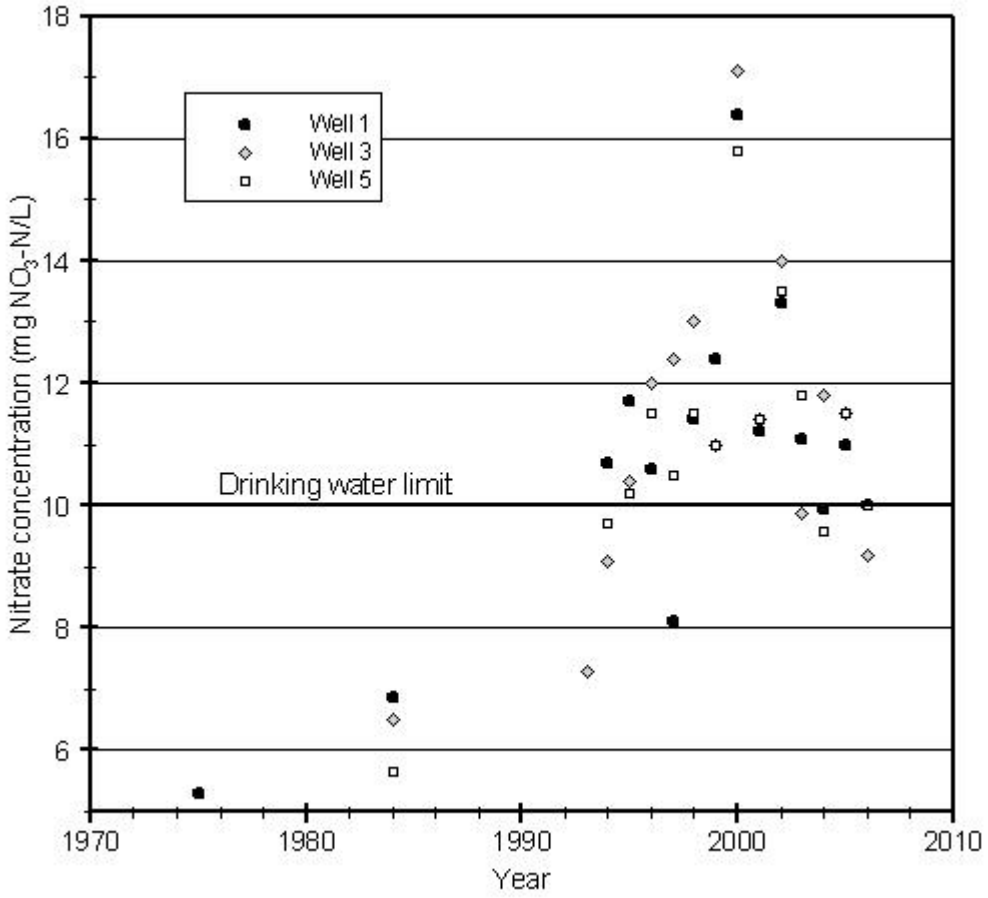

Figure 2.3. Temporal trends in nitrate concentration in municipal supply wells.

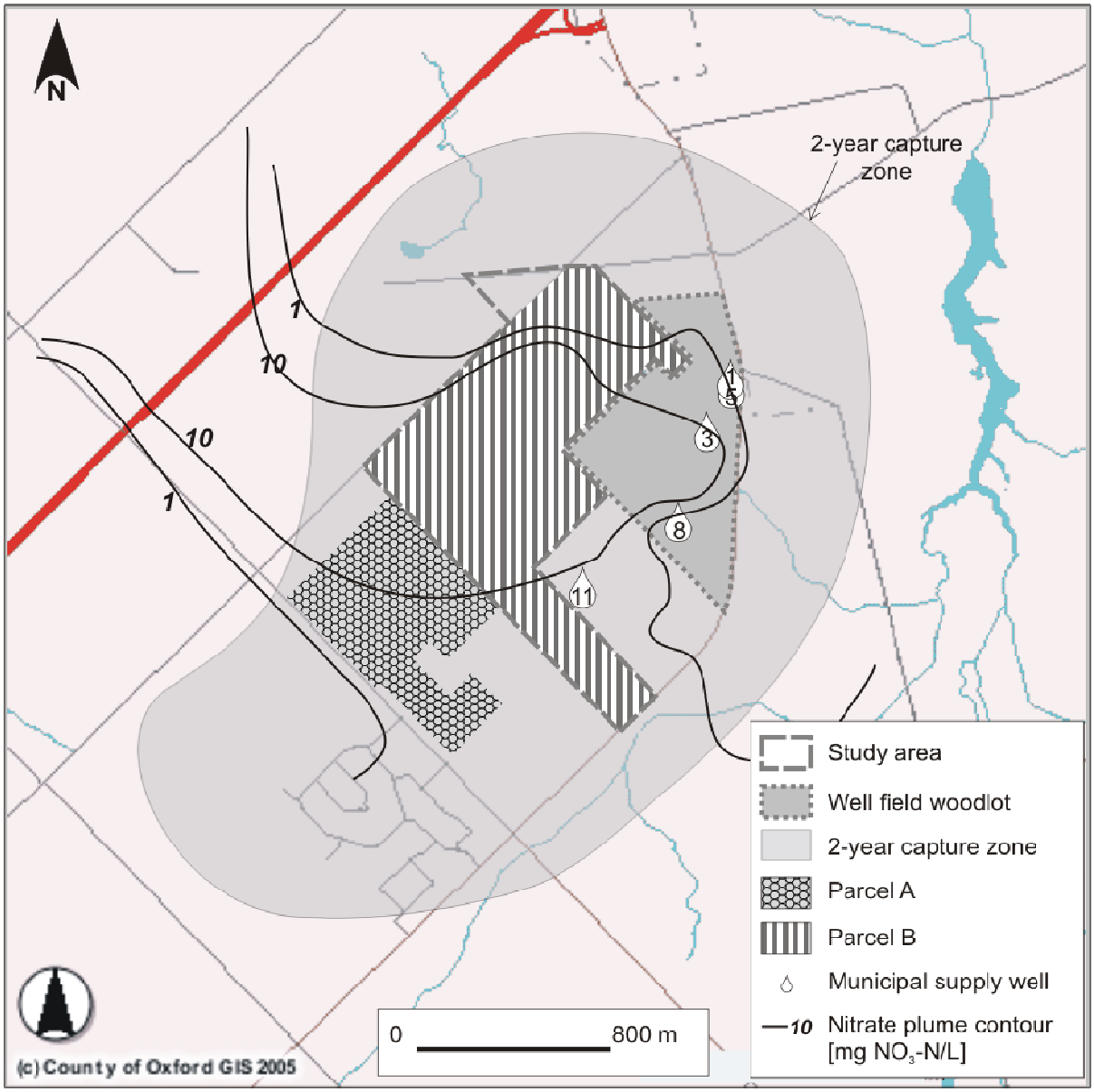

Figure 2.4. Groundwater nitrate concentration contours from Padusenko (2001), two-year time of travel capture zone from Golder Associates (2001) and Oxford County land purchases Parcels A and B.

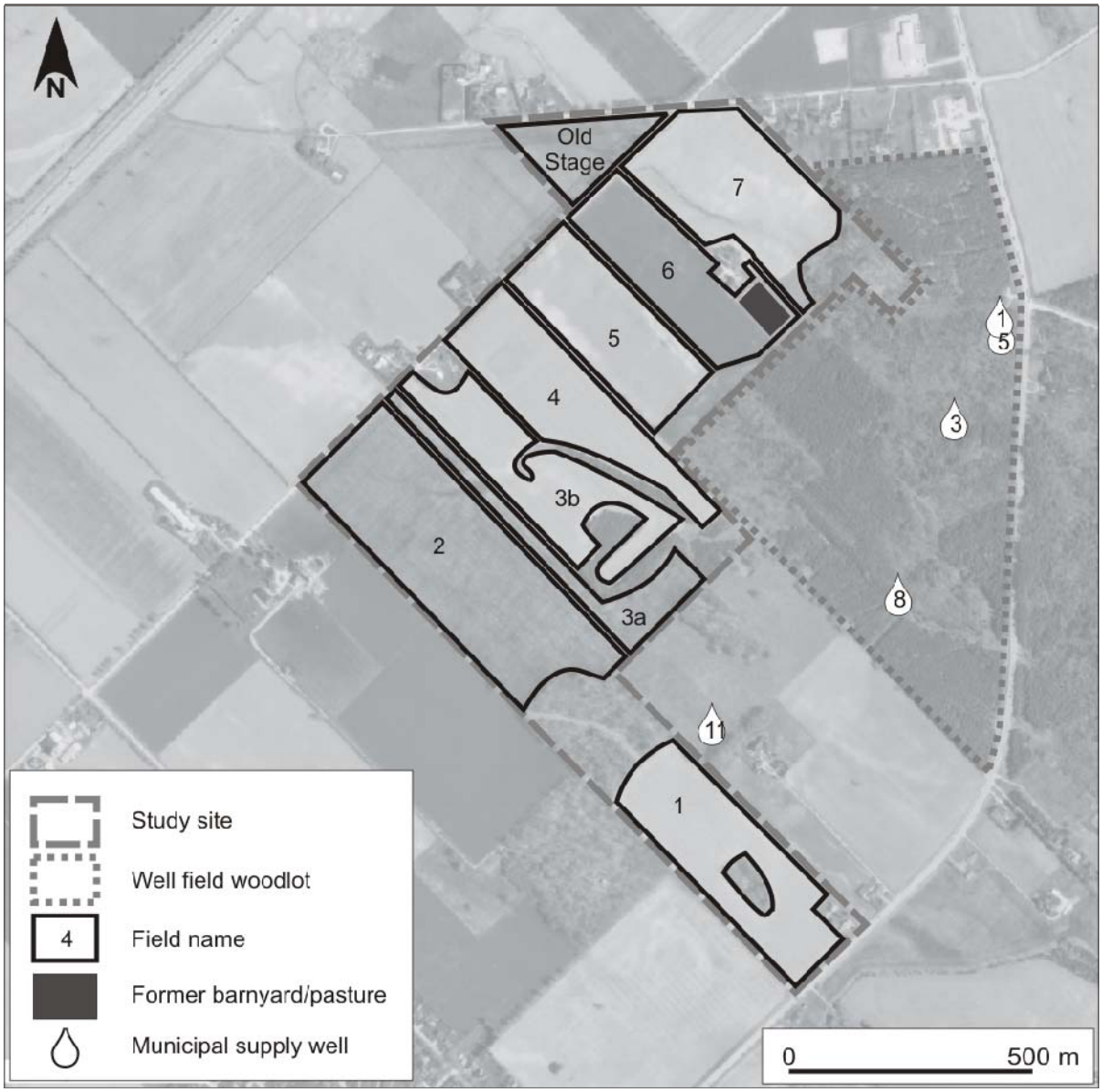

Figure 2.5. Study site field names. Contains data from The Corporation of the County of Oxford (2000).

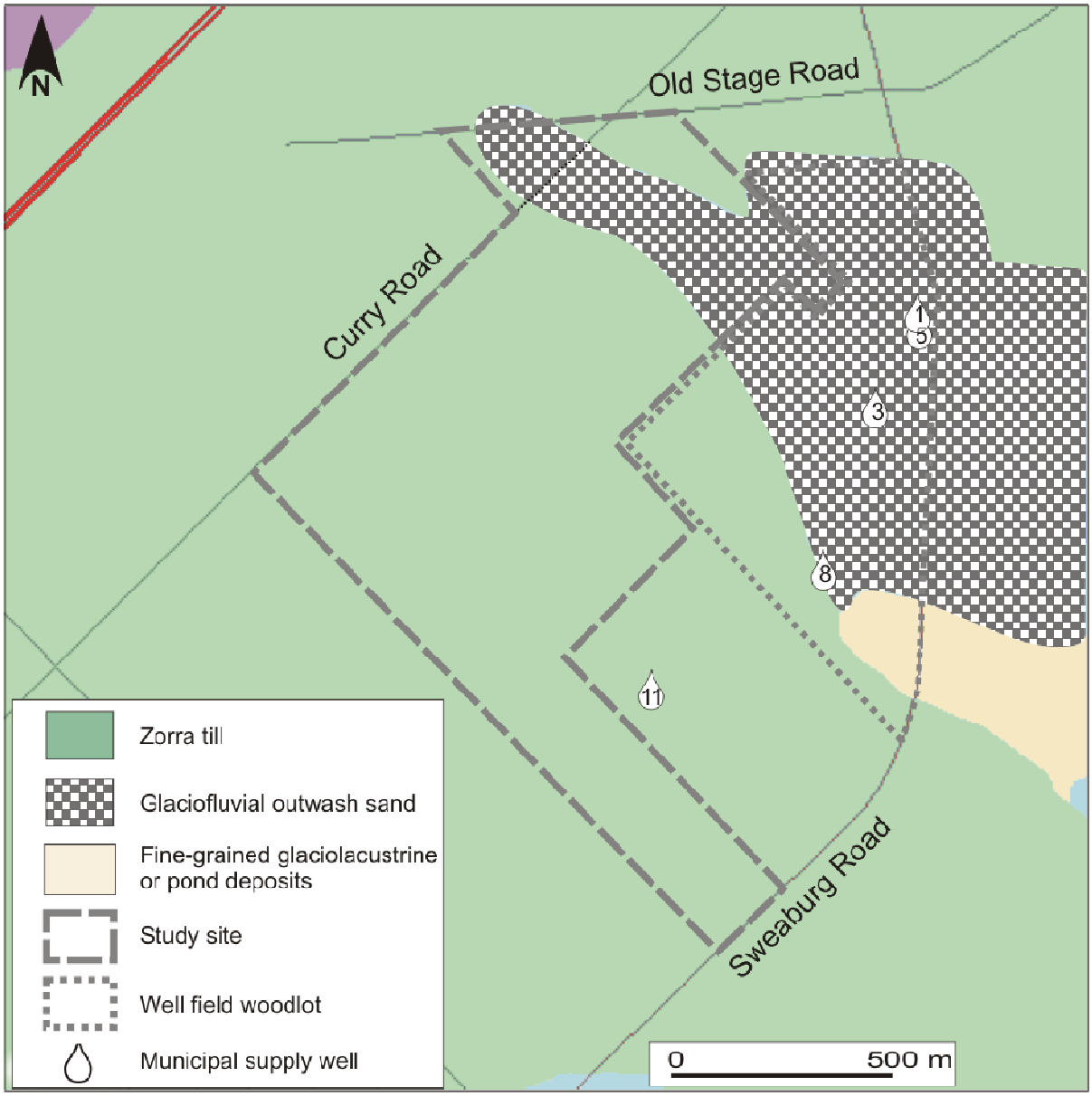

Figure 2.6. Study site Quaternary geology. Contains data from The Corporation of the County of Oxford (2001, 2003b, 2003c).

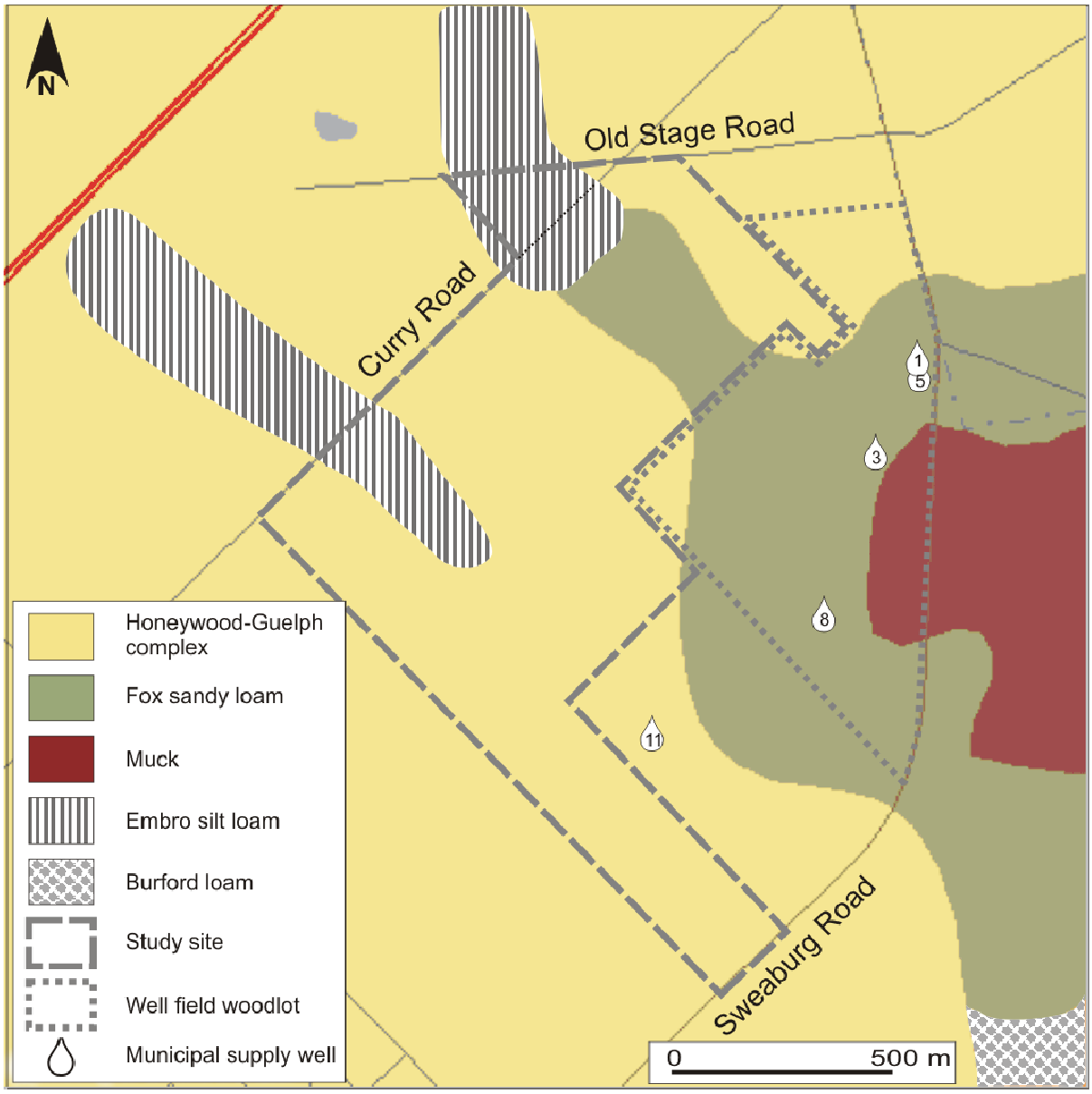

Figure 2.7. Study site soils. Contains data from The Corporation of the County of Oxford (1994, 2003b, 2003c).

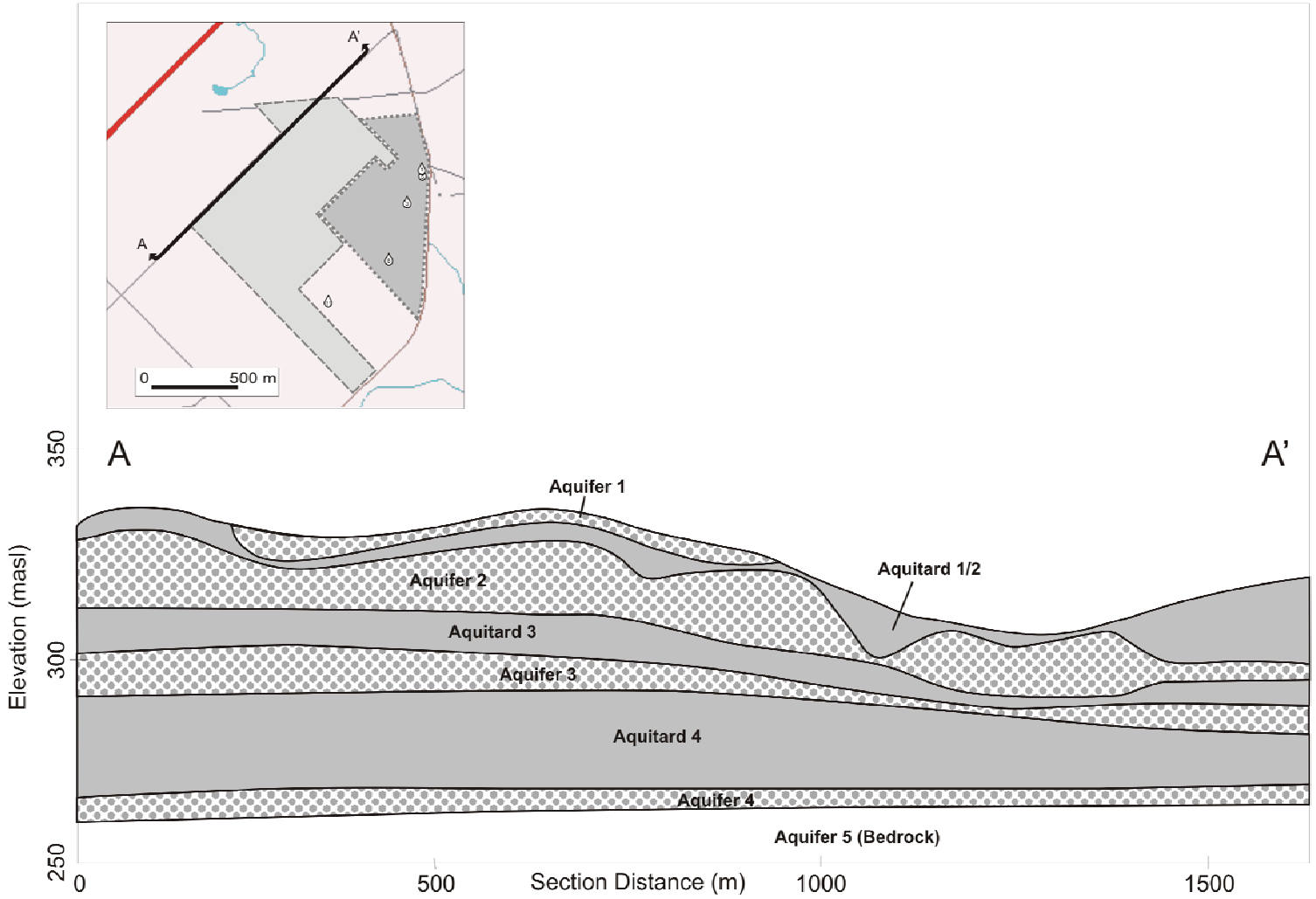

Figure 2.8. Geologic cross-section along Curry Road (north-west edge of study site). Contains data from The Corporation of the County of Oxford (2003b, 2003c) and Haslauer (2005).

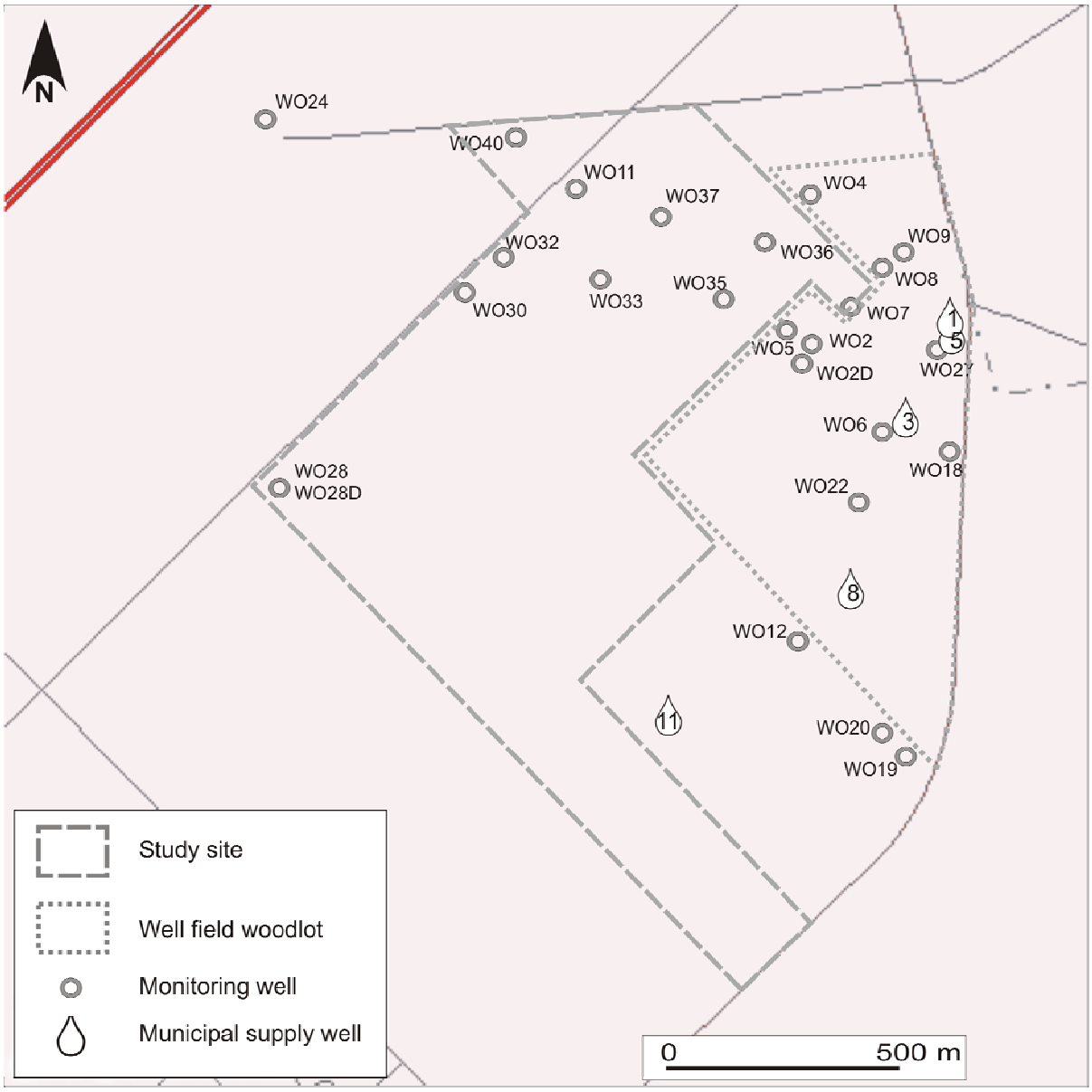

Figure 2.9. Study site and wellfield woodlot monitoring wells at study period outset. Contains data from The Corporation of the County of Oxford (2003b, 2003c) and Haslauer (2005).

3. Methods

This section describes the novel method designed to satisfy the thesis objectives stated in Chapter 1. The general approach was to estimate (at several locations across the study site) the groundwater recharge rate and the porewater nitrate concentration in the unsaturated zone, the product of which would yield an estimate of nitrate mass flux. Nitrate mass flux values corresponding to pre- and post-BMP conditions were then extrapolated to field-scale pre- and post-BMP nitrate mass load values which could be compared to assess the BMP's effect.

It was anticipated that within the timeframe of this study, BMP-driven changes in nitrate load below the root zone were most likely to be observed in the shallow unsaturated zone. The methods in this study were therefore focused on this zone. Groundwater recharge through the unsaturated zone at each study location across the site was estimated using several analytical techniques, as well as two computational models. The recharge rate was then used to define the maximum depth in the unsaturated zone potentially affected by the BMP at a given time, and analysis of soil samples from above this depth for water and nitrate content provided the porewater nitrate concentration. This concentration multiplied by the groundwater recharge rate at that location represented the average nitrate mass flux at that station since BMP implementation. Similarly, analysis of soil samples from below the depth of BMP effects allowed the calculation of the pre-BMP mass flux. As described above, these mass flux estimates were then distributed across the study site, such that each flux value was multiplied by a corresponding land area to determine pre- and post-BMP nitrate mass load estimates.

This chapter summarizes the field, laboratory and computational methods used to estimate groundwater recharge, porewater nitrate concentration and nitrate mass flux and load across the study site. Groundwater monitoring wells were installed in order to measure water level, temperature and nitrate concentration, while neutron moisture probe access tubes and other equipment were installed for soil water content measurement. A meteorological station and soil temperature sensors were also installed. Geologic cores collected during monitoring well and access tube installation and at other times were analysed for soil nitrate, bromide and water content. The time period over which these activities were conducted (the "study period") was from January 2005 to May 2006. The field and laboratory data collected during this period were

then used to estimate nitrate mass flux and mass load. Methods are distinguished as field equipment installation (3.1), field data collection (3.2), geologic core analysis (3.3), recharge estimation (3.4), modelling (3.5), porewater nitrate concentration estimation (3.6), nitrate mass load estimation (3.7), and up-scaling (3.8).

3.1. Field Equipment Installation

3.1.1. Meteorological Station

In order to collect detailed climatic data at the site, a meteorological station equipped with a Campbell Scientific Inc. (CSI) CR23X datalogger was installed on December 9, 2004 at the location indicated on Figure 3.1. The location was selected because of its locally flat topography and the absence of tree cover in the immediate vicinity. This station includes an extensive array of meteorological sensors for measurement of the following parameters: precipitation (including rainfall measurement with a tipping bucket, and snowfall measurement as rainfall equivalent using a snow adapter on the tipping bucket), temperature, relative humidity, wind speed and direction, solar radiation, barometric pressure and soil heat flux. The meteorological station also includes five soil temperature sensors and five soil moisture sensors, which are described in detail in Section 3.1.5.2. The datalogger was programmed to collect and record at an interval of 15 or 60 minutes for each sensor.

3.1.2. Recharge Station Selection

Data collection at various locations across the study site was critical for the evaluation of the spatial variability of groundwater recharge and nitrate mass load. Eight study locations ("recharge stations") were selected to represent a variety of topographic and geologic conditions present across the study site. The initial geologic characterization of the stations was based on previously drilled boreholes at or near the stations (Haslauer 2005) which often did not reach the water table, and therefore represented the shallow stratigraphy (3 to 10 m). No recharge stations were situated in Fields 1 and 2 (Figure 2.5) because these fields were inaccessible at the start of the study period. The locations of the recharge stations are shown on Figure 3.1, and their topography and assumed geologic characteristics based on prior geologic investigation are summarized in Table 3.1.

Each recharge station was equipped with a minimum of one monitoring well, one neutron probe access tube, six capacitance moisture probes and six soil temperature probes, and was subject to the surface application of a potassium bromide tracer, as described in the following sections. Additional equipment was installed at selected recharge stations. Table 3.2 includes a summary of the equipment installed at each station and figures showing the layout of each recharge station are provided in Appendix A.

3.1.3. Monitoring Wells

At the beginning of this study, an extensive network of monitoring wells existed in the vicinity of the study site around the Thornton well field. The number of wells on Parcel B was fairly limited, although some wells were in place in Fields 5, 6 and 7 and along Curry and Old Stage Roads. The only wells present at recharge stations were the 3.2-cm (1.25-in) diameter wells (WO37 and WO35) at recharge Stations 1 and 8. In order to determine the groundwater nitrate concentration, depth to water, stratigraphy and unsaturated zone nitrate content at each of the recharge stations, a geologic drilling and monitoring well installation program was conducted between March 29 and April 9, 2005.

Drilling was performed by SDS Drilling (Boart Longyear Inc.) using a Mini-Sonic track-mounted rig with a 4 x 6-inch continuous coring system. When possible, a split core barrel was used to allow the collection of continuous intact core in 10-cm (4-in) diameter, 1.5-m (5-ft) long Lexan tubes, which were then sealed to preserve soil moisture. These geologic cores were subsequently logged for stratigraphy and analyzed for soil water content and nitrate concentration in the laboratory as described in Section 3.3. In most boreholes, the collection of intact core was only possible to a depth of approximately 4.5 m below ground surface (bgs), below which the geologic material did not permit the use of a split barrel and the core sample was shaken into plastic sample bags. These samples were logged for stratigraphy, but were not analyzed for moisture content and nitrate. At Stations 3 and 5, intact core to depths of 20 and 15 m bgs respectively was collected and preserved in the Lexan tubes. Geologic cores were collected and bagged along the entire length of each borehole to the well screen depth.

A 5-cm (2-in) diameter Schedule 40 PVC monitoring well was installed in each borehole. All monitoring wells were screened over the bottom 3 m (10 ft), with a sandpack ending 0.6 m (2 ft)

above the screen and bentonite chips or slurry above the sandpack to ground surface. A total of seven monitoring wells were installed, at six of the eight recharge stations (wells numbered WO56, WO58, and WO60 to WO63) and at one extra location in Field 6 (WO64) (Figure 3.1). No monitoring well was installed at Station 8 because a well was already in place there, nor at Station 7 because site access had not been secured at that time. The monitoring well installed at Station 1 reached approximately 7 m deeper than the well already in place.

Two additional monitoring wells were installed at later dates. A 3.2-cm (1.25-in) diameter monitoring well (WO65) was installed at Recharge Station 7 using a Vibra-Push® direct push rig on May 9, 2005. The stratigraphy at this location was inferred from the continuous core collected during installation of the neutron access tube at 1.2 m from the well (Section 3.1.4). A 3.2-cm (1.25-in) diameter monitoring well (WO66) was also installed in Field 7 on November 21, 2005 (Figure 3.1). At this time, a Vibra-Push® direct push rig equipped with the Enviro-Core® sampling system was used to advance a 5-cm (2-in) diameter borehole and collect continuous geologic core. The 0.9-m (3-ft) long core samples were sealed in the field to preserve moisture content and refrigerated at the University of Waterloo until analysis as described in Section 3.3. The locations of all monitoring wells installed during this study are shown on Figure 3.1, and geologic logs are available on request.

3.1.4. Neutron Probe Access Tubes

Soil water content measurements were necessary for the estimation of recharge and porewater concentration across the study site. Several types of instrument were employed to allow comparison and the selection of the most appropriate instrument for the study site. The first of these instruments was a neutron moisture probe. Each recharge station was equipped with a 5-cm (2-in) diameter access tube for the probe. Tubes were installed at six of the stations (2 to 6, and 8) on February 9 and 10, 2005, while the access tubes at Stations 1 and 7 were installed on November 18, 2005 and May 9, 2005, respectively. At each station, a Vibra-Push® direct push rig equipped with the Enviro-Core® sampling system was used to advance a 5-cm (2-in) diameter borehole and collect continuous geologic core. The 0.9-m (3-ft) long core samples were sealed in the field to preserve moisture content and refrigerated at the University of Waterloo until analysis as described in Section 3.3. A 5-cm (2-in) diameter Schedule 40 PVC riser pipe with a threaded bottom cap was fitted snugly into the borehole. Air space and surface

water leakage between the access tube and the geologic material were minimized to ensure representative measurements. The average depth of the 5-cm access tubes was 4.5 m bgs.

In an effort to increase the depth of neutron probe measurements at the study site, a different installation method was used for a second set of access tubes in conjunction with the monitoring well installation described in Section 3.1.3. This method was employed at the six recharge stations where monitoring wells were installed with the Mini-Sonic rig; it was not required at Stations 7 and 8 due to their relatively short unsaturated zone which could be fully penetrated with the Vibra-Push® rig. A borehole measuring 8.9 cm (3.5 in) in diameter was advanced within 3 m (10 ft) of the existing access tube using a Mini-Sonic track-mounted rig and the rig's drill rods as a "core barrel". This advancement method did not allow for the collection of continuous core; however, each access tube was installed within 3 m of a monitoring well installation where a detailed stratigraphic log was available and assumed to adequately represent the access tube borehole stratigraphy. The boreholes were fitted with an 8.9-cm (3-in) diameter Schedule 40 PVC riser pipe with a threaded bottom cap. The average depth of the 8.9-cm neutron probe access tubes was 7.4 m bgs. The locations of all access tubes are shown on Figure 3.1 and in Appendix A.

3.1.5. Soil Water Content and Temperature Sensors

3.1.5.1. ECH_2O Probes and HOBO Temperature Sensors

Each recharge station was instrumented with six ECH_2O-20 dielectric aquameters (Decagon Devices, Inc.), in a vertical profile between 0.6 m and 2.4 m depth. The ECH_2O sensor is a capacitance-based probe that reports the volumetric water content (VWC) in a 2-cm zone of influence relative to its flat surface. The ECH_2O-20 probes used in this study measure an average VWC over their 20-cm length.

Laboratory soil-specific calibration of the ECH_2O probes was conducted for two material types: well-sorted fine sand, and silty clay. For each calibration, ten ECH_2O probes were deployed successively in the material, at moisture contents varying over the range of 0 to 30% VWC which were also measured gravimetrically or with a time-domain reflectometry (TDR) probe. A linear relationship between the ECH_2O probe's raw output in millivolts and the

gravimetrically-measured or TDR VWC results was established, and the equation of the line was subsequently used to convert the ECH_2O probe data to VWC.

A vertical profile of six ECH_2O probes was installed at each recharge station. A separate 10-cm (4-in) diameter borehole was advanced for each probe using the Vibra-Push® direct push rig and the extracted geologic material was retained. The ECH_2O probe installation tool was used to insert the probe vertically into intact material at the bottom of the borehole. Frequently, the geologic material was too compacted or stony to allow probe insertion, in which case the probe was set in the open borehole. In either case the borehole was backfilled with its original material and a layer of bentonite chips was placed in the upper one metre to prevent surface water infiltration. Probe installation depth (at the probe mid-point) ranged from 0.7 to 2.3 m bgs (Table 3.3).

A HOBO Weather Station 8-bit Temperature Smart Sensor (Model S-TMA-M006, Onset Computer Corporation) was also installed approximately 0.15 m above each ECH_2O probe. The ECH_2O probes and temperature sensors were connected to a HOBO Weather Station datalogger (Onset Computer Corporation) at surface which was programmed to record data hourly.

3.1.5.2. Meteorological Station Sensors

An additional set of soil water content and soil temperature sensors connected to the meteorological (MET) station datalogger was installed at Station 2 only, due to the proximity of the MET to the recharge station and the limited cable length connecting the sensors to the datalogger. These sensors included five CSI CS616 water content reflectometers, which use TDR methods but operate without the typical cable tester, and output a square wave whose period is converted to water content (Campbell Scientific, Inc., 2004). The CS616 sensors measure an average VWC along the 0.3-m length of the rods. Also installed were five CSI 107B soil/water temperature sensors, which use a thermistor to measure temperature (Campbell Scientific, Inc., 2003).

Like the ECH_2O probes, each CS616 water content sensor was installed at the bottom of a 10-cm (4-in) diameter borehole. The material from the deepest 30 cm of the borehole was

replaced in the borehole after any large stones were removed, and the sensor was inserted into this material. The borehole was then backfilled with the remaining original material with a thin seal of bentonite at the surface. The sensors were installed at approximately 0.4-m intervals (between sensor mid-points) between 0.95 and 2.45 m bgs. The CSI 107B soil/water temperature sensors were fastened to a 2.5-cm PVC pipe at 0.4-m intervals between 0.85 and 2.45 m bgs and installed in a separate borehole. The water content and temperature sensors were connected by buried cable to the MET station datalogger which was programmed to record their measurements hourly.

3.1.6. Bromide Tracer Application

In order to quantify vertical solute transport in the unsaturated zone and directly measure groundwater recharge rates, a potassium bromide (KBr) conservative tracer was applied at ground surface at each recharge station between July 20 and 22, 2005. An application area measuring 3 by 3 m (9 m^2) was established at each station, and was designed to overlap or abut the neutron access tubes without overlapping the ECH_2O probe installations. A solution of 6 kg KBr dissolved in 18 L deionized water was applied across the application area in 1-m^2 increments using a watering can. This application was equivalent to an aqueous concentration of 224 g Br/L in the tracer solution, or an applied surface concentration of 0.45 kg Br/m^2. Although crops were in place on the fields at the time of tracer application, efforts were made to ensure consistent tracer application to the soil surface.

3.1.7. Equipment Burial

In order to obtain field data that were more representative of groundwater recharge and nitrate mass load below active agricultural land, the recharge stations were located within active fields. Field equipment was buried during operations such as planting and harvesting to permit normal agricultural activities to take place over the recharge stations.

3.2. Field Data Collection

3.2.1. Neutron Moisture Probe

A Model 503 DR Hydroprobe Neutron Moisture Probe (CPN International Inc.) was used to measure soil water content along the length of the access tubes. The probe uses 50mCi

Americium-241/Beryllium as a source of fast neutrons, and measures the proportion of emitted fast neutrons that are redirected to the probe as slow neutrons after colliding with the hydrogen atoms in the water molecule. Moisture content is usually determined from the neutron probe count ratio (CR; raw neutron count/neutron count in a standard medium) using a linear calibration equation.

In order to collect CRs, the neutron moisture probe was lowered down the access tube with a usual depth interval of 0.15 m. At each measurement depth along the profile, the CR was determined based on neutron emission and reflection over a 16-second time interval. From March 1 to December 31, 2005, neutron probe measurements were performed in the field on average bi-weekly. In 2006 the approximate measurement frequency decreased to once per month, although several measurements were taken in March 2006 during spring melt.

The 503 DR Hydroprobe was supplied with a factory calibration equation for measurements taken in a 5-cm (2-in) PVC access tube. Literature suggests, however, that site- and soil-specific calibrations are necessary for reliable measurements (Yao et al., 2004; Greacen et al., 1981). Furthermore, no factory calibration equation was available for the 8.9-cm (3.5-in) PVC access tubes. Therefore a field calibration program was conducted at the study site in November 2005, and was based on the comparison of probe measurements in several newly-installed 5-cm access tubes and existing 8.9-cm access tubes with the gravimetric moisture content of the core collected during tube installation. The calibration effort required the installation of additional 5-cm access tubes not described in Section 3.1.4. The details and results of this calibration program are provided in Appendix B.

3.2.2. Geologic Cores

Geologic cores were collected during the neutron access tube installations in February 2005 and the monitoring well installations (March 2005) as described in Section 3.1. The purpose of this core collection was to determine stratigraphy, soil water content and soil nitrate and bromide concentration. To further monitor changes in the soil nitrate concentration and the transport of the bromide tracer, additional cores were collected from the bromide application areas on November 17-18, 2005 and May 8, 2006, approximately 4 and 9.5 months after tracer application. At both of these times, a continuous core sample (average depth of 5.0 m in

November and 3.0 m in May) was extracted from the approximate centre of the bromide application area at each recharge station, using the Enviro-Core® sampling system. The 5-cm (2-in) diameter, 0.9-m (3-ft) long geologic core tubes were sealed in the field and analyzed at the University of Waterloo as described in Section 3.3. The boreholes were immediately backfilled with bentonite chips.

3.2.3. Groundwater Monitoring and Sampling

A Levelogger pressure transducer equipped with temperature sensor (3001 Mini LT, Solinst Canada Ltd., Part No. 105818) was installed in the monitoring well at each recharge station in June 2005 and programmed to record water level and water temperature hourly. These pressure transducers were removed for repair in August 2005 and were replaced by Levelogger Gold pressure transducers (3001 LT Gold, Solinst Canada Ltd., Part No. 108083) in December 2005. No automated measurements of groundwater level were collected between August and December 2005. Groundwater levels in these wells were also measured manually at an average bi-weekly frequency during the study period in order to verify the electronic measurements.

To determine the groundwater nitrate concentration immediately underlying the eight recharge stations and to monitor regional groundwater nitrate trends, groundwater samples were collected from the monitoring well network on three occasions during this study. In January 2005 the entire network of wells in the well field woodlot (Figure 2.9) and existing wells in Fields 6 and 7 were sampled, which represented a total of 60 sampling points including the ports of multilevel monitoring wells. This round did not include the monitoring wells described in Section 3.1.3 which had not yet been installed. In August 2005 and January 2006, the monitoring wells installed at the recharge stations, other wells across the study site and selected wells in the woodlot were sampled. These sampling events included 38 and 27 sampling points, respectively.

Well sampling protocols were as follows. The static water level in each well was measured immediately prior to purging three well volumes. Groundwater samples were then pumped through 100μm and 0.45μm filters into 200 mL bottles. Wells in which the static water level was within 8 metres of ground surface were purged with a peristaltic or gas-powered centrifugal pump, and sampled with a peristaltic pump. Deeper wells were purged and sampled using

dedicated Waterra tubing with a foot valve, except for monitoring well WO28D which was purged and sampled using a submersible pump (Grundfos Rediflow 2 submersible pump, Model 1A107603). The samples were refrigerated until submission to one of two certified analytical laboratories (Maxxam Analytics Inc. and Enviro-Test Laboratories) where they were analyzed for nitrate.

3.3. Geologic Core Analysis

Geologic core samples collected during neutron access tube and monitoring well installation between February and May 2005 were analyzed in the laboratory for moisture content and nitrate content, while geologic samples collected in November 2005 and May 2006 were analyzed for moisture content, nitrate and bromide content.

Each core was opened and immediately sampled for moisture content analysis at intervals ranging from 0.10 to 0.30 m. A moist sample was extracted from the core, weighed, oven-dried at 110°C for 24 hours and reweighed (ASTM, 2005). The mass of the soil samples varied between 15 and 300 g, depending on grain size and the diameter of the core tube from which they were extracted. Gravimetric moisture content (θ_g) was calculated from

$$\theta_g = \frac{W_w}{W_s} \tag{3.1}$$

where W_w is the mass of water in the soil sample, and W_s is the mass of the solid particles in the soil sample. Volumetric moisture content (VWC; θ_v) was determined based on sample volume:

$$\theta_v = \frac{V_w}{V} = \frac{\left(\frac{W_w}{\rho_w}\right)}{A_{core} \cdot l_s} \tag{3.2}$$

where V is the volume of the sample, V_w is the volume of the water in the sample, ρ_w is the density of water, assumed to be 1 g/cm^3, A_{core} is the cross-sectional area of the core tube, and l_s is the length of the soil sample. Soil bulk density (ρ_b) was also calculated for soil samples as

$$\rho_b = \frac{W_s}{V} \tag{3.3}$$

At times, particularly when handling cores containing loose, coarse-grained material, cutting the core tube lengthwise and opening it to remove samples caused some material to fall out of the

tube. VWC and ρ_b could not be determined for samples from which material was lost since the exact sample volume was unknown.

Bulk soil nitrate analysis of selected oven-dried samples weighing 5 g was performed by the University of Guelph Laboratory Services using a colorimetric method as described in Tel and Heseltine (1990). Bulk soil bromide analysis of samples collected in November 2005 was performed by Enviro-Test Laboratories (ETL) in Waterloo. In this analysis, 5 g of soil were tumbled or shaken in 50 ml of Ultra-pure water for 30 minutes, after which the soil was centrifuged or settled out of solution. The supernatant was decanted, filtered and analyzed on an ICS 2000 ion chromatograph with AS18 and AG18 columns using a KOH eluent. For the May 2006 soil samples, bulk soil bromide analysis was conducted at the University of Waterloo with a method similar to the ETL method: soil samples (5 g) were mixed end-over-end in 50 ml of deionized water for 18 hours, and settled or centrifuged. The extract solution was analyzed using a Dionex ICS 3000 ion chromatograph equipped with a Dionex Ionpac AS 4 x 250 mm analytical column and a KOH eluent.

Assuming no sorption of the ions to the soil matrix, aqueous nitrate and bromide concentrations in the porewater of each sample were calculated from the bulk soil concentration (C_{soil}), the gravimetric water content and an assumed water density of 1 g/cm^3:

$$C_{aq} = \frac{C_{soil}}{\theta_g} \rho_w \tag{3.4}$$

Detailed stratigraphic logging based on the Unified Soil Classification System (ASTM, 2006) was completed on all cores. Complete stratigraphic logs of the first 3 to 6 m of the subsurface were required for the proper interpretation of soil nitrate, bromide and water content profiles, and for stratigraphic input to the unsaturated zone models. However, at times geologic conditions did not permit complete core recovery, such that portions of a borehole's stratigraphy were unknown, and the location of a soil sample in the core tube may have shifted and not represented its true depth in the subsurface. To determine the true depth of the soil samples and generate a complete shallow stratigraphic log for each recharge station, it was necessary to combine all available data for interpretation. A detailed analysis of all geologic logs, gravimetric moisture content and neutron moisture probe measurements was conducted for each of the eight recharge stations. Where geologic core was missing from a core tube and the

collected core had potentially shifted in the tube, other borehole logs from the same station, drilling notes and sharp variations in the neutron probe soil water content profile were used to estimate the true location of the core pieces in the tube. In this way, the true depth of the soil samples was determined and a complete shallow log ("composite log") was produced for each recharge station. These composite logs generally reached as deep as the neutron access tubes installed in February 2005 and therefore did not extend to the water table.

Finally, a profile of the cumulative stored nitrate mass along each core was derived. As further described in Section 3.6.1, the shallowest 0.5 m of the subsurface was excluded from calculations related to nitrate concentration and stored mass in order to reduce the effect of seasonal nitrate fluctuations. The cumulative (from 0.5 m) stored mass at given point *j* in the profile was defined as

$$M_{cum,j} = \sum_{i=1}^{j} \left[C_{soil,i} \cdot d_i \cdot \rho_{b,ave} \right] \tag{3.5}$$

where $C_{soil,i}$ and d_i are the soil nitrate concentration of a soil sample and the depth interval represented by the sample; $\rho_{b,ave}$ is the average bulk soil density of samples from across the site; and 1 through *j* are sampling points between 0.5 m depth and the point *j*.

3.4. Recharge Estimation

The following sections outline the analytical methods employed to estimate groundwater recharge from the collected field data. Recharge was estimated for a one-year period in which most field data were collected ("recharge measurement period"; May 1, 2005 to May 1, 2006).

3.4.1. Tracer Velocity Method

The tracer-based recharge rate may be estimated as the product of the tracer's vertical velocity (v) and the average volumetric water content ($\theta_{v,ave}$) in the zone of migration, as represented by

$$R_{tracer} = v\theta_{v,ave} = \frac{\Delta z_{tr}}{\Delta t}\theta_{v,ave} \tag{3.6}$$

where Δz_{tr} and Δt represent the distance traveled by the centre of mass or peak concentration of a tracer applied at ground surface, and the time of travel (Scanlon et al., 2002). Tracers at this

site included both the nitrate previously applied as fertilizer, and the bromide applied to the surface in July 2005 (Section 3.1.6). In the case of a controlled tracer application, such as bromide in this study, the tracer velocity is calculated from the depth of the tracer pulse centre of mass and the time since application, or from the time elapsed and the distance traveled by the centre of mass between two sampling events. For tracers such as nitrate, with repeated applications over several years and unknown application dates, two or more vertical concentration profiles must be compared in order to identify the same peak in both profiles and hence determine the peak velocity. It should be noted that while bromide is a conservative tracer, nitrate may be subject to transformation processes that may affect its concentration in the subsurface (Section 2.1).

For a given sampling event, the bromide tracer pulse centre of mass was calculated from

$$z_{centre} = \frac{\sum_{i=1}^{n} C_{soil,i} l_i z_i}{\sum_{i=1}^{n} C_{soil,i} l_i} \tag{3.7}$$

where $C_{soil,i}$ is the bulk soil bromide concentration (mg Br/kg soil) of a geologic core sample, l_i is the length of core represented by $C_{soil,i}$, z_i is the depth of the core sample, and n is the number of samples within a profile. The value of $\theta_{v,ave}$ within the zone of migration was determined from neutron probe data collected during the period of tracer migration. For movement in the upper 0.3 m of the soil profile where neutron probe measurements are unreliable, laboratory-measured water content values from the geologic cores were used to calculate $\theta_{v,ave}$. To derive likely upper and lower bounds on the recharge estimate, the standard deviation of all soil water content measurements within the spatial and temporal intervals of tracer migration was determined and used to derive a range of soil water content and therefore a range of recharge estimates.

A mass balance of the bromide tracer was completed by expanding the bromide concentration profile of the geologic core to the entire tracer application area. The total bromide mass M_{Br} at a recharge station during a given coring event was calculated from

$$M_{Br} = \left(\sum_{i=1}^{n} C_{soil,i} l_i \right) \rho_{b,ave} A_{Br} \tag{3.8}$$

where $\rho_{b,ave}$ is the average soil bulk density of samples across the site (3.3), and A_{Br} is the area of the bromide tracer application. This approach assumes a uniform bromide distribution below the tracer application area and no lateral transport of the tracer beyond the application area.

3.4.2. Zero-Flux Plane Method

The zero-flux plane (ZFP) method estimates groundwater recharge as the change in soil water storage below the plane of zero vertical hydraulic gradient. All water flow above this ZFP is upward due to evapotranspiration, and below the ZFP flow is downward due to drainage, constituting recharge. The depth of the ZFP changes through the year as water uptake by plants varies, and is generally determined from soil matric potential measurements (Scanlon et al., 2002). In the absence of these measurements, the ZFP or ET/drainage boundary has also been estimated from the observed plant root depth (Delin et al., 2000). In the case where the depth of the ET/drainage boundary varies between the successive soil water storage measurements, it has been suggested to use the average depth in the calculations (Román et al., 1996).

In this study, the depth of the ET/drainage boundary at each recharge station was estimated using root depth as a guide. The following values were estimated using the methods described by Allen et al. (1998) for the determination of crop evapotranspiration: the maximum root depth of the crop at the station ($z_{r\text{-}max}$); one-half of the maximum root depth ($z_{r\text{-}half}$); and the times during plant growth when these two depths were attained. For the time period from the development of $z_{r\text{-}half}$ until crop harvest, the ET/drainage boundary depth was approximated as $z_{r\text{-}max}$. For the rest of the year including winter months, the boundary depth was approximated as $z_{r\text{-}half}$ to reflect reduced crop uptake (or crop removal) with the continued effect of evaporation.

The soil water stored in a profile at a given time is expressed as

$$SWS = \sum_{i=1}^{n} \left(\theta_{v,i} d_i \right) \tag{3.9}$$

where SWS is the soil water stored between the ET/drainage boundary and the bottom of the profile, $\theta_{v,i}$ is the volumetric water content at measurement point i, d_i is the vertical interval represented by $\theta_{v,i}$, $\theta_{v,1}$ is the first VWC measurement below the ET/drainage boundary and $\theta_{v,n}$ is the deepest VWC measurement from the neutron probe in the profile. The effective profile length considered in the method is the interval covered by the neutron access tube.

The magnitude of recharge is based on the difference between high and low soil water storage values observed throughout the measurement period. A "high" SWS value is preceded and followed in time by lower SWS values, and a "low" SWS value by higher ones, and therefore there may be several relative highs and lows during the measurement period as the soil water content fluctuates. One recharge event is defined as the decrease from a high SWS value to a low one. In this context, a recharge event begins when water infiltrates into the unsaturated zone and drives up the water content, continues as the water content decreases, and ends when the water content begins to increase again due to infiltration from the surface which initiates another recharge event. The total recharge determined from the ZFP method is the sum of the recharge amounts from the individual events; that is

$$R_{ZFP} = \sum_{i=1}^{m} \left(SWS_{i,high} - SWS_{i,low} \right) \tag{3.10}$$

where SWS_{high} and SWS_{low} represent a high SWS and the subsequent low SWS to which the geologic material drains before increasing in water content again; and 1 through m represent the pairs of high and low values observed during the measurement period.

As mentioned above, the SWS value calculated in (3.9) represents only the soil water stored over the depth of water content measurement (i.e., the neutron probe access tube depth), which may not represent the entire unsaturated zone. As a result, in this study the ZFP method may have underestimated the magnitude of recharge since it did not capture the water content loss below the instrumented depth.

3.4.3. Water Balance

A basic water balance equates water inputs (precipitation, irrigation and run-on) on a given surface to water outputs (evapotranspiration, run-off and infiltration). The measurement of precipitation and the estimation of evapotranspiration (ET) using empirical methods allow the estimation of surplus water (i.e., the total of run-off and recharge) at a site.

3.4.3.1. Evapotranspiration Calculation

ET was estimated using a method described by the Food and Agriculture Organization of the United Nations (Allen et al., 1998). A daily reference ET value (ET_o), corresponding to the anticipated ET for a standard grass crop under optimal agronomic conditions, was calculated using many of climatic parameters measured at the site meteorological station including solar radiation, soil heat flux, air temperature, wind speed, relative humidity and atmospheric pressure. To determine the actual ET from the fields under their particular crops and growing conditions, calculations were performed to estimate the daily adjusted ET values for each of the crop types grown across the study site in 2005 and 2006, incorporating estimated crop growth, precipitation and the potential development of soil water stress conditions (see Appendix C).

The evapotranspiration was calculated with the dual crop coefficient method with the soil water stress adjustment, in which ET_o is multiplied by a factor combining three coefficients that reflect local agronomic conditions: $(K_s K_{cb} + K_e)$. K_{cb} is the basal crop coefficient representing primarily the transpiration portion of ET, K_s is the soil water stress coefficient and K_e is the soil evaporation coefficient. K_{cb} varies through the stages of crop growth which are defined as the initial, development, mid-season and late season stages. K_s and K_e also vary during the year and are primarily affected by root zone water depletion and the fraction of soil not covered by plants. The complexity involved in the assignment of K_{cb} values and the calculation of ET in non-growing periods was further complicated by the variable meteorological conditions experienced during the study; therefore the assumptions applied in the calculation of ET in each period of the year are described in more detail below.

Growing periods: For each crop type, the length of growth stages, their associated K_{cb} values and other required data including crop height and root depth were based on recommended

values (Allen et al., 1998). For the oat and grass crops planted together on Fields 3b and 7 in 2005, these input parameters were similar. Consequently for the period in which the oats and grass were growing together, the parameters for oats were applied. At the onset of the late season stage for the oats, however, the usual decrease in K_{cb} was omitted and the K_{cb} was maintained at the mid-season level for grass to reflect the continued growth of the grass after the oat harvest. Because the grass was kept on the fields until the end of the study period, the ET parameters for the grass crop were maintained on Fields 3b and 7, with the exception of the frozen winter period described below. On the Old Stage Road field, winter wheat was planted almost immediately after the soybean harvest. The growth parameters for each crop were incorporated in the ET calculations during the appropriate period. The K_{cb} was multiplied by the soil water stress coefficient (K_s) to reflect potential conditions in which the soil is dry and soil water has a low potential energy and is less easily extracted by the crop.

Bare soil: Between the start of the recharge measurement period and planting, all fields except Field 2 were bare. For bare fields, ET was approximated using the dual crop coefficient method with the basal crop coefficient (K_{cb}) set to zero (Allen et al., 1998).

Surface covered with dead vegetation: Fields 4, 5 and 6 were covered in plant residue following corn harvest in early November. For these conditions, ET was calculated using the adjustments recommended by Allen et al. (1998). The value of total evaporable water (TEW) was reduced by 30% to reflect an estimated 60% soil cover from residue.

Frozen or snow-covered surfaces: The estimation of ET from frozen or snow-covered surfaces is more difficult than for growing or above-freezing conditions. The use of ET_o is of limited value due to the violation of the assumption of a sustained grass reference crop (Allen et al., 1998), and the potential for ET depends on the varying degrees of soil freezing and snow cover. For these conditions, an average daily ET value of 1 mm/day was used as suggested by Allen et al. (1998). In this study, the period corresponding to frozen or snow-covered conditions was assumed to be period in which average air temperatures were below zero degrees Celsius.

3.4.3.2. Water Balance Calculation

The other main water balance components anticipated at the recharge stations are precipitation and recharge. Run-off was infrequently observed across the study site and was not measured or monitored during this study. The water balance for each station was completed by subtracting the adjusted ET value from the measured precipitation (P), where each term is the sum of daily values during the study period. The result represents the surplus water available at each station for either run-off or recharge. Since the magnitude of run-off is unknown, the surplus water value represents an upper bound on the potential recharge at each recharge station as expressed by

$$R_{water\ balance} < Surplus\ water = P - ET \tag{3.11}$$

3.5. One-dimensional Unsaturated Zone Modelling

The aim of modelling in this study was: to gain an additional estimate of recharge and nitrate mass flux at each station based on meteorological, agricultural and hydrogeological input parameters; to better understand the controls on recharge and mass load across the study site; and to evaluate the suitability of commonly applied water balance models for the estimation of recharge and mass load. Two models were used: Simultaneous Heat and Water model (SHAW, version 2.4; Flerchinger, 2000a) and the Hydrologic Evaluation of Landfill Performance (HELP; Schroeder et al., 1994) model within the Waterloo Hydrogeologic, Inc. Unsat Suite (version 2.2). The models were used to estimate groundwater recharge during the recharge measurement period.

3.5.1. Model Description

The SHAW model incorporates the effects of plant cover, dead plant residue and snow in order to simultaneously solve the heat, water and solute balance equations in a one-dimensional profile. The model can also account for soil freezing and thawing, snow accumulation and a multi-plant canopy (Flerchinger, 2000a). Unlike many other one-dimensional water balance models which calculate potential evapotranspiration, the SHAW model solves the energy budget equation to simulate actual evaporation (Scanlon et al., 2002). Infiltration of rainfall, snowmelt and ponded water into the soil is calculated using a Green-Ampt approach, while unsaturated

flow through the soil is determined by Richards' equation. The relationship between soil water content and soil water potential is (Brooks and Corey, 1966; Campbell, 1974, 1985)

$$\psi = \psi_e \left(\frac{\theta_v}{\theta_s} \right)^{-b} \tag{3.12}$$

where ψ is potential (m), ψ_e is air entry potential (m), θ_v is volumetric water content (m^3/m^3), θ_s is saturated water content (m^3/m^3), and b is a pore size distribution parameter.

Unsaturated hydraulic conductivity is represented by the Burdine function (Burdine, 1953), given as

$$K = K_s \left(\frac{\theta_v}{\theta_s} \right)^{(2b+3)} \tag{3.13}$$

where K and K_s are unsaturated and saturated hydraulic conductivity respectively.

The HELP model is a quasi-two-dimensional hydrologic model created for the evaluation of landfill hydrologic processes. It is often applied to estimate groundwater recharge in various other settings (Padusenko, 2001; Jyrkama et al., 2002; Gogolev, 2002). In the model, a surface water balance is used to indirectly determine the infiltration to the unsaturated zone, soil water in the evaporative zone is removed by evapotranspiration, and a storage-routing method is used to redistribute soil water within the profile. The model assumes unsaturated flow is Darcian and gravity-driven only, and unsaturated water retention and hydraulic conductivity are expressed by the Brooks-Corey and Campbell functions respectively (Schroder et al., 1994). The HELP model runs in one-year intervals only.

3.5.2. Input Data

3.5.2.1. Soil Properties

To use field measurements of soil water content for both of these models, the vertical profile simulated at each recharge station was chosen to be the depth of the 5-cm diameter neutron access tube installed at that station. Consequently the simulated profiles did not generally reach the water table. The model input describing the geologic layers was created based on the composite stratigraphic logs described in Section 3.3.

Input data for soil properties was generated from the results of Wendt (2005) who conducted laboratory investigations of the grain size and hydraulic properties of various soil types collected from the study site. These tests included sieve and hydrometer analyses for grain size distribution, permeameter tests for saturated hydraulic conductivity, and tempe cell analyses for soil water retention. Tempe cell results were used as input to the Retention Curve program (RETC; van Genuchten et al., 1991) to generate the water retention and unsaturated hydraulic conductivity parameters for both the Brooks-Corey and van Genuchten functions. Disturbed soil samples were used for the permeameter and tempe cell tests and the determination of bulk density, except when undisturbed core samples were available for bulk density analysis as described in Section 3.3.

The results of the grain size analysis were also entered into a subprogram of the Soil-Plant-Air-Water (SPAW) model (Saxton, 2002) that determines soil hydraulic characteristics. This subprogram generated independent estimates of hydraulic conductivity and bulk density based on soil texture. It also generated soil water potential values at various water contents, and the Brooks-Corey and van Genuchten parameters that best fit these data were determined by curve-matching. The initial estimate of soil hydraulic properties was based on the laboratory results which were compared to SPAW-generated values and literature values to identify any potentially anomalous laboratory measurements. Laboratory data was limited for the soils in the upper 50 to 60 cm at each station due to difficulties in both field collection and re-packing of samples in the laboratory. For these shallow soils, hydraulic properties were estimated with the SPAW subprogram using soil textures described in published soil maps (Wicklund and Richards, 1961) and estimated bulk density.

SHAW - The unsaturated zone profiles were generally created using the maximum of fifty nodes permitted by the SHAW model. Node spacing was decreased at the upper and lower boundaries and layer interfaces. Soil layers ranging in thickness from 0.1 to 3.0 m were created and assigned properties including porosity, bulk density, saturated hydraulic conductivity (K_s), and the b and ψ coefficients for the water retention function.

HELP – Each distinct geologic layer in the profile was designated as a vertical percolation layer, a material type in which unsaturated flow is downward due to gravity drainage controlled by soil hydraulic parameters and soil water content and upward flux due to ET is modeled as an extraction (Schroder et al., 1994). These layers were assigned porosity, saturated hydraulic conductivity and soil water retention parameters. The required soil water retention input data were the field capacity and wilting point, corresponding to the volumetric water content at 1/3 bars and 15 bars, respectively. These values were calculated using the van Genuchten parameters generated by RETC.

3.5.2.2. Weather Data

Daily meteorological data that were input directly from the weather station data files to the model included precipitation, temperature, total wind run (wind speed multiplied by elapsed time) and solar radiation measured during the study period. To simulate field conditions until the end of the recharge measurement period in May 2006, while satisfying the HELP model's requirements for year-long data sets, a simulation period of two full years (2005 and 2006) was used. Since weather data from June to December 2006 were not available, the weather data from June to December 2005 were used as "dummy data" to represent this period. The simulated results for June to December 2006 were ignored and the use of artificial data for that period was not expected to affect the results for the preceding time period. The HELP program includes a weather generator that produces synthetic weather data based on climate normals from regional measurement points; however, these data were only used in the sensitivity analysis described in Section 3.5.2.7.

3.5.2.3. Soil Water Content Data

The SHAW model requires an initial water content profile, while the lower boundary condition for water flux is either a unit hydraulic gradient or user-specified soil water content. In this study, the lower boundary condition of user-specified water content was selected to make use of field data. For each station, four to six water content profiles including the initial and final profiles were generated from the neutron probe water content data. Water content at each node was linearly interpolated from the neutron probe data at adjacent measuring points. Neutron probe measurements between ground surface and approximately 0.3 m were not considered reliable due to the possibility of neutron escape to the atmosphere, and therefore shallow model

nodes between zero and 0.3 m depth were assigned the value of the first measurement below 0.3 m. The specified water content at the lower boundary condition was determined by linear interpolation between the various water content profiles.

The HELP model allows the input of user-specified initial water contents for each layer, or it will simulate field processes for one year and then use the final water content profile in that simulation as input for the actual simulation. In order to compare the relative effects of these two options, separate simulations using each of the options for initial soil water content were performed. For the user-specified initial water content, the water content profile from December 21, 2005 was assumed to best represent field conditions on January 1, 2005 given the proximity of these dates in the annual cycle.

3.5.2.4. Soil Temperature Data

An initial soil temperature profile is required by the SHAW model. The lower boundary condition for temperature may either be user-specified or estimated by the model. For this study, the former option was used. Soil temperature input data was generated from the HOBO soil temperature sensors in most cases, and the soil temperature sensors connected to the meteorological station data logger were used for all stations when the HOBO sensor data were unavailable. Since the available soil temperature field data did not generally reach the bottom of the simulated profile, the deeper data was estimated by fitting a third-order polynomial curve to the upper data with all points below 4 m set to a constant temperature throughout the year. This constant temperature is 7.5 degrees C, equivalent to the average annual temperature (Flerchinger, 2000a). Soil temperature data is not required for the HELP model.

3.5.2.5. Crop Data

The data related to plant water uptake required by the SHAW model were numerous and are listed in detail in Appendix D. Where a default standard value was suggested by the user's manual (Flerchinger, 2000b) it was generally used (e.g., for stomatal, leaf and root resistance). Plant growth was accounted for in a separate input file, in which values for plant height, root depth, leaf dimension, dry biomass and leaf area index (LAI) for days throughout the growing season were estimated based on the literature and field observations. A separate plant growth file was required for each of the three crop types planted at the site in 2005: corn, soybean and

oats. Although the oats were intercropped with grass, published data (see Appendix D) suggested that the growth parameters (including LAI and root depth) of the oats and grass were sufficiently similar to represent the entire crop as oats. The growing period of the oat crop was extended beyond the oat harvest date to account for the continued presence of grass on the Fields 3b and 7.

Curves describing LAI evolution in time were taken from the literature, whereas height and root depth data were taken from evapotranspiration calculations (Section 3.4.3.1). For leaf dimension and dry biomass evolution, the shape of the curve was assumed to match the curves for height and root depth, with maximum values found in the literature.

Input data requirements for HELP related to crop growth were limited to start and end dates, evaporative zone depth and maximum LAI. These parameters were based on the more detailed data prepared for the SHAW model.

3.5.2.6. Calibration and Simulations

The SHAW model was used to simulate actual field conditions from the date of the first available soil water content profile at each station, ranging between March 10, 2005 at most stations and May 6, 2005 at Station 7, until the final water content measurement on May 25, 2006. Simulated soil water content profiles were compared to field-measured (neutron moisture probe) profiles from selected dates, and soil hydraulic properties (K_s, b and ψ) were adjusted within reasonable limits in order to better match the profiles. After this calibration exercise, a final simulation was performed and the simulated water balance components (evapotranspiration, run-off and recharge) were calculated. It should be noted that the SHAW model is often used in the absence of field water content data (Fallow et al., 2003), and calibrations of the type described above have not been found in the literature.

The HELP model was used to simulate field conditions between January 2005 and December 2006. The first simulations with the HELP model used a model-estimated initial soil water content. The only simulated water content profile provided by the model was the final one; therefore to allow calibration to a measured profile, the model was first run for 2005 only and the final profile (representing December 31, 2005) was compared to the December 21, 2005

field profile. Soil hydraulic properties (K_s, field capacity and wilting point) were adjusted to generate a better fit between the simulated and field data. The model was then run for 2005 and 2006 using the calibrated parameters.

The refined soil hydraulic properties were then also used in simulations with a user-specified initial soil water content profile as described in Section 3.5.2.3. The final 2005 water content profile under these conditions was compared to the December 2005 field data.

3.5.2.7. Sensitivity Analyses

Basic sensitivity analyses were also performed on simulations using both models at selected recharge stations. Stations 4 and 6 were selected for this sensitivity analysis because they represented different geologic and 2005 crop conditions. The sensitivity analyses were completed for the recharge measurement period from May 2005 to May 2006. Within the SHAW model, the effects of variations in both soil hydraulic properties and crop growth on the magnitude of recharge were evaluated. The influence on recharge of the saturated hydraulic conductivity (K_s) values was tested by increasing and decreasing by one order of magnitude first the K_s of the topsoil layers only and then of all of the geologic materials in the profile. The pore size distribution index (b) and air entry potential (ψ_e) were then increased and decreased by 1 and 0.1 m, respectively. The use of a unit gradient lower boundary condition was also evaluated for its effect on the water balance. Crop growth parameters were varied by increasing or decreasing the growing period by 30 days with a respective unit increase or decrease in leaf area index.

A similar sensitivity analysis of soil hydraulic properties and crop growth parameters was completed for the HELP model. The hydraulic conductivities of both the topsoil layers and then the entire profile were increased and decreased by one order of magnitude. Crop growth parameters were varied as described for the SHAW model. These changes were incorporated into model runs using the option of model-estimated initial soil water content. Also evaluated was the HELP model's method for estimating the initial water content profile, which is to simulate a one-year test period using the weather data from the first year of simulation, and then use the water content at the end of the test year as the initial water content in the actual simulation. The effect of using the first year's (2005) data in both the initial VWC estimation

and the actual simulation was evaluated by obtaining from the HELP program's synthetic weather generator one year of synthetic data appropriate for the study site. Rather than the 2005-2006 runs described earlier, HELP was run for the years 2004 to 2006 with the synthetic data used as 2004 data. In this way, the model applied the 2004 and not 2005 data to generate the initial estimated soil water content profile. Data from the recharge measurement period in 2005 and 2006 were then extracted.

3.6. Porewater Nitrate Concentration Estimation

In addition to the recharge rate, the porewater nitrate concentration was required to determine nitrate mass flux and ultimately nitrate mass load. To allow a comparison of the nitrate mass load before and after the BMP implementation (i.e., the reduction in nutrient application), the average porewater nitrate concentration was determined for both the BMP-affected (post-BMP) zone and the deeper, pre-BMP zone in all cores from all recharge stations. The approach for determining the maximum depth of potential BMP impacts is described below, followed by the calculations for porewater concentration.

3.6.1. Extent of BMP Effects

It was assumed that water recharging through the unsaturated zone below Parcel B after BMP implementation would potentially have a reduced nitrate concentration due to the decrease in nitrogen fertilizer applied at the surface. This recharge water, henceforth referred to as "BMP recharge water" to reflect the potential effect of the BMP on its nitrate concentration, was also assumed to be capable of displacing existing nitrate-laden porewater downward toward the water table. Therefore, at a given time and a given recharge station, the subsurface would be bisected at the depth attained by the earliest BMP water to infiltrate, i.e., at the maximum post-BMP depth, $d_{max,BMP}$ (Figure 3.2). The average post-BMP porewater nitrate concentration above this depth was anticipated to be lower than the average pre-BMP concentration below this depth. The successive geologic cores extracted at one recharge station would each have a distinct and increasing value of $d_{max,,BMP}$, depending on the station's recharge rate. Having multiple cores at one station would allow trends in the average post-BMP concentration to be monitored, and provide several estimates of the average pre-BMP porewater concentration.

For each recharge station, the annual recharge rate (R) anticipated to best represent conditions at the station was derived from the various recharge estimation methods described in Section 3.4 and the simulation models in Section 3.5. Using this recharge estimate, $d_{max,BMP}$ at the time of each coring event at the station could be estimated, assuming piston flow of the water and not including dispersion. An initial estimate of $d_{max,BMP}$ was made, and the annual average volumetric water content over this estimated depth ($\theta_{v,ave\text{-}BMP}$) was derived from neutron probe moisture content data for one year of measurement. The distance travelled by the BMP recharge water was then calculated from

$$d_{\max,BMP} = \frac{R \cdot t}{\theta_{v,ave-BMP}} \tag{3.14}$$

where t is time between BMP implementation, estimated as April 1, 2003, and the coring event. This new estimate of $d_{max,BMP}$ would then correspond to a new $\theta_{v,ave\text{-}BMP}$, which would be again applied in (3.14). The calculation was repeated in an iterative manner until the estimate of $d_{max,BMP}$ was unchanged within 0.05 m. This depth represented the lower bound of the unsaturated zone most likely to have been affected by the infiltration of BMP recharge water.

The upper bound of the post-BMP zone was, in theory, the ground surface. Incorporating the root zone in the nitrate mass calculation, however, would allow seasonal variation in crop uptake to skew estimates of nitrate mass load. For example, an elevated nitrate value at 0.20 m depth measured in a May 2006 core may not have necessarily represented an eventual nitrate mass load to the groundwater, since a crop growing at the core location might have removed a significant amount of the nitrogen before it leached downward past the root zone. To minimize the effect of seasonal nitrate variation and ensure that the mass load calculations reflected only the nitrogen that might be expected to reach the groundwater, the upper 0.5 m of the unsaturated zone was not included in the calculations of average porewater nitrate concentration and mass load. This depth represented approximately the shallowest effective rooting depth among the crops in rotation across the study site (Allen et al., 1998).

3.6.2. Concentration Calculations

The average concentration in a pre- or post-BMP segment of the unsaturated zone was based on a weighted average soil nitrate concentration and the average gravimetric soil water content.

A unit area (1 m^2) was used for ease of calculation. As described in Section 3.3, geologic cores were sampled at 0.1 to 0.3 m intervals and submitted for nitrate analysis. The distance-weighted average soil nitrate concentration from the post-BMP zone of a core was estimated from:

$$C_{soil,ave} = \frac{\sum_{i=1}^{n} C_{soil,i} \cdot l_i}{\sum_{i=1}^{n} l_i} \tag{3.15}$$

where $C_{soil,i}$ is the soil nitrate concentration in a geologic core sample, l_i is the vertical core interval corresponding to the $C_{soil,i}$ sample, and 1 through n represent core samples within the upper and lower bounds of the post-BMP unsaturated interval as defined in Section 3.6.1. For the deeper, pre-BMP section of a core, 1 through n represent core samples between the depth of BMP effects ($d_{max,BMP}$) and the bottom of the core.

The average annual gravimetric water content ($\theta_{g,ave}$) within either the post-BMP or pre-BMP zone was determined from volumetric water content measurements in the zone from the neutron moisture probe, and the average soil bulk density (ρ_b) from samples across the study site as expressed by:

$$\theta_{g,ave} = \frac{\theta_{v,ave}\,\rho_w}{\rho_b} \tag{3.16}$$

When the depth of the post-BMP zone exceeded the depth of available soil water content measurements, the average water content along the entire depth of neutron probe measurement (below 0.5 m) was applied as $\theta_{g,ave}$ for this zone. Similarly, the average water content between $d_{max,BMP}$ and the deepest neutron probe measurement was assumed to adequately represent $\theta_{v,ave}$ in the pre-BMP zone. If $d_{max,BMP}$ exceeded the depth of water content measurements, $\theta_{v,ave}$ within the range of neutron probe measurements was used as $\theta_{v,ave}$ in the pre-BMP zone.

Finally, the average porewater nitrate concentration $C_{aq,ave}$ in the post- or pre-BMP zone was determined as:

$$C_{aq,ave} = \frac{C_{soil,ave}}{\theta_{g,ave}}\,\rho_w \tag{3.17}$$

It should be noted that porewater nitrate concentrations might also have been computed from individual core samples' soil nitrate concentration and soil water content, and then averaged over the length of the core. This method, however, would have been susceptible to the influence of erroneously low water content values measured in the laboratory, which could have artificially increased both the sample and average porewater nitrate concentration by a significant amount. In order to avoid the influence of artificial spikes in the water content data, the average annual water content values from the neutron moisture probe were used.

3.7. Nitrate Mass Flux Estimation

The next step in the calculation of unsaturated zone nitrate mass load was to estimate nitrate mass flux at each recharge station using the groundwater recharge rate and the porewater nitrate concentration. More specifically, for each core pre-BMP and post-BMP nitrate mass flux values were estimated using the porewater concentrations from below and above the maximum depth attained by BMP recharge water ($d_{max,\ BMP}$).

3.7.1. Post-BMP Nitrate Mass Flux

Post-BMP nitrate mass flux was calculated for each recharge station for each coring event. This mass flux value represented the average rate (mass/time/area) at which nitrate was migrating through the post-BMP section of the unsaturated zone. It was assumed to also represent the average rate at which nitrate had passed through a plane corresponding to 0.5 m depth since BMP implementation. The mass flux values from cores extracted late in the study represented longer periods of time since BMP implementation, and hence a longer averaging period.

To calculate the nitrate mass flux ($Flux$) at each recharge station, the groundwater recharge rate at the station was multiplied by the average nitrate concentration in the recharging water, as follows:

$$Flux = C_{aq,ave} \cdot R \tag{3.18}$$

where $C_{aq,ave}$ is the average porewater nitrate concentration described in Section 3.6 and R is the recharge rate.

3.7.2. Pre-BMP Nitrate Mass Flux

The pre-BMP nitrate mass flux was also calculated with (3.18). Porewater nitrate concentrations were based on core samples in the vertical interval between $d_{max,\ BMP}$ and the bottom of each core. The resulting mass flux represented the nitrate migration rate through this vertical interval, as well as the assumed average mass flux into the unsaturated zone below 0.5 m depth between BMP implementation and some date before implementation. The amount of time prior to implementation represented by the pre-BMP mass flux depended on the length of core between $d_{max,\ BMP}$ and the bottom of the core.

3.8. Up-scaling to Nitrate Mass Load Values

The total nitrate mass load values were determined by extrapolating the point-scale nitrate mass flux estimates to the field scale, i.e., by multiplying mass flux by land area. The study site was subdivided into areas that were best represented by each station's recharge, porewater concentration and mass flux characteristics. Each station's represented area was then multiplied by its flux value to determine a nitrate mass load, and the individual stations' mass loads were combined to derive a total nitrate mass load across the site.

The partitioning of the study site for the assignment of different flux values was based on two principal criteria: topography and shallow geology, which were assumed to exert primary control on groundwater recharge. Cropping history was likely a major influence on the residual nitrate in the subsurface and hence the nitrate mass flux, given the varying nutrient requirements of the different crops as described in Section 2.5. However, the field-scale crop history at the study site has only been documented since the purchase by County of Oxford in 2003, which limits the possibility of subdividing the study site based on similar histories. Given the prevalence of the wheat-corn-soybean rotation in the area, it was assumed that the long-term average crop history and nitrogen application rate was relatively uniform across the site. Exceptions to this assumption are discussed in Section 4.10. Overall, topography and shallow stratigraphy were evaluated to partition the study site, with the addition of land use history where necessary.

The topographical designations (crest, slope or low) were determined from the contour map in Figure 2.2 and field observations of surface water flow. Geological characteristics were derived from the composite logs at each recharge station, as well as the additional borehole logs and stratigraphic cross-sections presented in Haslauer (2005). The soil map in Figure 2.7 was also used. Based on these data, each recharge station was assigned a description of topography and stratigraphy, and the portion of the study site with the same characteristics was defined. This area generally surrounded the recharge station but in some cases included other, more distant parts of the study site.

Table 3.1. Initial characterization of recharge stations based on data from Haslauer (2005) and field observations

Recharge Station	Field	Topography	Shallow stratigraphy
1	7	Low, flat	Sand and gravel
2	4	High, flat	Silt till
3	3a	Flat	Silt and sand
4	5	Slope	Silt till
5	3b	Low, flat	Sand and silt
6	7	Slope	Sand and gravel
7	Old Stage Rd.	Flat	Sand and gravel
8	6	Low, flat	Silt till

Table 3.2. Recharge station equipment summary

Recharge Station	Monitoring wells *(Depth in italics)*	Neutron access tubes *(Depth in italics)*	Number of ECH_2O moisture sensors	Number of HOBO temperature sensors	Surface bromide tracer
1	WO37 *(4.9 m)* WO63 *(13.7 m)*	AT13 *(3.0 m)*	6	6	Yes
2	WO60 *(35.1 m)*	AT2 *(4.3 m)* AT11 *(8.5 m)*	6 (+ 5 CSI CS616 sensors)	6 (+ 5 CSI 107B sensors)	Yes
3	WO56 *(19.8 m)*	AT4 *(5.8 m)* AT9 *(11.9 m)*	6	6	Yes
4	WO61 *(25.9 m)*	AT5 *(4.0 m)* AT14 *(9.8 m)*	6	6	Yes
5	WO58 *(29.0 m)*	AT3 *(5.8 m)* AT10 *(6.1 m)*	6	6	Yes
6	WO62 *(16.8 m)*	AT7 *(4.0 m)* AT12 *(5.2 m)*	6	6	Yes
7	WO65 *(8.2 m)*	AT15 *(5.5 m)*	6	6	Yes
8	WO35 *(6.7 m)*	AT6 *(3.8 m)*	6	6	Yes

Table 3.3. ECH_2O sensor installation depths. ECH_2O probe midpoint depth (below ground surface) is followed by temperature sensor depth (below ground surface) in italics. Blank cells indicate no sensor installed. See Appendix A for sensor locations.

Station	Depth, Sensor 1(m)	Depth, Sensor 2 (m)	Depth, Sensor 3 (m)	Depth, Sensor 4 (m)	Depth, Sensor 5(m)	Depth, Sensor 6 (m)	Depth, Sensor 7 (m)	Depth, Sensor 8 (m)
1	1.1 *0.85*	1.4 *1.15*	0.8 *0.55*	1.7 *1.45*	2.0 *1.75*	2.3 *2.05*		
2	0.8 *0.55*	1.1 *0.85*	1.4 *1.15*	1.7 *1.45*	2.1 *1.85*	2.35 *2.1*		
3	0.7 *0.45*	1.1 *0.85*	1.4 *1.15*	1.7 *1.45*	2 *1.75*	2.3 *2.05*		
4	0.8 *0.55*	1.1 *0.85*	1.4 *1.15*	install. failed	1.7 *1.45*	2.1 *1.85*	1.8 *1.55*	
5	0.7 *0.45*	1.1 *0.85*	1.35 *1.1*	1.5 *1.25*	2 *1.75*	2.3 *2.05*		
6	0.8 *0.55*	1.1 *0.85*	1.4 *1.15*	1.7 *1.45*	2 *1.75*	2.3 *2.05*		
7	0.9 *0.65*	1.1 *0.85*	install. failed	1.4 *1.15*	install. failed	1.8 *1.55*	1.6 *1.35*	2 *1.75*
8	0.7 *0.45*	1.1 *0.85*	1.4 *1.15*	1.7 *1.45*	1.7 *1.45*			

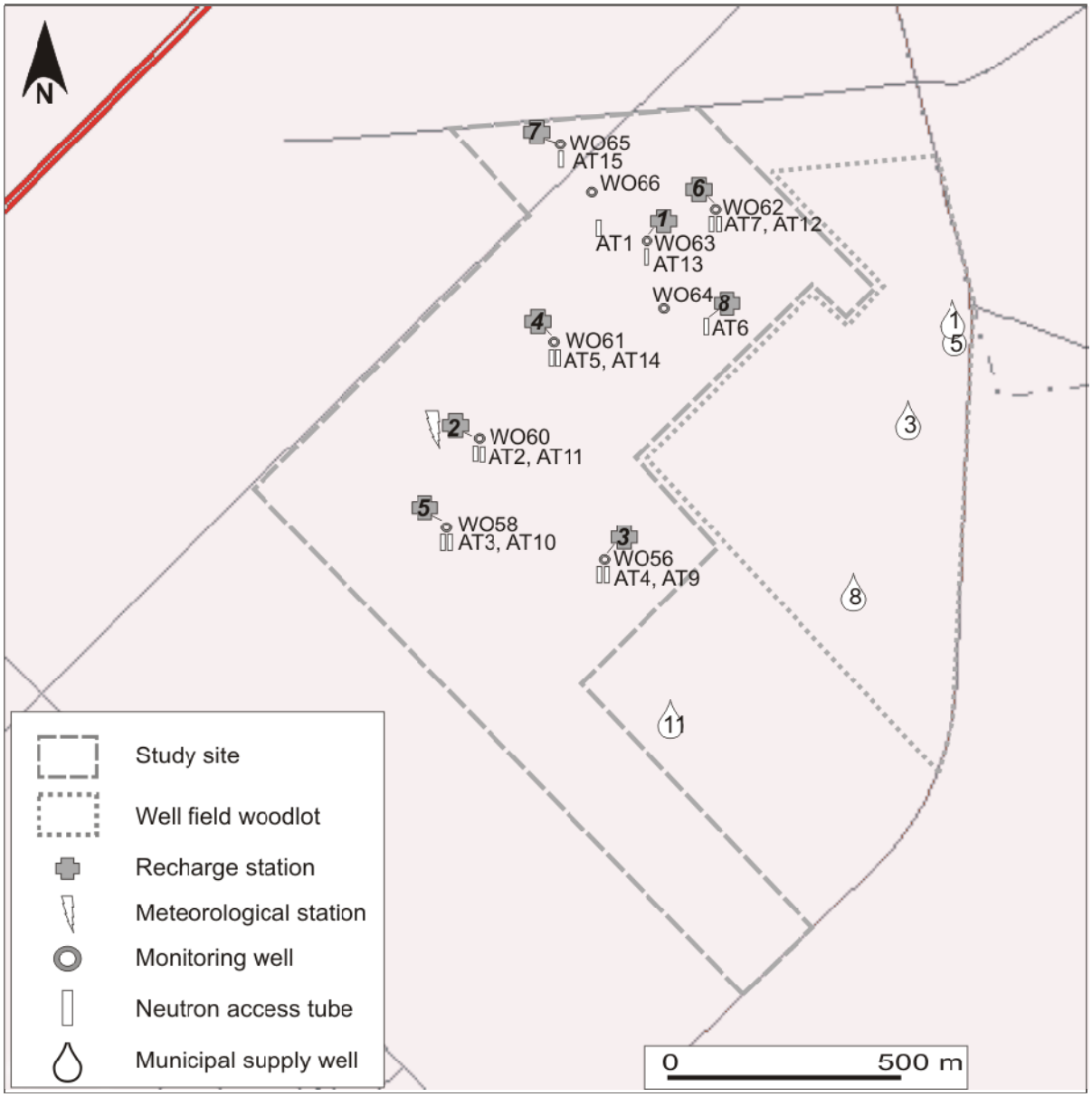

Figure 3.1. Location and components (monitoring wells and access tubes) of recharge stations and meteorological station location. Contains data from The Corporation of the County of Oxford (2003b, 2003c).

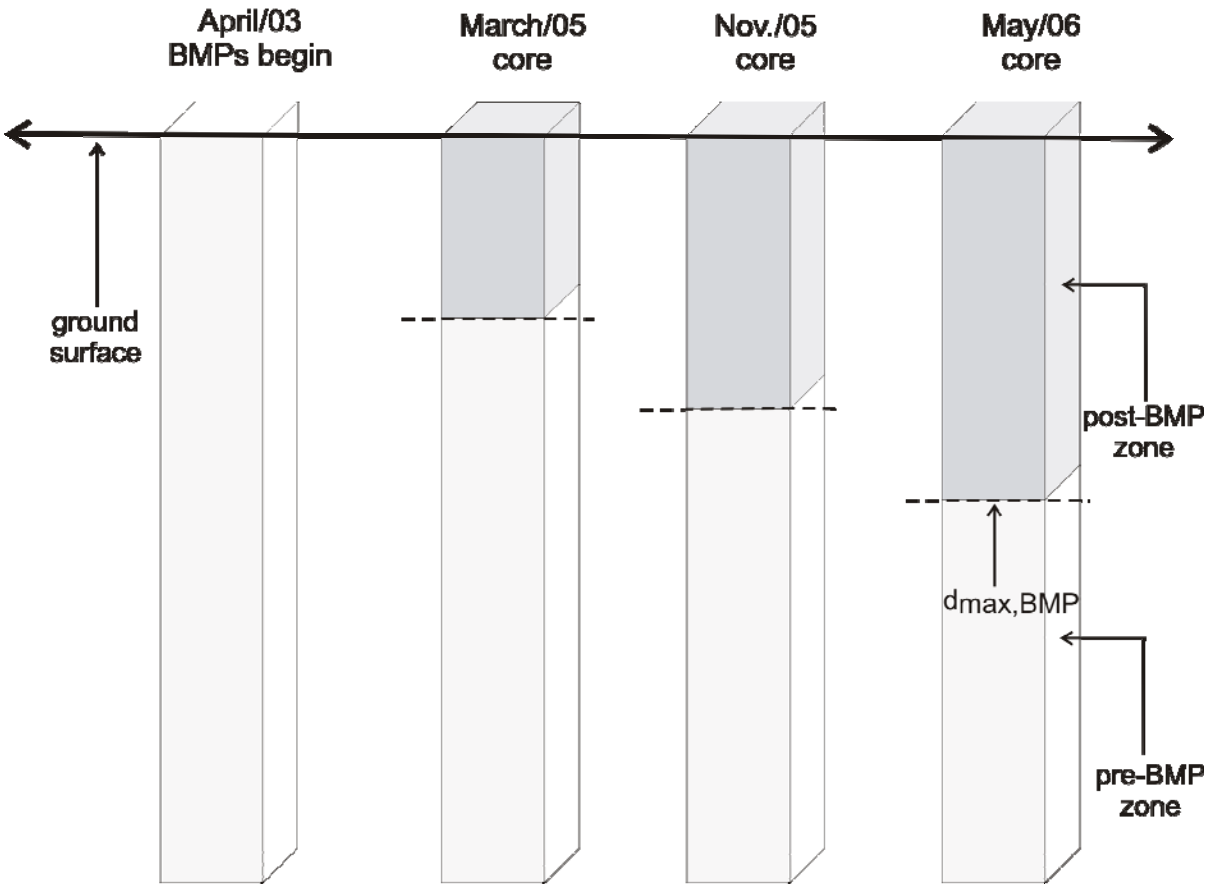

Figure 3.2. Conceptual drawing of the downward migration of the depth of anticipated BMP effects and associated pre- and post-BMP zones.

4. Results

This chapter summarizes the results of field, laboratory and computational methods used to estimate groundwater recharge, porewater nitrate concentration and nitrate mass load across the study site. Sections 4.1 to 4.5 present field data including meteorological data, recharge station stratigraphy, soil nitrate analysis, soil water content and temperature measurement and groundwater monitoring and sampling. Field data were applied in several methods for the estimation of the recharge rate, as described in Section 4.5, and in two one-dimensional unsaturated zone models (Section 4.6). Based on the results of the field and model estimates, a recharge rate range was determined for further analysis (Section 4.7). The anticipated depth of BMP impacts in the unsaturated zone was estimated from the recharge rate, and the average porewater nitrate concentrations above and below this depth corresponding to post- and pre-BMP conditions were calculated (Section 4.8). Finally, the porewater concentration and recharge rate were combined to determine the nitrate mass flux at each recharge station (Section 4.9) and these individual results scaled up to a total nitrate mass load across the study area (Section 4.10).

4.1. Meteorological data

The average daily air temperature and monthly precipitation data recorded between January 2005 and May 2006 at the meteorological station are shown on Figure 4.1. The annual precipitation and average daily temperature measured at the station in 2005 (961 mm and 8.2°C) were comparable to historical averages in Woodstock (950 mm and 7.5°C) (Environment Canada, 2006). However, the on-site measurements in the first five months of 2006 (479 mm and 3.6°C) were 30% and 140% higher than historical averages for the same five-month period (351 mm and 1.5°C) (Environment Canada, 2006), indicating a wetter and warmer start to the year than usual. Notable climatic observations during this period include the elevated monthly precipitation amounts in November 2005 and May 2006 which were 81 and 122 mm higher than historical averages (Environment Canada, 2006), and the temperature oscillations around the freezing point in January and February 2006. Additional meteorological data are included in Appendix E.

4.2. Study Site Stratigraphy and Soil Analysis

4.2.1. Study Site Stratigraphy

The shallow composite geologic logs constructed from all available borehole logs and soil water content information at each recharge station are presented in Figure 4.2. These include, where possible, the identification of aquifer and aquitard units described by Haslauer (2005) and in Section 2.7. The shallow composite logs were constructed for the upper 3 to 6 m of the subsurface to provide stratigraphic input to the various recharge estimation methods. At most stations, the unsaturated zone extended to a greater depth than shown in the composite logs. Stratigraphic data extending to the water table, which was available from the boreholes drilled in March 2005 and a limited number of boreholes from other drilling events, is described below. The original logs for boreholes drilled in February, March and November 2005 are available on request. Boreholes drilled in May 2006 were not logged due to their proximity to the November 2006 boreholes. The groundwater elevation data provided below were based on automated measurements described further in Section 4.4.

The unsaturated zone geology at the stations was generally consistent with the quaternary geology map shown in Figure 2.6. Stations 1 and 6, which lie within the glaciofluvial outwash channel shown on Figure 2.6 (see Figure 3.1 for station locations) were characterized by sand and gravel, with some silt layers at Station 6. The depth to the water table of Aquifer 2 from ground surface ranged annually from 2.2 to 3.3 m at Station 1 and from 8.9 to 10.0 m at Station 6. Station 7 is also located within the outwash channel across Curry Road from Stations 1 and 6. Its shallow stratigraphy was comprised of sand with some clay layers near ground surface. The depth to the Aquifer 2 water table ranged from 3.7 to 5.9 m at this station.

There was no new borehole drilled to the water table during this study at Station 8, which is also located in the outwash channel. The composite log at this location was based on cores reaching up to 3.8 m, and the deeper unsaturated zone stratigraphy was inferred from Haslauer (2005) who indicated that approximately 4 m of silty clay overlay the sand and gravel of Aquifer 2. The Aquifer 2 water table varied from 4.5 to 5.6 m depth.

Stations 2 and 4 had a shallow stratigraphy composed of clay-silt till (the Zorra till shown in Figure 2.6 also designated as Aquitard 1). At Station 2, the till was underlain by unsaturated silty sand, followed by a layer of clay, silt and sand interpreted to be Aquitard 2. The remainder of the unsaturated zone was composed of sand and silt, with some clay and sand layers between 24 and 28 m depth corresponding to Aquitard 3. The depth to the Aquifer 3 water table ranged from 26 to 26.4 m at Station 2. Station 4 had a similar stratigraphy, although Aquitard 2 was not encountered, and the depth to water in Aquifer 3 ranged from 20.5 to 21.1 m.

The shallow stratigraphy at Station 5 did not contain the clay-silt till encountered at most other sites and was dominated by layers of fine sand, silty sand and silt down to the Aquifer 3 water table which ranged from 21.4 to 21.7 m depth. At Station 3, the upper 2 m of clay-silt till were underlain by silt and sand, with thin clayey layers at 6 and 8 m interpreted to be Aquitard 2. Below this depth are the sand and silt layers associated with Aquifers 2 and 3 (Aquifer 3 water table varying from 16.4 to 17.4 m) and Aquitard 3.

4.2.2. Soil Analysis Results

Bulk soil nitrate, gravimetric water content and porewater nitrate concentration data from all coring events are presented graphically in Figures 4.3 to 4.17. These figures also include cumulative nitrate mass profiles as described in Section 3.3, while Table 4.1 summarizes the stored nitrate mass above a common depth for cores from each recharge station. The nitrate mass values in both the figures and the table excluded the upper 0.5 m of the soil profile due to the transience of nitrogen content in the root zone (Section 3.6.1). It should be noted that the common depth above which stored nitrate mass was calculated at each station was not selected to coincide with the maximum anticipated depth of BMP impacts ($d_{max,BMP}$), and at each station $d_{max,BMP}$ may have fallen above or below the depth for stored mass calculations. As a result the stored mass values may not represent a portion of the core completely affected by BMPs, but rather the stored mass over the shallowest core depth at each station. In addition, in most of the boreholes drilled to groundwater in March 2005, geologic core from deeper than 4.5 m could not be preserved in Lexan tubes since the split core barrel could not be used for core extraction (Section 3.1.3). Bulk soil nitrate concentration and gravimetric water content were only measured in samples from the preserved core. Soil bromide data are discussed in Section

4.5.1.1, and all laboratory-measured soil water content and soil quality results are included in Appendix F.

In most profiles, the highest bulk soil nitrate concentrations measuring up to 50 mg NO_3-N/kg were observed in the shallowest 0.5 m (the depth excluded from subsequent nitrate mass flux calculations), while deeper concentrations were relatively uniform with depth and 5 to 10 times lower than the shallow peaks. Gravimetric water content values varied with soil type between 0.04 g/g in sand to 0.3 g/g in the shallow topsoil layers. The porewater nitrate concentration values reflected variations in the bulk soil nitrate and soil water content values from which they were calculated, reaching 200 mg NO_3-N/L in the upper 0.5 m and usually ranging from 1 to 30 mg NO_3-N/L deeper in the profile. The total stored nitrate mass over the shallowest 2.3 to 3.0 m (excluding the first 0.5 m) in all cores was also highly variable, ranging from 1.9 to 23.4 g NO_3-N/m^2 (Table 4.1).

At Station 6 in the glaciofluvial outwash channel, cores from February and March 2005 had bulk soil nitrate concentrations between 2 and 6 mg NO_3-N/kg over the depth interval of 0.5 to 4 m, while concentrations over the same depth in November 2005 and May 2006 cores decreased to 0.1 to 2 mg NO_3-N/kg. The associated peak porewater nitrate concentrations similarly decreased from 150 to 35 mg NO_3-N/L, suggesting that in the sand and gravel unsaturated zone at this station high-nitrate porewater had been displaced downward by lower-nitrate porewater since BMP implementation. The stored nitrate mass to 2.8 m depth decreased from 14.8 g NO_3-N/m^2 in early 2005 to 2.9 g NO_3-N/m^2 in May 2006, suggesting that the reduction in nutrient application associated with a switch from wheat to grass crop may have had an observable effect on shallow stored nitrate. At Station 1 also in the outwash channel, no cores were extracted in February or March 2005 but bulk soil and porewater nitrate concentrations in cores from November 2005 and May 2006 were similar to Station 6 values (0.02 to 2 mg NO_3-N/kg and 0.5 to 20 mg NO_3-N/L). Stored nitrate mass to 3.0 m depth (average 3.0 g NO_3-N/m^2, similar to the May 2006 value at Station 6) was the lowest among the recharge stations and was likely also associated with the change in crop from wheat to grass at a location with high-conductivity geologic materials.

Bulk soil nitrate concentrations at Station 3 were more variable with depth than at most other stations with a range of 0.07 to 2.4 mg NO_3-N/kg (below 0.5 m depth) over the study period. Porewater nitrate concentrations ranged from 2 to 40 mg NO_3-N/L. There was no apparent correlation between nitrate concentration and soil type; however, as at Station 6, a marked decrease in stored nitrate mass (from 7.4 to 1.9 g NO_3-N/m^2 in the shallowest 2.3 m) appeared to coincide with the transition from a wheat crop to grass and associated decrease in applied fertilizer.

In the clay-silt till layer reaching 4 and 3 m depth at Stations 2 and 4, bulk soil nitrate concentrations were generally very uniform with depth and varied over the study period between 1.5 and 2.0 mg NO_3-N/kg at Station 2, and between 0.6 and 2.3 mg NO_3-N/kg at Station 4. The lowest concentrations were measured in November 2005 at both stations. Gravimetric water content was consistently 0.1 g/g in the till material, such that the porewater nitrate concentrations were also consistent with depth within the range of 5 to 25 mg NO_3-N/L during the study period. Stored nitrate mass values at the stations, measured to 2.9 and 2.6 m at Stations 2 and 4 respectively, fell within similar ranges (5.0 to 9.1 mg NO_3-N/m^2 overall) and no apparent trend in the data was discernable at either station although the highest values were measured in May 2006 after corn was grown at the stations. In contrast to Stations 1, 3 and 6, where a significant decrease in nitrogen fertilizer application combined with the presence of coarse-grained unsaturated zone materials led to a noticeable decrease in stored nitrate mass, the combination at Stations 2 and 4 of dense, fine-grained geologic material and a less significant reduction in fertilizer application on the corn crop resulted in no clear response in the stored nitrate mass. However, it should be noted that the shallow stored nitrate mass at the time of BMP implementation (2003) is unknown and may have been higher than was measured at Stations 2 and 4 during this study.

Bulk soil nitrate and porewater nitrate concentrations were also steady in time over the shallowest 5 m of sand and silt at Station 5. The average soil nitrate concentration between 0.5 and 5 m depth ranged from 0.3 mg NO_3-N/kg in November 2005 to 1.0 mg NO_3-N/kg in March 2005. These were among the lowest concentrations observed over the study site, as were the porewater nitrate concentrations at Station 5 which generally ranged from 7 to 10 mg NO_3-N/L. The deeper March 2005 soil samples reaching 15 m bgs at this station had a similar

average bulk soil nitrate concentration (1.1 mg NO_3-N/kg) but higher calculated porewater nitrate concentrations (average 20 mg NO_3-N/L) due to the lower gravimetric water contents between 5 and 15 m depth. In the shallowest 2.8 m, stored nitrate mass varied from 3.2 to 4.7 g NO_3-N/m^2 over the study period, a range slightly higher than at Station 1 in the outwash channel where the lowest stored mass was observed. The relatively low bulk nitrate concentrations and shallow stored mass are consistent with the fact that Station 5 was planted in the same lightly-fertilized grass crop as at Station 1 during the study period.

At Station 8, bulk soil nitrate concentrations were considerably higher than at other stations, generally ranging from 3 to 7 mg NO_3-N/kg with deeper measurements as high as 14 mg NO_3-N/kg in February 2005. As at Stations 2 and 4, the gravimetric water content in the clay-silt was approximately 0.1 g/g through the profile, such that porewater nitrate concentrations ranged from 15 to 150 mg NO_3-N/L. Stored nitrate mass to 2.6 m bgs increased over the study period from 12.4 to 23.4 g NO_3-N/m^2. The increase in stored nitrate mass may be due in part to the combined effects of low hydraulic conductivity materials and continued corn cropping as at Stations 2 and 4, but the amount of stored nitrate relative to other sites suggests that the soil nitrate content was also driven up by historical manure storage or cattle confinement at that location (Section 2.5).

Finally, Station 7 was the only recharge station not located within the limits of Parcel B on which BMPs were implemented. The range of bulk soil nitrate concentrations (0.4 to 3 mg NO_3-N/kg) at this location was comparable to the concentrations within Parcel B. Porewater concentrations generally ranged from 8 to 35 mg NO_3-N/L, while stored nitrate mass to 3.8 m bgs decreased from 13.4 to 8.9 g NO_3-N/m^2 from May 2005 to May 2006. This decrease coincided with the switch from a corn crop to the nitrogen-fixing soybean crop and may reflect a progressive decrease in leached excess nitrate.

Some variation in the soil nitrate profile between successive cores was also likely attributable to spatial variability. For example, the apparent differences in the nitrate profile between the February 2005 and March 2005 cores at Station 2 were likely not due to nitrate transport, due to the short time interval between the collection of the cores and the presence of low-conductivity clay-silt material, but rather due to local spatial variability of nitrate mass storage in the

unsaturated zone since the two cores were approximately 5 metres apart. This local spatial variability may have also affected nitrate profiles at other recharge stations, although it is difficult to estimate the magnitude of its influence. Finally, an average bulk soil density of 1.7 g/cm^3 was calculated from samples across the study site and was used in subsequent calculations as required.

4.3. Soil Water Content and Temperature Data

Soil water content measurements from the neutron moisture probe and the ECH$_2$O and CS616 sensors were compared to identify the most accurate data set for this study. The data and instrument analysis are presented below. Soil temperature, as measured by the HOBO Temperature Smart Sensors at each recharge station, was applied only in the SHAW model simulations and is not presented below. Soil temperature measurements were consistent between the HOBO sensors and the CS107B sensors installed at Station 2.

4.3.1. Neutron Probe Measurements

Count ratios (CRs) measured with the neutron moisture probe were converted to volumetric water content (VWC) values using the calibration equation developed in Appendix B. The CRs measured during the study period ranged from 0.4 to 1.3, corresponding to VWCs of 0.05 to 0.35 m^3/m^3. The potential error in these measurements ranged from 0.04 m^3/m^3 for the lowest CR to 0.09 m^3/m^3 for the highest CR. The seasonal variation of VWC profiles is illustrated in Figure 4.18, which show the profiles at Stations 2, 5 and 7 at 3-4 month intervals on dates when complete profiles were available. This figure also includes the laboratory measurements of VWC in cores extracted at the stations on November 17, 2005. The seasonal profiles at the remaining stations are included in Appendix G. The 5-cm diameter access tubes at Stations 1, 2, 4 and 8 suffered intermittent flooding during the study period, which prevented the collection of a full set of measurements for these stations.

The VWC profiles at Stations 2 and 5 exhibited the site's lowest and highest amounts of seasonal variation, which appeared to be controlled primarily by soil type. Station 2 had a shallow stratigraphy of 4 m of clay-silt till which drained slowly and showed little variation (maximum 3%) in VWC below 1 m depth over the course of six months. Station 5, in contrast, experienced 5-10% variations in VWC throughout its upper 5.8 m of sand and silt. At the

remaining recharge stations including Station 7, the stratigraphy was generally a combination of the fine and coarse materials encountered at Stations 2 and 5, and the extent of seasonal VWC variations was accordingly greater in the coarse-grained geologic layers and lowest in the clay-silt layers. During the study period the magnitude of VWC across the site ranged from 6% in some fine to coarse sand layers at Stations 4, 5 and 6, to 30% in the shallow organic layers at several stations. The VWC in the clay-silt till across the site was generally steady in time at 24%.

The VWC profiles determined from laboratory analysis of cores from November 17, 2005 also matched well to the neutron probe profiles from October and November 2005 at Stations 2 and 5. Local peaks in laboratory-measured VWC between 2.5 and 3.2 m depth at Station 5 were not measured by the neutron probe, but otherwise VWC measurements along the two profiles varied by no more than approximately 4% VWC at both stations. At Station 7, the difference between laboratory and neutron probe VWC measurements increased to 5-7% in the well-graded sand layers. This discrepancy may have been due to the difficulties associated with sampling the coarse-grained material (Section 3.3), which may have either artificially decreased laboratory VWC measurements or affected the accuracy of the neutron probe calibration (Appendix B) by limiting the number of coarse-grained samples obtained. Although it could not be determined whether the neutron probe measurements were biased for coarse-grained material, the accuracy of the probe's measurements for other soil types and the probe's vertical range (up to 6 m depth) made the probe's VWC dataset the most appropriate among those available for use in recharge and porewater nitrate concentration calculations.

4.3.2. ECH_2O Probe Measurements

Several of the ECH_2O moisture content probes reported negative or error values during the study period, suggesting that the probes had perhaps been damaged during installation or by rodents, or had malfunctioned. Thirteen of the 47 ECH_2O probes across the study site recorded negative water content values over periods of at least two weeks at some time during the study period. Due to these prolonged errors, the entire data set from these 13 probes was deemed questionable and was not used.

Comparison of data from the functioning ECH_2O probes to the neutron moisture probe and laboratory data also revealed some discrepancies (Figure 4.19). At Station 5, the ECH_2O probes

reported VWC values consistently higher than laboratory and neutron probe measurements at the same depth, whereas at Station 2 the ECH_2O probes reported maximum and minimum values outside the range of values estimated by both the neutron probe and laboratory measurements. At Station 7, the ECH_2O probes also reported maximum and minimum values beyond the range of neutron probe measurements, although the minimum ECH_2O values remained higher than the low laboratory measurements of VWC in well-graded sand. In addition to the potential measurement error associated with both the neutron moisture probe (CPN, 1984) and the ECH_2O probes (Decagon Devices, Inc., 2006), the installation method for the ECH_2O probes may have also affected the accuracy of their measurements. Each ECH_2O probe was either driven into the native material at the bottom of a 10-cm borehole or placed at the bottom of the borehole. In either case, the borehole was backfilled and compacted, but the compaction of the backfill material may not have attained the material's original density, resulting in preferential pathways down which infiltrating water may have travelled to accumulate and cause artificially high water content.

The utility of the ECH_2O probe readings was further limited by the short vertical interval of the unsaturated zone (approximately 1.6 m) in which the profile of probes was installed. As a result of the various factors limiting the utility of the ECH_2O probe readings, they were not used. However, the measurements from the soil temperature sensors installed with the ECH_2O probes were used as input in the SHAW model (Section 3.5.2.4).

4.3.3. CS616 Water Content and 107B Temperature Measurements

The soil water content and soil temperature data from the CS616 and 107B sensors attached to the meteorological station are included in Appendix E with the climate data. Data from the CS616 sensors at Station 2 are presented on Figure 4.19. Like the ECH_2O probes, the CS616 sensors were installed in 10-cm boreholes which were then backfilled and compacted. The elevated water content measurements in July (one greater than 40%) suggest that these boreholes may have acted as preferential pathways to collect and retain infiltrating water, resulting in prolonged periods of high water content readings following recharge events. Furthermore, like the ECH_2O probe profiles, the profiles of these sensors were also limited in vertical range; therefore the CS616 data were not used for analysis in this study.

4.4. Groundwater Monitoring and Sampling Results

Figure 4.20 depicts the hydraulic head contours for Aquifers 2 and 3 based on measurements from August 2005. Contours in January 2005 and January 2006 were consistent with the August 2005 contours (Appendix G). In Aquifer 2, locally saturated within the glacifluvial outwash channel, the groundwater flow within the limits of the study site and woodlot was from west to east with an average horizontal hydraulic gradient of 0.009 m/m, except under the Old Stage Road field where groundwater flowed toward the northeast. In Aquifer 3 in which the Thornton supply wells are screened, the local groundwater flow direction was toward the east-northeast, with a 0.007 m/m average horizontal hydraulic gradient. In both aquifers, the hydraulic gradient increased in the vicinity of the Thornton well field. These hydraulic head distributions are consistent with Haslauer's (2005) findings of a regional groundwater flow direction of southwest to northeast in Aquifer 3.

The spatial distribution of groundwater nitrate in Aquifers 2 and 3 in August 2005 is provided in Figure 4.21; figures from January 2005 and January 2006 are in Appendix G and data are included in Appendix F. The magnitude and spatial extent of the zone of elevated nitrate in Aquifer 2 were relatively steady over the course of the three monitoring events. Nitrate concentrations during these monitoring events ranged from minima of 0.2 to 2.5 mg NO_3-N/L along the east edge of the woodlot, to maxima of 14.7 to 15.9 mg NO_3-N/L, which were consistently measured in WO35, the monitoring well located at Station 8.

The spatial groundwater nitrate distribution in Aquifer 3 was also relatively constant between the three monitoring events. The zone of elevated groundwater nitrate appeared to extend from the vicinity of municipal wells 1, 3 and 5 toward WO28D on the western edge of the study site. The lowest nitrate concentrations (0.2 mg NO_3-N/L) and non-detectable concentrations (less than 0.1 mg NO_3-N/L) were found along the east and north edges of the monitoring well network, while high concentrations ranging from 13.3 to 13.9 mg NO_3-N/L were measured at wells in the central to eastern portion of the study site, including at WO61 (Station 4). Haslauer (2005) noted that nitrate concentrations measured at the study site in 2005 were slightly higher than in 2003, and noticeably higher than in 1998.

As described by Haslauer (2005), groundwater with elevated nitrate content in Aquifer 2 (in the glaciofluvial outwash channel) spreads into Aquifer 3 where there are discontinuities in Aquitard 3. This nitrate transport between aquifers appears to occur in the vicinity of WO37, WO07 and WO02 where the nitrate concentrations in the two aquifers were similar during the three monitoring events, ranging from 12.3 to 15.6 mg NO_3-N/L in Aquifer 2 and from 11.8 to 13.9 mg NO_3-N/L in Aquifer 3.

To evaluate the seasonal and potentially precipitation-driven responses in the groundwater at each recharge station, the groundwater level, temperature and nitrate concentration during the study period are shown for Stations 1, 2, 3 and 7 on Figure 4.22 (data at remaining stations are shown in Appendix G). Questionable water level data were recorded by the Leveloggers beginning in early September 2005 after the instruments were brought to ground surface for downloading. The Leveloggers were removed from the wells for repair and were replaced approximately three months later, such that only manual water level measurements were available between September and December 2005. As a result, the hourly groundwater response to the most intense precipitation event during the study period in November 2005 was not recorded. At Station 5, difficulties in securing the casing of WO58 and deploying the Levelogger limited the electronic measurements to the period from June to September 2005.

Observed trends in groundwater level were similar at Stations 1, 6 and 8 in the outwash channel, where the maximum variation in water level between June 2005 and May 2006 was approximately 1.1 m. There was a 0.5 m decrease in water level between June and August 2005 coinciding with a period of minimal precipitation, and a 0.4 m increase in February 2006 during the spring melt. The most rapid change in groundwater level (approximately 0.3 m in 10 days at Station 1) was observed in March 2006 and appeared to be related to intense precipitation events. The maximum variation in groundwater temperature at the stations varied depending on the depth to water, ranging from 1.0 ºC at Station 6 (with a depth to water of 8.9 to 10.0 m) to 5.0 ºC at Station 1 (with a depth to water of 2.2 to 3.3 m).

At Stations 2 and 4, there was less variation in water level (maximum 0.5 m during the period of measurement) than at Stations 1, 6 and 8, and minimal variation in groundwater temperature. The smaller variation in groundwater level and temperature is likely due to the greater depth to

the Aquifer 3 water table at these stations, which ranged from 20 to 26 m. At Station 3, the average depth to groundwater was approximately 17 m. The groundwater temperature at this station was also steady but the maximum variation in groundwater level was 0.8 m, with the same seasonal variations as observed at Station 1. At Station 5, where WO58 is also screened in Aquifer 3, the groundwater level and temperature data were limited, but their trends appeared to most closely match those observed at Stations 2 and 4.

The largest and fastest variations in groundwater level were observed at Station 7 in the Old Stage Road field. In February and March 2006, there were five instances in which the water level increased by 0.3 to 0.9 m over 1 to 4 days. These sudden jumps in water level were accompanied by decreases in groundwater temperature. The greatest of the water level increases coincided with daily precipitation amounts exceeding 10 mm. It appeared that the groundwater at Station 7 responded very quickly to heavy precipitation events, suggesting rapid infiltration of surface water. The groundwater response recorded in monitoring well WO40 nearby was very similar, indicating that the jumps were a true reflection of field conditions and not caused by leakage along the well casing.

4.5. Field Recharge Estimates

Results of the three field methods for recharge estimation are presented and discussed in this section. The final recharge estimate made for each method represented the annual recharge rate based on the May 1, 2005 to May 1, 2006 measurement period. However, because the methods relied on field measurements obtained on different dates, the exact length of field data collection for the tracer and ZFP methods deviated from the one-year period. For these methods, the recharge amount calculated from the field data was scaled proportionally to a one-year period. The selection of a final range of recharge rates is described in Section 4.7.

4.5.1. Tracer Velocity Method

4.5.1.1. Bromide Tracer Migration

Profiles of bromide concentration (normalized by dividing by the maximum observed concentration) and centre of mass based on core data from November 2005 and May 2006 at Stations 1, 2, 3 and 4 are shown in Figure 4.23 with profiles from remaining stations in

Appendix G. The core samples collected at Stations 3, 4, 5 and 7 in May 2006 were not deep enough to capture the leading edge of the bromide pulse and therefore for these stations the bromide profile was extrapolated to allow the calculation of the tracer centre of mass. For this extrapolation, the slope of the lowest part of the observed bromide profile was assumed to adequately represent the deeper bromide profile and the profile was extended to the zero concentration axis with the same slope.

Table 4.3 lists the depth of the bromide centre of mass for each coring event, the average volumetric water content (θ_{ave}) within the temporal and spatial range of tracer migration (Section 3.4.1), monthly recharge rates for the periods of July 2005 to November 2005 and November 2005 to May 2006, and the recharge rate from July 2005 to May 2006 scaled to a yearly rate. Because there was less than a full year of bromide tracer data available, it was necessary to estimate an annual rate from the 9.5 months of observed tracer migration. In the absence of data on seasonal recharge variations at the site, it was assumed that the average monthly recharge rate between July 2005 and May 2006 was representative of the average monthly rate between May and July, and therefore the bromide tracer migration over 9.5 months was scaled proportionally to one year. As a result, the accuracy of the recharge estimates from the bromide tracer method may be affected if this assumption were not valid, as discussed further in Section 4.7.

The upper and lower bounds of the recharge estimate were calculated from the standard deviation of the soil water content for all periods in which the tracer moved below 0.3 m and there were multiple neutron probe water content measurements available. This was not possible at any of the stations in the period between July and November 2005, and at Station 2 between November 2005 and May 2006, since the depth of the tracer centre of mass was too shallow.

The bromide profiles for the November 2005 cores showed that 90% of the applied mass was within the upper 0.6 m at all of the recharge stations, except at Stations 6 and 7 where this mass was within the first 1.1 m. The depth of the centre of mass ranged from 0.29 to 0.51 m bgs. The associated monthly recharge rate calculated for the period between July and November 2005 varied from 0.023 m/mo at Station 8 to 0.042 m/mo at Station 7. The variation in recharge depth between stations was more pronounced in the bromide profiles for the May 2006

cores, with the bromide centre of mass varying from 0.49 to 2.11 m bgs and recharge rates for the period from November 2005 to May 2006 ranging from 0.009 m/mo at Station 2 to 0.065 ± 0.011 m/mo at Station 3. The total estimated recharge at all stations from July 2005 to May 2006 varied from 0.21 m/yr at Station 2 to 0.64 ± 0.08 m/yr at Station 7. Generally the trend in bromide tracer recharge estimates matched variations in geology and topography among the recharge stations. The lowest recharge rates were measured at Stations 2 and 8 where there was approximately 4 m of clay-silt, although at Station 4 which had a similar shallow stratigraphy but a sloping topography the recharge rate was twice as high as at Station 2. A common recharge rate (0.43 m/yr) was observed at Stations 1 and 6 which had similar stratigraphies and exhibited similar groundwater and soil nitrate characteristics. The highest recharge rate was measured at Station 7 located in the outwash channel, where there was rapid groundwater response to precipitation events as presented earlier.

The total bromide mass below the application area was estimated from the mass profile observed in each core, as summarized in Table 4.3. The total mass estimates for Stations 1 and 7 based on the November 2005 core data were significantly higher than the applied bromide mass of 4.05 kg. Conversely, mass estimates between 5 and 15 times less than the applied amount were measured at three stations in November and four stations in May. One possible reason for the discrepancy between applied and recovered bromide mass is the average vertical spacing of the core samples. In November 2005 this spacing was 0.1 m above 0.5 m depth, 0.5 m below 0.5 m depth, and in May 2006 was 0.2 m. This spacing may have caused unrealistically long core intervals to be assigned to the highest or lowest measured concentrations. This outcome appeared likely at Stations 2, 3 and 4 where the recovered mass was at least 80% less than the applied amount in November 2005 and then increased from November to May. It is also possible that the peak of the bromide mass pulse was deeper than the extracted core; however, Station 3 is the only location for which the bromide profile shape suggested this possibility. Bromide uptake by crops is possible as observed by Kung (1990) but would only explain mass losses between July and November, during the growing period. Alternatively, the apparent loss of bromide at all stations between July 2005 and May 2006 may potentially indicate a horizontal component of dispersive spreading that transported the bromide laterally beyond the midpoint of the application area where the core was extracted.

Despite the loss of bromide mass, the bromide tracer method was considered robust, since the tracer movement was a direct result of groundwater recharge phenomena in the field and the location of its centre of mass was relatively easy to identify. At most recharge stations, each bromide breakthrough curve in the unsaturated zone had a distinct peak indicating that it had adequately captured the migration of the tracer by advection and dispersion. Exceptions to these peaked profiles were observed at Station 4 in May 2006, where a long flat bromide profile may have been caused by repeated variations between downward recharge and upward flow controlled by ET, and at Stations 5 and 7 in May 2006 where multiple peaks in the profile may have been caused by two-dimensional flow effects, or by the presence in deep core samples of pieces of surface soil that had fallen into the borehole during drilling. The main limitations associated with the bromide tracer method in particular were the temporal scaling described earlier, and the fact that the application of the tracer compromised crop growth in the application area at several stations, which may in turn have reduced evapotranspiration and increased the recharge rate.

4.5.1.2. Nitrate Tracer Migration

Across the study site, soil nitrate concentrations below a depth of 1 m bgs varied within a relatively narrow range (0 to 3 mg/kg at most stations) with no apparent trend along the borehole depth. These variations often prevented the identification of distinct peaks in the concentration profiles as required by the tracer migration method. It was particularly difficult to discern the same concentration peak in multiple cores at one recharge station. Migrating peaks were identified in consecutive cores at four stations, including Station 3 as shown in Figure 4.24. At other locations including Station 8 (Figure 4.24), nitrate profiles in two consecutive cores exhibited little change, suggesting near-zero recharge. Recharge rates determined from the nitrate profiles are provided in Table 4.2 but were not available for each station due to the limitations of the variable soil nitrate data.

4.5.2. Zero-Flux Plane Method

Recharge estimates were derived from fluctuations in the soil water content profile using the zero-flux plane (ZFP) method as discussed in Section 3.4.2. The profiles corresponding to consecutive high and low water contents during the study period are included in Appendix G. Recharge estimates equal to the sum of the water content losses are provided in Table 4.4 for the

three comparison periods. At Stations 1, 2, 4 and 8, occasional flooding of the access tubes precluded water content data collection and the estimation of recharge for the complete study period. The annual recharge rates calculated for these stations are marked in the table as incomplete due to the lack of a full dataset. At the four remaining stations, the annual recharge estimate ranged from 0.11 m/yr at Station 6 to 0.50 m/yr at Station 5.

At most of the recharge stations, three distinct recharge events were observed during the study period. In the context of the zero-flux plane method, a recharge event is the decrease of soil water storage from a high to a low value below the ET/drainage boundary (as based on root depth in this study). At all stations except 7, the first high soil water storage value was measured in mid-April (the closest measurement date to the start of the recharge measurement period on May 1, 2005), and the subsequent relative low in soil water storage was not measured until October or November 2005. Therefore the progressive decrease in soil water storage below the ET/drainage boundary during the 2005 growing season represented a single recharge event through the unsaturated zone. The stored soil water at all stations began to increase in mid to late November 2005 following two heavy rainfall events on November 9 and 15. At Stations 3, 5, 6 and 7 where a complete neutron probe water content dataset was available, two additional recharge events were observed between January and early March 2006, and between mid-March and May 2006. The divide between these two recharge events (the reversal of the trend in soil water content from decreasing to increasing) also coincided with a heavy rainfall on March 9.

At three of the four recharge stations at which a full year of data was available for the ZFP method, the ZFP recharge estimate was less than half of the bromide tracer estimate. At Station 5, however, the ZFP estimate was only 0.01 m different from the bromide tracer estimate. In addition to limitations in the bromide tracer method, the discrepancy between bromide tracer and ZFP recharge estimates at the three other stations may be explained by several factors related to the ZFP method, as described below.

The unsaturated zone depth over which this method was applied at each station, i.e., the depth of the neutron probe access tube used for water content measurements, is listed in Table 4.4. Although the access tube at Station 1 reached the water table, the instrumented depth at the remaining stations was up to 23 m (at Station 2) less than the depth to the water table, such that

potential water content loss below the instrumented depth could not be measured. The VWC profiles (Figures 4.18, G.1 and G.2) suggest that the water content may have remained constant below the instrumented depth at Stations 2, 6 and 8. At Stations 3, 4, 5 and 7, water content was variable near the bottom of the instrumented depth suggesting that water content may have also varied at greater depth. In this case, the ZFP method may have underestimated the recharge estimate since it would not have captured the water content loss below the instrumented depth.

Even when the soil water content profile remained unchanged over time, however, downward water flow (recharge) may still have occurred but would not have been captured by the ZFP method. At Station 2, for example, the water content in the silt-clay material between the ZFP and 4 m bgs remained relatively constant from April to November 2005, although recharge did occur as captured by the bromide tracer movement. Due to this limitation, the recharge estimates at all stations may have been underestimated by this method.

A final limitation in the use of the ZFP method was the potential for wetting fronts to pass through the shallow unsaturated zone between successive measurements without being observed and included in the recharge estimate. However, the average neutron probe measurement frequency of two weeks in 2005 and one month in 2006 was anticipated to adequately capture variations in soil water content. Overall, results from the ZFP method may be considered a lower bound on the recharge rate since there are several circumstances in which the method will not detect recharge.

4.5.3. Water Balance

In the water balance method, numerous types of data from the study site meteorological station were applied in an empirical equation to estimate the evapotranspiration rate, which was then subtracted from the observed precipitation rate. The result was an estimate of the surplus water which represented an upper bound on recharge (Table 4.5). Detailed ET and water balance data are included in Appendix C.

Precipitation was assumed to be uniform across the study site. The only factor creating spatial variability in the water balance was the ET, which in turn was controlled mainly by the crop type. As a result, the water balance yielded identical surplus water estimates for fields and

recharge stations under the same crops in 2005-06. The eight recharge stations were planted with three crop types (grass/oats, corn and soybean) and Field 2 which contained no stations was planted in winter wheat in late 2004, which grew during the 2005 season. It should be noted that the crop over Station 5 in Field 3a was in fact grass only, but was approximated as the grass/oats crop in Fields 3b and 7 due to the similarities in crop growth parameters between oats and grass.

The water surplus estimates for the recharge measurement period of May 1, 2005 to May 1, 2006 varied by approximately 17% between the three recharge station crop types, from 0.160 m under oats/grass to 0.187 m under soybean. The water surplus for winter wheat during this period was 2.5 to 3 times smaller than for the other crops, due to the earlier planting and development of the crop. Negative values of water surplus were calculated during the growing season or bare conditions at all stations, indicating that during those periods the magnitude of evapotranspiration exceeded precipitation which resulted in a decrease in soil water storage with no recharge. The annual recharge rates calculated by the water balance method were significantly lower (by 24 to 73%) than those estimated by the bromide tracer method.

Although the water balance method makes use of local precipitation measurements and other meteorological data for deriving ET_o, the calculation of actual ET is based on empirical crop coefficients and numerous other field parameters including crop height, root depth, growth stage lengths and soil water availability which, in the absence of detailed field observations, are also estimated from the literature (Section 3.4.3.1). The assumptions required to calculate actual ET limit the accuracy of water balance method for the estimation of recharge. This is particularly true of ET calculations for non-growing periods, for which even literature data is limited (Allen et al., 1998).

Site-specific difficulties in estimating ET were also caused by the fluctuating temperatures during the winter of 2005-06. Unfrozen, bare soil and frozen or snow-covered soil required the use of different coefficients and assumptions in the ET calculation. However, due to the fact that average daily winter temperatures often varied around the freezing point, the distinction between these conditions was often unclear. The snow cover/frozen period was identified as

December 1, 2005 to March 7, 2006 because most average daily temperatures during this period were below zero degrees Celsius.

4.6. Modelling

4.6.1. Soil Hydraulic Parameters

The soil hydraulic parameters selected for initial parameterization for the models are listed in Table 4.6. These parameters were determined by laboratory analysis of core samples, followed by comparison of the results to computer-generated (SPAW) and literature values to identify any anomalies (Appendix H). The Brooks-Corey hydraulic parameters b and ψ derived from tempe cell tests in the laboratory were significantly different from the SPAW and literature values (up to 7 units and 0.43 m higher respectively) for the finer-grained clay-silt till and sandy silt, due perhaps to difficulties in adequately re-packing the samples for laboratory analysis. For these materials the values used for model parameterization were based primarily on the SPAW and literature values. Hydraulic parameters for coarser-grained materials were more similar to published and SPAW values (within 1.7 units for b and 0.17 m for ψ). Laboratory-measured values of saturated hydraulic conductivity were within the range of published values, while porosities were either inside or less than 0.06 outside of published ranges. As a result those parameters were maintained or minimally adjusted for model input.

Hydraulic parameters for the upper 1.0 to 1.3 m of soil were estimated by the SPAW computer program based on published soil texture characteristics. In keeping with their grain size distributions and parent material, the hydraulic parameters of the Guelph-Honeywood soil horizons resembled those of the clay-silt till, while the hydraulic parameters of the Fox and Embro horizons resembled those of the sand and silt encountered at the study site. The porosities of the soil horizons were increased slightly to reflect the reduced compaction of these shallow layers.

4.6.2. SHAW

The water balance components calculated using the SHAW model are presented in Table 4.7, and represent the final results after adjusting the soil hydraulic parameters within a reasonable range to best match the simulated and field-measured soil water content profiles. The largest

adjustments to saturated hydraulic conductivity (K_s) were 10- to 20-fold decreases at Stations 3 and 4 and increases of the same magnitude at Station 6. The maximum change in simulated VWC along each recharge station's profile during calibration of the soil hydraulic parameters ranged from 0 to 0.10 m^3/m^3. The recharge estimate for the May 2005 to May 2006 period based on initial hydraulic parameters was from 0.028 m/yr lower to 0.066 m/yr higher than the calibrated estimate, and the average difference (absolute value) between initial and calibrated recharge estimates was 0.019 m/yr. Below 1 m bgs, the maximum difference in VWC between calibrated simulations and observed field data at each station averaged 0.06 m^3/m^3 among the recharge stations. This difference was slightly higher in the soil layers between 0.3 and 1.0 m bgs (0.09 m^3/m^3 on average) due to parameterization based on grain size distribution and hydraulic parameters from the literature and SPAW rather than from core samples which were difficult to collect from the shallow, easily compressed material. Calibration to VWC between 0 and 0.3 m depth was not attempted because neutron probe measurements in this zone were unreliable.

The SHAW model's calibrated recharge estimates for the recharge measurement period (May 2005 to May 2006) varied from 0.000 m/yr at Station 8 to 0.135 m/yr at Station 5. The zero recharge rate at Station 8 was a product of equal downward drainage and upward flow controlled by the hydraulic gradient. Precipitation during the measurement period was 0.969 m, of which 90 to 97% was removed by evapotranspiration (ET), except at Station 5 where the absence of clay in the shallow stratigraphy allowed increased recharge and reduced ET to 75% of precipitation. The magnitude of simulated run-off was 1 to 15 times that of recharge. There was a poor correlation between the magnitude of simulated recharge and the shallow stratigraphy. Although the highest recharge rate (0.135 m/yr) was estimated for Station 5 where the shallow stratigraphy was comprised of sand and silt without clay, the second-highest recharge rate (0.052 m/yr) was estimated for Station 2 which had the thickest layer of clay-silt till (to 4.3 m bgs). Apart from the zero value at Station 8, the lowest recharge rate (0.010 m/yr) at Station 7, where there was over 5 m of sand and silt below surface and where the highest recharge rate was measured with the bromide tracer method.

The SHAW model's recharge estimates for the recharge measurement period (0.00 to 0.14 m/yr) were significantly lower than those derived from field methods. For example, the recharge estimates from the bromide tracer method ranged from 0.21 to 0.64 m/yr (based on 9.5

months of observation), and were 3 to 64 times higher than the SHAW model's estimates at individual stations.

4.6.2.1. Sensitivity Analysis

Sensitivity analyses were performed for Stations 4 and 6 since these stations represented varying shallow stratigraphies and 2005 crop conditions. At Station 4, corn was grown over 3 m of clay-silt till underlain by fine sand, while at Station 6 oats and grass were grown over layers of fine and well-graded sand. As described in Section 3.5.2.7, the parameters evaluated for their effect on recharge depth included the saturated hydraulic conductivity (K_s), pore size distribution index (b), air entry potential (ψ_e), crop growth parameters and soil albedo. The use of the unit gradient lower boundary condition in place of specified soil water content was also assessed. The initial recharge estimates for these stations during the May 2005 to May 2006 period were 0.014 m and 0.048 m/yr, respectively. Results of the sensitivity analyses at Stations 4 and 6 are summarized in Table 4.8 and below. However, as previously discussed, the base recharge estimates from the SHAW model appeared to be significantly underestimated, such that like the recharge estimates themselves, the results of the sensitivity analysis may serve to illustrate trends only. For instance a variation in recharge of only 0.007 m/yr, which corresponds to 2% of the average recharge estimate from the bromide tracer method, represents a 50% change in recharge magnitude at Station 4. The magnitude of changes in the sensitivity analysis should therefore be interpreted with caution.

Saturated hydraulic conductivity: A ten-fold increase in hydraulic conductivity in the upper soil layers caused a 45% rise in recharge at Station 6, although a similar adjustment at Station 4 caused a premature stop of the simulation due to non-convergence. A ten-fold increase in K_s along the entire simulated profile also caused recharge to increase at both stations (by 100 - 145% relative to its base value), with a corresponding decrease in soil water storage. Conversely, when the K_s of the shallow soil layers was reduced by one order of magnitude, the effect was negligible at Station 4 but drainage decreased by 35% at Station 6. A similar reduction in K_s along the entire profile reduced recharge to 1 and 6 mm at Stations 4 and 6, respectively (i.e., a 88 to 93% decrease). The results indicate that a variation in hydraulic conductivity of one order of magnitude, which may not even exceed the published range for a particular soil type, may have a significant effect on recharge and alter its magnitude by up to 93%. The influence of the

K_s of the shallow soil layers relative to the K_s of the deeper geologic material depends on their relative magnitudes. Where the shallow soil layers have a higher K_s than the underlying till as at Station 4, the recharge rate was primarily controlled by the low K_s of the till and was minimally affected by variations in the soil K_s. At Station 6, the shallow soil and the underlying sand had similar hydraulic conductivities which both affected the magnitude of recharge.

Soil water retention parameters (b and ψ): The pore size distribution index (b) is a factor in the SHAW model's expressions for both unsaturated water content and unsaturated hydraulic conductivity. As a result, its influence on recharge depends on the magnitude of other parameters such as saturated hydraulic conductivity and saturated water content. At both Stations 4 and 6, a unit increase in b caused reductions in the magnitude of recharge (of 17 to 21%) and ET, with an associated increase in the final soil water storage. This result is consistent with the decrease in unsaturated hydraulic conductivity potentially caused by an increase in b, which would restrict both upward and downward flow out of the profile. Meanwhile, a unit decrease in b at Station 6 caused a 30% drop in recharge, with increased runoff and decreased soil water storage. This result suggests that the overall effect of the decrease in b was to reduce soil water content and therefore K, which favoured runoff over recharge. Based on observed changes, the SHAW model's recharge estimates appear to be less sensitive to reasonable variations in b than to similar changes in saturated hydraulic conductivity. A decrease in b at Station 4 resulted in the premature end of the simulation due to convergence problems, despite the fact that the altered parameters were still reasonable estimates for the soil types at the station.

At Station 6, a 0.1 m increase in air entry potential (ψ_e) (to a higher tension and more negative potential) increased recharge by 42%, while a 0.1 m decrease in ψ_e reduced recharge by 27%. These results are consistent with the influence of ψ_e in the Brooks-Corey function: for a given soil water potential, an increase in ψ_e increases soil water content, which in turn increases the unsaturated hydraulic conductivity. However, at Station 4 similar increases and decreases in ψ_e were insufficient to affect the magnitude of recharge. Overall, like the pore size distribution index, the air entry pressure had less influence on recharge than did the value of K_s.

Unit gradient lower boundary: The application of a unit gradient to the lower boundary, rather than the specified soil water content lower boundary condition used in the base run, lowered drainage by 43% at both Stations 4 and 6. At Station 4, the decrease was explained by the fact that the hydraulic gradient throughout the year in the base simulation was greater than one (ranging from 2 to 5) and therefore allowed greater recharge out of the profile. At Station 6, the hydraulic gradient in the base simulation varied above and below unity during the year, with an overall recharge rate in the base simulation that was slightly higher than with the unit gradient. As would be expected, the SHAW model was most sensitive to the use of the unit gradient in circumstances where the field and original calibrated conditions had a significantly different gradient.

Crop variations: Increasing the length (by 30 days) and leaf area index (by one unit) of crop growth had no effect on drainage at Station 4 and actually increased recharge by 58% at Station 6 due to the decreased run-off potential during the longer plant growth period. A decrease of the same magnitude in crop growth parameters again had a negligible effect on recharge at Station 4 and increased it by 52% at Station 6. Whether crop growth was increased or decreased, the magnitude of evapotranspiration varied by less than 5%, indicating that evaporation rather than transpiration was the dominant component of ET. With parameters (Flerchinger, 2000b) selected to maximize soil albedo in order to minimize evaporation, ET still accounted for at least 86% of precipitation. When the crops were removed entirely in the simulations, recharge at Station 4 was unchanged and it increased by 52% to 0.073 m/yr at Station 6, but ET (i.e., evaporation in this case) still accounted for 82 – 88% of precipitation, indicating that under the study conditions the SHAW model was relatively insensitive to any type of crop growth.

4.6.2.2. Discussion

The sensitivity analysis of the SHAW model indicated that its recharge estimates were relatively insensitive to any changes to the input parameters. Only increases in K_s caused the recharge rate to increase through both the clay-silt till at Station 4 and the sand at Station 6. However, changing the K_s through the profiles would have affected the match between observed and simulated soil water content profiles achieved during the calibration of the soil hydraulic parameters.

One potential source of the discrepancy between the SHAW model and other recharge estimation methods is the magnitude of evapotranspiration (ET) estimated by SHAW, which exceeded the estimate from the water balance method by up to 0.09 m/yr at Stations 4 and 6. Modelling the stations without crops had no effect at Station 4, and at Station 6 increased the recharge to only two thirds of the lowest estimate from field methods. Soil evaporation therefore appears to be the dominant component of the high ET values, but variations in soil albedo had little effect on ET and recharge values (Table 4.8). Scanlon et al. (2002) found that the SHAW model overestimated evaporation and underestimated recharge (by factor of up to 14.8) compared to other one-dimensional unsaturated flow models for non-vegetated engineered covers in semiarid settings. They attributed this phenomenon to the use of the Brooks-Corey water retention function, which increased upward flow rather than drainage. The SHAW model results in this study, which included high evaporation rates (90 to 97% of precipitation) at seven recharge stations, were consistent with Scanlon et al.'s observations.

For humid regions, the SHAW model's ability to simulate recharge has not been evaluated in the literature, but Preston and McBride (2004) have noted the model's tendency to overestimate volumetric water content. They suggested that as a result, the recharge estimates from the model might be similarly overestimated due to increased unsaturated hydraulic conductivity. In this study, however, simulated water content profiles were used to calibrate the model. Therefore the overestimation of VWC may have resulted in the assignment of artificially low hydraulic conductivity values in order to match the simulated profiles, which may have reduced the simulated recharge. As noted earlier, the maximum decreases in Ks applied during calibration were by a factor of 10 to 20 at Stations 3 and 4, where simulated recharge rate was the lowest (0.01 m). Overall, the SHAW model's significant underestimation of recharge relative to field methods and previous recharge estimates for the site (Section 2.8) casts doubt on its utility to accurately reproduce field conditions. Therefore the results from the SHAW model may only be useful for the evaluation of trends between recharge stations.

4.6.3. HELP

As described in Section 3.5, the HELP model was employed in several ways to estimate recharge. Simulations were first conducted using an initial soil water content profile estimated

by the model. Using this initial condition, the soil hydraulic properties were calibrated to match observed and simulated soil water content profiles in December 2005. Using the calibrated hydraulic parameters, the simulations were repeated with a specified soil water content profile corresponding to the December 2005 field-measured profile, which was estimated to best represent the initial conditions in January 2005. The recharge amounts based on both model-estimated and user-specified initial soil water content are provided in Table 4.9. The difference between recharge estimates based on the two initial conditions ranged from 0 to 21% at individual recharge stations. The recharge estimates from the model-estimated initial condition, which varied from 0.28 to 0.34 m/yr, corresponded to 53 to 138% of the bromide tracer estimate at each station and were on average 16 times higher than the SHAW estimate. They also exceeded the range (0.11 to 0.25 m/yr) determined by Padusenko (2001), who applied the HELP model to an area including the study site and used topographic and soils maps to generate the input data.

When the model-estimated initial soil water content was used, the simulated recharge amounts in early 2006 were identical to those in early 2005. This can be explained by the model's use of 2005 weather data to estimate soil water content at the beginning of 2005. As a result, the simulated soil water conditions and unsaturated flow in both early 2005 and early 2006 were affected by climatic conditions in late 2005. In the early months of 2006, the freezing conditions at surface limited the effect of the weather on drainage, such that despite experiencing different precipitation amounts from 2005, the simulated profile drained the same way as in early 2005.

As previously mentioned, the difference between the recharge estimates using the two different soil water content initial conditions ranged from 0 to 21%. When the user-specified initial condition was applied, the simulated soil water content profile for December 31, 2005 at each station was unchanged from the earlier runs with the model-estimated initial condition. The simulated recharge rates decreased from 9 to 22% at Stations 3, 4 and 5 (Table 4.9) but were unchanged at the remaining stations. This indicated that at some stations, the model's estimate of initial water content was higher than the user-specified initial profile, although this could not be verified because the model does not provide that output.

The results of the sensitivity analysis in HELP are summarized in Table 4.9. The sensitivity of the simulated recharge rates to soil hydraulic properties and crop growth was tested at Stations 4 and 6, since these stations represented varying geologic and 2005 crop conditions.

Saturated hydraulic conductivity: Four sets of varying hydraulic properties were used. When the hydraulic conductivity of the shallow geologic material above 1 m depth was increased or decreased by one order of magnitude, there was an associated increase or decrease in recharge of 11 to 18%. Extending the increase in conductivity to lower layers further increased the recharge by another 3 to 4%, but decreasing their conductivity did not further change the recharge. The results indicate that the K_s of the topsoil exerted more control on recharge than did the K_s of the underlying layers. The sensitivity of the recharge rate to K_s was almost identical at the two stations, contrary to the results of the SHAW model sensitivity analysis in which the results varied between the stations because of different changes in K_s between topsoil and underlying layers. However, due to the comparatively low estimates of recharge rate from the SHAW model which suggest that even minimal changes in recharge (5 to 10 mm) represent changes of more than 50%, it is difficult to identify the reason for the difference in trends between the HELP and SHAW models' results.

Crop variations: The effects of varying the length of the growth stage by 30 days and the maximum leaf area index by one unit were negligible (less than 5% change). Like the SHAW model, the HELP model appeared to be relatively insensitive to crop growth parameters under the simulation conditions.

Weather generator: The sensitivity of the model to the type of weather data used to estimate the initial water content was evaluated by replacing field data with synthetic data for the first year and conducting the simulation for the years 2004 to 2006, as described in Section 3.5.2.7. In this way, 2004 synthetic data rather than 2005 field data were used to generate the initial soil water content profile. The total annual precipitation within the synthetic data set was 1.082 m, which was 11 and 15% higher than the 2005 total measured at the site (0.961 m) and the 2004 total measured at a local Environment Canada station (0.915 m) (Environment Canada, 2006). The use of the artificially high synthetic precipitation data set resulted in an increase of 0.02 m/yr (6 to 7%) in the recharge rate relative to simulations in which 2005 weather data was used to

estimate the initial condition. Compared to the saturated hydraulic conductivity, the weather data set employed was less significant in the estimation of recharge rate.

In contrast to the SHAW model, the HELP model yielded recharge estimates that were among the highest at each station (Table 4.2). The HELP model has previously been observed to overestimate recharge compared to measured values in both humid and semi-arid climates (Scanlon et al., 2002; Albright et al., 2002; Khire et al., 1997), potentially due to its use of a unit downward hydraulic gradient boundary condition. The HELP model was also difficult to calibrate to field conditions since it only output water content profiles at the end of the simulation period. Furthermore, the model based crop growth and associated ET on significantly fewer site-specific parameters than did the SHAW model. This may in part explain the decreased variability in recharge estimates between stations compared to other methods: the ratio between the highest and lowest HELP recharge estimates was 1.5, whereas the ratios for the bromide tracer method and the SHAW model were 3 and 12. Overall, these limitations suggest that HELP model results should be used with caution.

4.7. Recharge Estimate Summary

The recharge estimates generated by the various field and computational methods varied significantly, with the difference between the highest and lowest recharge estimates at individual recharge stations ranging from 0.17 to 0.69 m/yr (Table 4.2). All of the methods used to estimate recharge were subject to inherent limitations and potential errors, as discussed in Sections 4.5 and 4.6. It was not possible to quantify the error associated with each method because of the numerous factors (sampling limitations, analytical precision, steady-state flow, etc.) that may have simultaneously contributed to these errors. Instead, all methods were considered and a best estimate of recharge at each station was determined, in addition to lower and upper bounds to the potential range of recharge which accounted for potential errors in the estimates and the variability between methods.

As previously discussed, the bromide tracer method was considered the most robust of the recharge estimation methods since the movement of the tracer was a direct result of recharge processes. Potential limitations affecting accuracy were more significant for the other field methods than for the bromide tracer method: the nitrate tracer method was not applicable for all

recharge stations nor for the entire recharge measurement period, the zero-flux plane method did not account for steady-state flow, and the water balance method relied on empirical estimates of evapotranspiration with no consideration of site-specific geologic properties. Between the unsaturated zone models, the HELP model was assumed to provide more realistic recharge estimates since the SHAW model appeared to significantly overestimate evapotranspiration and underestimate recharge.

Based on this comparison between methods, the *best estimate* of the recharge rate at each station was designated as the estimate from the bromide tracer method. The initial estimate of the lower and upper bound on the recharge rate were from the bromide tracer method, as determined from the standard deviation of the soil water content. The Station 2 bromide tracer recharge estimate lacked upper and lower bounds because the standard deviation of soil water content could not be calculated (Section 4.5.1.1); this station was assigned a bromide tracer range (± 0.03) with the same magnitude as at Station 8, which had the closest bromide recharge estimate to Station 2.

Consideration was also given to the recharge estimates from the HELP model, which was considered to be the more accurate of the models used in this study. Where the HELP recharge estimate fell beyond the upper or lower bound of the bromide estimate, the revised bound was assumed to be the average of the HELP estimate and the initial bound. For example, at Station 3 the bromide tracer and HELP recharge estimates were 0.59 ± 0.08 and 0.29 m/yr respectively. Because the HELP estimate was lower than the initial lower recharge bound (0.51 m/yr), the revised lower bound was adjusted to 0.40 m/yr, the average of the lower bromide bound and the HELP estimate. The final estimate range of recharge rates at each recharge station is listed in Table 4.2.

The final recharge rates (i.e., the bromide tracer method recharge rates) varied among recharge stations from 0.21 to 0.64 m/yr, with an average of 0.45 m/yr. This average was almost double the highest recharge rate (0.25 m/yr) calculated by Padusenko (2001) for the study area. Padusenko's estimates were based on more indirect input data such as soils maps rather than geologic core data, which may have affected their accuracy. In the current study, several of the recharge stations were located in topographical lows where surface water run-on

may have increased the recharge rate. However, the recharge rates in this study may also have been driven up by the above-average precipitation amounts in early 2006 (Section 4.1), or by the proportional scaling-up of the bromide tracer recharge rate from 9.5 months of data to an annual rate, since the period for which data was unavailable (May to July) was likely a period of relatively high evapotranspiration and low recharge.

Because the HELP model and the water balance method are commonly and independently used to estimate recharge rates in other hydrologic studies, the recharge rates determined from these methods were also used to calculate nitrate mass load in subsequent sections, in order to compare their results to those from the final recharge rates described above. In total, five recharge rates (the best estimate, the upper and lower bounds on this estimate, the HELP and the water balance estimates) were carried through the calculations for porewater nitrate concentration and nitrate mass load.

4.8. Porewater Nitrate Content

4.8.1. Anticipated Depth of BMP Effects

The groundwater recharge estimates listed in Table 4.2 were used to calculate the maximum depth potentially attained by the BMP recharge water ($d_{max,\ BMP}$) at each station since BMP implementation, as described in Section 3.6.1. Five potential values of $d_{max,\ BMP}$, based on the five recharge rates described in the previous section, were derived for each core extracted in March and November 2005 and May 2006 (Table 4.10). The February 2005 cores were not used in the nitrate mass load calculations due to the proximity in time to the March 2005 cores. However, the February 2005 core was used at Station 8 and the May 2005 core at Station 7, because no cores were collected in March 2005 at those locations.

As described in Section 3.6.1, the May 2006 cores represented post-BMP conditions integrated over the longest period among the cores: from BMP implementation in April 2003 to the date of core extraction in May 2006. The nitrate concentrations measured in the March and November 2005 cores also represented average nitrate application conditions since BMP implementation, but over shorter periods than in the May 2006 cores. As a result of their longer integrated time period, the May 2006 data related to $d_{max,\ BMP}$, porewater nitrate concentration

and nitrate mass flux were assumed to better represent post-BMP conditions and are therefore discussed in detail in the following sections.

Recharge station 7 was located in the Old Stage Road field, outside the limits of Parcel B where nutrient applications had been reduced. In order to gain an additional estimate of nitrate mass load under non-BMP conditions, the calculations for nitrate mass load were applied to Station 7. For simplicity, they were performed and presented in the same manner as for the other stations, although at Station 7 there were no post-BMP conditions. Post-BMP conditions as presented for Station 7 represent simply the nitrate mass load since April 2003 when the BMP began on Parcel B. The presentation of "pre- and post-BMP" conditions for Station 7, which are in reality all pre-BMP conditions, provides additional insight into the temporal variability of nitrate mass load.

The estimated depth below ground surface attained by BMP recharge water in May 2006 based on the best estimate of recharge varied from 1.8 m at Station 2 to 10.6 m at Station 3. As expected, relatively high and low values of $d_{max,\ BMP}$ generally corresponded to high and low recharge rates, although $d_{max,\ BMP}$ at Station 7 (where the highest recharge rate was observed) was slightly lower than at Station 3 due to a greater average soil water content at Station 7. The value of $d_{max,\ BMP}$ based on the other recharge estimates varied from 1.3 to 12.0 m.

The value of $d_{max,BMP}$ calculated for May 2006 based on the best recharge estimate exceeded the depth of the May 2006 core at all stations but Station 2. As a result, pre-BMP conditions were not represented anywhere in the cores, and the conditions through the entire post-BMP portion of the unsaturated zone had to be approximated from the available length of core, which represented only a portion of the total post-BMP zone. The $d_{max,BMP}$ also exceeded the depth of 60% of the cores from March and November 2005. In the remaining 40% of those cores and in the May 2006 core at Station 2, where $d_{max,BMP}$ fell within the length of core, the length of pre-BMP core available ranged from 0.1 to 12 m. There were also numerous cores in which $d_{max,BMP}$ was deeper than the range of soil water content measurements from the neutron probe. In these cases, the value of $\theta_{v,ave}$ in both the pre- and post-BMP zones was approximated from $\theta_{v,ave}$ within the interval of neutron probe measurements. The implications of the limited pre-BMP

data and the use of post-BMP data from a portion of the post-BMP zone are further discussed in the following sections.

4.8.2. Porewater Concentration

Average porewater concentrations were calculated within the post-BMP zone (below 0.5 m depth) and the pre-BMP zone of each core extracted at the recharge stations (Table 4.11). These values were determined from the average annual neutron probe soil water content and the weighted average bulk soil nitrate concentration in each zone. The pre- and post-BMP nitrate concentrations were determined for cores from March and November 2005 and May 2006, based on each of the five recharge estimates at each recharge station. As described earlier, where the anticipated depth of BMP impacts exceeded the core depth, the post-BMP nitrate concentration was estimated using the soil nitrate concentration and water content measurements between 0.5 m and the bottom of the core, but the pre-BMP concentration could not be determined.

In May 2006, the average porewater nitrate concentration in the post-BMP zone as defined by best recharge estimates ranged from 8.1 mg NO_3-N/L at Station 1 to 48.9 mg NO_3-N/L at Station 8. At some recharge stations, the average post-BMP porewater nitrate concentration varied significantly between cores taken at different times (e.g., by 79% from 46.1 to 9.7 mg NO_3-N/L at Station 6). This was due to differences in the bulk soil nitrate concentration within the zone of BMP impacts.

Where the pre-BMP nitrate concentrations were available in cores from any date, they were lower than the post-BMP concentration in five of seven cores (based on $d_{max,\ BMP}$ determined from best recharge estimates). Similar trends were observed when the other recharge estimates were applied. The greatest differences between pre- and post-BMP concentrations were observed at Station 8, where in the February 2005 core the pre-BMP value exceeded the post-BMP value by 49.8 mg NO_3-N/L, but conversely in November 2005 the pre-BMP value was 10.6 mg NO_3-N/L lower than the post-BMP value.

The apparent increases in average porewater nitrate concentration in response to reduced nutrient application were counterintuitive, and it was speculated that they were related to the

exclusion of the upper 0.5 m of the subsurface to reduce the influence of seasonal nitrogen variations in the root zone (3.6.1). This depth was selected because it corresponded to the shallowest assumed root depth of the crops across the study site. Given the complexity of the nitrogen cycle and the deeper roots of other crops, however, it is possible that even below the 0.5 m depth, there was continued cycling of nitrogen that may have affected the nitrate mass load calculations. Figures 4.3 to 4.17 indicate that at many stations, the slope of cumulative stored nitrate mass versus depth decreased noticeably around 1.0 m bgs depth, below which it was generally constant. This suggests that the depth below which nitrate concentrations are no longer affected by nitrogen cycling in the root zone may be closer to 1.0 than 0.5 m bgs. As a result, the elevated bulk soil nitrate concentration values (up to 11 mg NO_3-N/kg) measured between 0.5 and 0.9 m in cores at several stations may have artificially raised the post-BMP porewater nitrate concentrations at many stations.

It should also be noted that the geologic cores from which soil samples were extracted rarely reached the water table, such that in the few cases where the pre-BMP concentration could be estimated, it was determined from a portion of core representing a fraction of the distance between $d_{max,\ BMP}$ and the water table. For example, the pre-BMP concentration determined from the May 2006 core at Station 2 was based on soil nitrate samples between $d_{max,\ BMP}$ (2.8 m) and the deepest soil sample (4.2 m), but the distance between $d_{max,\ BMP}$ and the water table was in fact approximately 23.4 m. Therefore the 1.4-m interval of unsaturated zone for which samples were available may not have adequately represented the overall pre-BMP conditions through the entire unsaturated zone. Overall, the contrast between pre- and post-BMP concentrations presented in Table 4.11 requires a cautious interpretation due to the assumptions and data limitations required for their calculation.

4.9. Nitrate Mass Flux

The nitrate mass flux at each recharge station was determined from the porewater nitrate concentration (Section 4.8.2) and recharge estimate (Section 4.7). The mass flux was determined for post- and pre-BMP conditions for each core based on each of the five recharge estimates at the station (Table 4.12). The pre- and post-BMP recharge rates were assumed to be equal. As described in Section 3.7.1, the nitrate mass flux value through the post-BMP zone of a core represents the average mass flux since BMP implementation required to have generated the

average nitrate concentration measured in the post-BMP zone. The pre-BMP mass flux was determined from recharge and porewater nitrate concentrations (when available) below the anticipated depth of BMP effects ($d_{max, BMP}$). All available core data at each station were used to calculate an average pre-BMP mass load; however, as described earlier, at several stations the value of $d_{max, BMP}$ exceeded the depth over which nitrate samples were available in the cores and therefore pre-BMP mass flux could not be calculated for those coring events.

The post-BMP nitrate mass flux values based on the best recharge estimates and the May 2006 core data ranged from 3.4 g/yr/m^2 at Station 2 to 13.2 g/yr/m^2 at Station 8. The average nitrate mass flux among the stations was 6.6 g NO_3-N/m^2/yr with a standard deviation of 3.5 g NO_3-N/m^2/yr. Individual nitrate mass flux values were 12 to 101% different from the average value. There was no apparent correlation between recharge station stratigraphy and the magnitude of post-BMP nitrate mass flux. The lowest mass flux values, ranging from 3.4 to 4.6 g/yr/m^2, were observed at Stations 1, 2, 5 and 6 which had stratigraphies varying from clay-silt till (Station 2) to sand and gravel (Station 6). At Station 8, where the highest mass flux was measured, the shallow subsurface was dominated by clay-silt and the recharge rate (best estimate) was the second lowest among the recharge stations. However an elevated porewater nitrate concentration (48.9 mg NO_3-N/L in May 2006) at Station 8, potentially due to its location in the former barnyard, resulted in a calculated nitrate mass flux that was significantly higher than at the other stations.

The trends in nitrate mass flux over time and between post- and pre-BMP zones at each station were the same as for the porewater nitrate concentrations because of the common recharge rate by which the concentrations were multiplied to determine mass flux. As a result, the post-BMP nitrate mass flux was greater than the pre-BMP mass flux at several stations. At six of the seven stations in Parcel B, the post-BMP nitrate mass flux was also greater than the average annual nitrogen application rate between 2003 and 2005 (Table 4.13). Due to their unexpected magnitude compared to application rates, the nitrate mass flux results appear questionable, and may be related to the potentially inappropriate use of bulk soil nitrate data from depths between 0.5 and 1.0 m as discussed in the previous section. They may also have been affected by the potential overestimation of the recharge rate due to above-average precipitation or less than a full year of data (Section 4.7).

The potential influence of these factors was tested by re-calculating the nitrate mass flux with the best recharge estimate reduced by 50% and with soil nitrate data excluded to a depth of 1.0 m rather than 0.5 m. The results (Table 4.13) indicate that under these alternative conditions, the post-BMP nitrate mass flux would be significantly lower than previously calculated at all stations. Furthermore, $d_{max, BMP}$ would be reduced such that the pre-BMP conditions would be captured in more cores than before, and the post-BMP mass flux would be lower than pre-BMP mass flux in five of these ten cores. In four of the five remaining cores in which post-BMP mass flux was higher than pre-BMP mass flux, the difference between the two values would be only 7% on average. The post-BMP fluxes at all stations would also be reduced to 27 to 89% of the 2003-05 application rate, except at Station 5 where there was no fertilizer application, and in one core at Stations 6 and 8. Overall, the results suggest that potential overestimation of the recharge rate or the use of nitrate data from 0.5 to 1.0 m may have caused an overestimation of post-BMP nitrate mass flux across the site. This in turn led to the implication that the BMP had caused nitrate mass flux to increase. If these two potential sources of error were mitigated, the results would suggest improvements in nitrate mass flux at 3 of the 7 Parcel B stations and relatively steady mass flux at 3 other stations (pre-BMP data would remain unavailable at Station 1 under the alternative analysis). Because the significance of the potential errors could not be verified or quantified, the results of the hypothetical analysis were not carried through in the remaining sections. However, the results of the analysis indicate that nitrate load estimates based on the original nitrate mass fluxes should be interpreted with caution.

4.10. Up-scaling of Nitrate Mass Load Values

4.10.1. Study Site Partitioning

The up-scaling of nitrate mass flux values across the study site to determine total post- and pre-BMP nitrate mass load values required the partitioning of the study site into areas best represented by each of the recharge stations. The characteristics of each station that influenced its mass load (topography, geology, crop history) were discussed in part in Table 3.1 and Sections 2.5 and 3.8. This section further describes the stations and the rationale for the distribution of nitrate mass flux values across the study site. The partitioning of the study site into sections of similar nitrate mass flux is illustrated on Figure 4.25. Both the pre- and post-

BMP nitrate mass flux for each station was assigned to the area that it represented. The approach for stations at which no pre-BMP data were available is discussed in the following section.

Station 1(post-BMP mass flux 3.5 mg NO_3-N/m^2/yr) – This station had an average groundwater recharge estimate among all stations (0.43 m/yr) and the lowest post-BMP porewater nitrate concentration (8.1 mg NO_3-N/L). The anticipated depth of BMP effects exceeded the water table depth as of November 2005, suggesting that the nitrate concentration was comparatively low because a significant amount of nitrate had already flushed through the 3-m unsaturated zone at this station. The nitrate mass flux characteristics at Station 1 were likely controlled by its location in the low of the glaciofluvial outwash channel, which may have encouraged surface water run-on, and the absence of Aquitards 1 and 2 in its stratigraphy. Therefore the nitrate mass flux value from Station 1 was assigned along the low of the outwash channel where there was no aquitard at surface.

Station 2 (post-BMP mass flux 3.4 mg NO_3-N/m^2/yr) – Station 2, situated along the relatively flat crest of a drumlin, had a shallow subsurface comprised of clay-silt till. The estimated recharge rate (0.21 m/yr) at this station was the lowest across the study site, and the post-BMP porewater concentration (16.4 mg NO_3-N/L) was average. The station was assumed to represent areas where relief was low, run-on unlikely and with till below surface. Haslauer (2005) showed that these characteristics existed along Curry Road from the western end of the study site to the border between Fields 4 and 5 (Figure 2.5). Based on the quaternary geology map (Figure 2.6), the flat till surface represented by Station 2 was assumed to extend southeast from Curry Road into Field 2, although no borehole logs were available to confirm this.

Station 3 (post-BMP mass flux 5.8 mg NO_3-N/m^2/yr) – Station 3 was located at the confluence of two swales and has a shallow unsaturated zone of silt and sand. As a result it was determined to have relatively high groundwater recharge (0.59 m/yr). Post-BMP porewater concentrations were relatively low (9.8 mg NO_3-N/L). Due to the potential for topographically focused recharge, Station 3 was assumed to represent the two swales adjacent to it.

Station 4 (post-BMP mass flux 9.1 mg NO_3-N/m^2/yr) – Station 4 had a similar stratigraphy to Station 2, but was located along a 300 m slope of approximately 7 percent. Despite the prevalence of clay-silt till in its shallowest 4 m, this station had the third-highest recharge rate (0.52 m/yr) among the stations. The post-BMP porewater nitrate concentration was also comparatively high (17.4 mg NO_3-N/L). The nitrate mass flux determined for this station was applied to other sloped areas underlain by the clay-silt till. This included most of Fields 5 and 6 surrounding Station 4, as well as Field 1, which had an overall slope of 3% and was assumed to be underlain by the till, although no borehole logs were available for this field. Haslauer (2005) also determined that the subsurface of the northernmost corner of Field 7 was also comprised of till; therefore this area was added to Station 4's portion of the study site.

Station 5 (post-BMP mass flux 4.6 mg NO_3-N/m^2/yr) – This station was located in a topographic low, where a frozen pond was observed after a brief midwinter thaw in January 2005. It was also located in a local discontinuity of Aquitards 1 and 2 (Haslauer, 2005), with a shallow stratigraphy of sand and silt. The recharge rate at the station was above-average (0.51 m/yr), while porewater nitrate concentrations among core samples at this station were comparatively low (9.0 mg NO_3-N/L), indicating that as at Station 1, large amounts of nitrate may have been flushed from the upper four to five metres of the subsurface. Field 3a in which Station 5 is located had been planted in grass since 2003 which may also have contributed to the lower nitrate concentrations. Due to the localized nature of the topographic and geologic controls on nitrate load at this station, it was assumed to represent only the swale in which it was located.

Station 6 (post-BMP mass flux 4.2 mg NO_3-N/m^2/yr) – Station 6 was located on a slope in Field 7 along the edge of the outwash channel. Its subsurface of sand and gravel was similar to the subsurface at Station 1, and its recharge rate (0.43 m/yr) and porewater nitrate concentration (9.7 mg NO_3-N/L) were very similar to those measured at Station 1. The main difference between Stations 1 and 6 appeared to be the deeper unsaturated zone and sloped surface at Station 6. The nitrate mass load at this station was assigned to the slope on which it was located, between the area represented by Station 1 and the northern border of the study site.

Station 7 (post-BMP mass flux 8.7 mg NO_3-N/m^2/yr) - Station 7 was located in the Old Stage Road field, outside the limits of Parcel B on which the BMP were applied. It is also situated near

the outlet of a tile drain, fed by fields to the west, which was observed to discharge water onto the Old Stage Road field during spring melt. Given the enhanced surface water run-on and the subsurface of sand and silt with some clayey layers, recharge here was determined to be highest across the site (0.64 m/yr), while the porewater nitrate concentration was 13.6 mg NO_3-N/L, lower than at three of the recharge stations under BMPs. Since the nitrate mass load at this station was not affected by BMPs, it was assigned only to the Old Stage Road field.

Station 8 (post-BMP mass flux 8.7 mg NO_3-N/m^2/yr) – This recharge station was located in a local topographic low in the general location of the former barnyard. Here the thickness of the till above Aquifer 2 was approximately three metres, and recharge was comparatively low (0.24 m/yr). The average porewater concentration, however, reached almost 50 mg NO_3-N/L, indicating the influence of the heavy historic nitrogen load. The station's mass load was assigned to the area of the former barnyard.

The partitioning of the study site into areas of differing nitrate mass load is shown in Figure 4.25 and in Table 4.14. Recharge stations 2 and 4 were estimated to represent 43% and 33% respectively of the study site, while Stations 5 and 8 represented the smallest portions of the site.

4.10.2. Total Distributed Nitrate Mass Load

To determine the post-BMP nitrate mass load, the area of the study site represented by each recharge station was multiplied by the station's nitrate mass flux to determine the nitrate mass load across the station's representative area. The total post-BMP nitrate mass load across the site was the sum of these individual stations' mass loads. The post-BMP mass flux values determined from the May 2006 cores were used because of their longer averaging period compared to the other cores. Due to the limited number of pre-BMP nitrate mass flux data, particularly from May 2006 cores, the pre-BMP mass load was determined using the pre-BMP mass flux value from the core at each station in which the distance between $d_{max, BMP}$ and the core bottom was maximized. In other words, the core containing the longest pre-BMP interval was used in order to use the most available data.

At four recharge stations, no pre-BMP mass load estimate was available because $d_{max, BMP}$ exceeded the core depth at all drilling events. As a result, the total site pre-BMP mass load was

determined from the pre-BMP mass flux values where available. The average mass flux for the study site (weighted based on the representative areas of stations where pre-BMP mass flux values were available) was multiplied by the total area of the study site. Because the pre-BMP nitrate mass load estimates were based on data from only four of the eight recharge stations, it was considered to be significantly less representative of field conditions than was the post-BMP mass load estimate. Post-BMP and pre-BMP mass loads were calculated for the five recharge estimates, and both with and without Station 7 which was the only station outside of the BMP implementation area.

The total nitrate mass load below Parcel B based on best recharge estimates was 4.1 t NO_3-N/yr post-BMP implementation, and 2.2 t NO_3-N/yr pre-BMP implementation. Again, the apparent trend in mass load in response to BMPs was unexpected, and was potentially due to the susceptibility of the nitrate mass flux calculations to high recharge rates or high soil nitrate concentrations in the shallow subsurface which could have artificially raised post-BMP values. Furthermore, the length of pre-BMP core available at Stations 2 and 8 ranged from 0.1 to 2.4 m which may have represented only one or two years of historical agricultural production; if this period coincided with a legume crop or a below-average fertilizer application, the long-term pre-BMP nitrate mass flux may have been underestimated.

As described in Section 2.8, previous estimates of nitrate mass load below Parcel B determined by Haslauer (2005) ranged from 1.1 to 2.5 t NO_3-N/yr. These estimates were based on aqueous nitrate concentrations in cores with an average depth of 5.5 m extracted in September 2004, and therefore likely represented a combination of pre- and post-BMP conditions. The fact that the post-BMP nitrate mass load determined in this study was 64% higher than the upper limit of Haslauer's range also suggests that the post-BMP mass load may have been overestimated due to the factors discussed above.

In contrast to the apparent increase in nitrate mass load, the trend in the shallow stored nitrate mass (Table 2.1) suggested a beneficial response to reductions in applied fertilizer, even though the stored mass calculations included soil nitrate data from 0.5 to 1.0 m depth. These stored mass figures were calculated independently of the recharge rate and the magnitude of $d_{max, BMP}$, which may have improved their reliability given the unexpectedly high recharge rates

measured across the site. Overall, the response in stored nitrate mass at each station had a logical connection to crops and geology: noticeable decreases in stored mass occurred where a significant fertilizer reduction associated with a switch to a grass crop was implemented over an unsaturated zone of sand and gravel as at Stations 1, 3 and 6. More stable trends in stored mass were observed where corn was planted over fine-grained material (Stations 2 and 4) or where there was a consistent grass crop (Station 5).

The nitrate mass load and stored nitrate mass data presented differing responses of the agricultural system to the implementation of the BMP. However, the mass load method was hindered by its dependence on accurate recharge estimates, given the difficulty in obtaining reproducible recharge estimates in this study, and on deep soil nitrate data representing pre-BMP conditions. The mass load method would have been considerably more robust if a core representing exclusively pre-BMP conditions, i.e. extracted before BMP implementation in 2003, were available at each station. In this case, the comparison of pre- and post-BMP nitrate mass loads would not be dependent on the proper estimation of $d_{max,\ BMP}$ which is in turn dependent on the recharge rate. However, within the constraints of this study where there is no core data from 2003, the nitrate mass load method appears significantly more limited than the stored nitrate mass comparison.

Table 4.1. Comparison of stored nitrate mass over a common depth in successive cores at each recharge station, and associated crop cover.

		Feb./05	Mar./05	Nov./05	May/06
Station 1	Comparison depth (m)	0.5 - 3.0			
	Cumulative N ($g\ NO_3\text{-}N/m^2$)			3.1	2.9
	Most recent crop			Oats/Grass	Grass
Station 2	Comparison depth (m)	0.5 - 2.9			
	Cumulative N ($g\ NO_3\text{-}N/m^2$)	7.1	7.3	6.1	9.1
	Most recent crop	Wheat/clover	Wheat/clover	Corn	Corn
Station 3	Comparison depth (m)	0.5 - 2.3			
	Cumulative N ($g\ NO_3\text{-}N/m^2$)	7.1	7.4	1.9	3.1
	Most recent crop	Wheat	Wheat	Oats/Grass	Grass
Station 4	Comparison depth (m)	0.5 - 2.6			
	Cumulative N ($g\ NO_3\text{-}N/m^2$)	6.2	5.0	5.1	8.0
	Most recent crop	Wheat/clover	Wheat/clover	Corn	Corn
Station 5	Comparison depth (m)	0.5 - 2.8			
	Cumulative N ($g\ NO_3\text{-}N/m^2$)	3.7	4.7	3.2	3.5
	Most recent crop	Grass	Grass	Grass	Grass
Station 6	Comparison depth (m)	0.5 - 2.8			
	Cumulative N ($g\ NO_3\text{-}N/m^2$)	14.8	15.3	9.5	2.9
	Most recent crop	Wheat/clover	Wheat/clover	Oats/Grass	Grass
Station 7	Comparison depth (m)	0.5 - 3.8			
	Cumulative N ($g\ NO_3\text{-}N/m^2$)		13.4	12.9	8.9
	Most recent crop		Corn	Soybean	Soybean
Station 8	Comparison depth (m)	0.5 - 2.6			
	Cumulative N ($g\ NO_3\text{-}N/m^2$)	12.4		19.5	23.4
	Most recent crop	Wheat/clover	Wheat/clover	Corn	Corn

Table 4.2. Field- and model-estimated recharge rates and final recharge rate estimates. All estimates were scaled from the measurement period indicated to a one-year interval. Incomplete estimates due to missing water content data are shaded, although still scaled to one year. Notes: a) Station 2 standard deviation estimated from Station 8 standard deviation.

Station	Recharge estimate, Bromide tracer method (m/yr)	Recharge estimate, Nitrate tracer method (m/yr)		Recharge estimate, Zero-flux plane method (m/yr)	Recharge estimate, Water balance (m/yr)	Recharge estimate, HELP model (m/yr)	Recharge estimate, SHAW model (m/yr)	Final recharge estimates (m/yr)		
	Jul./05 to May/06	Apr./05 to Nov./05	Nov./05 to May/06	Apr./05 to May/06	May/05 to May/06	May/05 to May/06	May/05 to May/06	Best	Low	High
1	0.43 ± 0.09			0.05	0.19	0.34	0.05	0.43	0.34	0.52
2	0.21 ± 0.03[a]	0.48		0.04	0.16	0.29	0.05	0.21	0.18	0.27
3	0.59 ± 0.08	0.15		0.17	0.19	0.29	0.02	0.59	0.40	0.67
4	0.52 ± 0.04		0.70	0.11	0.16	0.28	0.01	0.52	0.38	0.56
5	0.51 ± 0.08			0.50	0.19	0.29	0.14	0.51	0.36	0.59
6	0.43 ± 0.06	0.20		0.11	0.19	0.33	0.05	0.43	0.35	0.49
7	0.64 ± 0.08			0.30	0.17	0.34	0.01	0.64	0.45	0.72
8	0.27 ± 0.03		0.00	0.24	0.16	0.33	0.00	0.27	0.24	0.32

Table 4.3. Tracer centre of mass, soil volumetric water content (VWC), recharge rate and mass recovery related to the bromide tracer method.

	Nov./05 core				May/06 core				Jul./05 to May/06
Station	Centre of mass (m)	Ave. VWC (m^3/m^3)	Recovered bromide (kg) (proportion of applied)	Recharge estimate, Tracer method (m/month) Jul./05 to Nov./05	Centre of mass (m)	Ave. VWC (m^3/m^3) (std. dev.)	Recovered bromide (kg) (proportion of applied)	Recharge estimate, Tracer method (m/month) Nov./05 to May/06 (± range)	Recharge estimate, Tracer method (m/year) (± range)
1	0.32	0.34	7.41 (183%)	0.027	1.77	0.16 (0.05)	0.44 (11%)	0.042 ± 0.016	0.43 ± 0.09
2	0.35	0.36	0.44 (11%)	0.032	0.49	0.34	0.98 (24%)	0.009	0.21
3	0.38	0.33	0.74 (18%)	0.031	1.88	0.24 (0.04)	1.48 (37%)	0.065 ± 0.011	0.59 ± 0.08
4	0.48	0.33	0.41 (10%)	0.040	1.38	0.27 (0.03)	0.70 (17%)	0.044 ± 0.005	0.52 ± 0.04
5	0.39	0.32	1.99 (49%)	0.031	1.88	0.18 (0.04)	0.29 (7%)	0.049 ± 0.011	0.51 ± 0.08
6	0.51	0.32	4.36 (108%)	0.041	1.74	0.15 (0.04)	0.53 (13%)	0.034 ± 0.009	0.43 ± 0.06
7	0.47	0.36	8.40 (207%)	0.042	2.11	0.20 (0.04)	1.23 (30%)	0.060 ± 0.012	0.64 ± 0.08
8	0.29	0.32	4.46 (110%)	0.023	0.79	0.26 (0.04)	1.41 (35%)	0.024 ± 0.004	0.27 ± 0.03

Table 4.4. Unsaturated zone water balance (UZWB) recharge estimates, including date and magnitude of each high and low soil water storage event. Incomplete estimates due to missing water content data are shaded.

		Recharge Event 1		Recharge Event 2		Recharge Event 3				
Station	Meas. Depth (m)	Date of high meas.	Date of low meas.	Date of high meas.	Date of low meas.	Date of high meas.	Date of low meas.	Missing data	Total recharge depth (m)	Recharge rate (m/yr)
1	2.23	13/04/05	26/10/05					7/12/05 and on	0.030	0.045
2	3.98	13/04/05	05/10/05					17/11/05 and on	0.038	0.041
3	5.66	13/04/05	26/10/05	31/01/06	08/03/06	17/03/06	25/05/06		0.189	0.170
4	3.86	13/04/05	27/09/05	31/01/06	08/03/06			17/3/06 and on	0.103	0.111
5	5.70	13/04/04	10/11/05	23/02/06	08/03/06	17/03/06	25/05/06		0.557	0.499
6	3.74	13/04/05	10/11/05	31/01/06	08/03/06	17/03/06	25/05/06		0.127	0.114
7	5.47	09/05/05	10/11/05	31/01/06	08/03/06	21/03/06	25/05/06		0.316	0.303
8	3.09	13/04/05	10/11/05	31/01/06	13/03/06			13/3/06 and on	0.216	0.237

Table 4.5. Water balance components (precipitation, evapotranspiration (ET) and surplus water) under the various crop conditions across study site in 2005-06. Negative water surplus values indicate a decrease in soil water storage with no recharge. Notes: a) Grass crop in Field 3a approximated as the oats/grass crop.

Field	Stations	2005-06 Field Cover	Start Date	End Date	Precip. (m)	ET (m)	Surplus water (P – ET) (m)	Max. recharge rate (m/yr) May 1/05 – May 1/06
3a[a], 3b, 7	1, 3, 5[a], 6	Grass/Oats	01/05/2005	24/11/2005	0.621	0.550	0.071	0.187
		Frozen/Snow	25/11/2005	01/04/2006	0.258	0.128	0.130	
		Grass	02/04/2006	01/05/2006	0.091	0.105	-0.014	
				SUM	0.970	0.783	0.187	
4, 5, 6	2, 4, 8	Bare soil	01/05/2005	14/05/2005	0.035	0.034	0.001	0.160
		Corn	15/05/2005	31/10/2005	0.459	0.527	-0.069	
		Residue	01/11/2005	30/11/2005	0.167	0.049	0.118	
		Frozen/Snow	01/12/2005	07/03/2006	0.163	0.097	0.066	
		Residue	08/03/2006	01/05/2006	0.146	0.102	0.044	
				SUM	0.970	0.809	0.160	
1, Old Stage	7	Bare soil	01/05/2005	26/05/2005	0.039	0.060	-0.021	0.165
		Soybean	27/05/2005	14/10/2005	0.410	0.457	-0.047	
		Winter Wheat	15/10/2005	30/11/2005	0.211	0.080	0.131	
		Frozen/Snow	01/12/2005	07/03/2006	0.163	0.097	0.066	
		Winter Wheat	08/03/2006	01/05/2006	0.146	0.110	0.036	
				SUM	0.969	0.804	0.165	
2		Winter Wheat	01/05/2005	05/10/2005	0.440	0.562	-0.122	0.062
		Bare soil	06/10/2005	30/11/2005	0.220	0.093	0.127	
		Frozen/Snow	01/12/2005	07/03/2006	0.163	0.097	0.066	
		Bare soil	08/03/2006	01/05/2006	0.146	0.155	-0.009	
				SUM	0.969	0.907	0.062	

Table 4.6. Initial estimate of hydraulic parameters based on laboratory analyses and adjusted as necessary based on literature data (Campbell (n.d.) and Leij et al. (1996)) and SPAW program results. Notes: a) b = pore size distribution index; b) ψ = air entry pressure; c) K_{sat} = saturated hydraulic conductivity; d) ρ_b = bulk soil density; e) n= porosity; f) organic matter content unknown and assumed to be zero. See Appendix H for background data from laboratory, literature and SPAW program.

Material	b[a]	ψ[b] (m)	K_{sat}[c] (cm/s)	ρ_b[d] (kg/m^3)	n[e]	% sand	% silt	% clay	% org. matter	Field capacity (m^3/m^3)	Wilting point (m^3/m^3)
Clay-silt till	5	-0.4	7.E-06	1980	0.23	35	45	20	0[f]	0.14	0.06
Sandy silt	4	-0.3	4.E-05	1700	0.34	35	50	15	0[f]	0.19	0.07
Silt	3.4	-0.3	7.E-05	1723	0.35	5	85	10	0[f]	0.17	0.06
Fine sand	1.5	-0.1	7.E-04	1860	0.3	95	0	5	0[f]	0.03	0.002
Silty sand	3.5	-0.1	7.E-05	1690	0.36	55	30	15	0[f]	0.13	0.04
WG sand	3	-0.1	7.E-04	1740	0.34	90	0	10	0[f]	0.10	0.03
Guelph Honeywood soil											
0 - 0.15 m	4.5	-0.55	1.E-02	1100	0.59	20	55	25	5	0.39	0.17
0.15 - 0.28 m	4	-0.55	3.E-03	1380	0.48	36	49	15	2.5	0.31	0.12
0.28 - 0.45 m	4	-0.45	7.E-04	1510	0.43	43	43	14	1	0.26	0.10
0.45 - 0.6 m	5	-0.45	5.E-05	1470	0.45	44	28	28	2	0.30	0.14
0.6 - 1.0 m	4.7	-0.3	6.E-05	1590	0.40	48	33	19	0.5	0.24	0.11
Embro soil											
0 - 0.38 m	3.2	-0.7	4.E-02	1170	0.56	20	67	13	5	0.34	0.10
0.38 - 0.58 m	4	-0.4	8.E-04	1430	0.46	32	51	17	2.5	0.27	0.10
0.58 - 0.75 m	4.5	-0.4	1.E-04	1450	0.45	24	42	34	1	0.28	0.12
0.75 - 1.0 m	5.5	-0.35	7.E-06	1660	0.37	34	46	20	0.5	0.25	0.12
1.0 - 1.3 m	3.3	-0.35	5.E-03	1640	0.38	72	27	1	0.5	0.19	0.06
Fox soil											
0 - 0.3 m	3.1	-0.35	1.E-02	1370	0.48	91	2	7	3	0.23	0.07
0.3 - 0.6 m	3.2	-0.25	5.E-03	1630	0.39	91	2	7	1	0.17	0.05
0.6 - 0.75 m	4.5	-0.2	5.E-04	1620	0.39	65	23	12	0.5	0.21	0.09
0.75 - 1.0 m	3.7	-0.15	3.E-03	1780	0.33	91	3	6	0	0.14	0.05

Table 4.7. SHAW model water balance components from May 1/05 to May 1/06

Station	Precip. (m)	Evapo-transpiration (m) (proportion of precip. in parentheses)	Run-off (m)	Recharge (m)	Change in storage (m)
1	0.969	0.868 (90%)	0.125	0.048	-0.056
2	0.969	0.900 (93%)	0.166	0.052	-0.113
3	0.969	0.864 (89%)	0.146	0.015	-0.046
4	0.969	0.886 (91%)	0.108	0.014	-0.020
5	0.969	0.722 (75%)	0.140	0.135	-0.014
6	0.969	0.872 (90%)	0.062	0.048	0.005
7	0.969	0.859 (89%)	0.150	0.010	-0.029
8	0.969	0.942 (97%)	0.059	0.000	-0.019

Table 4.8. Results of SHAW model sensitivity analysis, expressed as water balance components from May 1, 2005 to May 1, 2006 at Stations 4 and 6.

	Station 4					Station 6				
Modification	Prec. (m)	ET (m)	Run-off (m)	Δ storage (m)	Rech. (m)	Prec. (m)	ET (m)	Run-off (m)	Δ storage (m)	Rech. (m)
Base run	0.969	0.886	0.108	-0.020	0.014	0.969	0.872	0.062	0.005	0.048
Increase topsoil Ks (factor of ten)	Model did not converge					0.969	0.890	0.019	0.003	0.069
Decrease topsoil Ks (factor of ten)	0.969	0.886	0.205	-0.006	0.014	0.969	0.858	0.095	0.001	0.031
Increase all Ks (factor of ten)	0.969	0.888	0.165	-0.121	0.028	0.969	0.881	0.010	-0.027	0.118
Decrease all Ks (factor of ten)	0.969	0.896	0.097	-0.011	0.001	0.969	0.861	0.086	0.032	0.006
Increase b (one unit)	0.969	0.867	0.124	0.124	0.011	0.969	0.846	0.057	0.027	0.040
Decrease b (one unit)	Model did not converge					0.969	0.866	0.132	-0.043	0.034
More negative ψ (0.1 m)	0.969	0.905	0.088	0.009	0.014	0.969	0.839	0.074	-0.012	0.068
Less negative ψ (0.1 m)	0.969	0.885	0.097	0.009	0.013	0.969	0.891	0.061	-0.003	0.035
Unit gradient	0.969	0.88	0.112	-0.012	0.008	0.969	0.866	0.118	-0.024	0.027
Increase crop growth (30 days; one LAI unit)	0.969	0.924	0.156	-0.115	0.014	0.969	0.883	0.016	0.004	0.076
Decrease crop growth (30 days; one LAI unit)	0.969	0.863	0.138	-0.014	0.014	0.969	0.875	0.029	0.007	0.073
Remove crop	0.969	0.794	0.113	0.060	0.014	0.969	0.856	0.058	-0.001	0.073
Maximize albedo	0.969	0.863	0.095	0.027	0.013	0.969	0.835	0.188	-0.050	0.021

Table 4.9. HELP model recharge rates from base simulations and sensitivity analyses, May 1/05 to May 1/06

	Recharge estimate (m/yr)								
Station	Base simulation (model-generated initial VWC)	Base simulation (user-input initial VWC)	Increase topsoil Ks (factor of ten)	Decrease topsoil Ks (factor of ten)	Increase all Ks (factor of ten)	Decrease all Ks (factor of ten)	Increase crop growth (30 days; one LAI unit)	Decrease crop growth (30 days; one LAI unit)	Meteorologic data from weather generator
1	0.34	0.34							
2	0.29	0.29							
3	0.29	0.27							
4	0.28	0.25	0.31	0.23	0.32	0.23	0.28	0.28	0.30
5	0.29	0.23							
6	0.33	0.33	0.37	0.29	0.38	0.29	0.34	0.32	0.34
7	0.34	0.33							
8	0.33	0.33							

Table 4.10. Anticipated depth of BMP effects based on various recharge estimates. Note: a) No BMPs implemented at Station 7.

		Anticipated depth of BMP effects (m)				
Station	Core date	Best estimate	Lower estimate	Upper estimate	HELP estimate	Water balance estimate
1	Nov./05	6.6	5.2	8.0	5.2	2.9
	May/06	7.9	6.2	9.5	6.2	3.5
2	Mar./05	1.8	1.4	2.3	2.5	1.3
	Nov./05	2.4	1.9	3.0	3.2	1.8
	May/06	2.8	2.3	3.6	3.9	2.1
3	Mar./05	6.8	4.3	7.7	2.8	1.6
	Nov./05	8.9	6.1	10.1	4.0	2.2
	May/06	10.6	7.2	12.0	5.2	2.9
4	Mar./05	4.8	3.1	5.1	2.2	1.3
	Nov./05	6.2	4.5	6.7	2.9	1.6
	May/06	7.4	5.4	8.0	4.0	1.9
5	Mar./05	6.0	4.5	7.0	3.8	2.5
	Nov./05	7.8	5.5	9.0	4.7	3.4
	May/06	9.3	6.6	10.8	5.4	3.8
6	Mar./05	6.8	5.5	7.7	5.2	2.9
	Nov./05	8.8	7.2	10.1	6.8	3.9
	May/06	10.5	8.6	12.0	8.1	4.7
7[a]	May/05	6.8	4.8	7.7	3.7	1.6
	Nov./05	8.5	5.9	9.5	4.5	2.1
	May/06	10.1	7.1	11.4	5.4	2.6
8	Feb./05	2.3	2.0	2.7	2.8	1.4
	Nov./05	2.8	3.7	3.1	3.8	1.9
	May/06	3.7	3.3	4.4	4.5	2.2

Table 4.11. Average post-BMP and pre-BMP porewater NO_3 concentration in all cores based on the $d_{max,BMP}$ from various recharge estimates. Pre-BMP value in parentheses follows post-BMP value and is indicated as not available (n/a) where the depth of BMP impacts exceeded the core depth. Note: a) No BMPs implemented at Station 7.

		Average porewater concentration (mg NO_3-N/L)				
Station	Core date	Best estimate	Lower estimate	Upper estimate	HELP estimate	Water balance estimate
1	Nov./05	7.3 (n/a)	7.3 (n/a)	7.3 (n/a)	7.3 (n/a)	7.3 (n/a)
	May/06	8.1 (n/a)	8.1 (n/a)	8.1 (n/a)	8.1 (n/a)	8.1 (n/a)
2	Mar./05	11.5 (13.2)	12.9 (12.0)	11.8 (13.2)	12.3 (12.7)	15.2 (11.8)
	Nov./05	10.8 (9.4)	11.4 (9.4)	10.9 (9.0)	10.8 (8.8)	11.5 (9.4)
	May/06	16.4 (14.6)	17.3 (13.5)	16.3 (n/a)	16.3 (n/a)	17.7 (13.1)
3	Mar./05	12.6 (10.0)	13.3 (12.9)	12.6 (9.8)	16.7 (11.7)	21.2 (11.3)
	Nov./05	5.4 (n/a)	5.4 (n/a)	5.4 (n/a)	5.1 (6.1)	4.8 (5.8)
	May/06	9.8 (n/a)	9.8 (n/a)	9.8 (n/a)	9.8 (n/a)	8.3 (n/a)
4	Mar./05	10.2 (n/a)	9.6 (16.8)	10.2 (n/a)	9.7 (11.7)	14.6 (9.2)
	Nov./05	7.3 (n/a)	7.4 (3.1)	7.3 (n/a)	9.0 (5.1)	12.8 (5.0)
	May/06	17.4 (n/a)	17.4 (n/a)	17.4 (n/a)	17.4 (n/a)	15.2 (19.4)
5	Mar./05	12.2 (11.8)	12.2 (9.9)	12.7 (11.3)	10.9 (10.4)	10.2 (11.0)
	Nov./05	6.0 (n/a)	6.1 (n/a)	6.0 (n/a)	6.5 (1.1)	9.3 (1.6)
	May/06	9.0 (n/a)	9.0 (n/a)	9.0 (n/a)	9.2 (n/a)	9.9 (n/a)
6	Mar./05	46.1 (n/a)	46.1 (n/a)	46.1 (n/a)	46.1 (n/a)	50.1 (36.3)
	Nov./05	26.0 (n/a)	26.0 (n/a)	26.0 (n/a)	26.0 (n/a)	26.0 (n/a)
	May/06	9.7 (n/a)	9.7 (n/a)	9.7 (n/a)	9.7 (n/a)	9.7 (n/a)
7[a]	May/05	19.0 (n/a)	20.5 (15.6)	19.0 (n/a)	20.7 (16.9)	25.9 (17.5)
	Nov./05	17.6 (n/a)	17.3 (n/a)	17.6 (n/a)	19.7 (6.1)	27.8 (11.7)
	May/06	13.6 (n/a)	13.6 (n/a)	13.6 (n/a)	13.6 (n/a)	16.9 (7.1)
8	Feb./05	24.5 (74.3)	23.6 (67.7)	26.6 (90.3)	27.6 (93.4)	21.8 (55.9)
	Nov./05	42.9 (32.3)	42.0 (44.0)	42.6 (n/a)	42.6 (n/a)	32.6 (51.8)
	May/06	48.9 (n/a)	48.9 (n/a)	48.9 (n/a)	48.9 (n/a)	46.3 (n/a)

Table 4.12. Average post-BMP and pre-BMP nitrate mass flux in all cores based on the $d_{max,BMP}$ from various recharge estimates. Pre-BMP value in parentheses follows post-BMP value and is indicated as not available (n/a) where the depth of BMP impacts exceeded the core depth. Note: a) No BMPs implemented at Station 7.

		Nitrate mass flux (g NO_3-N/m^2/yr)				
Station	Core date	Best estimate	Lower estimate	Upper estimate	HELP estimate	Water balance estimate
1	Nov./05	3.1 (n/a)	2.5 (n/a)	3.8 (n/a)	2.5 (n/a)	1.4 (n/a)
	May/06	3.5 (n/a)	2.7 (n/a)	4.2 (n/a)	2.7 (n/a)	1.5 (n/a)
2	Mar./05	2.4 (2.8)	2.2 (2.1)	3.2 (3.6)	3.6 (3.7)	2.4 (1.9)
	Nov./05	2.3 (2.0)	1.9 (1.6)	3.0 (2.4)	3.1 (2.6)	1.8 (1.5)
	May/06	3.4 (3.1)	2.9 (2.3)	4.4 (n/a)	4.7 (n/a)	2.8 (2.1)
3	Mar./05	7.5 (5.9)	5.3 (5.2)	8.5 (6.6)	4.8 (3.4)	4.0 (2.1)
	Nov./05	3.2 (n/a)	2.1 (n/a)	3.6 (n/a)	1.5 (1.8)	0.9 (1.1)
	May/06	5.8 (n/a)	3.9 (n/a)	6.6 (n/a)	2.8 (n/a)	1.6 (n/a)
4	Mar./05	5.3 (n/a)	3.7 (6.4)	5.7 (n/a)	2.7 (3.3)	2.3 (1.5)
	Nov./05	3.8 (n/a)	2.8 (1.7)	4.1 (n/a)	2.5 (1.4)	2.1 (0.8)
	May/06	9.1 (n/a)	6.6 (n/a)	9.8 (n/a)	4.9 (n/a)	2.4 (3.1)
5	Mar./05	6.2 (6.0)	4.4 (3.6)	7.5 (6.7)	3.2 (3.0)	1.9 (2.1)
	Nov./05	3.1 (n/a)	2.2 (n/a)	3.6 (n/a)	1.9 (0.3)	1.8 (0.3)
	May/06	4.6 (n/a)	3.2 (n/a)	5.3 (n/a)	2.7 (n/a)	1.9 (n/a)
6	Mar./05	19.8 (n/a)	16.1 (n/a)	22.6 (n/a)	15.2 (n/a)	9.5 (6.9)
	Nov./05	11.2 (n/a)	9.1 (n/a)	12.8 (n/a)	8.6 (n/a)	4.9 (0.4)
	May/06	4.2 (n/a)	3.4 (n/a)	4.8 (n/a)	3.2 (n/a)	1.9 (n/a)
7[a]	May/05	12.1 (n/a)	9.2 (7.0)	13.7 (n/a)	7.0 (5.7)	4.4 (3.0)
	Nov./05	11.3 (n/a)	7.8 (n/a)	12.7 (n/a)	6.7 (2.1)	4.7 (2.0)
	May/06	8.7 (n/a)	6.1 (n/a)	9.8 (n/a)	4.6 (n/a)	2.9 (1.2)
8	Feb./05	6.6 (20.1)	5.7 (16.3)	8.5 (28.9)	9.1 (30.8)	3.5 (9.0)
	Nov./05	11.6 (8.7)	10.1 (10.6)	13.6 (n/a)	14.0 (n/a)	5.2 (8.3)
	May/06	13.2 (n/a)	11.7 (n/a)	15.7 (n/a)	16.2 (n/a)	7.4 (9.6)

Table 4.13. Comparison of calculated post-BMP nitrate mass flux and average nitrogen application rate

Station	Field	Original post-BMP nitrate mass flux (May cores) (g NO_3-N/m^2/yr)	Average nitrogen fertilizer application rate, 2003-05 (g N/m^2/yr)	Reduced recharge (50%) and 1.0 m root zone		
				Core date	Post-BMP nitrate mass flux (g NO_3-N/m^2/yr)	Pre-BMP nitrate mass flux (g NO_3-N/m^2/yr)
1	7	3.5	3.0	Nov./05	0.80	n/a
				May/06	1.87	n/a
2	4	3.4	6.0	Mar./05	n/a	n/a
				Nov./05	n/a	n/a
				May/06	1.65	1.60
3	3b	5.8	3.0	Mar./05	2.67	3.45
				Nov./05	1.42	1.78
				May/06	2.27	n/a
4	5	9.1	5.6	Mar./05	1.62	3.03
				Nov./05	1.49	1.39
				May/06	4.85	n/a
5	3a	4.6	0	Mar./05	2.94	2.58
				Nov./05	1.82	0.39
				May/06	2.39	n/a
6	7	4.2	3.0	Mar./05	8.14	7.75
				Nov./05	2.36	n/a
				May/06	1.86	n/a
7	Old Stage	8.7	n/a	May/05	5.33	5.52
				Nov./05	3.78	2.46
				May/06	3.80	n/a
8	6	13.2	3.6	Feb./05	n/a	n/a
				Nov./05	2.07	6.88
				May/06	5.12	8.10

Table 4.14. Total distributed pre- and post-BMP nitrate mass loads over study site based on various recharge estimates. Note: a) No BMPs implemented at Station 7.

		Nitrate mass load (t NO_3-N/yr)									
		Best recharge estimate		Low recharge estimate		High recharge estimate		HELP recharge estimate		Water balance recharge estimate	
Station	Area (ha)	Post-BMP mass load	Pre-BMP mass load	Post-BMP mass load	Pre-BMP mass load	Post-BMP mass load	Pre-BMP mass load	Post-BMP mass load	Pre-BMP mass load	Post-BMP mass load	Pre-BMP mass load
1	3.08	0.11	n/a	0.08	n/a	0.13	n/a	0.08	n/a	0.05	n/a
2	32.8	1.13	0.65	0.96	0.53	1.45	1.17	1.55	1.21	0.93	0.49
3	4.58	0.27	0.27	0.18	0.24	0.30	0.30	0.13	0.15	0.07	0.10
4	24.6	2.23	n/a	1.63	1.57	2.40	n/a	1.20	0.81	0.60	0.36
5	1.97	0.09	0.12	0.06	0.06	0.10	0.13	0.05	0.06	0.04	0.04
6	4.89	0.20	n/a	0.17	n/a	0.23	n/a	0.16	n/a	0.09	0.34
7[a]	2.84	0.25	n/a	0.17	0.20	0.28	n/a	0.13	0.16	0.08	0.08
8	0.87	0.11	0.17	0.10	0.14	0.14	0.25	0.14	0.27	0.06	0.08
SUM (Study site)	75.6	4.39	2.27	3.37	3.06	5.03	3.48	3.45	2.97	1.92	1.56
SUM (Parcel B)	72.8	4.14	2.19	3.19	2.94	4.75	3.35	3.32	2.86	1.84	1.50

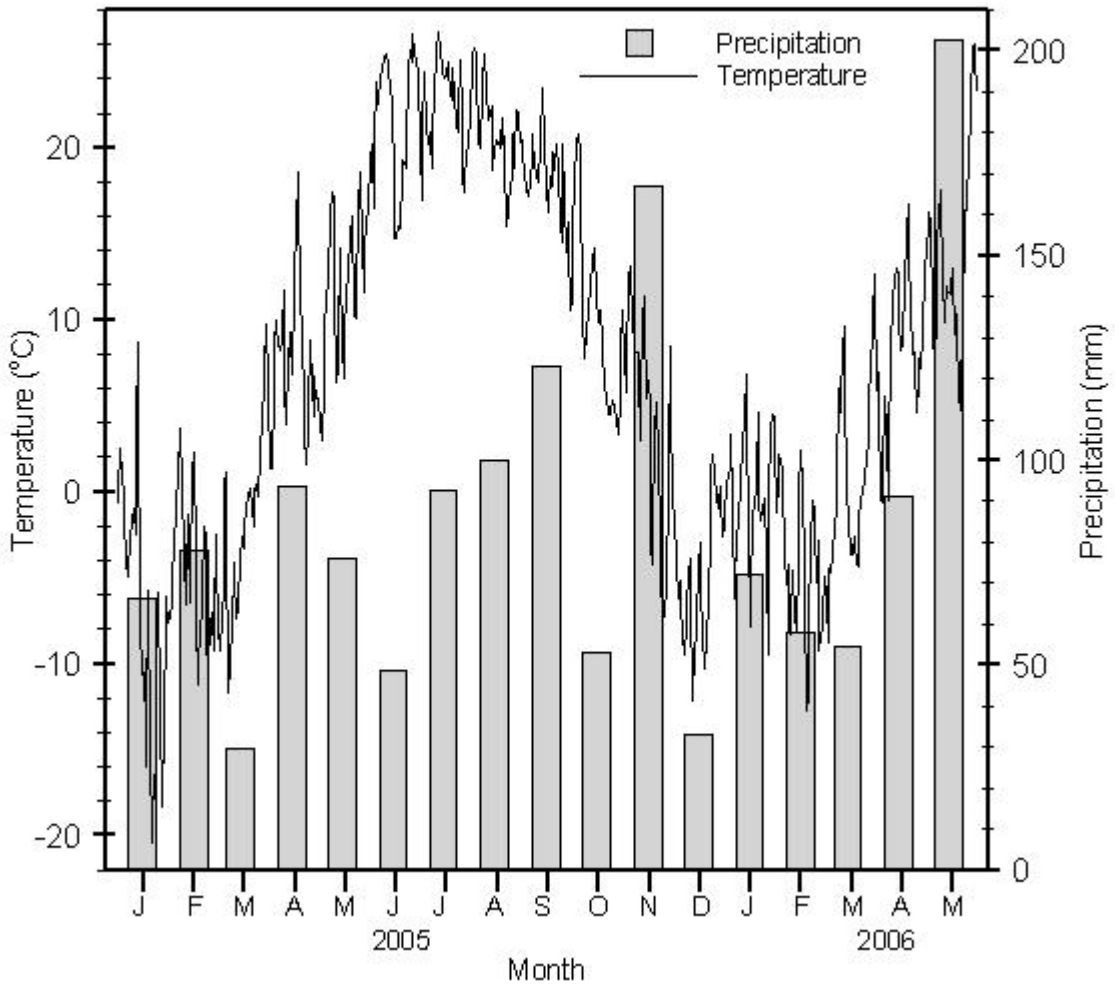

Figure 4.1. Monthly precipitation and daily air temperature observed at the study site meteorological station during the study period.

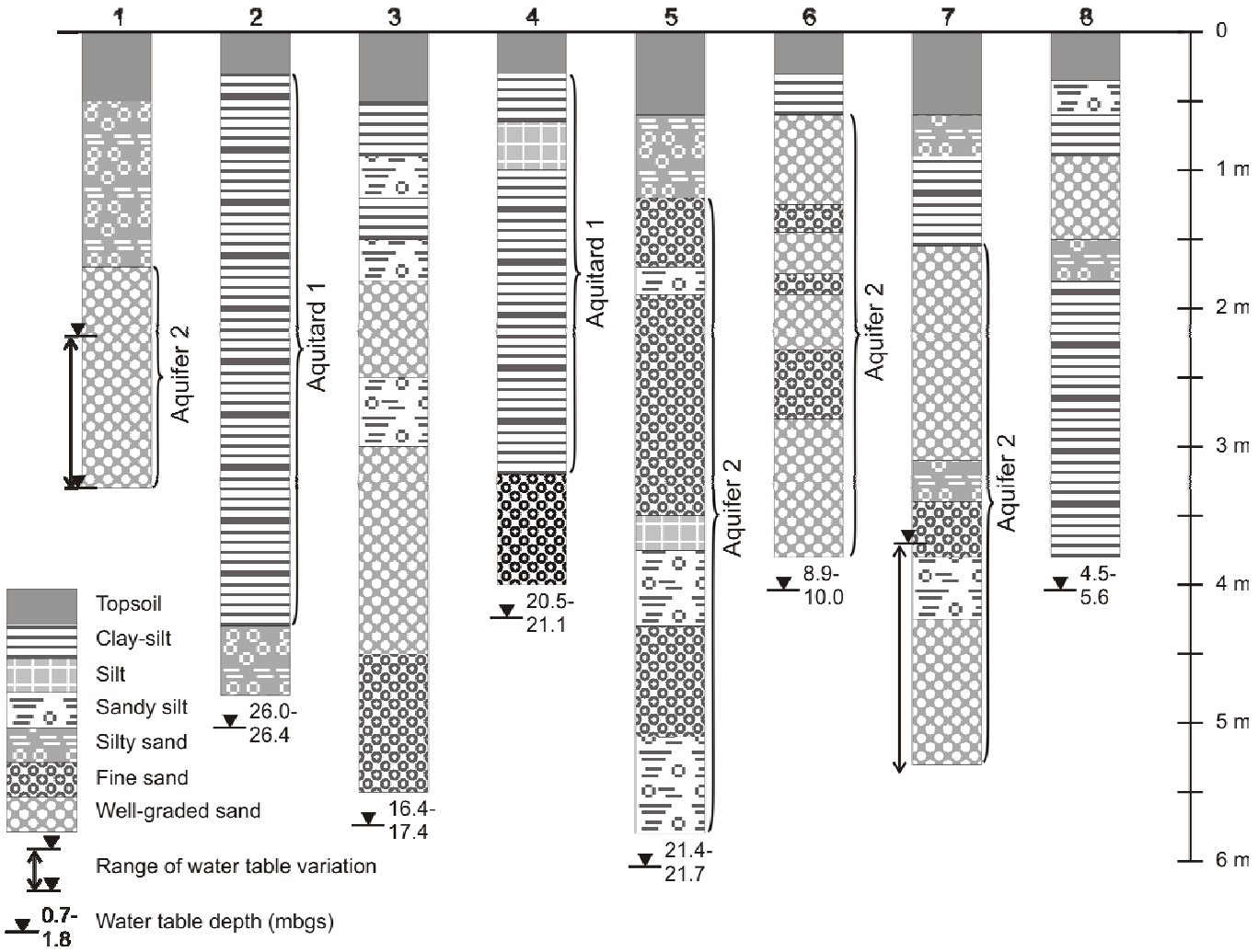

Figure 4.2. Shallow composite geologic log at each recharge station within zone of water content measurement, based on all available cores and water content profiles.

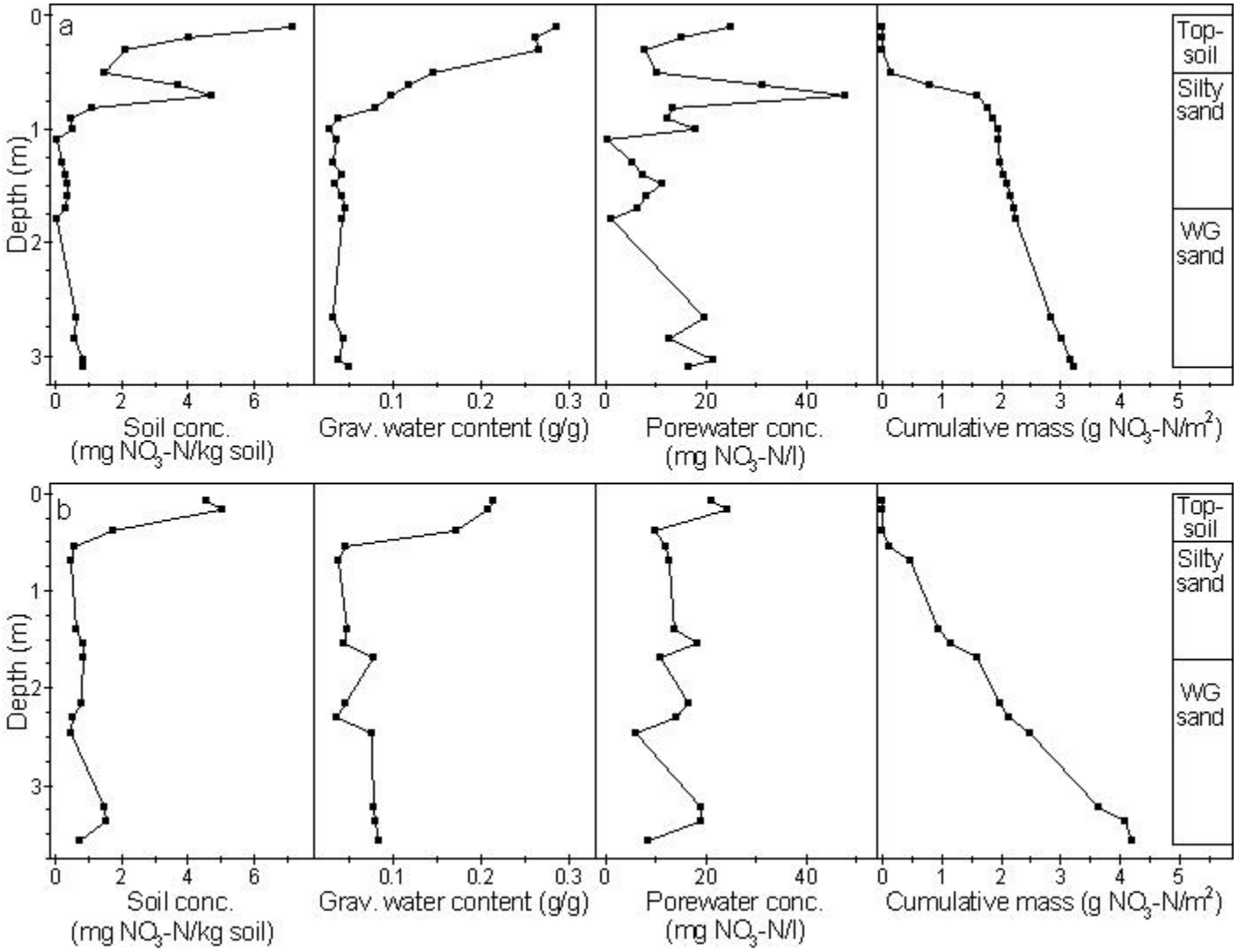

Figure 4.3. Station 1 profiles of bulk soil nitrate concentration, gravimetric soil water content, porewater nitrate concentration and cumulative stored nitrate mass from cores collected in a) November 2005 and b) May 2006.

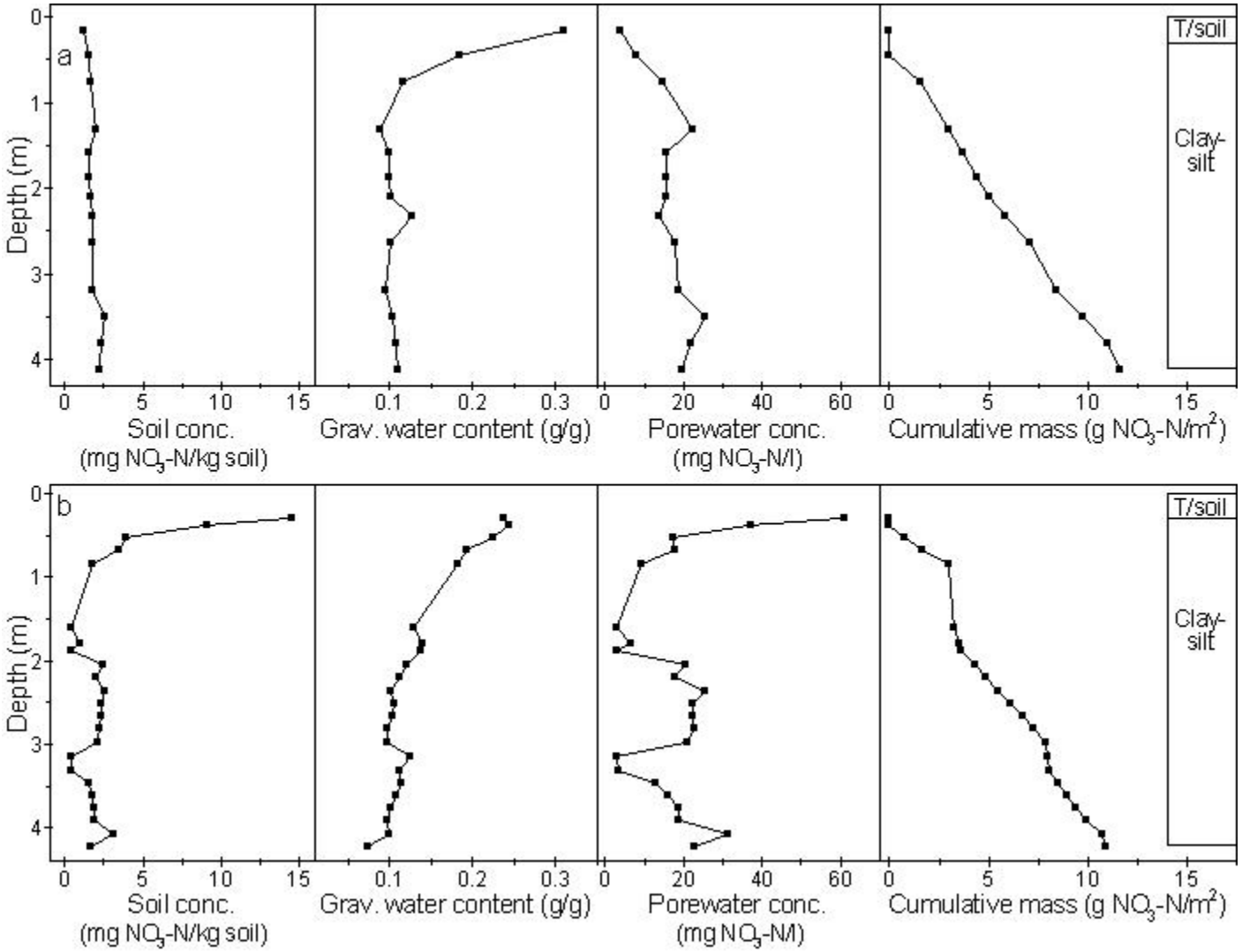

Figure 4.4. Station 2 profiles of bulk soil nitrate concentration, gravimetric soil water content, porewater nitrate concentration and cumulative stored nitrate mass from cores collected in a) February 2005 and b) March 2005.

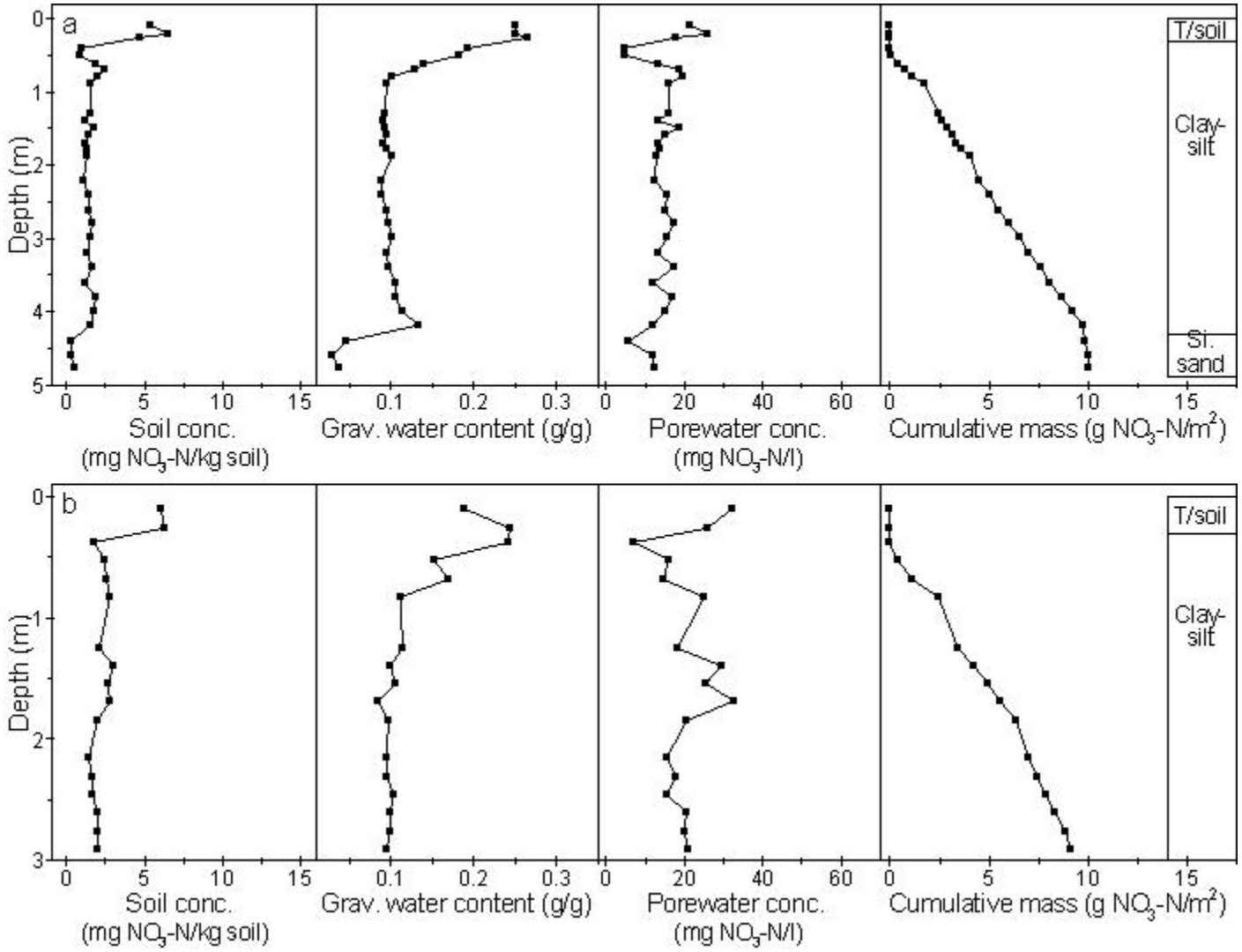

Figure 4.5. Station 2 profiles of bulk soil nitrate concentration, gravimetric soil water content, porewater nitrate concentration and cumulative stored nitrate mass from cores collected in a) November 2005 and b) May 2006.

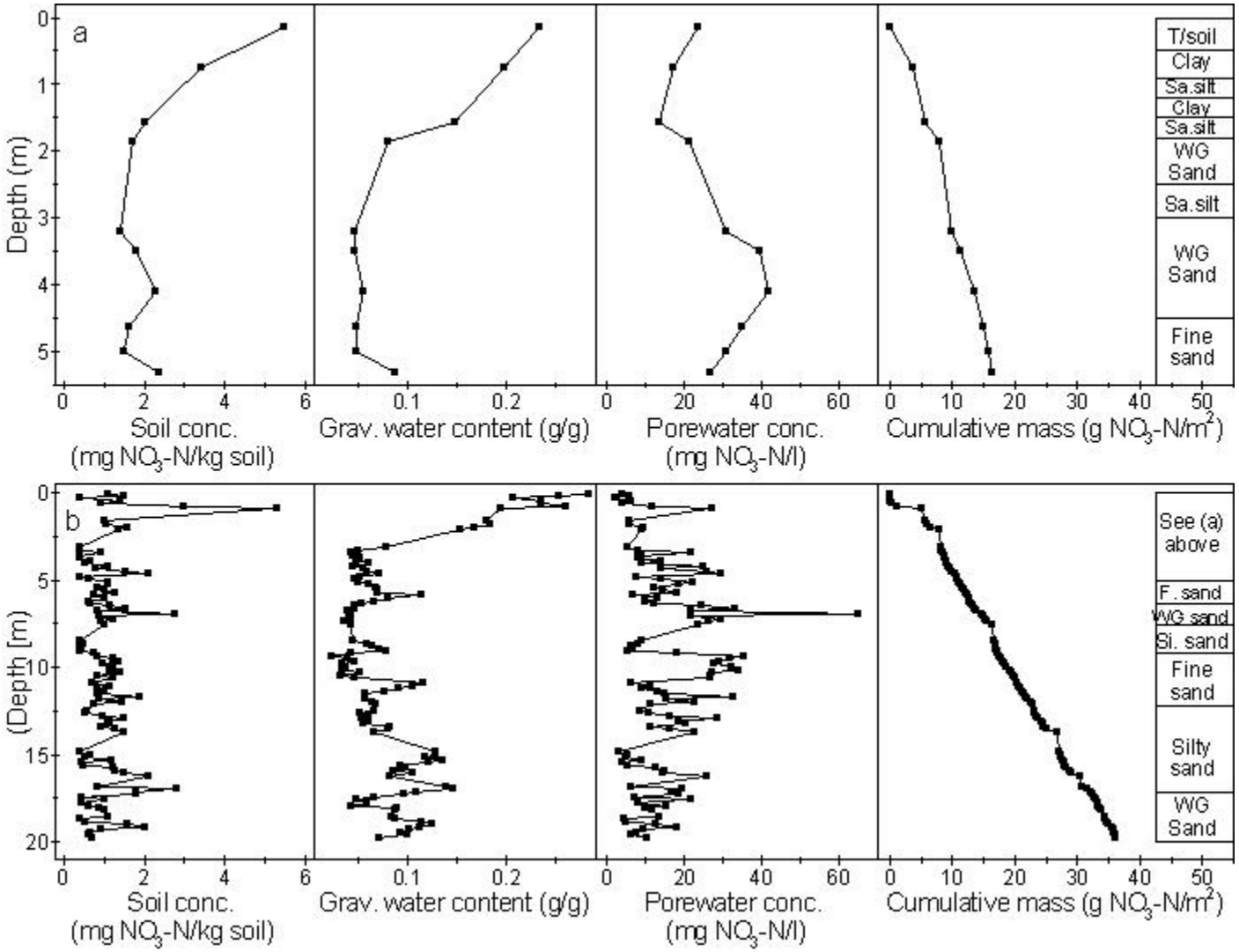

Figure 4.6. Station 3 profiles of bulk soil nitrate concentration, gravimetric soil water content, porewater nitrate concentration and cumulative stored nitrate mass from cores collected in a) February 2005 and b) March 2005.

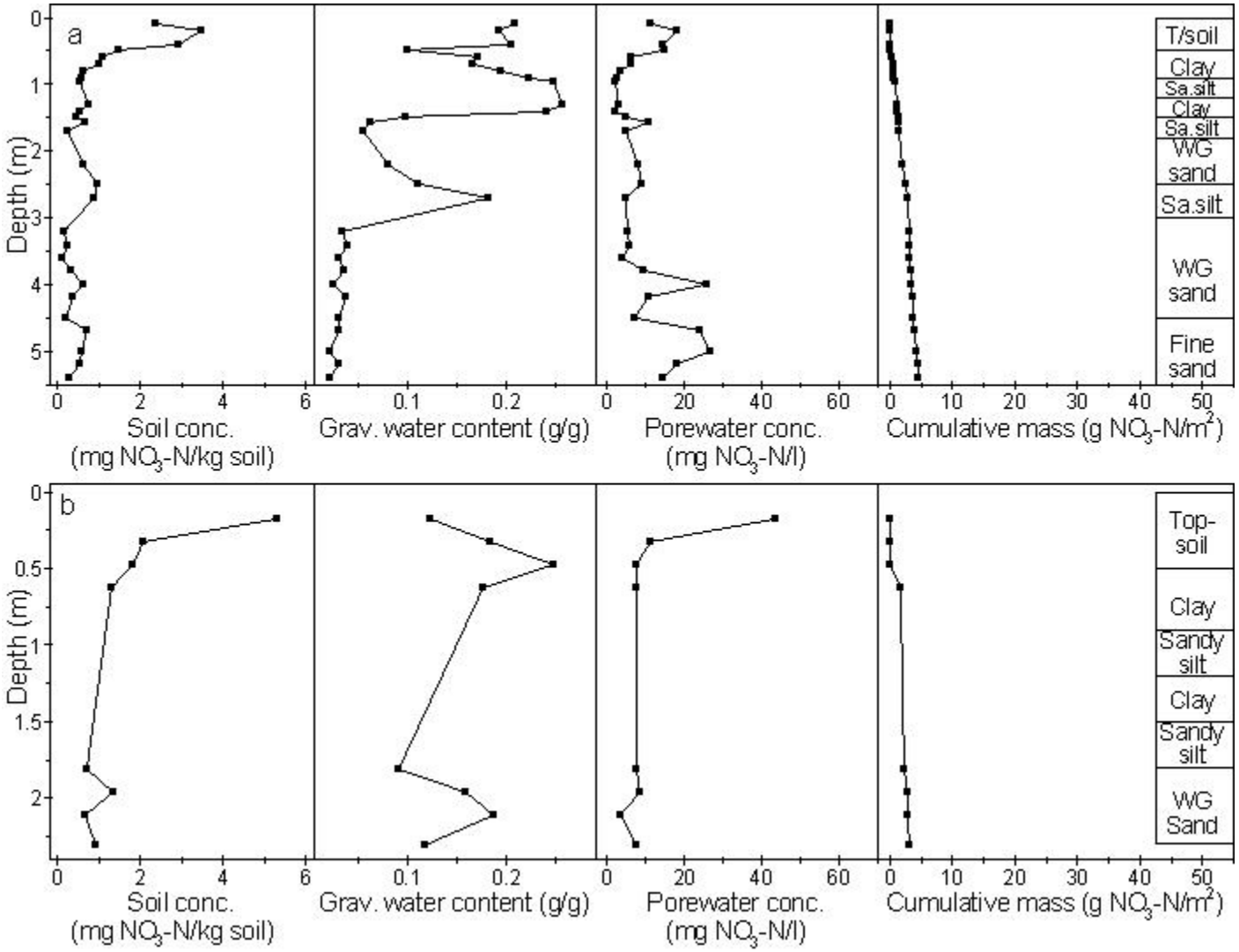

Figure 4.7. Station 3 profiles of bulk soil nitrate concentration, gravimetric soil water content, porewater nitrate concentration and cumulative stored nitrate mass from cores collected in a) November 2005 and b) May 2006.

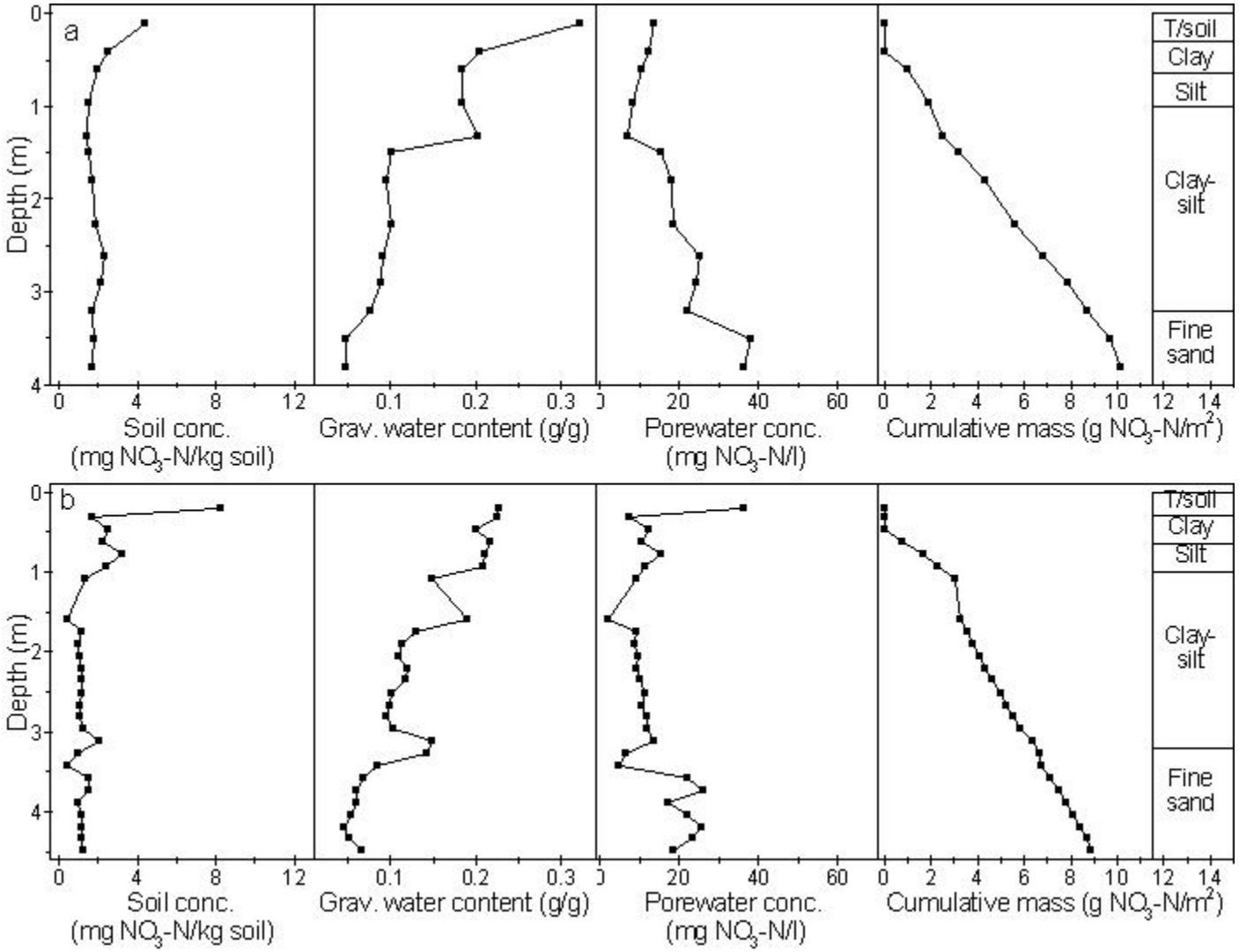

Figure 4.8. Station 4 profiles of bulk soil nitrate concentration, gravimetric soil water content, porewater nitrate concentration and cumulative stored nitrate mass from cores collected in a) February 2005 and b) March 2005.

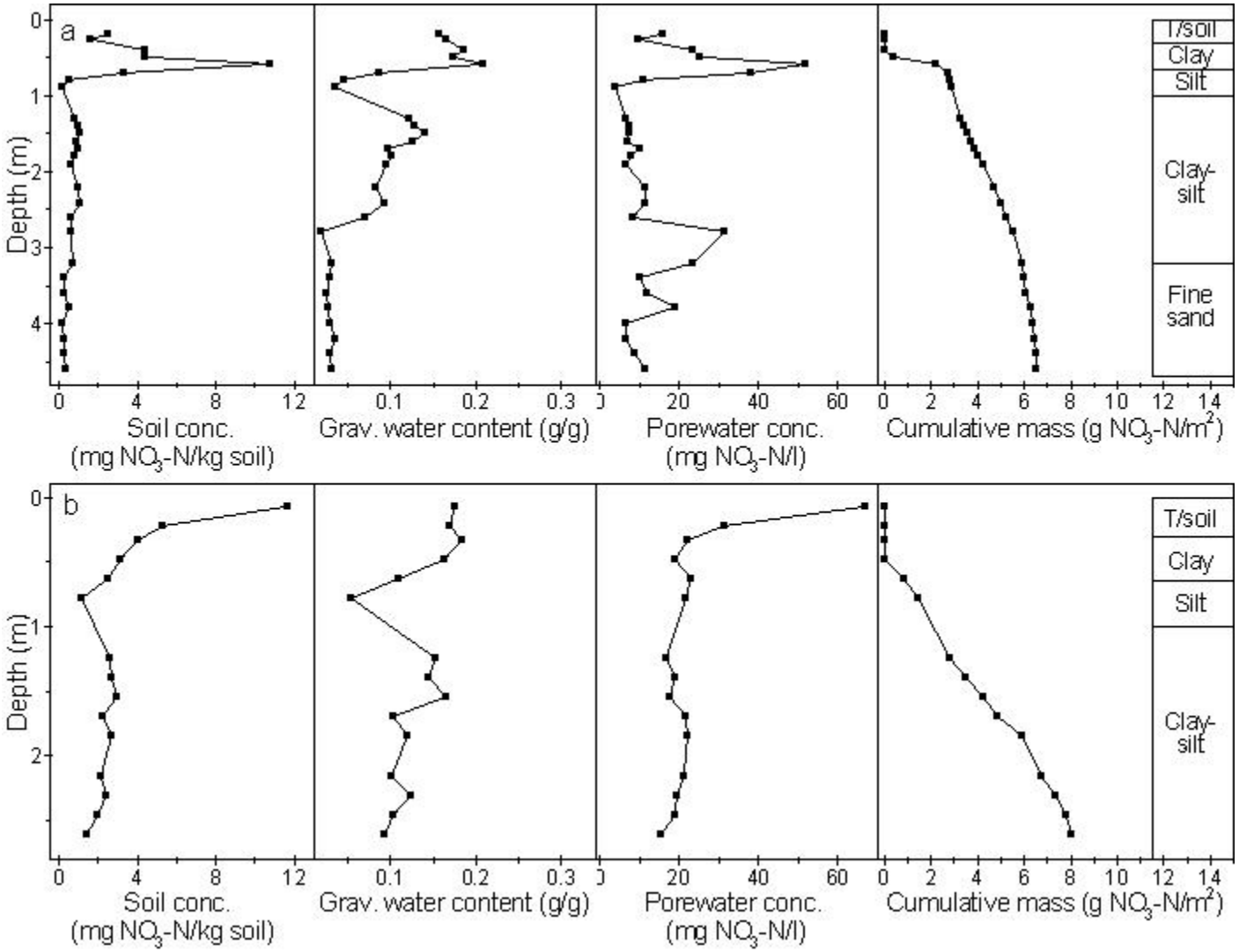

Figure 4.9. Station 4 profiles of bulk soil nitrate concentration, gravimetric soil water content, porewater nitrate concentration and cumulative stored nitrate mass from cores collected in a) November 2005 and b) May 2006.

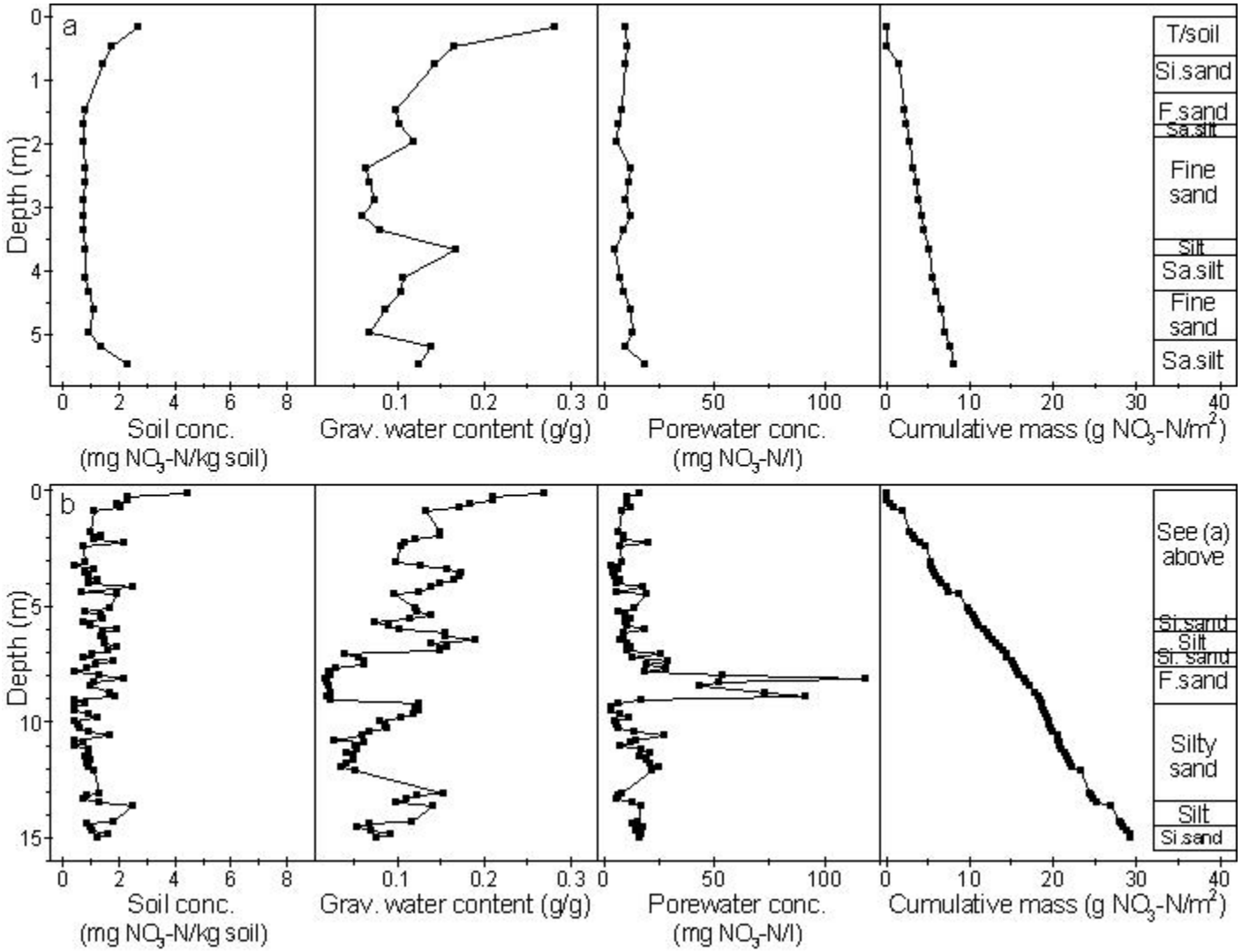

Figure 4.10. Station 5 profiles of bulk soil nitrate concentration, gravimetric soil water content, porewater nitrate concentration and cumulative stored nitrate mass from cores collected in a) February 2005 and b) March 2005.

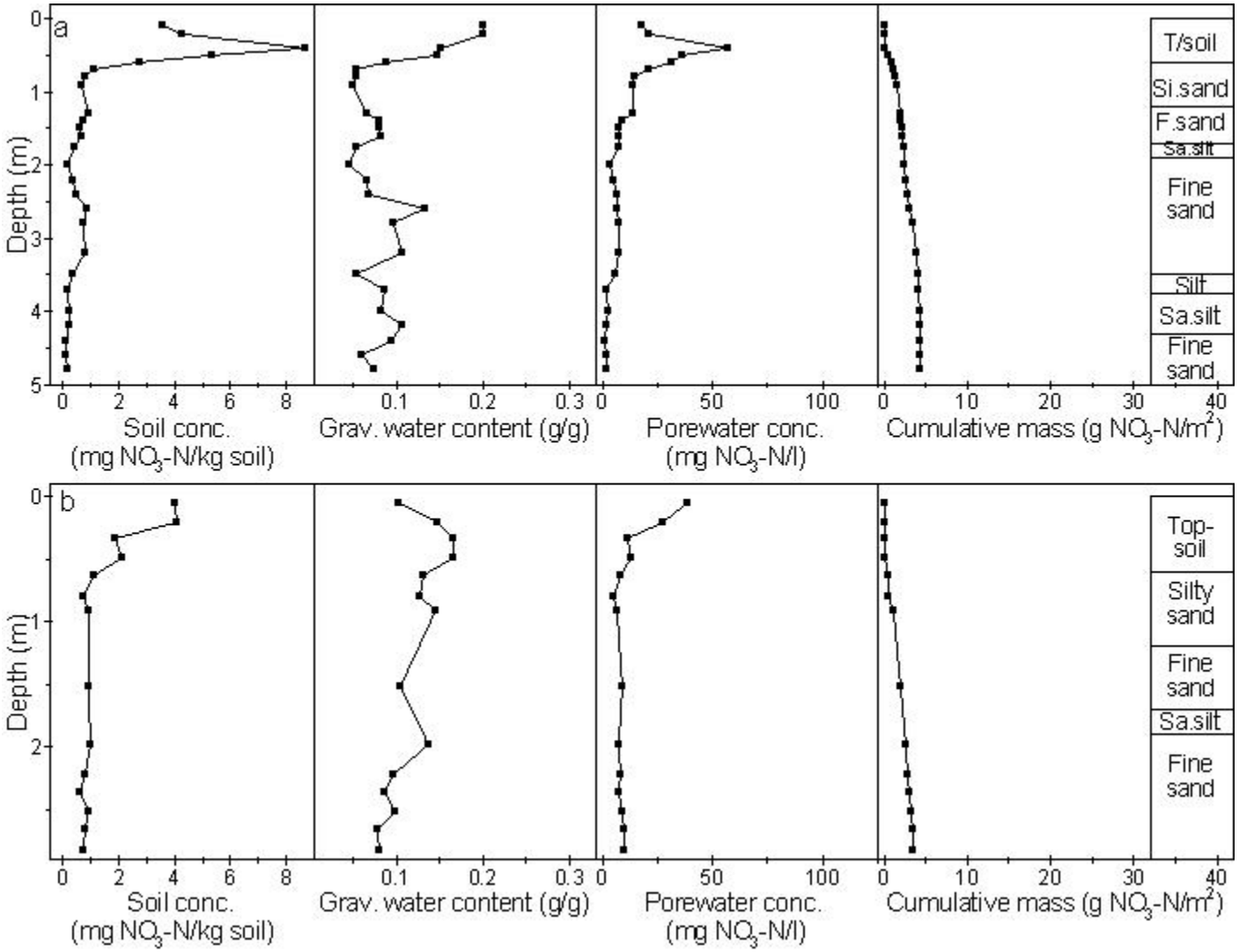

Figure 4.11. Station 5 profiles of bulk soil nitrate concentration, gravimetric soil water content, porewater nitrate concentration and cumulative stored nitrate mass from cores collected in a) November 2005 and b) May 2006.

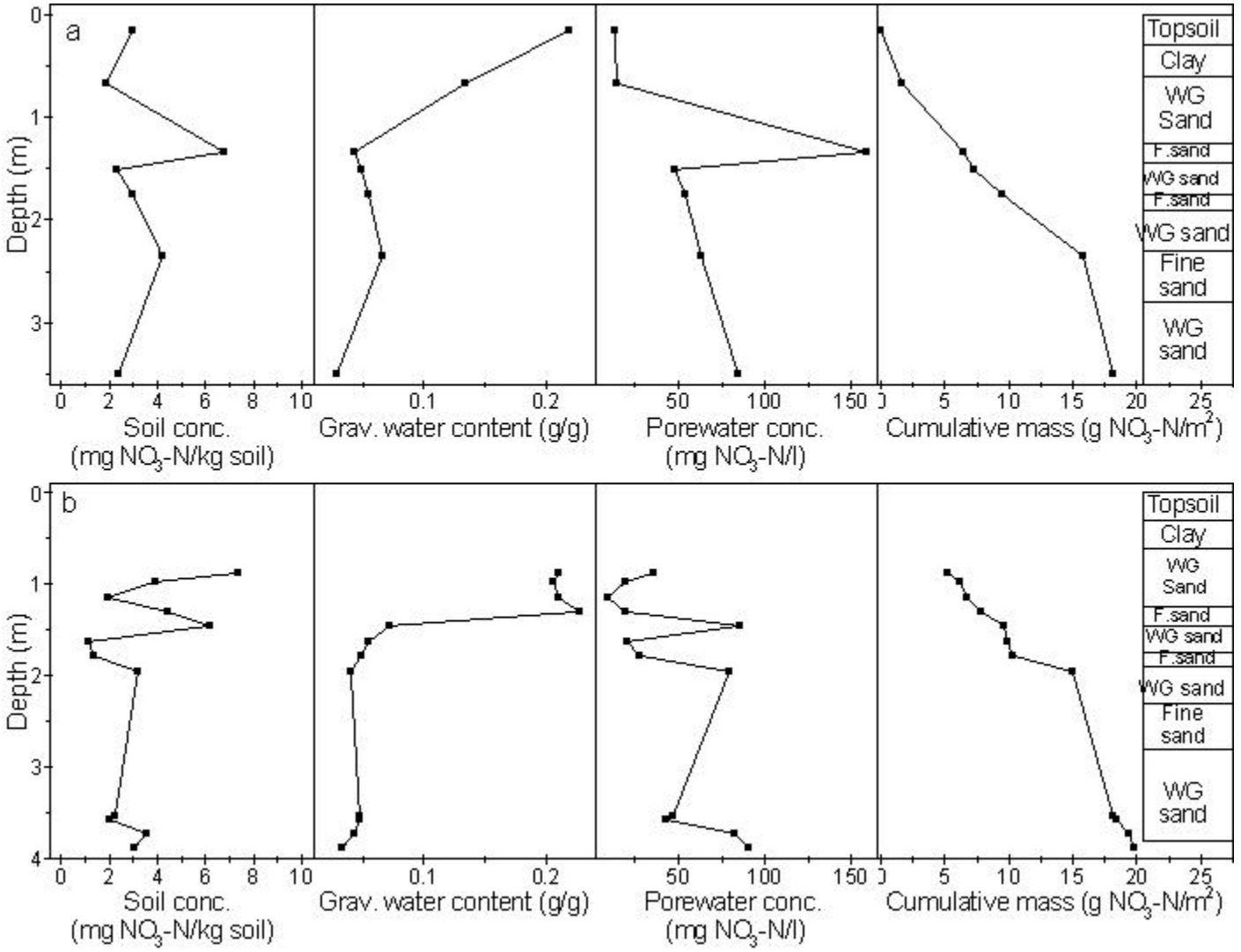

Figure 4.12. Station 6 profiles of bulk soil nitrate concentration, gravimetric soil water content, porewater nitrate concentration and cumulative stored nitrate mass from cores collected in a) February 2005 and b) March 2005.

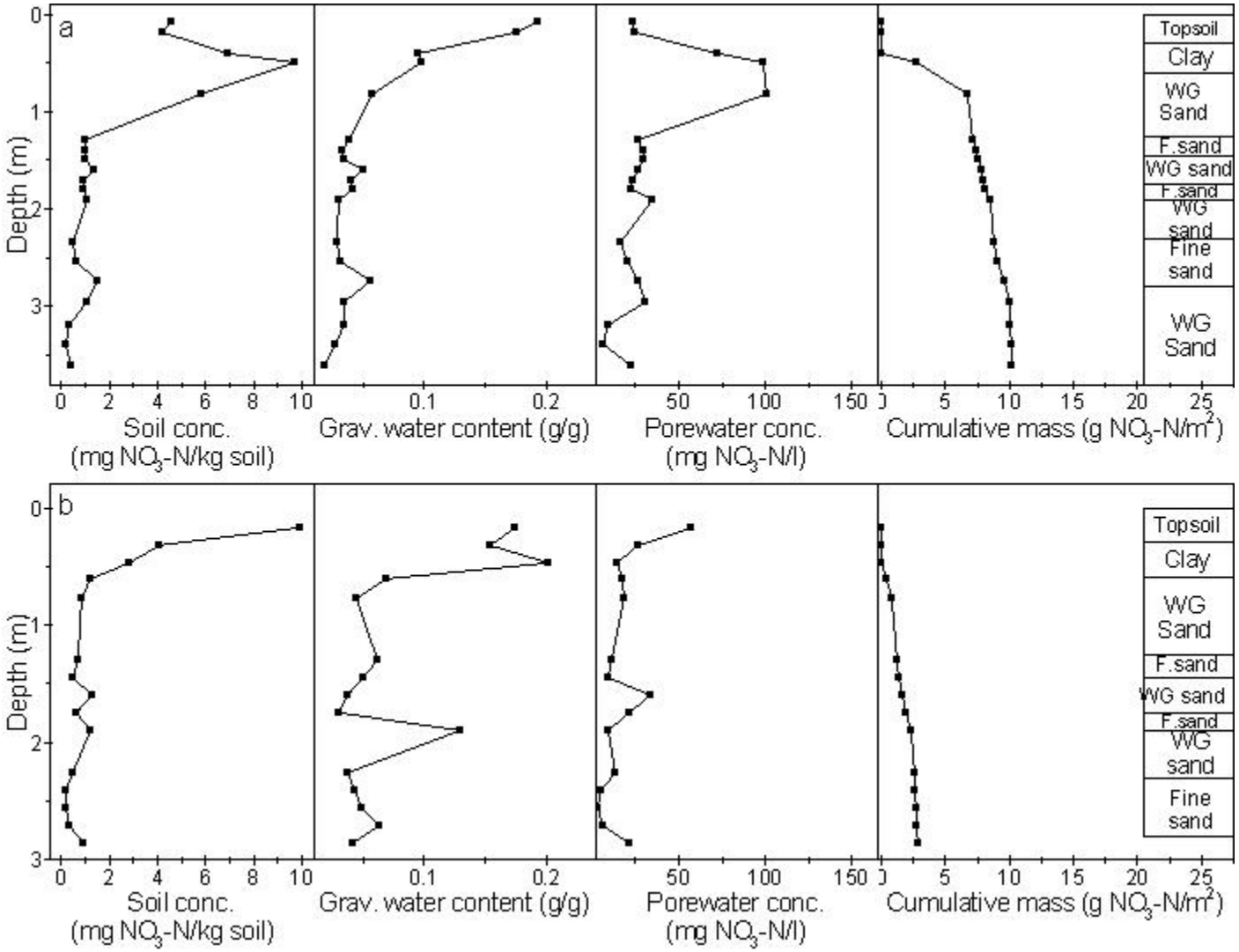

Figure 4.13. Station 6 profiles of bulk soil nitrate concentration, gravimetric soil water content, porewater nitrate concentration and cumulative stored nitrate mass from cores collected in a) November 2005 and b) May 2006.

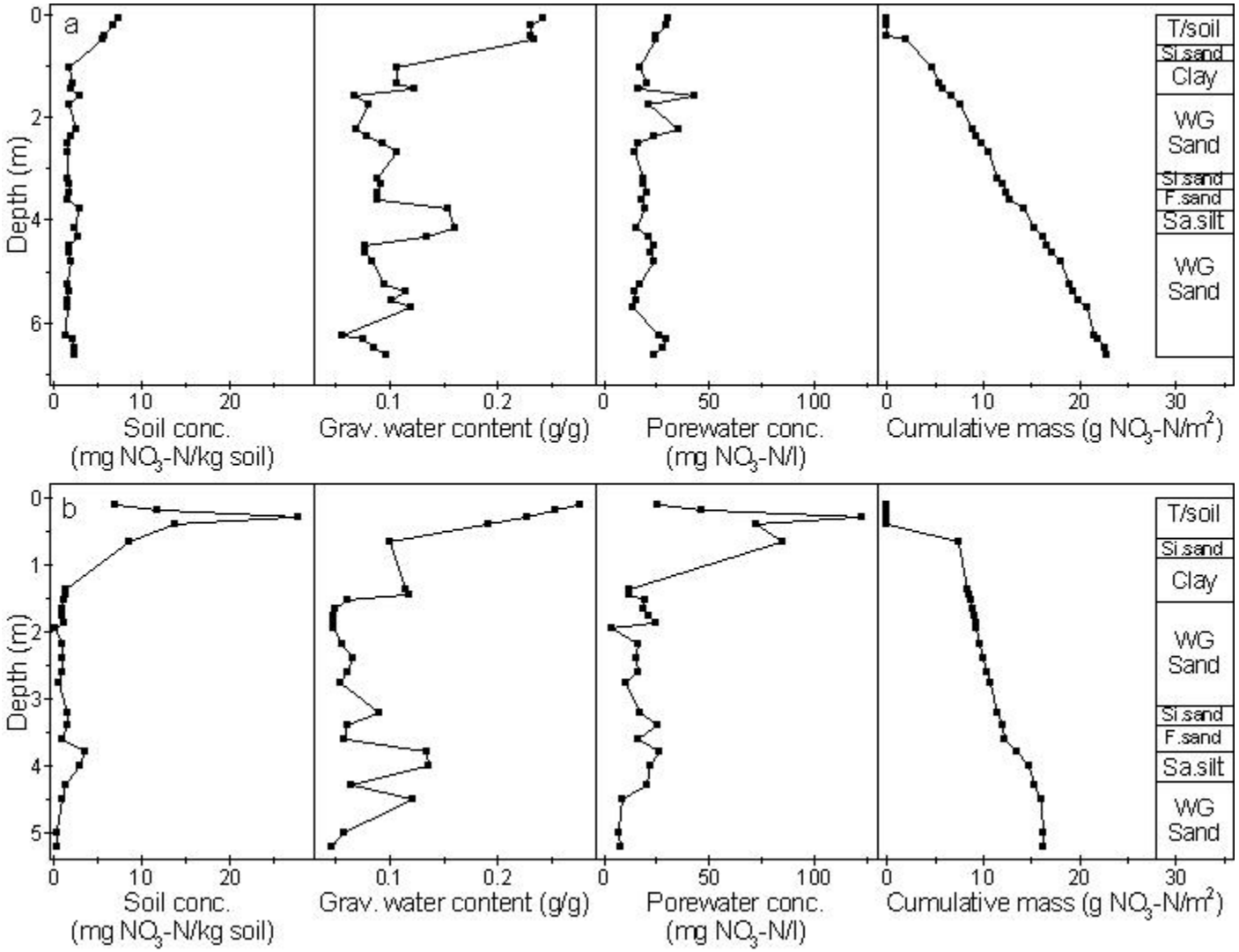

Figure 4.14. Station 7 profiles of bulk soil nitrate concentration, gravimetric soil water content, porewater nitrate concentration and cumulative stored nitrate mass from cores collected in a) May 2005 and b) November 2005.

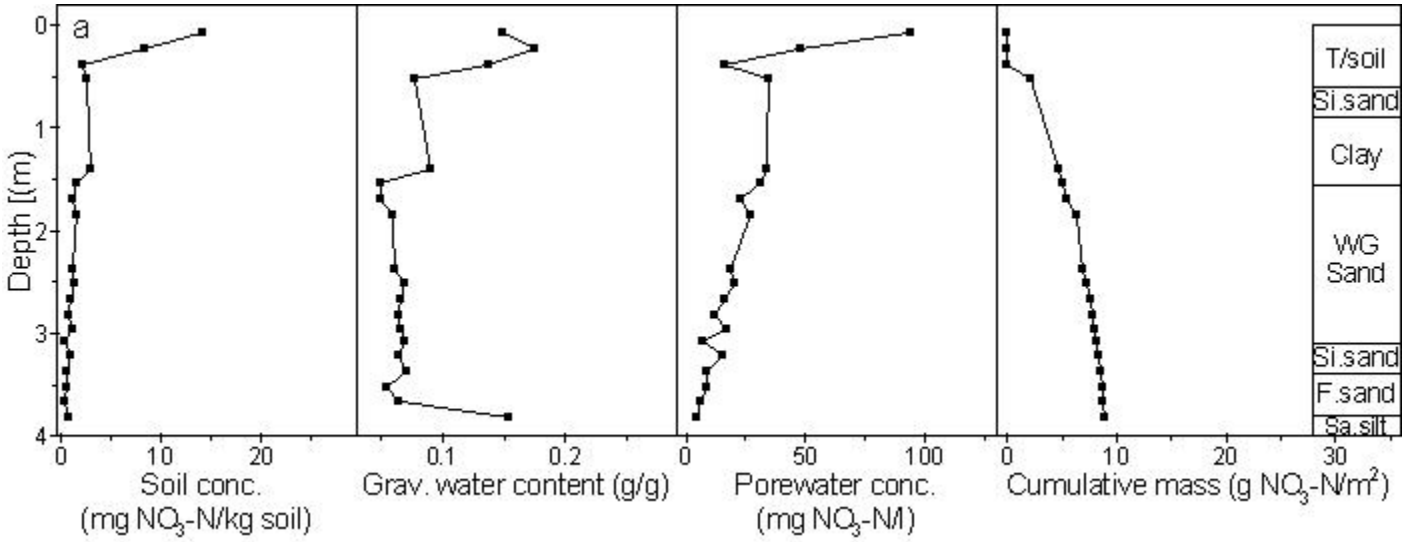

Figure 4.15. Station 7 profiles of bulk soil nitrate concentration, gravimetric soil water content, porewater nitrate concentration and cumulative stored nitrate mass from cores collected in a) May 2006.

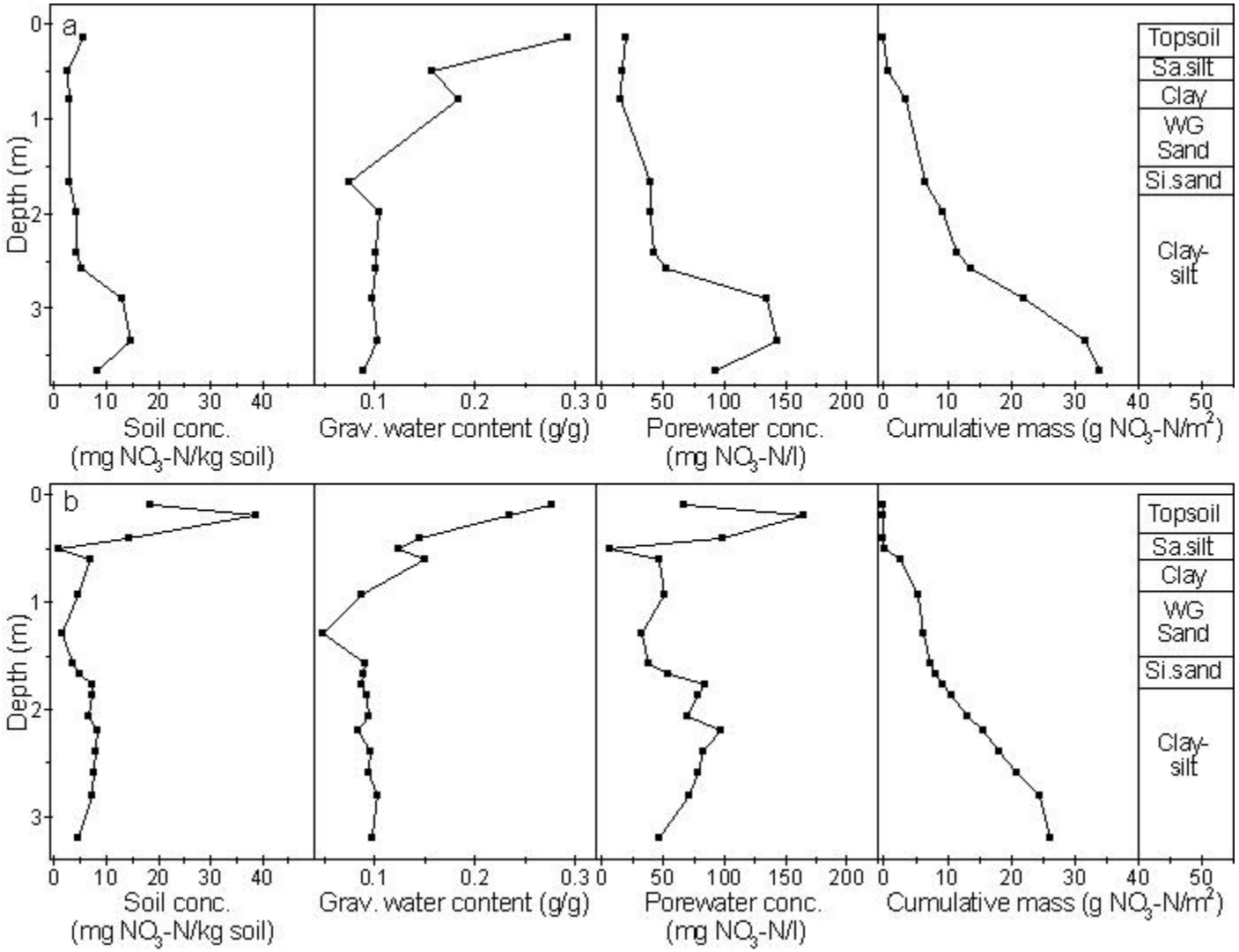

Figure 4.16. Station 8 profiles of bulk soil nitrate concentration, gravimetric soil water content, porewater nitrate concentration and cumulative stored nitrate mass from cores collected in a) February 2005 and b) November 2005.

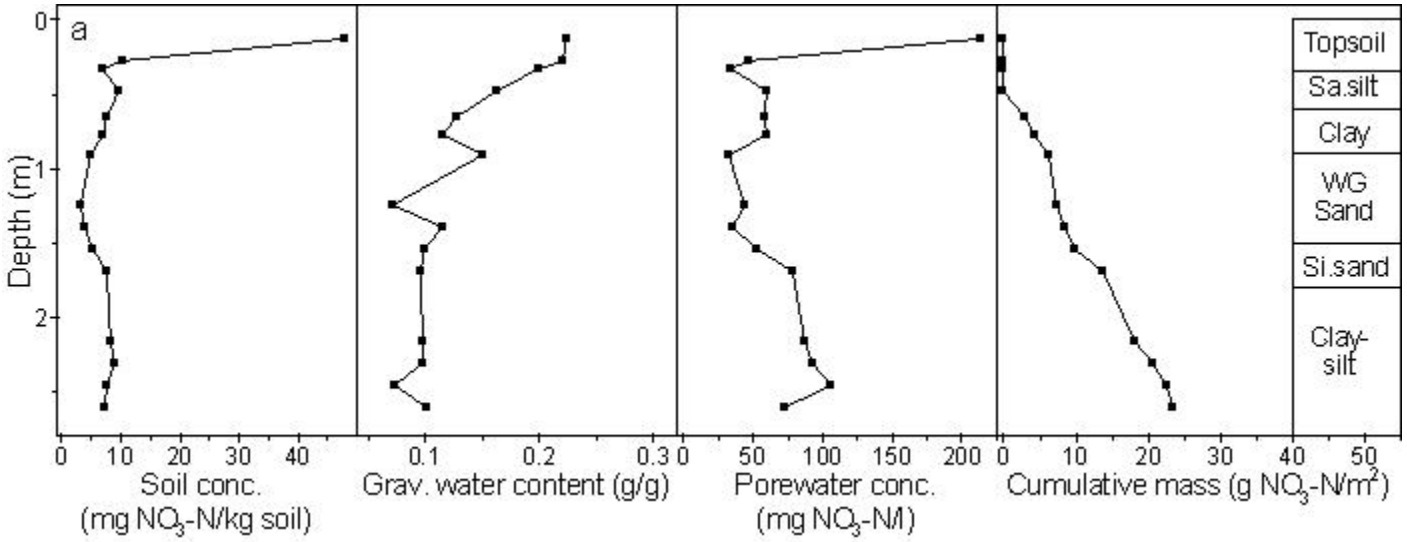

Figure 4.17. Station 8 profiles of bulk soil nitrate concentration, gravimetric soil water content, porewater nitrate concentration and cumulative stored nitrate mass from cores collected in a) May 2006.

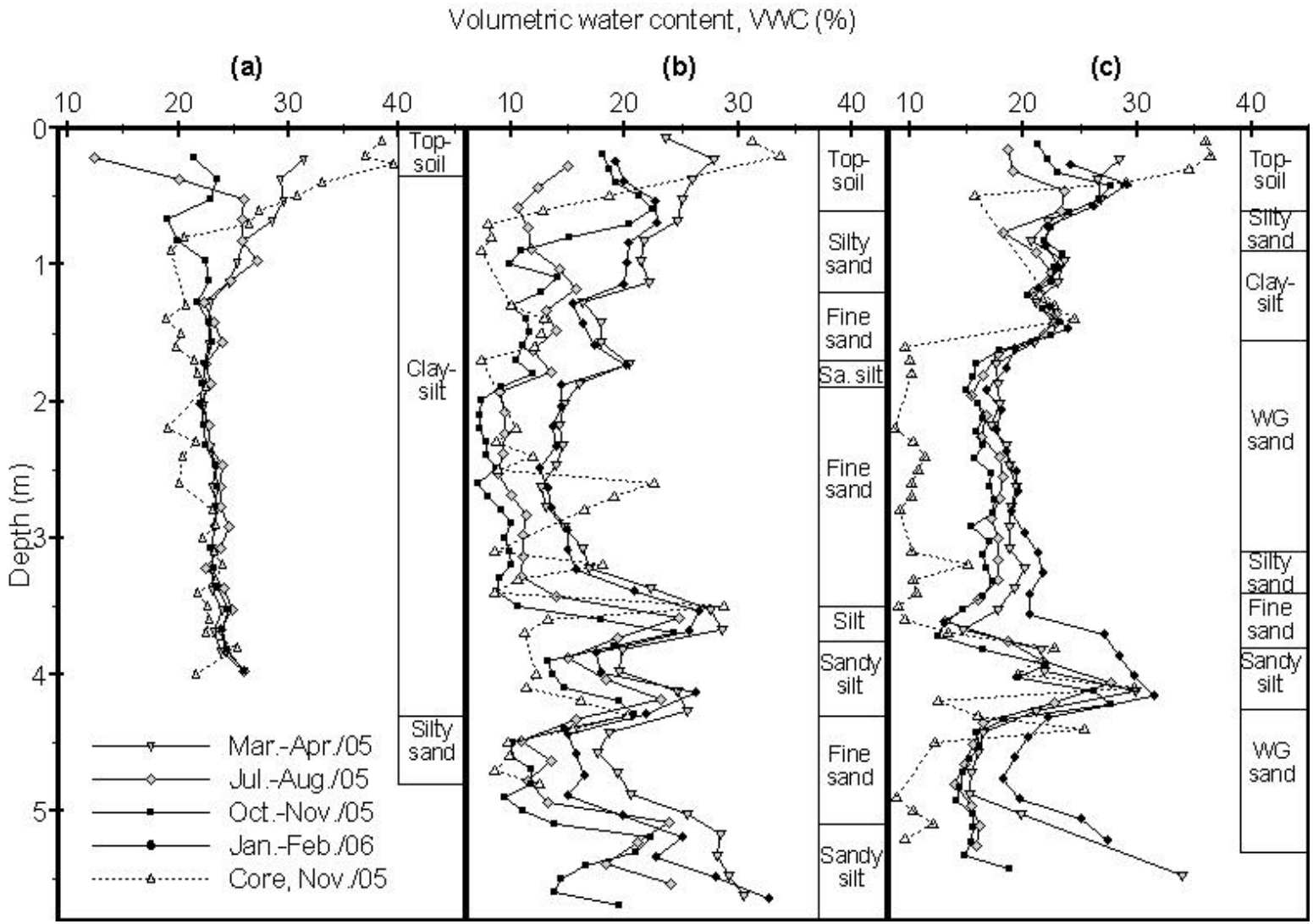

Figure 4.18. Seasonal variation in volumetric soil water content (as measured with the neutron probe and in core samples) at Stations a) 2; b) 5; c) 7.

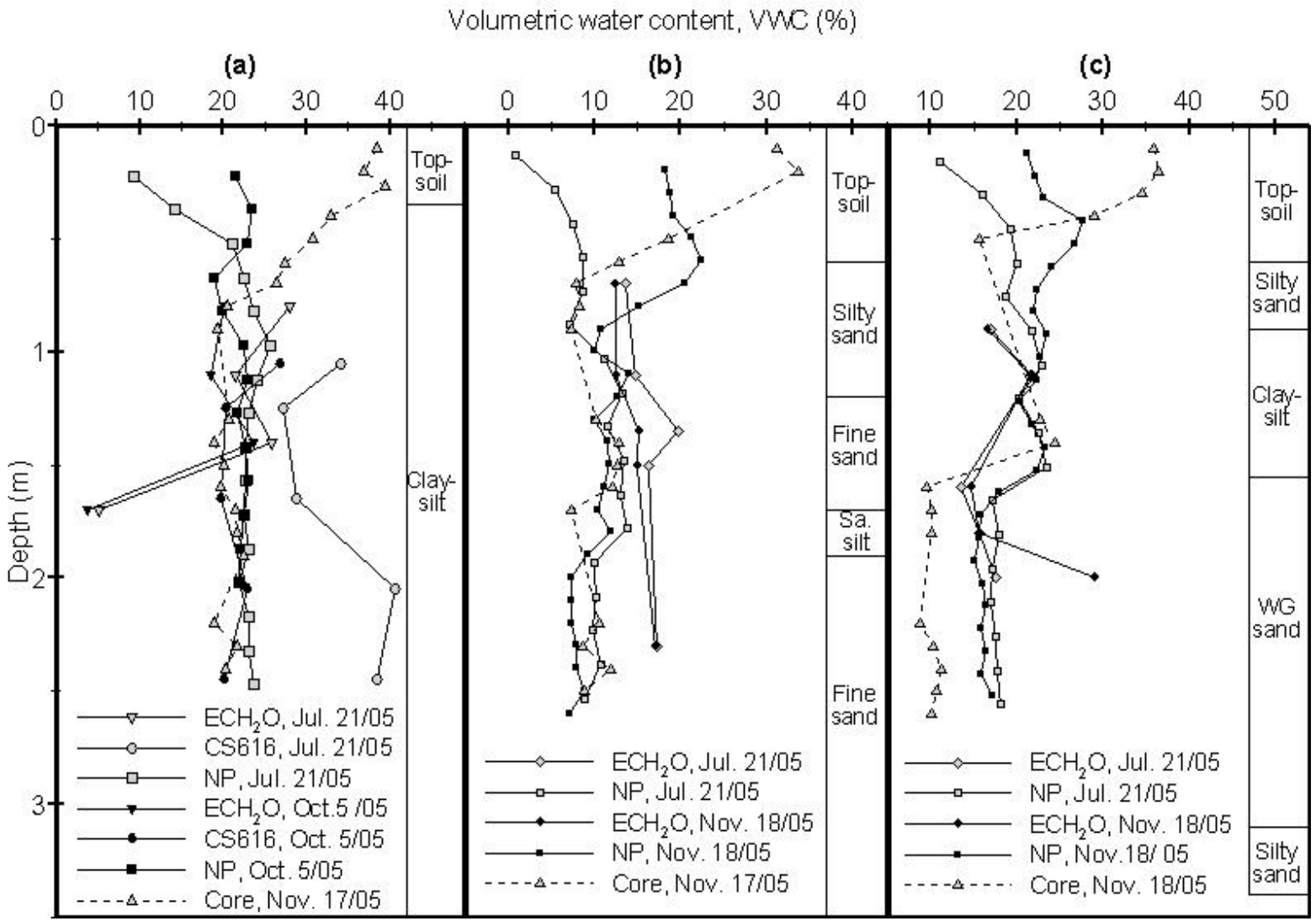

Figure 4.19. Comparison of soil volumetric water content measurements from ECH_2O probes, CS616 probes and the neutron probe (NP) in July 2005 and October-November 2005 at Stations a) 2; b) 5; and c) 7.

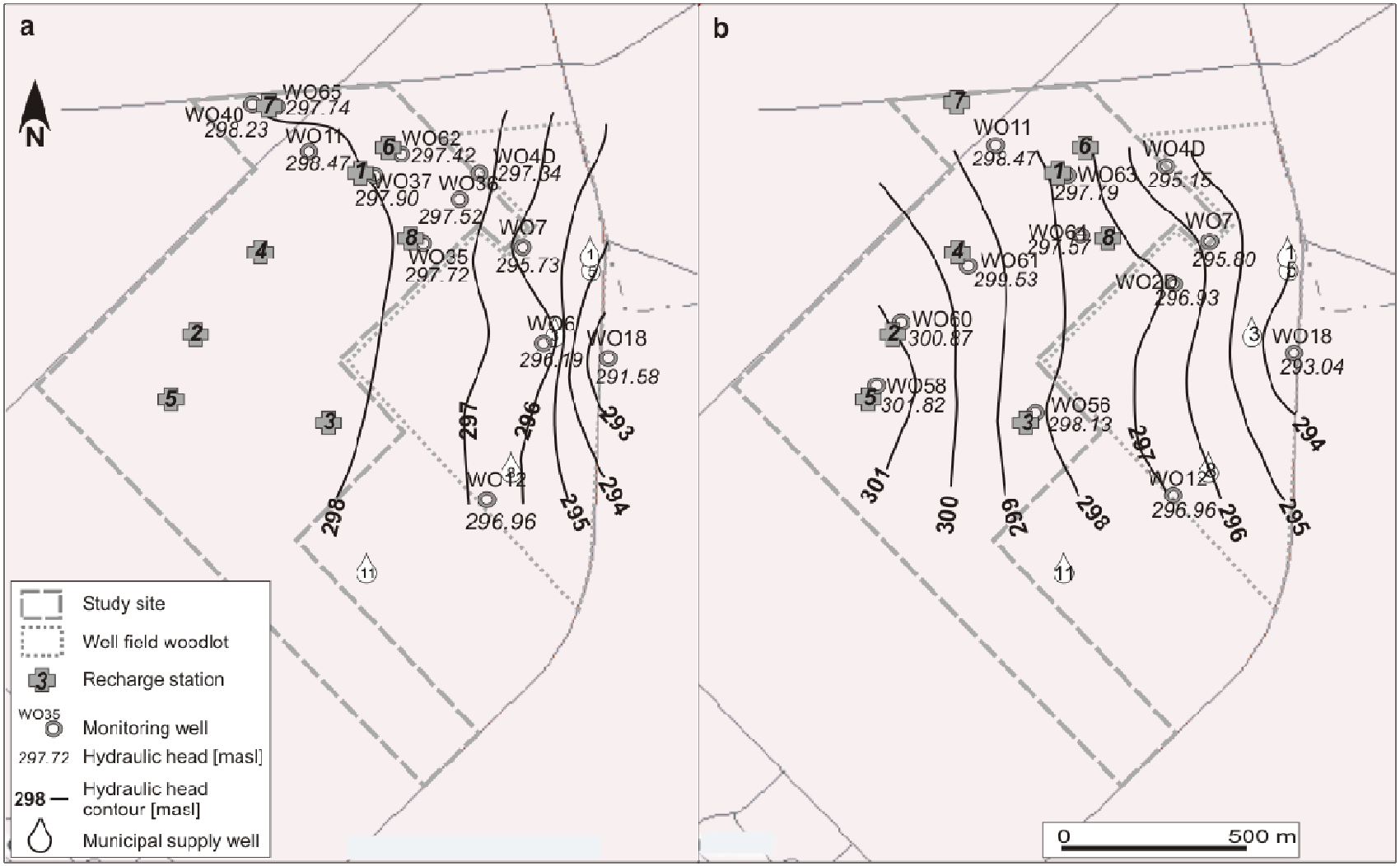

Figure 4.20. August 2005 hydraulic head contours as estimated from wells across the study site and well field screened in a) Aquifer 2 and b) Aquifer 3. Contains data from The Corporation of the County of Oxford (2003b, 2003c).

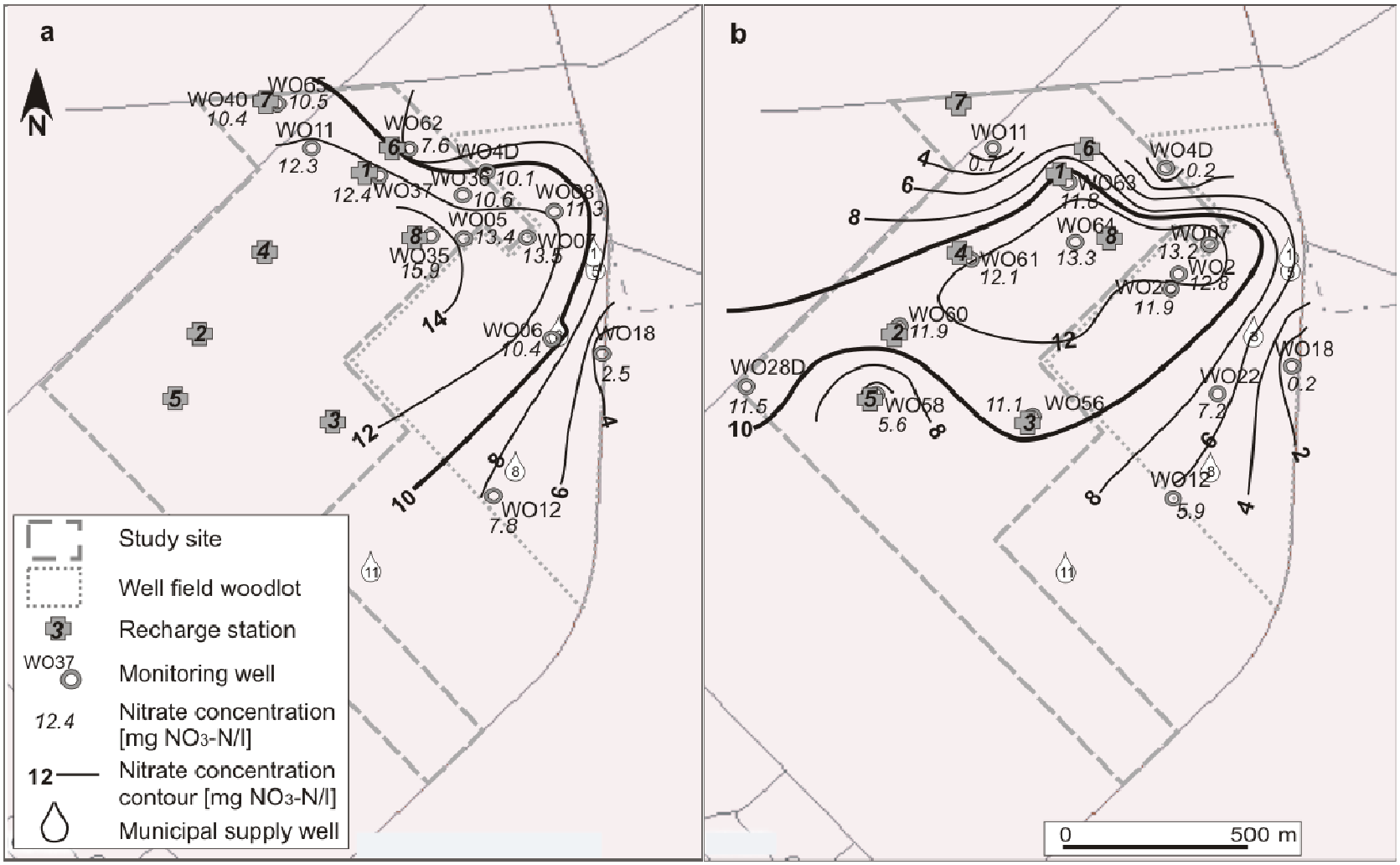

Figure 4.21. August 2005 groundwater nitrate concentration contours as estimated from wells across the study site and well field screened in a) Aquifer 2 and b) Aquifer 3. Contains data from The Corporation of the County of Oxford (2003b, 2003c).

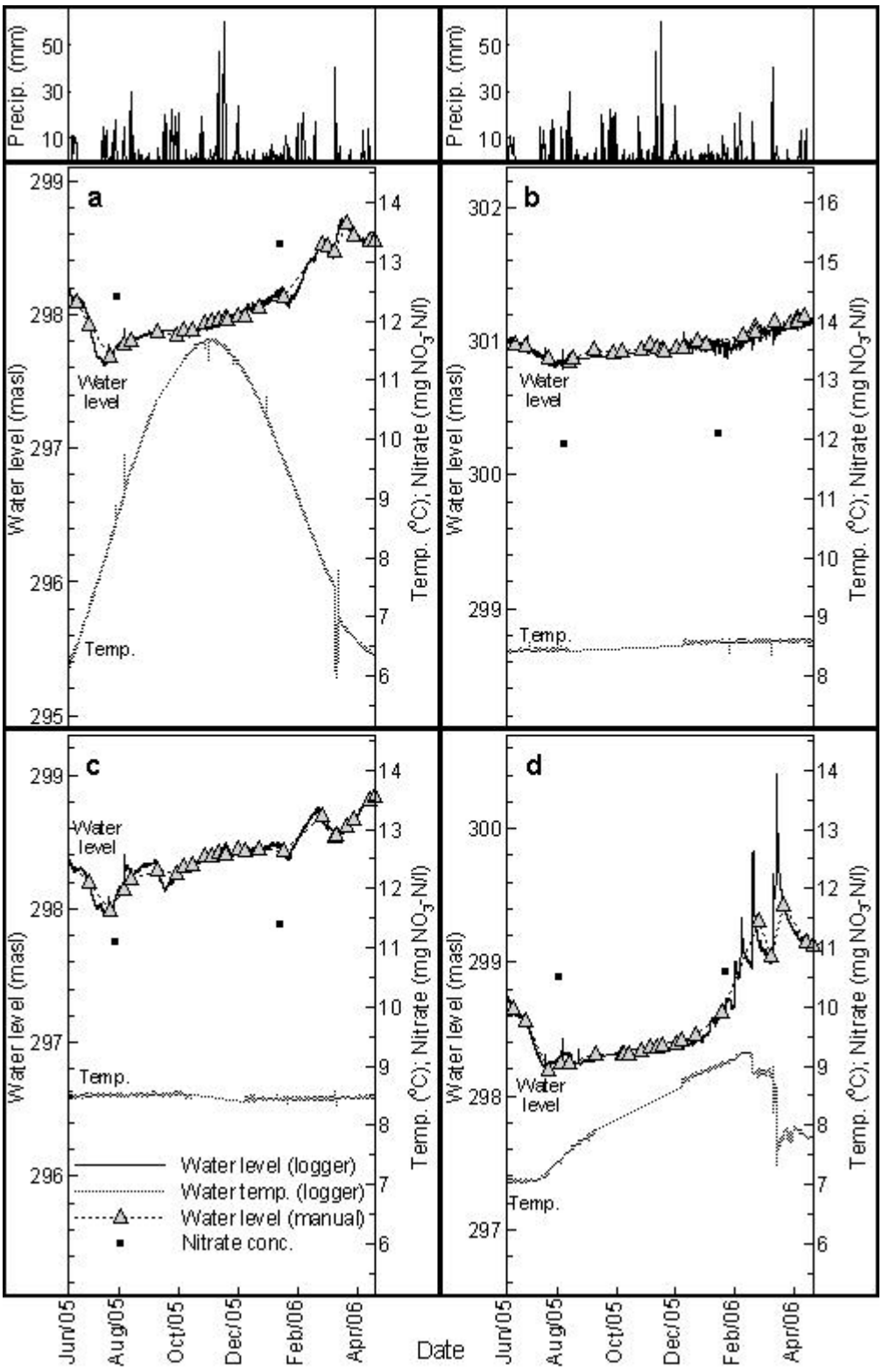

Figure 4.22. Groundwater data including automated water level and temperature measurements, manual water level measurements and nitrate concentration at Stations a) 1; b) 2; c) 3; and d) 7.

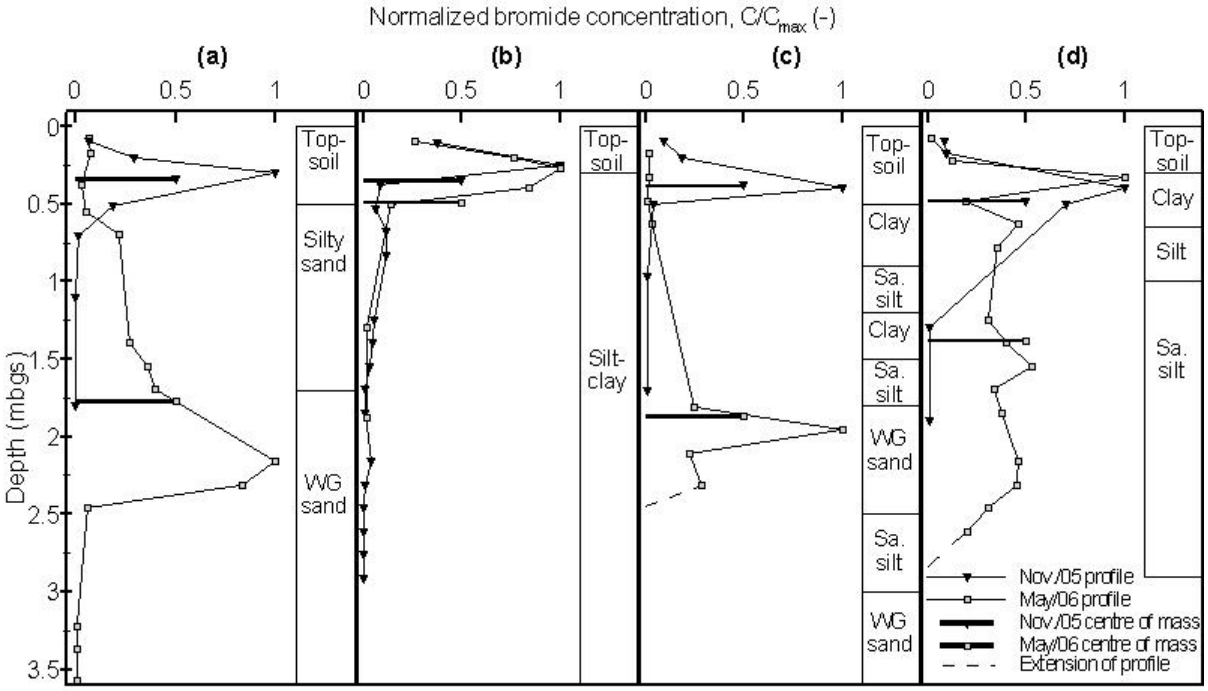

Figure 4.23. Profiles of bromide concentration (normalized by dividing by the maximum concentration) from cores extracted in November 2005 and May 2006 at Stations a) 1; b) 2; c) 3; and d) 4.

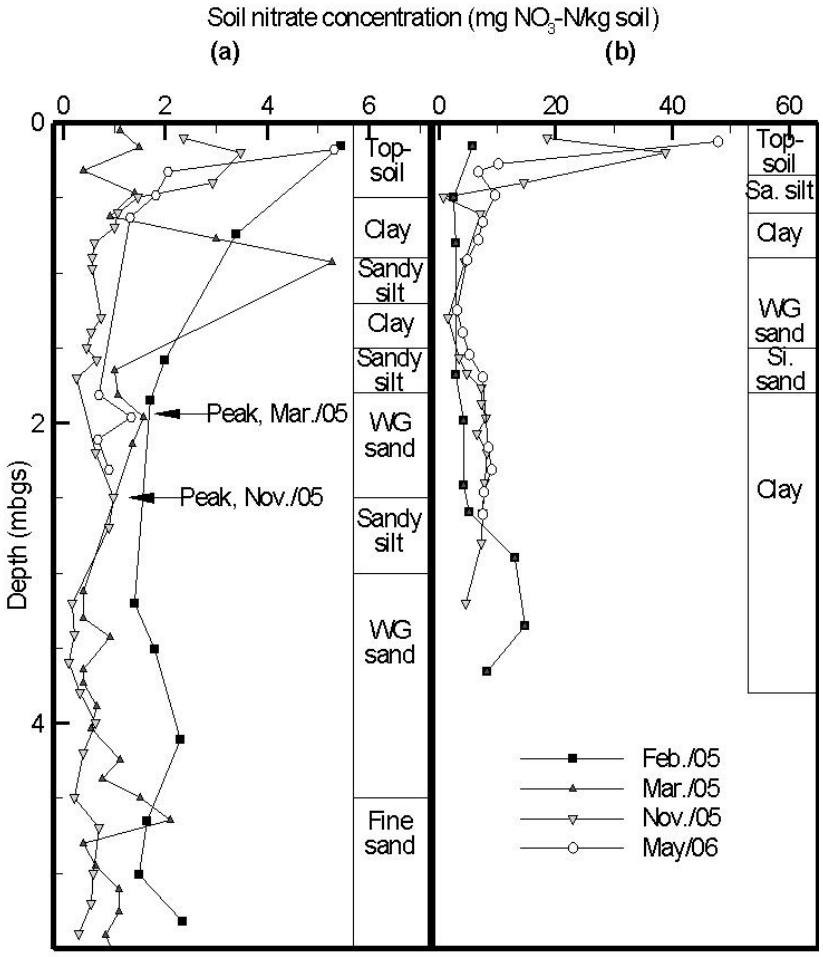

Figure 4.24. Comparison of seasonal profiles of bulk soil nitrate concentration at Stations a) 3 and b) 8.

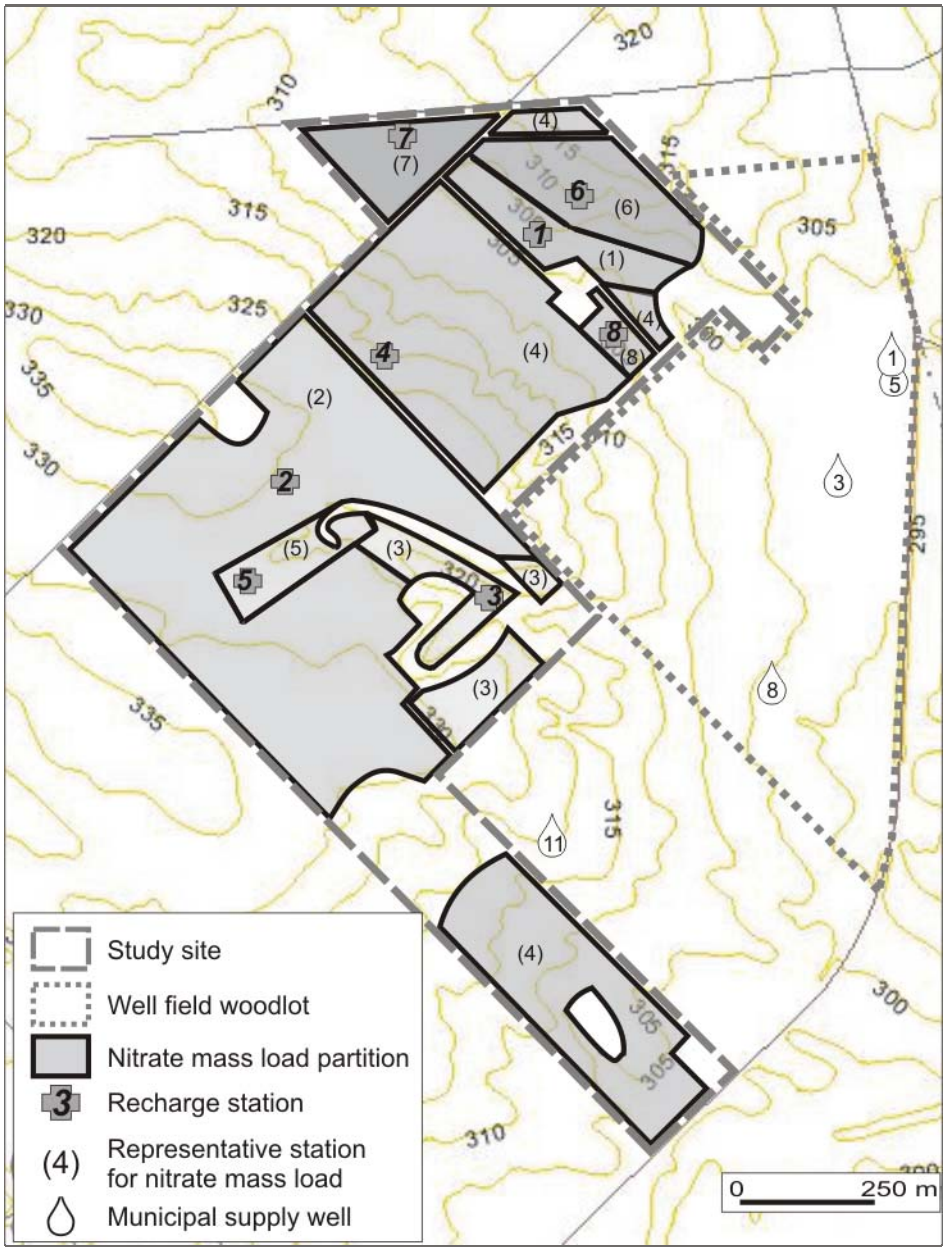

Figure 4.25. Partitioning of study site into areas of similar nitrate mass load. Contains data from The Corporation of the County of Oxford (2003b; 2003c; 2003f).

5. Discussion

This chapter evaluates the study results relative to objectives, and their implications to the study site and to the assessment of BMPs in agricultural and other settings. As described in Chapter 1, the impetus for the study was the lack of published research about the effect of agricultural BMPs on groundwater quality, particularly under deep unsaturated zones, and the potential utility of nitrate mass load measurements for this purpose. A novel study approach was necessary in order to satisfy the objectives of the study, which were to: (1) develop field techniques for the measurement of nitrate mass flux; (2) assess the contribution of computational models to this effort; (3) establish a method to upscale mass flux values and derive a nitrate mass load estimate across the site; and (4) evaluate the utility of mass load measurements in the assessment of agricultural BMPs. These objectives are addressed in the following sections and are followed by the implications of this research.

5.1. Determination of Nitrate Mass Flux

It was possible to estimate nitrate mass flux at locations across the study site by estimating groundwater recharge and the porewater nitrate concentration in pre- and post-BMP sections of the unsaturated zone. However, the analysis proved challenging due to several factors, some of which were limitations on the use of the method in general and others which were particular to the study site and conditions. These factors are discussed in the following sections.

5.1.1. Limitations to the Method

A primary challenge in the estimation of nitrate mass flux at each recharge station was the variability in results among recharge measurement methods. The difference between the highest and lowest recharge estimates at individual recharge stations (excluding the nitrate tracer and zero-flux plane estimates which were generally incomplete) ranged from 0.24 to 0.63 m/yr, a difference equivalent to 73 to 122% of the best recharge estimate based on the bromide tracer method. Among the recharge estimates, even the closest to the best estimate was 12 to 70% lower than it. This variability may be partly due to study-specific limitations to the use of the bromide tracer recharge estimates, as described in the following section.

One implication of this recharge estimate variability is that the accuracy of the nitrate mass flux estimates across the site is highly dependent on the accuracy of the bromide tracer estimates, since no other results can corroborate them. In addition, it appears that the use of a single indirect but simple and inexpensive recharge estimation method, such as the HELP model or the water balance method, may result in the underestimation of recharge for some field conditions. However, the deviation between the best recharge estimate and the HELP and water balance estimates was greatest at stations in topographic lows where local surface water run-on was likely. Therefore the agreement between estimates (and apparent accuracy of the HELP and water balance methods) could potentially be improved at those stations by measuring any occasional precipitation-driven surface water flow across the site and incorporating the results into the analyses.

The methods used in this study for the calculation of nitrate mass flux were also based on several key simplifying assumptions which must be considered in the evaluation of the results. The first of these assumptions was that in the vertical interval of nitrate mass load measurements, the nitrate was not subject to any of the transformation processes of the nitrogen cycle. As described in Section 2.1, in the shallow subsurface of high organic content and root growth, the fate of nitrogen is subject to a range of simultaneous transformation processes including mineralization, nitrification and denitrification. In this study, the parameter of interest in this study was the nitrate mass load that would pass beyond the root zone and ultimately reach the water table. The detailed investigations of soil characteristics and crop growth necessary to properly account for all of the effects of the nitrogen cycle on the mass load measurements were beyond the scope of this study. As a result, the cut-off depth of 0.5 m was used to minimize its effects. As discussed in Sections 4.8.2 and 4.9, however, the soil nitrate profiles revealed that the zone of root growth and nitrogen cycling may have reached a depth of 1.0 m, and therefore soil nitrate data to 1.0 m rather than 0.5 m should have been excluded. As a result, elevated bulk soil nitrate concentrations between 0.5 and 0.9 m may have artificially increased the apparent post-BMP nitrate mass flux.

The other primary assumption in the nitrate mass load calculations was of one-dimensional plug flow in the unsaturated zone; i.e. it was assumed that all water flow was downward and spatially uniform across a measurement location (recharge station). This assumption was first

applied in the estimation of groundwater recharge. In the bromide tracer method, changes in the centre of mass depth were attributed to one-dimensional downward flow and were assumed to represent the movement of water across the bromide application area. Similarly, decreases in soil water storage below the ET/drainage boundary were attributed to downward groundwater recharge. The loss of bromide mass between application and subsequent coring events, however, indicates that horizontal flow may have been substantial at some stations (Section 4.5.1.1). Furthermore, geologic heterogeneities, preferential flow pathways and dispersion processes were likely to have affected unsaturated flow and transport processes in various ways at a single recharge station, such that the assumption of plug flow may have been violated.

The other important application of the one-dimensional plug flow assumption was in the estimation of the depth of BMP effects for the calculation of pre- and post-BMP mass flux. Since the conceptual basis for this depth calculation was the same as for the tracer migration method, its results were equally susceptible to the effects of horizontal or preferential flow. The result was that the zone of a core determined to be theoretically BMP-affected may still have contained pockets of porewater as yet untouched by BMP recharge water. Alternatively, the post-BMP zone may have been re-contaminated by pre-BMP water migrating horizontally. The potential inaccuracies associated with this assumption were difficult to overcome in the context of this study. As with the nitrogen cycle, it was anticipated that the long-term reduction in nutrient input would have a measurable overall effect on nitrate load such that these inaccuracies would not affect the observed mass flux trend.

5.1.2. Site-Specific Limitations

In addition to the limitations inherent to this study's method for estimating nitrate mass flux, certain study- and site-specific characteristics also presented challenges to the determination of either recharge or porewater nitrate concentration. The first of these challenges came in the estimation of recharge with the bromide tracer method, which was ultimately deemed the most direct and best recharge estimate method. In the bromide tracer analysis, the monthly recharge rate measured over 9.5 months from July 2005 to May 2006 was proportionally scaled up to derive an annual recharge rate. This extrapolation assumes that the recharge rate in the May to July period, which was not measured in the field, is equivalent to the average recharge rate during the rest of the year. However, given the crop growth occurring in the late spring and

early summer, it is likely that recharge during that period is relatively low and the proportional scaling may have overestimated the annual recharge rate. The possibility of the overestimation of recharge is further increased by the above-average precipitation and temperature measured at the site in the first five months of 2006 (Section 4.1). The occurrence of wetter and warmer conditions during a period of reduced evapotranspiration may have driven the observed recharge rate higher than would have been observed under average conditions.

The potential effect of these two factors (scaling and high precipitation) on recharge rates may be very roughly estimated, assuming an extreme scenario in which recharge from May to July was in fact zero and all of the excess precipitation in early 2006 (above the historical average) caused an equal amount of excess recharge. In this case, the use of above-average precipitation and proportionally scaled recharge would have caused an approximately 50% overestimation of recharge. This calculation is intended for illustration only, as it required several assumptions and the accuracy of the recharge estimates is dependent on other factors as previously discussed (Section 4.5.1.1). Nonetheless, the consequences of overestimating recharge are two-fold: it would affect the nitrate mass load not only as one of the two factors in the mass load calculation, but also by causing an overestimation of the depth of BMP effects, which would influence the pre- and post-BMP porewater nitrate concentrations.

The estimation of porewater nitrate concentration for nitrate mass flux calculations was also affected by the availability of soil samples from deep in the profile. With the drilling rigs used in this study, the maximum depth to which geologic core could be collected for water content and nitrate analysis generally ranged from 3 to 6 m. At some recharge stations, the depth of anticipated BMP effects exceeded the core depth for all coring events. At these stations, the pre-BMP nitrate mass flux could not be calculated, and the post-BMP flux was determined from soil samples over an incomplete depth. Even at the remaining stations the accuracy of the pre-BMP mass flux results may have been affected by the fact that the available soil samples represented only a fraction of the unsaturated zone.

5.2. Utility of Models

Two unsaturated zone models were applied to supplement the recharge estimates used to calculate nitrate mass flux. These models, the SHAW model and the HELP model, were of

varying use. As described in Section 4.6.2, the SHAW model recharge estimates were 3 to 64 times (average 24 times) lower than the best estimates from the bromide tracer method. Due to its apparent underestimation of the recharge rate, results from this model were not used in the derivation of the best recharge estimate or any other subsequent calculations. The HELP model provided recharge estimates that were more comparable to the other methods and were therefore used to determine the range of likely recharge rates among the recharge stations. As described earlier, the accuracy of the HELP model results may have been further improved by incorporating run-on measurements.

Overall, direct field measurements were preferable to modelling results for the selection of the best recharge estimate in this study. However, the accuracy and utility of the SHAW and HELP models may be potentially be improved by incorporating refined, site-specific crop growth, soil albedo and soil hydraulic parameters. Other one-dimensional, unsaturated zone models may also help to narrow the range of potential recharge rates.

5.3. Upscaling

The third objective – the development of an upscaling technique for nitrate mass flux values - was prompted by the anticipated spatial variability of the mass flux results among the recharge stations. The mass flux values determined in Section 4.9 confirmed the assumption of spatial variability. Therefore the study site was subdivided based on topography, geology and site observations in order to best distribute the nitrate mass flux values measured at individual recharge stations.

The up-scaled post-BMP nitrate mass load across the study site was 4.4 t NO_3-N/yr. In comparison, the non-weighted average of the eight recharge stations' mass flux values was 6.56 g NO_3-N/m^2/yr, which, when applied to the entire study area, yielded a nitrate mass load of 4.97 t NO_3-N/yr, 13% higher than the distributed up-scaled load. Despite the spatial variability of the individual nitrate mass flux values, the relative sizes of the stations' representative areas resulted in a final mass load that was not significantly different than would have been calculated without the partitioning of the field. However, it should also be noted that the partitioning and upscaling effort required assumptions about the geology in areas of limited geologic core data, such as in Fields 1 and 2. Future geologic investigations may yield new information and demand

a revised partitioning of the field. If, for example, significantly more area was found to be represented by Station 4 or 1, the distributed mass load would exhibit a marked increase or decrease, respectively.

5.4. BMP Utility

The final objective of the study was to assess the potential for measurements of nitrate mass load through the unsaturated zone to be used to evaluate and predict the eventual effects of an agricultural BMP on groundwater quality. Due to time required for water to travel through the deep unsaturated zone across much of the site, it was unlikely that the BMP implemented in 2003 had exerted their full influence on the underlying groundwater quality at the time of the study in 2005-06. This time lag in groundwater effects, which first necessitated the nitrate mass load measurements, also somewhat hindered the assessment of the method since the trends suggested by the mass load analyses could not yet be verified nor disproved by the trends in water quality. However, analysis of the nitrate mass load results themselves and the objectives discussed above offered some indication of their utility.

The post-BMP mass load across Parcel B was 4.1 t NO_3-N/yr, almost twice the estimated pre-BMP mass load. This was an unexpected increase in response to a reduction in applied nitrate, but given the limitations associated with the estimation of recharge rate and porewater nitrate concentration at the site, it should be interpreted with caution. In contrast, the stored nitrate mass in the shallow subsurface (Table 4.1) suggested more potential improvement to the groundwater quality than did the pre- and post-BMP nitrate mass load values. The trends at Stations 1, 3 and 6 indicated that the decrease in fertilizer application associated with the switch from winter wheat to grass cover, combined with the high hydraulic conductivity of the shallow materials at these stations, had had a noticeable effect on the shallow stored nitrate mass. Low stored mass values were also observed at Station 5 which had been planted in grass since 2003. The trend at Stations 2 and 4 was a slight decrease (15-20%) in stored nitrate during 2005, and an increase in May 2006 potentially due to mineralization of nitrogen during the early spring. Meanwhile, steady increases in stored mass were observed at Station 8.

The stored mass results may also provide insight about the unsaturated flow assumptions in this study. As described in Section 3.3, the stored nitrate mass was calculated for all cores at

each station, over a common depth that did not necessarily coincide with the maximum depth of BMP impacts. At all but Stations 2 and 8, the common depth was within the post-BMP zone in every core. As a result, these stored mass values did not juxtapose pre- and post-BMP conditions, but rather represented on-going post-BMP conditions, assuming the calculation of $d_{max,\ BMP}$ was accurate. If one-dimensional plug flow were occurring through the unsaturated zone, a one-time decrease in stored mass would be expected as $d_{max,\ BMP}$ passed through the common depth for calculation. The fact that stored nitrate mass showed a progressively decreasing trend at some stations suggests that the assumption of one-dimensional plug flow is not accurate and that the shallow unsaturated zone is in fact being progressively flushed of nitrate-laden porewater over time as the recharging water reaches new pockets of a heterogeneous area.

Overall, the utility of nitrate mass load measurements in the assessment of the agricultural BMP appeared to be limited by challenges in the estimation of groundwater recharge and the use of shallow soil nitrate data, the lack of deep soil nitrate data, and the assumption of uniform downward flow. Seasonal variations in mineralized nitrogen may also hinder the identification of a trend in nitrate mass load that can be linked to reduced nitrogen application. As a result, the nitrate mass loads measured to this point may not be useful in the prediction of eventual impacts on groundwater nitrate concentration. However, the variations in nitrate mass load observed in the unsaturated zone are also likely to manifest themselves in the groundwater quality, such that it may be difficult to predict future groundwater quality by any means. It is anticipated that over time, the effects of nitrogen cycling and heterogeneous flow will be smoothed out by a long-term decrease in nitrogen input and nitrogen mass load.

5.5. Overall Study Implications

5.5.1. Study Site Implications

The area adjacent to the Thornton Well Field in the County of Oxford was selected as the site of this study due to the need to determine: whether the agricultural BMP (reduced nutrient application) in the area had affected the field conditions; when improvements to groundwater quality could be anticipated; and how significant the improvements could be. As discussed in the previous sections, the limitations associated with estimating the recharge rate and porewater

nitrate concentration cast doubt on the utility of nitrate mass load estimates to answer these questions. Stored nitrate mass in the shallow subsurface, however, did exhibit a decrease in response to reductions in surface nitrogen application.

In spite of the limited use of nitrate mass load results for assessing the BMP, the analysis undertaken in this study yielded important information about the spatial variability of recharge and nitrate mass flux across the site. In particular, the former barnyard area represented by Station 8 was confirmed as a location of high nitrate mass flux (13.2 g NO_3-N/m^2/yr based on the May 2006 core and the best recharge estimate). Meanwhile, the Old Stage Road field, which is neither currently owned by the County of Oxford nor subject to minimal nutrient inputs, is subject to a high recharge rate and hence relatively high nitrate mass flux (8.7 g NO_3-N/m^2/yr) directly upgradient of Parcel B. These two areas may require a focused effort to mitigate their contributions to the overall groundwater nitrate load.

The effect of reduced nutrient application at surface was not expected to have fully revealed itself in the groundwater underlying Parcel B, since the anticipated depth of BMP effects at the recharge stations was consistently shallower than the water table depth, except at Stations 1 and 6. As a result of the varying unsaturated zone depth and groundwater mixing below the water table, it is anticipated that the BMP will affect the groundwater nitrate levels gradually.

As described in Section 2.8, the average annual nitrate extraction from the supply wells in the Thornton Well Field was calculated as 14 to 36 t NO_3-N/yr by Haslauer (2005). Haslauer also estimated a potential 6 to 17% decrease in supply well nitrate concentration achievable by completely eliminating nitrate leaching below Parcel B. Since the post-BMP nitrate mass load estimated in this study was considerably higher than Haslauer's mass load estimate, the associated potential decrease in supply well nitrate concentration also increased to 11 to 30% of current concentrations. However, this estimate is limited by the same factors that potentially affected the accuracy of the post-BMP nitrate mass load estimate. The refinements to the method described in the following section may improve the use of nitrate mass load estimates in estimating potential improvements to groundwater quality.

5.5.1.1. Future Use

Although the monitoring of nitrate mass load through the unsaturated zone yielded equivocal results about the short-term benefits from the implementation of the agricultural BMP at the study site, the continued application of the method may yield more insight into site conditions. Refinement of the recharge estimate may considerably improve the accuracy of mass load estimates and reveal a more logical response to reduced fertilizer application. As previously discussed the heterogeneity of flow through the unsaturated zone may have delayed the removal of high-nitrate porewater in some areas. Therefore, cores taken progressively after the BMP implementation may become more and more representative of post-BMP conditions. However, it should be noted that as the zone of anticipated of BMP effects deepens, it will become increasingly difficult to collect core samples from near or below the maximum BMP depth. However, measurements of stored nitrate mass in the unsaturated zone over a consistent depth at each station will indicate whether the decrease in nitrate below grass crops is sustained and whether similar long-term decreases can be observed below other crops including corn.

A further application of nitrate mass load results is in the development of a three-dimensional flow and transport model for the capture zone of the Thornton Well Field. Field-based data describing the magnitude and spatial variability of recharge and porewater nitrate concentration will contribute to the calibration and application of the model.

5.5.2. Application beyond the Study Site and the Agricultural Context

The nitrate mass load monitoring method described in this study could be carried out at any agricultural site in order to compare pre- and post-BMP results or to quantify the overall mass load through the unsaturated zone. Mass load calculations can also serve to evaluate trends in other contaminants in settings beyond the agricultural context. They would likely be most useful for conservative contaminants such as chloride which would not be subject to conversion processes which might affect the results. However, even conservative contaminant mass load calculations would require some assumptions about the nature of flow in the unsaturated zone and accurate estimates of the recharge rate.

6. Conclusions and Recommendations

6.1. Conclusions

This study described the development and application of a novel method for measuring nitrate mass load through the unsaturated zone in order to assess agricultural Best Management Practices (BMPs). Measurements at distinct locations across the study site revealed considerable spatial variability in recharge rate, porewater nitrate concentration and hence nitrate mass flux. The monitoring of stored nitrate mass in the shallow subsurface indicated a beneficial response under some conditions. In contrast, the pre- and post-BMP nitrate mass load estimated by up-scaling the mass flux values suggested limited effects to date from the implementation of the BMP; however the method was also deemed to be hindered by the challenge of properly estimating the recharge rate and nitrate concentration.

The recharge rate measured at the recharge stations was generally correlated to shallow stratigraphy and topography, with the highest recharge rates observed at stations in topographic lows underlain by sand and gravel materials. The bromide tracer method was selected as the most direct and robust technique for estimating recharge, although its application in this study was limited by the lack of a full year of data and an above-average precipitation rate. The HELP model estimates of recharge were comparable to some field estimates, and were therefore used to develop a range for the estimated recharge rate, while the SHAW model appeared to significantly underestimate recharge under the study conditions and its results were not used in nitrate mass flux calculations.

Porewater nitrate concentration profiles often showed variation with depth which in some cases could be linked to geology and soil water content. In cores from most of the recharge stations, the average post-BMP porewater nitrate concentration was in fact higher than the average pre-BMP concentration. As a result, the nitrate mass flux estimates were similarly higher for post-BMP than for pre-BMP conditions. However, the post-BMP estimates were potentially skewed by elevated soil nitrate concentrations between 0.5 and 1.0 m, while the calculation of the pre-BMP mass flux was often limited by the maximum depth from which soil samples for nitrate concentration could be collected. Nonetheless, the post-BMP mass flux results revealed

locations of relatively high nitrate mass flux, including the former barnyard location (Station 8) and within the Old Stage Road field (Station 7).

The scaling-up of the nitrate mass flux values to a field-scale mass load, based on geology, topography and field observation, was also hindered by the difficulty in measuring pre-BMP conditions at all recharge stations. Like the mass flux, the nitrate mass load exhibited an increase across the study site since the implementation of the agricultural BMP. The results should be considered with caution due to the challenges of accurately measuring recharge, the significantly higher-than-average precipitation observed during the study period, and the limited number of deep nitrate concentration measurements as previously described. In contrast, estimates of stored nitrate mass in the shallow subsurface revealed a beneficial response to the BMP, particularly at recharge stations where a grass crop with low nutrient requirements was cultivated and the shallow stratigraphy consisted primarily of sand.

Overall, the utility of nitrate mass load measurements in assessing the agricultural BMP is hindered by some inherent limitations in the technique. However, it is likely that many of the limitations will be overcome during ongoing monitoring of the site and application of the method. Furthermore, monitoring of the stored nitrate mass in the shallow subsurface, which is independent of groundwater recharge measurements, appears to be very useful in revealing beneficial response to reduced nutrient inputs as the geologic material is progressively flushed of nitrate-laden porewater.

6.2. Recommendations

In light of the results and limitations of the techniques used in this study, the following recommendations should be considered.

- Continued site monitoring: geologic core collection, field data collection, bulk soil bromide and nitrate analysis, and the calculation of nitrate mass load and stored nitrate mass should continue. The resulting data will allow the refinement of groundwater recharge, porewater nitrate concentration and nitrate mass flux estimates. In particular, estimates of the groundwater recharge rate will be improved by using a longer averaging period that is a minimum of one year.

The results of all analyses will reveal whether the BMP effects seen in the stored nitrate mass are sustained, and whether they are reproduced in the nitrate mass load calculations.

- Examine horizontal flow: the apparent existence of horizontal flow in the shallow subsurface at most recharge stations should be confirmed and better characterized. If confirmed, the horizontal flow should be incorporated into the conceptual hydrogeologic model and be used to adapt the nitrate mass flux estimates. If horizontal flow is not significant, the reason for the loss of the bromide tracer requires further investigation.

- Improved modelling efforts: alternative one-, two- or even three-dimensional computational models should be used in order to improve estimates of groundwater recharge, particularly below the range of soil water content measurement and core collection for bromide analysis. These models may also assist in the evaluation of horizontal flow effects.

- Refined up-scaling method: geologic core collection, geophysical methods or other site characterization tools should be applied in order to obtain additional shallow stratigraphic data, especially in Fields 1 and 2 where stratigraphic data are limited. New data may be used to refine the up-scaling of nitrate mass flux values to field scale.

- Continued groundwater monitoring: groundwater nitrate concentrations should be monitored in order to detect any trends in response to the BMP.

Bibliography

AAFC. *See* Agriculture and Agri-Food Canada.

Addiscott, Tom M. 2004. *Nitrate, agriculture and the environment.* Wallingford, UK: CABI Publishing.

Agriculture and Agri-Food Canada. 1997. Profile of production trends and environmental issues in Canada's agriculture and agri-food sector. Ottawa: Agriculture and Agri-Food Canada.

Albright, W. H., G. W. Gee, G. V. Wilson, and M. J. Fayer. 2002. *Alternative Cover Assessment Project: Phase I Report.* Desert Research Institute, Publication No. 41183. DRI, Division of Hydrological Sciences, Reno, NV. http://www.acap.dri.edu/

Allen, Richard G., Luis S. Pereira, Dirk Raes, and Martin Smith. 1998. *Crop evapotranspiration: Guidelines for computing crop water requirements.* Food and Agriculture Organization of the United Nations, FAO Irrigation and Drainage Paper 56. Rome: FAO.

Almasri, Mohammad N. and Jagath J. Kaluarachchi. 2004. Assessment and management of long-term nitrate pollution of ground water in agriculture-dominated watersheds. *Journal of Hydrology* 295: 225-245.

American Society for Testing and Materials. 2005. *D2216-05, Standard Test Methods for Laboratory Determination of Water (Moisture) Content of Soil and Rock by Mass.*

American Society for Testing and Materials. 2006. *D2487-06, Standard Practice for Classification of Soils for Engineering Purposes (Unified Soil Classification System).*

Appelo, C.A.J., and D. Postma. 1999. *Geochemistry, groundwater and pollution.* Rotterdam, Netherlands: A.A. Balkema.

ASTM. *See* American Society for Testing and Materials.

Azevedo, A. S., P. Singh, R. S. Kanwar, L. R. Ahuja. 1997. Simulating nitrogen management effects on subsurface drainage water quality. *Agricultural Systems* 55(4):481-501.

Boumans, L. J. M., B. Fraters, and G. van Drecht. 1999. Nitrate in the upper groundwater of "De Marke' and other farms. *Netherlands Journal of Agricultural Science* 49: 163-177.

Brock University Map Library. n.d. Southern Ontario-Regional Municipality Boundaries. St. Catharines, Ontario: Brock University Map Library. Available: Brock University Map Library Controlled Access http://www.brocku.ca/maplibrary/images/sontbase.jpg.

Brooks, R. H. and A. T. Corey. 1966. Properties of porous media affecting fluid flow. *Journal of the Irrigation and Drainage Division, ASCE* 92(IR2):61-88.

Burdine, N. T. 1953. Relative permeability calculation from pore size distribution data. *Transactions of the American Institute of Mining, Metallurgical, and Petroleum Engineers* 198:71-78.

Burkart, M. and J. Stoner. 2002. Nitrate in aquifers beneath agricultural systems. *Water Science and Technology* 9:19-29.

Burr, S. and M. Goss. 2003. *The Partners in Nitrogen Use Efficiency project, biophysical component: Nitrogen balances between 1997 and 2002.* Prepared for the Ontario Federation of Agriculture.

Campbell, G. S. n.d. *Modeling available soil moisture.* Decagon Devices, Inc., Pullman, WA.

Campbell, G. S. 1974. A simple method for determining unsaturated conductivity from moisture retention data. *Soil Science* 117:311-314.

Campbell, G. S. 1985. *Soil physics with BASIC: Transport models for soil-plant systems.* New York: Elsevier.

Campbell Scientific, Inc. 2003. *Model 107 & 107B Temperature Probes, Instruction Manual.* Campbell Scientific, Inc.

Campbell Scientific, Inc. 2004. *CS616 and CS625 Water Content Reflectometer, Instruction Manual.* Campbell Scientific, Inc.

Corporation of the County of Oxford. 1990. Limits: The Corporation of the County of Oxford, Woodstock, Ontario, Canada.

Corporation of the County of Oxford. 1994. Soils: The Corporation of the County of Oxford, Woodstock, Ontario, Canada.

Corporation of the County of Oxford. 2000. County of Oxford Ortho Imagery: The Corporation of the County of Oxford, Woodstock, Ontario, Canada.

Corporation of the County of Oxford. 2001. Quaternary Geology: The Corporation of the County of Oxford, Woodstock, Ontario, Canada.

Corporation of the County of Oxford. 2003a. Wetlands: The Corporation of the County of Oxford, Woodstock, Ontario, Canada.

Corporation of the County of Oxford. 2003b. Municipal Water Wells: The Corporation of the County of Oxford, Woodstock, Ontario, Canada.

Corporation of the County of Oxford. 2003c. Roads: The Corporation of the County of Oxford, Woodstock, Ontario, Canada.

Corporation of the County of Oxford. 2003d. Surface Water Bodies: The Corporation of the County of Oxford, Woodstock, Ontario, Canada.

Corporation of the County of Oxford. 2003e. Surface Water Channels: The Corporation of the County of Oxford, Woodstock, Ontario, Canada.

Corporation of the County of Oxford. 2003f. Topography - Contours: The Corporation of the County of Oxford, Woodstock, Ontario, Canada.

Cowan, W. R. 1975. *Quaternary geology of the Woodstock area, Southern Ontario.* Geological Report 119, Ontario Division of Mines, Ministry of Natural Resources.

CPN. 1984. *503DR Hydroprobe operating manual.* CPN Corporation.

Decagon Devices, Inc. 2006. *ECH$_2$O soil moisture sensor operator's manual for models EC-20, EC-10, and EC-5, version 2.2.* Pullman, WA: Decagon Devices, Inc.

Delin, Geoffrey N., Richard W. Healy, Matthew K. Landon, and John Karl Böhlke. 2000. Effects of topography and soil properties on recharge at two sites in an agricultural field. *Journal of the American Water Resources Association* 36:1401-1416.

Dermody, O., S. P. Long, and E. H. DeLucia. 2006. How does elevated CO2 or ozone affect the leaf-area index of soybean when applied independently?. *New Phytologist* 169(1): 145-155.

Donahue, R. L., R. W. Miller, and John C. Shickluna. 1983. *Soils: an introduction to soils and plant growth.* Englewood Cliffs, N.J.: Prentice-Hall Inc.

Environment Canada. 2006. Canadian Climate Normals 1971-2000. http://www.climate .weatheroffice.ec.gc.ca/climate_normals/results_e.html..

Fallow, D. J., D. M. Brown, G. W. Parkin, J. D. Lauzon, and C. Wagner-Riddle. 2003. *Identification of critical regions for water quality monitoring with respect to seasonal and annual water surplus.* Land Resource Science Technical Memo No. 2003-1. Guelph, ON: University of Guelph.

Fertilizer Institute of Ontario Foundation. 2001. *The next best thing to rain: The history of the fertilizer industry in Ontario.* Guelph, ON: The Fertilizer Institute of Ontario.

Flerchinger, G.N. 2000a. *The Simultaneous Heat and Water (SHAW) Model: Technical Documentation.* Technical Report NWRC 2000-9, Northwest Watershed Research Center, USDA Agricultural Research Service, Boise, Idaho.

Flerchinger, G.N. 2000b. *The Simultaneous Heat and Water (SHAW) Model: User's Manual.* Technical Report NWRC 2000-10, Northwest Watershed Research Center, USDA Agricultural Research Service, Boise, Idaho.

Food and Agriculture Organization of the United Nations. 1998. *Crop evapotranspiration: guidelines for computing crop water requirements.* FAO Irrigation and Drainage Paper 56.

Follett, R. F. 1995. NLEAP model simulation of climate and management effects on N leaching for corn grown on sandy soil. *Journal of Contaminant Hydrology* 20:241-252.

Foth, Henry D. 1984. *Fundamentals of soil science.* New York: John Wiley & Sons.

French, Christine, Laosheng Wu, Thomas Meixner, Darren Haver, John Kabashima, and William A. Jury. 2006. Modeling nitrogen transport in the Newport Bay/San Diego Creek watershed of Southern California. *Agricultural Water Management* 81(1-2):199-215.

Gogolev, Mikhail I. 2002. Assessing groundwater recharge with two unsaturated zone modeling technologies. *Environmental Geology* 42:248-258.

Golder Associates. 2001. *Report on Phase II Groundwater Protection Study County of Oxford Volume I.* Technical Report.

Greacen, E. L., B. L. Correll, R. B. Cunningham, G. G. Johns, and K. D. Nicolls. 1981. Calibration. In *Soil water assessment by the neutron method,* ed. E. L. Greacen, 50-81. East Melbourne, Australia: CSIRO.

Greacen, E. L. and C. T. Hignett. 1979. Sources of bias in the field calibration of a neutron meter. *Australian Journal of Soil Research* 17:405-415.

Grismer, Mark E., S. Bachman, and T. Powers. 2000. A comparison of groundwater recharge estimation methods in a semi-arid, coastal avocado and citrus orchard (Ventura County, California). *Hydrological Processes* 14:2527-2543.

Grismer, M. E., K. M. Bali, and R. E. Robinson. 1995. Field-scale neutron probe calibration and variance analysis for clay soil. Journal of Irrigation and Drainage Engineering 121(5):354-362.

Hall, D. W., P. L. Lietman, and E. H. Koerkle. 1997. *Evaluation of agricultural best-management practices in the Conestoga River headwaters, Pennsylvania: Effects of nutrient management on quality of surface runoff and ground water at a small carbonate-rock site near Ephrata, Pennsylvania, 1984-1990, Water-Quality study of the Conestoga River headwaters, Pennsylvania,* U.S. Geological Survey Water-Resources Investigations Report 95-4143, Lemoyne, PA.

Haslauer, C.P. 2005. Hydrogeologic analysis of a complex aquifer system and impacts of changes in agricultural practices on nitrate concentrations in a municipal well field: Woodstock, Ontario. Master's thesis, University of Waterloo.

Heagle, D.J. 2000. Nitrate Geochemistry of a Regional Aquifer in an Agricultural Landscape, Woodstock, Ontario. Master's thesis, University of Waterloo.

Health Canada. 2006. *Guidelines for Canadian Drinking Water Quality Summary Table.* Prepared by the Federal-Provincial-Territorial Committee on Drinking Water.

Healy, Richard W. and Peter G. Cook. 2002. Using groundwater levels to estimate recharge. *Hydrogeology Journal* 10:91-109.

Jyrkama, Mikko I., Jon F. Sykes, and Stefano D. Normani. 2002. Recharge estimation for transient groundwater modelling. *Ground Water* 40(6):638-648.

Khire, Milind, Craig H. Benson, and Peter J. Bosscher. 1997. Water balance modeling of earthen final covers. *Journal of Geotechnical and Geoenvironmental Engineering* 123(8): 744-754.

Koo, B. K. and P. E. O'Connell. 2006. An integrated modelling and multicriteria analysis approach to managing nitrate diffuse pollution: 2. A case study for a chalk catchment in England. *Science of the Total Environment* 358:1-20.

Kraft, George J. and Will Stites. 2003. Nitrate impacts on groundwater from irrigated-vegetable systems in a humid north-central US sand plain. *Agriculture, Ecosystems and Environment* 100:63-74.

Kung, K.-J.S. 1990. Influence of plant uptake on the performance of bromide tracer. *Soil Science Society of America Journal* 54 (4-6): 975-979.

Leij, F.J., W.J. Alves, M. Th. van Genuchten, and J.R. Williams. 1996. *The UNSODA Unsaturated Soil Hydraulic Database, User's Manual Version 1.0.* Cincinnati: National Risk Management Research Laboratory, Office of Research and Development, U. S. Environmental Protection Agency.

Lombardo, L. A., G. L. Grabow, J. Spooner, D. E. Line, D. L. Osmond, and G. D. Jennings. 2000. *Section 319 Nonpoint Source National Monitoring Program Successes and Recommendations.* NCSU Water Quality Group, Biological and Agricultural Engineering Department, NC State University, Raleigh, North Carolina.

Manassaram, Deana M., Lorraine C. Backer, and Deborah M. Moll. 2006. A review of nitrate in drinking water: Maternal exposure and adverse reproductive and developmental outcomes. *Environmental Health Perspectives* 114(3):320-327.

McMahon, P. B., Dennehy, K. F., Bruce, B. W., Böhlke, J. K., Michel, R. L., Gurdak, J. J., Hurlbut, D. B. 2006. Storage and transit time of chemicals in thick unsaturated zones under rangeland and irrigated cropland, High Plain, United States. *Water Resources Research* 42: W03413.

Meissner, R., J. Seeger, and H. Rupp. 2002. Effects of agricultural land use changes on diffuse pollution of water resources. *Irrigation and Drainage* 51:119-127.

Molénat, J. and C. Gascuel-Odoux. 2002. Modelling flow and nitrate transport in groundwater for the prediction of water travel times and of consequences of land use evolution on water quality. *Hydrological Processes* 16:479-492.

Nakamura, K., Harter, T., Hirono, Y, Horino, H., Mitsuno, T. 2004. Assessment of root zone nitrogen leaching as affected by irrigation and nutrient management practices. *Vadose Zone Journal* 3:1353-1366.

Nolan, Bernard T., Arthur L. Baehr, and Leon J. Kauffman. 2003. Spatial variability of groundwater recharge and its effect on shallow groundwater quality in southern New Jersey. *Vadose Zone Journal* 2:677-691.

Nutrient Management Act. S.O. 2002, c.4.

OMAF. *See* Ontario Ministry of Agriculture and Food and Agriculture Canada.

Onsoy, Yuksel S., Thomas Harter, Timothy R. Ginn, William R. Horwath, W. 2005. Spatial variability and transport of nitrate in a deep alluvial vadose zone. *Vadose Zone Journal* 4:41-54.

Ontario Ministry of Agriculture and Food and Agriculture Canada. 1994. *Nutrient Management - Best Management Practices.* Ontario Ministry of Agriculture and Food.

Padusenko, G. 2001. Regional hydrogeologic evaluation of a complex glacial aquifer system in an agricultural landscape: Implications for nitrate distribution. Master's thesis, University of Waterloo.

Pedersen, P. and J. G. Lauer. 2004. Soybean growth and development in various management systems and planting dates. *Crop Science* 44:508-515.

Preston, G. M. and R. A. McBride. 2004. Assessing the use of poplar tree systems as a landfill evapotranspiration barrier with the SHAW model. *Waste Management & Research* 22: 291-305.

Rice, R. C., R. S. Bowman, and D. B. Jaynes. 1986. Percolation of water below an irrigated field. Soil Science Society of America Journal 50:855-859.

Rodvang, S. J., D. M. Mikalson, and M. C. Ryan. 2004. Changes in ground water quality in an irrigated area of southern Alberta. *Journal of Environmental Quality* 33:476–487.

Román, R., R. Caballero, A. Bustos, J. A. Diez, M. C. Cartgena, A. Vallejo, and A. Caballero. 1996. Water and solute movement under conventional corn in central Spain: I. Water balance. *Soil Science Society of America Journal* 60:1530-1536.

Rudolph, David, Will Robertson, Greg Padusenko, Tim Lotimer, and Tony Lotimer. 2002. Impact on water quality from agricultural practice in urban-rural well fields: Influence of time delay in the vadose zone. Paper presented at The National Conference on Agricultural Nutrients and Their Impact on Rural Water Quality. Hosted by the Agricultural Institute of Canada Foundation, Waterloo, ON.

Saxton, Keith E. 2002. *Soil-Plant-Atmosphere-Water Field and Pond Hydrology, User's Manual version 6.1.* USDA-ARS, Washington State University.

Scanlon, Bridget R., Marty Christman, Robert C. Reedy, Indrek Porro, Jirka Simunek, and Gerald N. Flerchinger. 2002. Intercode comparisons for simulating water balance of surficial sediments in semiarid regions. *Water Resources Research* 38(12):1323.

Scanlon, Bridget R., Richard W. Healy, and Peter G. Cook. 2002. Choosing appropriate techniques for quantifying groundwater recharge. *Hydrogeology Journal* 10:18-39.

Schroeder, P. R., N. M. Aziz, C. M. Lloyd, and P. A. Zappi. 1994. *The Hydrologic Evaluation of Landfill Performance (HELP) Model: User's Guide for Version 3,* EPA/600/R-94/168a, September 1994, U.S. Environmental Protection Agency Office of Research and Development, Washington, DC.

Schuh, W., R. Meyer, M. Sweeney, and J. Gardner. 1993. Spatial variation of root-zone and shallow vadose-zone drainage on a loamy glacial till in a sub-humid climate. *Journal of Hydrology* 148:1-26.

Sebol, L.A. 2000. Determination of Groundwater Age Using CFC's in Three Shallow Aquifers in Southern Ontario. Master's thesis, University of Waterloo.

Sebol, L.A. 2004. Evaluating Shallow Groundwater Age Tracers: Br−, CFCs, $^{3}H/^{3}He$, SF6, and HCFCs/HFCs. Ph.D. thesis, University of Waterloo.

Soil Resource Group. 2006. *Agronomic Services for County of Oxford Lands within the Thornton Well Field.* Final Report (draft).

Stöckle, C.O. and R. Nelson. 2006. *Cropping systems simulation model user's manual.* Washington State University, Biological Systems Engineering Department. http://www.sipeaa .it/tools/CropSyst/CropSyst_manual.pdf.

Tel, D. A. and Heseltine, C. 1990. The analysis of KCl soil extracts for nitrate, nitrite and ammonium using a TRAACS 800 analyzer. *Communications in Soil Science and Plant Analysis* 21:1681-1688.

van Genuchten, M. Th., F. J. Leij, and S. R. Yates. 1991. *The RETC code for quantifying the hydraulic functions of unsaturated soils.* Robert S. Kerr Environmental Research Laboratory, Office of Research and Development, U. S. Environmental Protection Agency, Ada, OK.

Vieira, S. R., D. R. Nielsen, J. W. Biggar. 1981. Spatial variability of field-measured infiltration rate. *Soil Science Society of America Journal* 45:1040-1048.

Ward, Mary H., Theo M. deKok, Patrick Levallois, Jean Brender, Gabriel Gulis, Bernard T. Nolan, and James VanDerslice. 2005. Workgroup report: Drinking-water nitrate and health – Recent findings and research needs. *Environmental Health Perspectives* 113(11):1607-1614.

Wassenaar, Leonard I., M. Jim Hendry, and Nikki Harrington. 2006. Decadal geochemical and isotopic trends for nitrate in a transboundary aquifer and implications for agricultural beneficial management practices. *Environmental Science and Technology* 40: 4626-4632.

Wellings, S. R. 1984. Recharge of the upper chalk aquifer at a site in Hampshire, England: I. Water balance and unsaturated flow. *Journal of Hydrology* 69:259-273.

Wendt, S. 2005. Hydraulic parameter investigation and 1D-modelling of water flow and solute transport in the vadose zone of the Thornton well field in Woodstock, Ontario, Canada. Student project in hydrogeology, Department of Earth Sciences, University of Waterloo.

Wicklund, R. E. and N. R. Richards. 1961. *The Soil Survey of Oxford County,* Report No. 28 of the Ontario Soil Survey, Research Branch, Canada Department of Agriculture and the Ontario Agricultural College.

Yao, T., P. Wierenga, A. Graham, and S. Neuman. 2004. Neutron probe calibration in a vertically stratified vadose zone. *Vadose Zone Journal* 3:1400-1406.

Appendix A

Recharge Station Layout Sketches

Approx. Slope = 0.01
downward to East

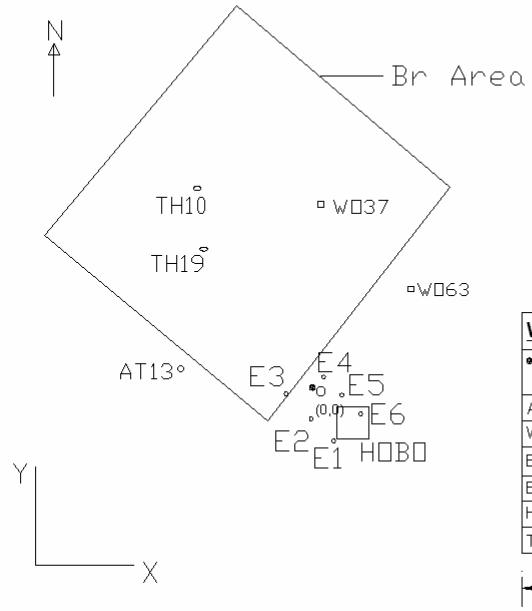

Woodstock Recharge Station 1 - Legend
• O (0,0) - Origin: x = 519847.397m East, y = 4770359.122m North.
AT - Access Tube for Neutron Moisture Probe
WO - Waterloo Observation Monitoring Well
E - ECHO Soil Water Content/Temp. Probes
Br Area - Bromide Application Area
HOBO - HOBO Dataloger
TH - Test Hole

5.00m

Approx. Slope = 0.01
downward to East

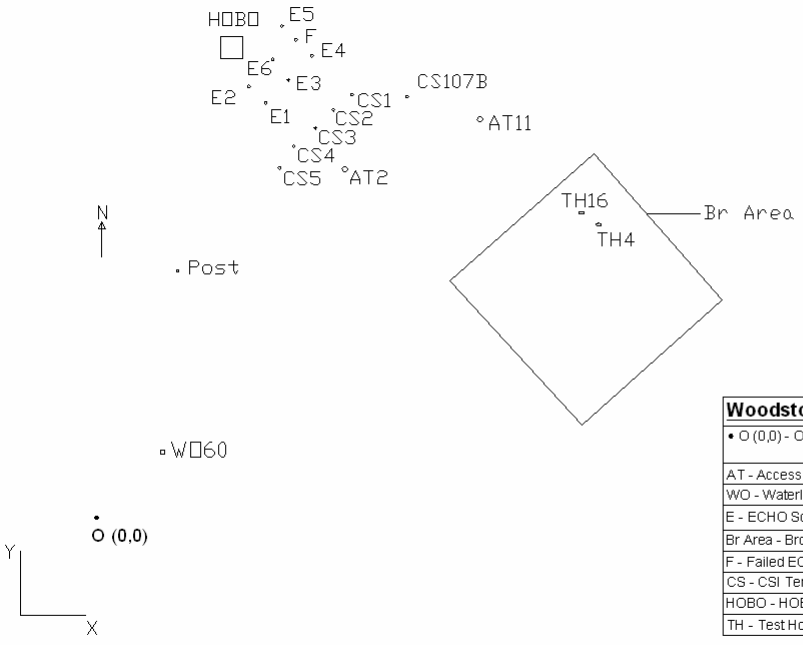

Woodstock Recharge Station 2 - Legend
• O (0,0) - Origin: x = 519405.1871m East, y = 4769959.682m North.
AT - Access Tube for Neutron Moisture Probe
WO - Waterloo Observation Monitoring Well
E - ECHO Soil Water Content/Temp. Probes
Br Area - Bromide Application Area
F - Failed ECHO Probe Installation
CS - CSI Temp. and Soil Water Content Probes
HOBO - HOBO Datalogger
TH - Test Hole

5.00m

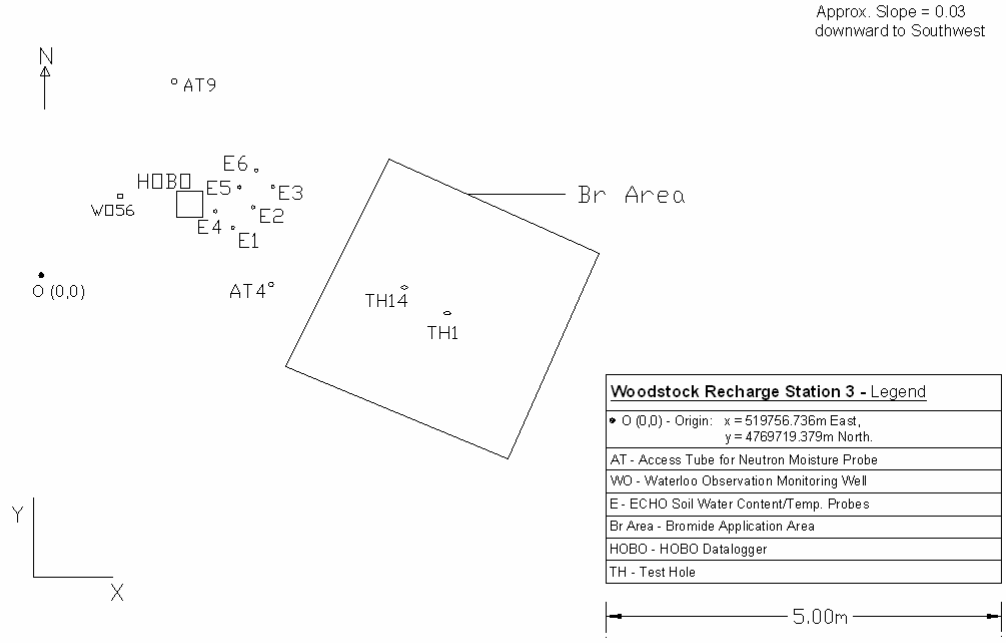
Approx. Slope = 0.03
downward to Southwest
N
AT9
E6
HOBO
E5
E3
WO56
E2
E4
E1
O (0,0)
AT4
Br Area
TH14
TH1
Y
X
Woodstock Recharge Station 3 - Legend
O (0,0) - Origin: x = 519756.736m East, y = 4769719.379m North.
AT - Access Tube for Neutron Moisture Probe
WO - Waterloo Observation Monitoring Well
E - ECHO Soil Water Content/Temp. Probes
Br Area - Bromide Application Area
HOBO - HOBO Datalogger
TH - Test Hole
5.00m

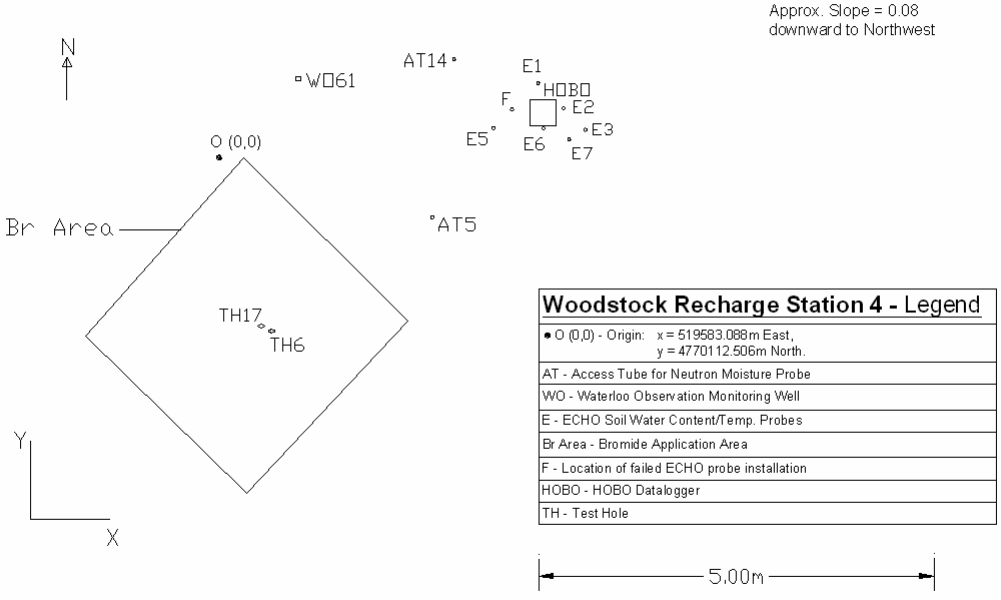
Approx. Slope = 0.08
downward to Northwest
N
AT14
E1
WO61
HOBO
F
E2
E5
E6
E3
E7
O (0,0)
Br Area
AT5
TH17
TH6
Y
X
Woodstock Recharge Station 4 - Legend
O (0,0) - Origin: x = 519583.088m East, y = 4770112.506m North.
AT - Access Tube for Neutron Moisture Probe
WO - Waterloo Observation Monitoring Well
E - ECHO Soil Water Content/Temp. Probes
Br Area - Bromide Application Area
F - Location of failed ECHO probe installation
HOBO - HOBO Datalogger
TH - Test Hole
5.00m

Approx. Slope = 0.02
downward to Northeast

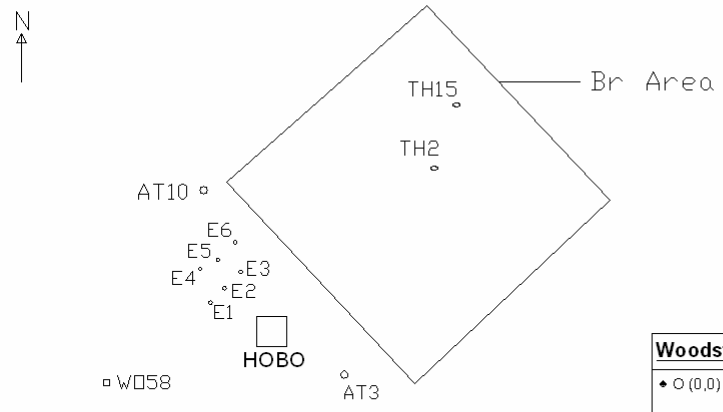

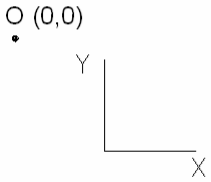

Woodstock Recharge Station 5 - Legend
O (0,0) - Origin: x=519342.981m East, y= 4769788.934m North
AT - Access Tube for Neutron Moisture Probe
WO - Waterloo Observation Monitoring Well
E - ECHO Soil Water Content/Temp. Probes
Br Area - Bromide Application Area
HOBO - HOBO Datalogger
TH - Test Hole

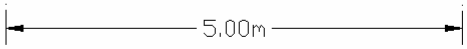

Approx. Slope = 0.2
downward to Southwest

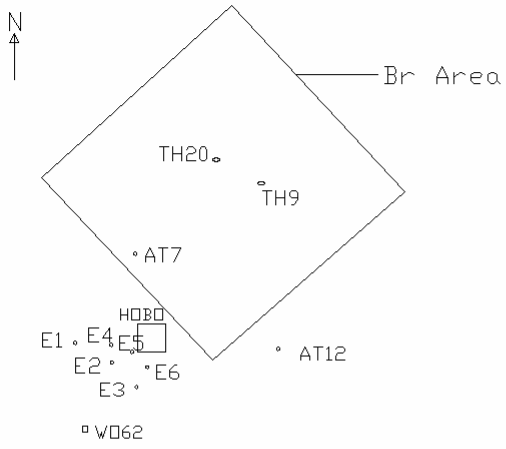

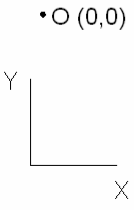

Woodstock Recharge Station 6 - Legend
O (0,0) - Origin: x = 519919.725m East y = 4770426.854m North.
AT - Access Tube for Neutron Moisture Probe
WO - Waterloo Observation Monitoring Well
E - ECHO Soil Water Content/Temp. Probes
Br Area - Bromide Application Area
HOBO - HOBO Datalogger
TH - Test Hole

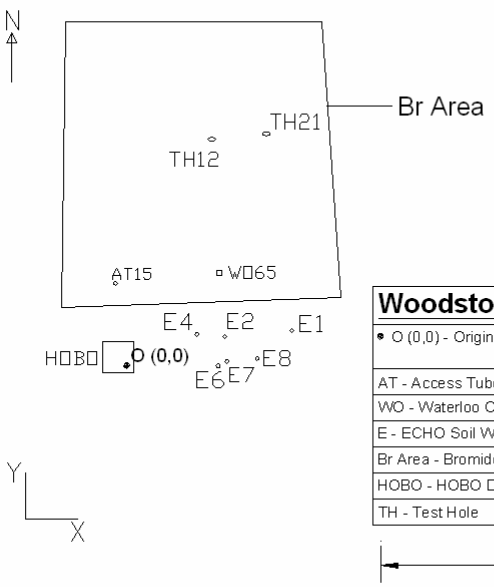

Approx. Slope = 0.007
downward to South

Woodstock Recharge Station 7 - Legend
• O (0,0) - Origin: x = 519576.336m East, y = 4770549.039m North
AT - Access Tube for Neutron Moisture Probe
WO - Waterloo Observation Monitoring Well
E - ECHO Soil Water Content/Temp. Probes
Br Area - Bromide Application Area
HOBO - HOBO Datalogger
TH - Test Hole

5.00m

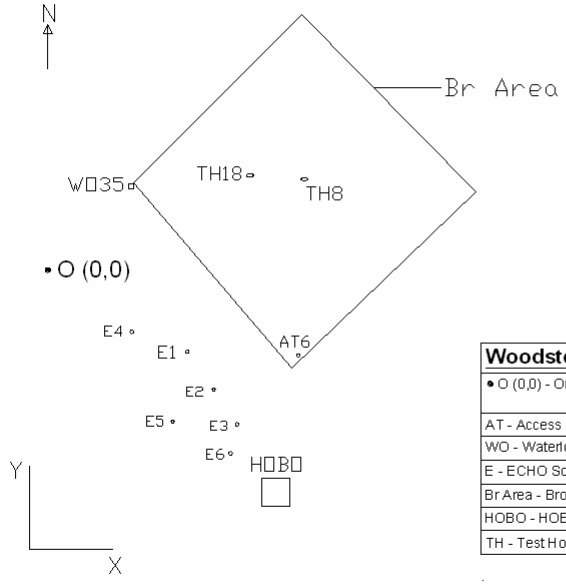

Approx. Slope = 0.04
downward to Northeast

Woodstock Recharge Station 8 - Legend
• O (0,0) - Origin: x = 519975.292m East y = 4770190.891m North
AT - Access Tube for Neutron Moisture Probe
WO - Waterloo Observation Monitoring Well
E - ECHO Soil Water Content/Temp. Probes
Br Area - Bromide Application Area
HOBO - HOBO Datalogger
TH - Test Hole

5.00m

Appendix B

Neutron Moisture Probe Calibration Program

Description: Soil water content was estimated with the Model 503 DR Hydroprobe Neutron Moisture Probe (CPN International Inc.). The probe uses 50mCi Americium-241/Beryllium as a source of fast neutrons, and measures the proportion of emitted fast neutrons that are redirected to the probe as slow neutrons after colliding with the hydrogen atoms in the water molecule. Moisture content is usually determined from the neutron probe count ratio (CR; raw neutron count/neutron count in a standard medium) using a linear calibration equation. In order to collect CRs, the neutron moisture probe is lowered down an access tube at user-specified intervals. At each measurement point along the profile, the probe emits fast neutrons and measures reflected slow neutrons.

Calibration: The 503 DR Hydroprobe was supplied with a factory calibration equation for measurements taken in a 5-cm (2-in) PVC access tube. Literature suggests, however, that site- and soil-specific calibrations are necessary for reliable measurements (Yao et al., 2004; Greacen et al., 1981). Therefore a field calibration program was conducted in the study area on November 17 and 18, 2005, and was based on the comparison of probe measurements in several newly-installed access tubes with the volumetric water content of the core collected during tube installation. These access tubes are not included in the set installed for regular water content measurements as described in Section 3.1.4.

The locations of the calibration access tubes were Recharge Stations 2, 4 and 5. At each station, a Vibra-Push® direct push rig equipped with the Enviro-Core® sampling system was used to advance a 5-cm (2-in) diameter borehole and collect continuous geologic core. The 0.9-m (3-ft) long core samples were sealed in the field to preserve moisture content and refrigerated at the University of Waterloo until analysis as described below. A 5-cm (2-in) diameter Schedule 40 PVC riser pipe with a bottom cap was fitted snugly into the borehole. Air space and surface water leakage between the access tube and the geologic material were minimized to ensure representative measurements. The riser pipe was cut at 0.2 m above ground surface and raw neutron counts were measured at 0.1-m intervals along the access tube within 30 minutes of

installation. The standard count of the neutron probe was determined in the field using the probe shield as an adsorber before the field measurements began.

The geologic cores from the access tube boreholes were subsequently sampled at 0.1 m intervals and analyzed in the laboratory for volumetric water content (VWC) and bulk density as described in Section 3.3.

Analysis: To determine the site-specific calibration equation for the neutron probe, the CR at each measurement point was compared to the corresponding VWC determined from the core samples. The radius of influence of the probe is approximately 0.15 m (Greacen et al., 1981); therefore for the CR measured at a given depth, the corresponding VWC was calculated as the average of the VWC measurements at that depth, 0.1 m above and 0.1 m below that depth. In the case where core material was missing from the core tube, one or two VWC measurements were used instead of three, with the measurement at the depth of the CR weighted twice as much as the adjacent VWC value. If the VWC could not be accurately estimated due to loss of a non-cohesive material from the core tube, the CR/VWC data pair was excluded from the analysis.

VWC was then regressed on CR to determine the calibration equation. This is contrary to Greacen et al.'s (1981) recommendation to regress CR on VWC based on greater confidence in and reliability of VWC measurements. In this study, as in Grismer et al.'s (1995), greater reliability was assigned to CR values, due to their reproducibility and the potential error associated with having only one VWC measurement at each depth.

Two additional corrections to the calibration data recommended in the literature were also applied and evaluated for their effect on the calibration equation. A correction for soil bulk density was recommended by Greacen and Hignett (1976) to account for the potential "trapping" of fast neutrons in higher density material. Based on an empirical relationship between count rate at constant VWC and the square root of density, the correction factor to CR was $(\rho_b/\rho_{bi})1/2$ where ρb is the average bulk density at the site and ρbi is the soil bulk density at a given depth. The regression of VWC on CR was repeated after this adjustment.

The presence of constitutionally bound hydrogen in clay minerals and organic matter also affects the response of the neutron moisture probe. The equivalent water content θ_e of hydrogen may be estimated as $0.124(\pm 0.012)C + 0.015$, where C is the fractional clay content of the soil (Greacen et al., 1981). The maximum clay content of any of the site materials is 10-15%, which corresponds to θ_e of approximately 2.7 to 3.4%. The regression was repeated after increasing the overall VWC for materials assumed to have clay content of >10% by 3%, to reflect the θ_e contribution.

Results: The uncorrected VWC and CR data are shown in Figure B.1. The calibration equation ($r^2 = 0.83$) for the conversion of CR to VWC is

$$VWC = 35.8(\pm 3.4) \cdot CR - 10.1(\pm 2.7) \quad \text{(B.1)}$$

where

VWC is the volumetric water content (percentage)

CR is the count ratio (raw neutron count/standard count)

For the density correction, an average ρ_b of 1.8 g/cm^3 was calculated from the laboratory analysis of all the samples. The ranges for ρ_{bi} and $(\rho_b/\rho_{bi})^{1/2}$ were 1.2 to 2.6 g/cm^3 and 0.8 to 1.2, respectively. Applying the density correction reduced the r^2 value from 0.83 to 0.74 and yielded the following calibration equation:

$$VWC = 33.7(\pm 4.1) \cdot CR - 8.4(\pm 3.3) \quad \text{(B.2)}$$

The coefficients in the density-corrected equation are within the 95% confidence interval of the uncorrected equation. Applying the density correction to the calibration would require that subsequent neutron probe measurements at the site be corrected for density, and density values along the entire profile of every access tube are unknown. Given this limitation and the reduction in the correlation coefficient, the density correction was omitted from the final calibration. Grismer et al. (1995) also found that the density correction were of limited value for field calibrations.

When the correction for clay content was applied to the original uncorrected data, the correlation coefficient was unchanged (0.83) and again the coefficients of the calibration equation fell within the 95% confidence interval of the uncorrected data:

$$VWC = 39.0(\pm 3.6) \cdot CR - 11.4(\pm 3.0) \quad \text{(B.3)}$$

Given the limited benefit of applying this correction and the increased labour required to correct all future readings for clay content, this correction was also omitted for the final calibration. Consequently the final site-specific calibration equation for the neutron moisture probe is Equation B.1.

A soil-specific calibration was also attempted for each of the clay, silt, fine sand and well-graded sand units common to the site. This analysis required subsets of the uncorrected data set, grouped by soil type and limited to CRs at points more than 0.15 m from soil type interfaces and their associated VWC data. This criterion was applied to encompass the 0.15 m radius of influence of the probe and to avoid bias related to averaging across different units. The distribution of soil-specific data is shown in Figure B.2. Linear regression was attempted on the individual data sets for each soil type, but the data sets were found to be too limited in range to be used for soil-specific calibration. The data set for silty clay, for example, consisted of 22 data pairs, 18 of which were clustered between 20 and 24% VWC. The soil-specific calibration was not possible for the available data set. Although the use of one equation for all soil types may result in decreased accuracy (Yao et al., 2004), it is convenient for sites where the detailed stratigraphy and soil characteristics along each access tube are unknown.

Additional sources of error in the derivation of the calibration equation include:

- Spatial variability in the soil water content, which limits the accuracy of comparing volumetric water content of material collected from the access tube hole to the neutron counts of the material surrounding the access tube;
- Compaction of the soil around the tube during installation.

Although there are numerous neutron probe calibration efforts described in the literature, few of these employed PVC access tubes. Yao et al. (2004) conducted soil-specific calibrations for a vertically-stratified vadose zone using two-inch Sch. 40 PVC access tubes. For a general calibration line fitted through all soil types, they reported a similar slope (38.6) as in this calibration but a significantly different intercept (-30). Their soil-specific calibration lines had significantly shallower slopes than the general calibration. The fact that Yao et al. reported a

similar range of measured water content values as in this calibration, but count ratios that ranged from 1 to 1.6, as compared to 0.4 to 1.3 here, suggests that other elements of the installation, sampling, or measurement processes differed between the two studies, or there are variations in site characteristics that preclude comparison of the results. For example, Yao et al. obtained standard count measurements with the probe at 2 m depth in an access tube, which may have yielded different standard count values compared to this study and consequently may have affected the slope of the calibration line.

Large diameter tube calibration: A separate analysis of the calibration data was conducted to derive a calibration equation for the larger 7.5 cm (3 in) diameter access tubes present at the site. The use of 7.5 cm access tubes is not ideal, as the larger diameter increases neutron loss and the potential for eccentric positioning of the probe (Greacen et al., 1981). The 7.5 cm tubes, however, are deeper on average than the 5 cm tubes and offer additional information about the general water content profile at each station.

The 7.5 cm tube calibration followed the method described for the 5 cm tubes described above. The raw neutron counts were measured in the existing 7.5 cm tubes at Stations 2, 4 and 5 at the time of installation of the 5 cm calibration tubes and collection of geologic core. The maximum distance between the 7.5 cm access tube and the 5 cm hole at each station was approximately one metre. The data is plotted in Figure B.3. The calibration equation ($r^2 = 0.75$) for the 7.5 cm tubes is

$$VWC = 54.7(\pm 7.2) \cdot CR - 17.1(\pm 4.3) \qquad \text{(B.4)}$$

In addition to the potential errors associated with the use of a 7.5 cm tube described above, this calibration is also limited by the fact that the gravimetric moisture content values were measured on core material from a borehole approximately one metre from the 7.5 cm tube.

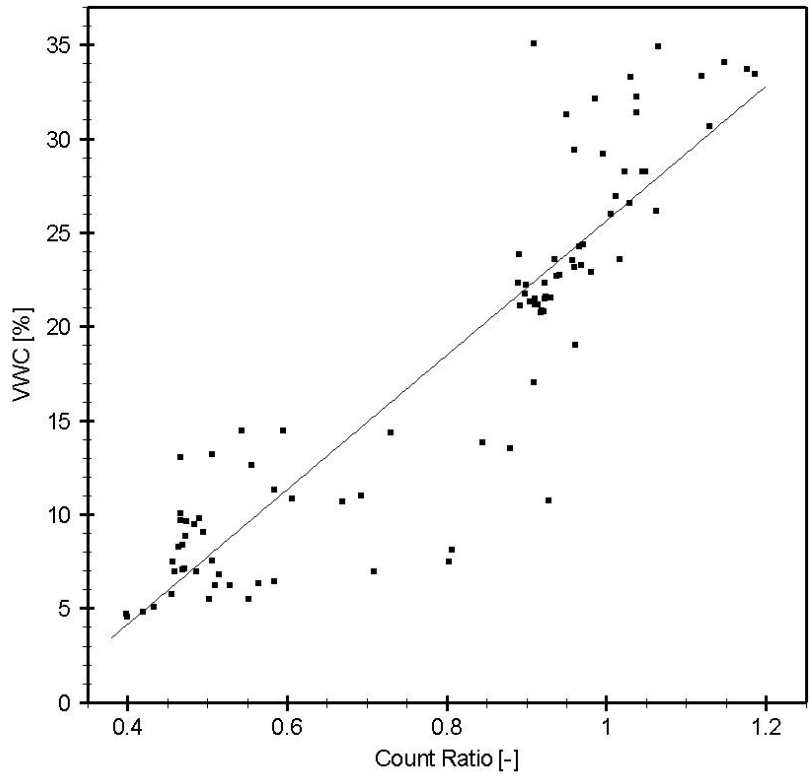

Figure B.1. Calibration data for 5-cm access tube

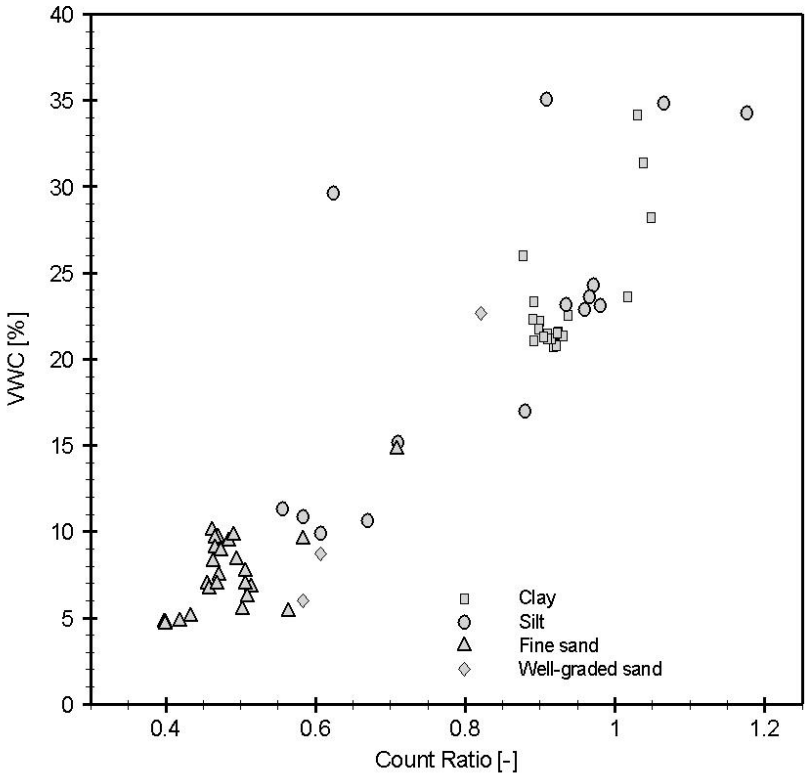

Figure B.2. Soil-specific calibration data (5-cm access tube)

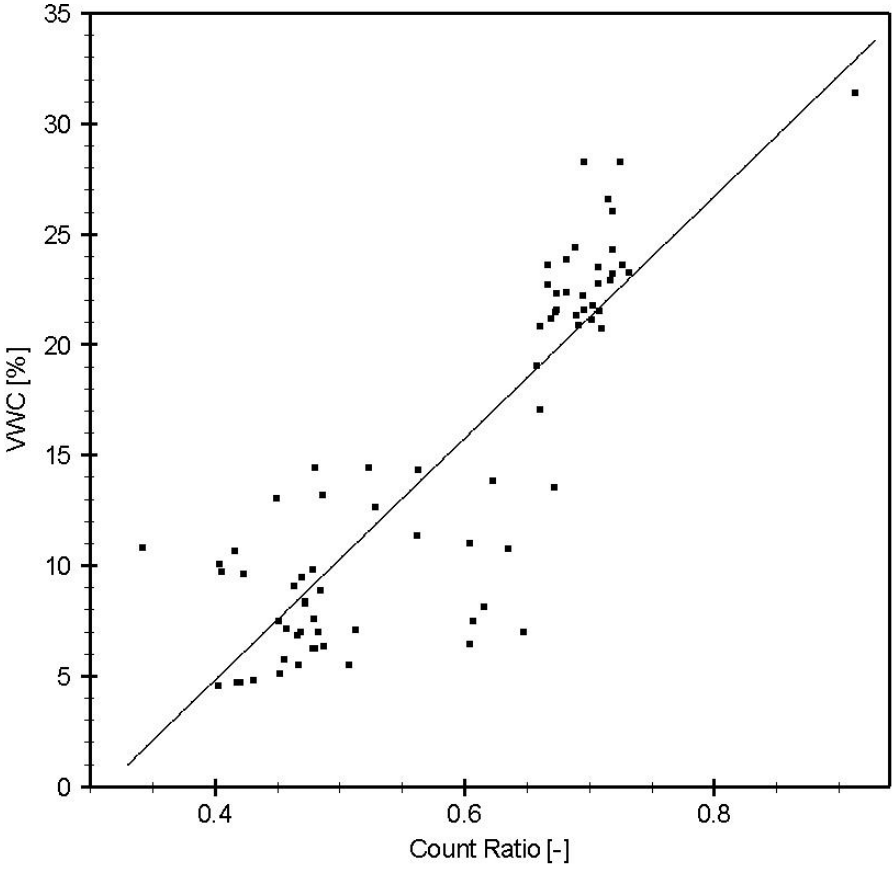

Figure B.3. Calibration data for 7.5-cm access tube

Appendix C

Evapotranspiration Calculations

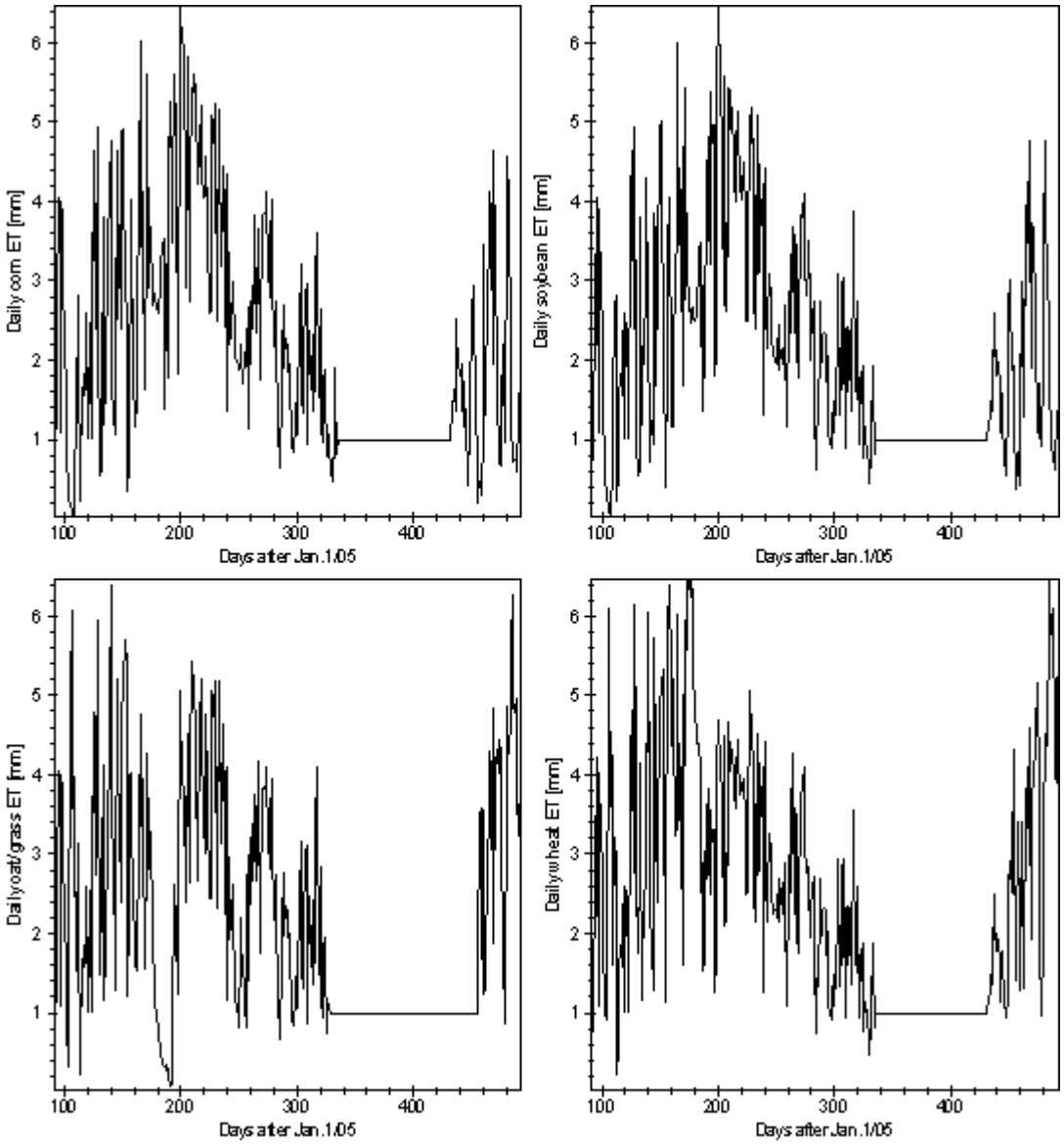

Figure C.1. Daily evapotranspiration (mm) for various crop types

CALCULATION OF REFERENCE EVAPOTRANSPIRATION (ET_o)

Based on a method described in Allen et al. (1998).

Reference evapotranspiration is expressed as

$$ET_o = \frac{0.408\Delta(R_n - G) + \gamma \frac{900}{T+273} u_2 (e_s - e_a)}{\Delta + \gamma(1 + 0.34u_2)}$$

where

ET_o	reference evapotranspiration [mm day^{-1}]
R_n	net radiation at the crop surface [MJ m^{-2} day^{-1}]
G	soil heat flux density [MJ m^{-2} day^{-1}]
T	air temperature at 2 m height [^{o}C]
u_2	wind speed at 2 m height [m s^{-1}]
e_s	saturation vapour pressure [kPa]
e_a	actual vapour pressure [kPa]
$e_s - e_a$	saturation vapour pressure deficit [kPa]
Δ	slope vapour pressure curve [kPa ^{o}C^{-1}]
γ	psychrometric constant [kPa ^{o}C^{-1}]

Saturation vapour pressure is expressed as

$$e_s = 0.3054\left[\exp\left(\frac{17.27 T_{max}}{T_{max} + 237.3}\right) + \exp\left(\frac{17.27 T_{min}}{T_{min} + 237.3}\right)\right]$$

where

e_s	saturation vapour pressure [kPa]
T_{max}	maximum temperature in daily period [^{o}C]
T_{min}	minimum temperature in daily period [^{o}C]

Slope of vapour pressure curve is expressed as

$$\Delta = \frac{4098\left[0.6108\exp\left(\frac{17.27 T}{T + 237.3}\right)\right]}{(T + 237.3)^2}$$

where

Δ	slope vapour pressure curve [kPa ^{o}C^{-1}]
T	mean air temperature [^{o}C]

Actual vapour pressure is expressed as

$$e_a = \frac{\exp\left(\frac{17.27 T_{min}}{T_{min} + 237.3}\right)\frac{RH_{max}}{100} + \exp\left(\frac{17.27 T_{max}}{T_{max} + 237.3}\right)\frac{RH_{min}}{100}}{2}$$

where

e_a actual vapour pressure [kPa]
T_{max} maximum temperature in daily period [°C]
T_{min} minimum temperature in daily period [°C]
RH_{max} maximum relative humidity in daily period [%]
RH_{min} minimum relative humidity in daily period [%]

Psychrometric constant is expressed as

$$\gamma = 0.665 \cdot 10^{-3} P$$

where
γ psychrometric constant [kPa °C^{-1}]
P atmospheric pressure [kPa]

Net radiation is expressed as

$$R_n = R_{ns} - R_{nl}$$

where
R_n net radiation [MJ m^{-2} day^{-1}]
R_{ns} incoming net shortwave radiation [MJ m^{-2} day^{-1}]
R_n outgoing net shortwave radiation [MJ m^{-2} day^{-1}]

Net outgoing longwave radiation is expressed as

$$R_{nl} = \sigma \left[\frac{T_{\max,K}^{\ 4} + T_{\min,K}^{\ 4}}{2} \right] (0.34 - 0.14\sqrt{e_a}) \left(1.35 \frac{R_s}{R_{so}} - 0.35 \right)$$

where
R_{nl} net outgoing longwave radiation [MJ m^{-2} day^{-1}]
σ Stefan-Boltzmann constant [4.903 x 10^{-9} MJ K^{-4} m^{-2} day^{-1}]
$T_{max,K}$ maximum absolute temperature during the 24-hour period [K]
$T_{min,K}$ minimum absolute temperature during the 24-hour period [K]
e_a actual vapour pressure [kPa]
R_s measured or calculated solar radiation [MJ m^{-2} day^{-1}]
R_{so} calculated clear-sky radiation [MJ m^{-2} day^{-1}]

Calculated clear-sky radiation is expressed as

$$R_{so} = (0.75 + 2 \cdot 10^{-5} z) R_a$$

where
z station elevation above sea level [m]
R_a extraterrestrial radiation [MJ m^{-2} day^{-1}]

Extraterrestrial radiation is expressed as

$$R_a = \frac{24 \cdot 60}{\pi} G_{sc} d_r \left[\omega_s \sin\varphi \sin\delta + \cos\varphi \cos\delta \sin\omega_s \right]$$

where

R_a	extraterrestrial radiation [MJ m^{-2} day^{-1}]
G_{sc}	solar constant [0.0820 MJ m^{-2} day^{-1}]
d_r	inverse relative distance Earth-Sun
ω_s	sunset hour angle [rad]
φ	latitude [rad]
δ	solar declination [rad]

Inverse relative distance Earth-Sun and solar declination are expressed as

$$d_r = 1 + 0.033 \cos\left(\frac{2\pi}{365} J\right)$$

$$\delta = 0.409 \sin\left(\frac{2\pi}{365} J - 1.39\right)$$

where

J	number of the day in the year

Sunset hour angle is expressed as

$$\omega_s = \arccos[-\tan\varphi \tan\delta]$$

CALCULATION OF CROP EVAPOTRANSPIRATION (ET_c)

$$ET_{c\,adj} = (K_s K_{cb} + K_e) ET_o$$

where

$ET_{c\,adj}$	crop evapotranspiration adjusted for soil water stress
K_s	water stress coefficient
K_{cb}	basal crop coefficient
K_e	soil evaporatation coefficient

Three values for K_{cb} are required to describe and construct the crop coefficient curve: those during the initial stage ($K_{cb\ ini}$), the mid-season stage ($K_{cb\ mid}$) and at the end of the late season stage ($K_{c\ end}$).

SAMPLE CALCULATION:

	A	B	C	D	E	F	G	H	I	J	K	L	M	N
	Day	ET_o	P-RO	I/f_w	height	K_{cmax}	f_c	f_w	f_{ew}	K_{cb}	$D_{e,i\ start}$	K_r	K_e	E
1	135	1.350	0	0	0.261	1.186	0.01	1	0.99	0.15	0	1	1.036	1.398
2	136	1.812	0	0	0.261	1.183	0.01	1	0.99	0.15	1.41	1	1.033	1.873

	O	P	Q	R	S	T	U	V	W	X	Y	Z
	DP_e	$D_{e,i\ end}$	K_c	ET_c	Root depth	Ending D	Irr. Applied	Drainage	K_s	$K_{c\ adj}$	Corrected Ending D	$Et_{c\ adj}$
1	0	1.412	1.186	1.600	0	1.600	0	0	1	1.186	1.600	1.600
2	0	3.303	1.183	2.144	0	3.744	0	0	1	1.183	3.744	2.144

Columns:

A	day of year
B	reference evapotranspiration [mm]
C	precipitation minus runoff [mm]
D	net irrigation depth [mm]
E	plant height [m]
F	maximum K_c immediately following wetting [-]
G	effective fraction of soil surface covered by vegetation [-]
H	fraction of soil surface wetted by irrigation or precipitation [-]
I	exposed and wetted soil fraction [-]
J	basal crop coefficient [-]
K	initial depth of evaporation (depletion) [mm]
L	dimensionless evaporation reduction coefficient [-]
M	soil evaporation coefficient [-]
N	evaporation on day i [mm]
O	deep percolation from evaporating layer [mm]
P	depth of evaporation (depletion) at end of day [mm]
Q	dual crop coefficient [-]
R	crop evapotranspiration, uncorrected for soil water stress [mm]
S	root depth [m]
T	root zone depletion at end of day i (soil water stress correction) [mm]
U	net irrigation depth on day i (soil water stress correction) [mm]
V	deep percolation (soil water stress correction) [mm]
W	dimensionless transpiration reduction factor [-]
X	evapotranspiration coefficient [-]
Y	corrected root zone depletion at end of day i [mm]
Z	final crop evapotranspiration value [mm]

Equations for Row 2:

A	day of year
B	ET_o

C	P - RO
D	Irrigation on day 1/H1
E	max((J2/Kcb mid) x max height, E1)
F	max((1.2+(0.04*(u_2-2)-0.004*(RH_{min}-45))*(E2/3)^0.3),(J2+0.05))
G	max((((J2-$K_{c\ min}$)/($K_{c\ max}$ – $K_{c\ min}$))^(1*0.5E2)), 0.01)
H	1 (no irrigation)
I	min(1-G2, H2)
J	basal crop coefficient, varies with crop growth stage
K	max(P1-C2-D2,0)
L	max(if(K2<REW,1,((TEW-K2)/(TEW-REW))),0)
M	min(L2*(F2-J2),I2*F2)
N	M2 x B2
O	max(C2+D2-P1,0)
P	min(K2-C2-D2+N2/I2+O2,0)
Q	M2 + J2
R	Q2 x B2
S	max(min.root+(max.root-min.root)*(J2-$K_{cb\ ini}$)/($K_{cb\ mid}$ – $K_{cb\ ini}$),0)
T	Y1-C2-U2+R2
U	0 (no irrigation)
V	max(C2+U1-R2-Y1,0)
W	if(T2>RAW,(TAW-T2)/(TAW-RAW),1)
X	W2 x J2 + M2
Y	Y1-C2-U2+X2*B2+V2
Z	X2 x B2

Appendix D

SHAW Model Crop Growth Parameters

	Day	Year	Height (m)	Characteristic dimension (m)	Dry biomass (kg/m^2)	Leaf area index	Root depth (m)
Corn	69	2005	0.00	0.00	0.00	0.00	0.00
	134	2005	0.00	0.00	0.00	0.00	0.00
	135	2005	0.26	0.30	0.24	0.00	0.20
	165	2005	0.26	0.30	0.24	0.43	0.20
	177	2005	0.78	5.50	0.53	0.60	0.44
	193	2005	1.48	9.50	0.91	4.00	0.76
	203	2005	1.91	12.00	1.15	4.50	0.96
	205	2005	2.00	12.50	1.20	4.48	1.00
	221	2005	2.00	12.50	1.20	4.30	1.00
	255	2005	2.00	12.50	1.20	3.30	1.00
	275	2005	2.00	12.50	1.20	2.00	1.00
	276	2005	0.00	0.00	0.00	0.00	0.00
	152	2006	0.00	0.00	0.00	0.00	0.00
Source			Allen et al. (1998)	Fallow et al. (2003)	estimated from Fallow et al. (2003)	Fallow et al. (2003)	Allen et al. (1998)
Soybean	69	2005	0.00	0.00	0.00	0.00	0.00
	89	2005	0.00	0.00	0.00	0.00	0.00
	147	2005	0.10	1.00	0.24	0.00	0.20
	167	2005	0.10	1.00	0.24	0.00	0.20
	168	2005	0.11	1.11	0.27	0.00	0.22
	196	2005	0.60	4.31	1.04	2.70	0.86
	202	2005	0.70	0.70	1.20	3.60	1.00
	217	2005	0.70	0.70	1.20	6.00	1.00
	231	2005	0.70	0.70	1.20	5.00	1.00
	259	2005	0.70	0.70	1.20	2.70	1.00
	287	2005	0.70	0.70	1.20	2.00	1.00
	288	2005	0.00	0.00	0.00	0.00	0.00
	152	2006	0.00	0.00	0.00	0.00	0.00
Source			Allen et al. (1998)	field estimate	estimated from Fallow et al. (2003)	Pedersen and Lauer (2004); Dermody, Long, and DeLucia (2006)	Allen et al. (1998)

	Day	Year	Height (m)	Characteristic dimension (m)	Dry biomass (kg/m^2)	Leaf area index	Root depth (m)
Oats/ grass	69	2005	0.00	0.00	0.00	0.00	0.00
	89	2005	0.00	0.00	0.00	0.00	0.00
	105	2005	0.14	0.40	0.48	0.00	0.20
	125	2005	0.14	0.40	0.48	0.00	0.20
	135	2005	0.48	0.64	0.77	0.00	0.32
	140	2005	0.65	0.76	0.91	1.50	0.38
	150	2005	1.00	1.00	1.20	4.00	0.50
	160	2005	1.00	1.00	1.20	5.00	0.50
	170	2005	1.00	1.00	1.20	6.00	0.50
	180	2005	1.00	1.00	1.20	5.00	0.50
	195	2005	1.00	1.00	1.20	4.50	0.50
	240	2005	0.30	0.50	1.20	4.00	0.50
	323	2005	0.30	0.50	1.20	4.00	0.50
	324	2005	0.00	0.00	0.00	0.00	0.00
	152	2006	0.00	0.00	0.00	0.00	0.00
Source			Allen et al. (1998)	field estimate	estimated from Fallow et al. (2003)	Stöckle and Nelson (2006)	Allen et al. (1998)

Appendix E

Meteorological Station Data

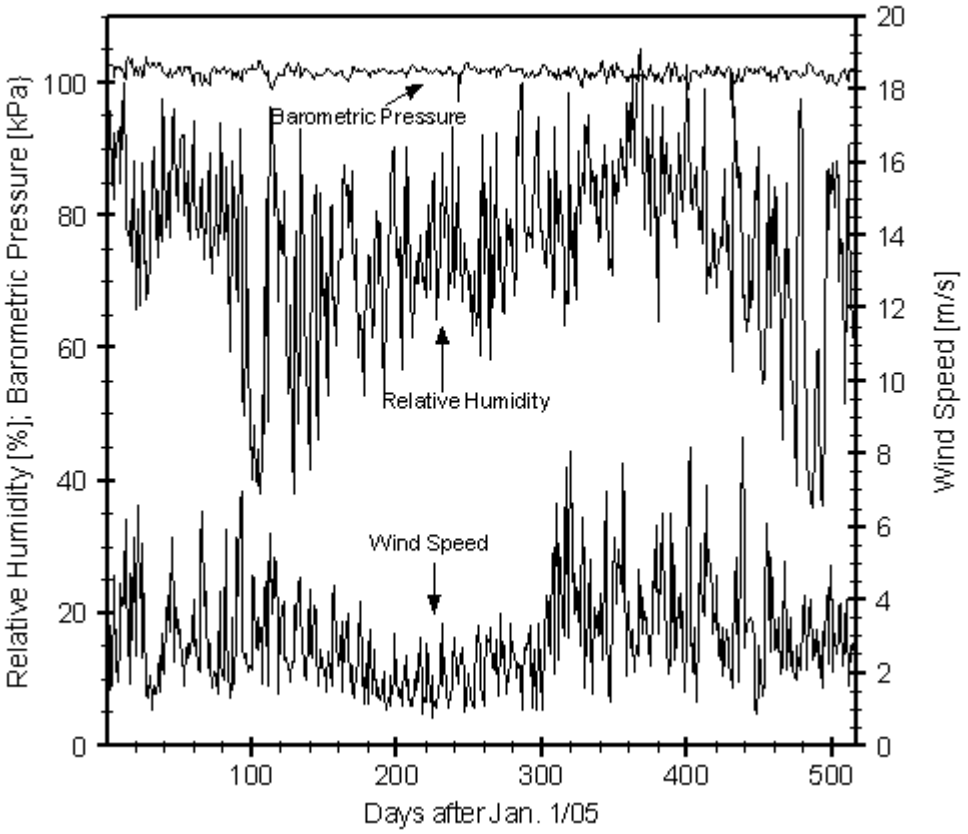

Figure E.1. Meteorological station data

Table E.1. Meteorological station CSI soil water content and temperature data

Day after Jan.1/05	CSI Soil Water Content Sensors					CSI Soil Temperature Sensors				
	0.95 m	1.25 m	1.65 m	2.05 m	2.45 m	0.85 m	1.25 m	1.65 m	2.05 m	2.45 m
127	0.365	0.427	0.441	0.42	0.353	6.668	6.12	5.12	5.925	5.78
128	0.371	0.427	0.442	0.421	0.392	6.992	6.271	3.721	5.947	5.802
129	0.375	0.426	0.442	0.422	0.397	7.31	6.46	1.824	5.987	5.828
130	0.378	0.426	0.442	0.422	0.398	7.71	6.68	-0.806	6.044	5.86
131	0.381	0.426	0.442	0.423	0.398	8.1	6.935	-0.723	6.117	5.901
132	0.382	0.426	0.442	0.423	0.398	8.45	7.19	-0.582	6.207	5.949
133	0.382	0.425	0.442	0.423	0.398	8.68	7.44	-0.387	6.314	6.013
134	0.383	0.425	0.441	0.423	0.397	8.74	7.64	-0.187	6.433	6.09
135	0.383	0.425	0.441	0.423	0.397	8.77	7.75	-0.134	6.55	6.169
136	0.383	0.424	0.441	0.423	0.397	8.83	7.86	-0.008	6.661	6.252
137	0.382	0.424	0.44	0.424	0.396	8.76	7.93	0.105	6.765	6.337
138	0.382	0.424	0.44	0.424	0.396	8.68	7.95	0.193	6.859	6.42
139	0.381	0.424	0.44	0.424	0.396	8.69	7.97	0.238	6.941	6.498
140	0.381	0.424	0.439	0.424	0.396	8.82	8.02	0.307	7.01	6.569
141	0.381	0.424	0.439	0.424	0.396	8.96	8.1	0.355	7.08	6.636
142	0.38	0.423	0.439	0.424	0.395	9.22	8.21	0.421	7.14	6.694
143	0.379	0.423	0.438	0.424	0.394	9.51	8.38	0.528	7.21	6.755
144	0.378	0.423	0.438	0.424	0.394	9.68	8.56	0.644	7.29	6.818
145	0.376	0.423	0.438	0.424	0.394	9.66	8.69	0.792	7.38	6.892
146	0.374	0.423	0.438	0.424	0.394	9.67	8.75	0.909	7.47	6.966
147	0.374	0.423	0.437	0.424	0.394	9.98	8.85	0.932	7.55	7.04
148	0.388	0.423	0.437	0.424	0.393	10.41	9.05	1.042	7.63	7.1
149	0.503	0.423	0.437	0.424	0.393	10.63	9.28	1.187	7.72	7.18
150	0.504	0.423	0.437	0.425	0.394	10.67	9.44	1.332	7.83	7.26
151	0.504	0.423	0.437	0.425	0.393	10.81	9.57	1.458	7.94	7.34
152	0.504	0.423	0.437	0.425	0.393	11.03	9.71	1.586	8.05	7.43
153	0.502	0.423	0.437	0.425	0.393	11.35	9.89	1.709	8.15	7.52
154	0.494	0.423	0.436	0.425	0.393	11.77	10.13	1.848	8.26	7.61
155	0.48	0.423	0.436	0.425	0.392	12.12	10.4	2.041	8.38	7.7
156	0.467	0.423	0.436	0.425	0.392	12.34	10.65	2.274	8.52	7.8
157	0.455	0.423	0.436	0.425	0.392	12.69	10.88	2.405	8.65	7.91
158	0.444	0.423	0.435	0.425	0.392	13.17	11.16	2.605	8.8	8.02
159	0.434	0.423	0.435	0.425	0.392	13.63	11.49	2.79	8.95	8.14
160	0.425	0.423	0.435	0.425	0.392	14.14	11.84	3.017	9.12	8.26
161	0.413	0.423	0.435	0.425	0.392	14.67	12.22	3.257	9.3	8.39
162	0.403	0.423	0.435	0.425	0.392	15.19	12.61	3.553	9.49	8.53
163	0.397	0.423	0.435	0.425	0.392	15.67	13	3.8	9.7	8.68
164	0.395	0.423	0.434	0.425	0.391	16.08	13.39	4.109	9.91	8.83
165	0.394	0.423	0.434	0.424	0.391	16.35	13.73	4.417	10.14	9
166	0.424	0.423	0.434	0.425	0.392	16.49	14.02	4.698	10.36	9.17
167	0.473	0.423	0.435	0.426	0.392	16.51	14.16	4.985	10.58	9.34
168	0.459	0.422	0.435	0.425	0.392	16.35	14.25	5.207	10.79	9.52
169	0.446	0.422	0.434	0.425	0.392	16.09	14.26	5.393	10.98	9.69
170	0.433	0.422	0.435	0.425	0.392	15.85	14.22	5.523	11.14	9.86

Day after Jan.1/05	CSI Soil Water Content Sensors					CSI Soil Temperature Sensors				
	0.95 m	1.25 m	1.65 m	2.05 m	2.45 m	0.85 m	1.25 m	1.65 m	2.05 m	2.45 m
171	0.418	0.422	0.434	0.425	0.392	15.66	14.16	5.623	11.28	10.01
172	0.404	0.421	0.434	0.425	0.391	15.57	14.11	5.636	11.39	10.15
173	0.396	0.421	0.434	0.425	0.391	15.65	14.1	5.693	11.48	10.27
174	0.393	0.421	0.433	0.425	0.391	15.79	14.15	5.739	11.55	10.37
175	0.393	0.421	0.433	0.425	0.39	15.98	14.25	5.874	11.64	10.48
176	0.392	0.421	0.433	0.425	0.39	16.22	14.38	5.94	11.73	10.58
177	0.393	0.413	0.432	0.425	0.39	16.58	14.55	6.029	11.82	10.67
178	0.393	0.372	0.432	0.425	0.39	16.95	14.77	6.173	11.92	10.77
179	0.393	0.349	0.431	0.425	0.389	17.32	15.01	6.326	12.03	10.87
180	0.394	0.334	0.431	0.424	0.389	17.66	15.27	7.04	12.16	10.98
181	0.394	0.328	0.432	0.424	0.389	17.93	15.52	6.943	12.3	11.09
182	0.393	0.327	0.431	0.424	0.389	18.15	15.74	6.897	12.45	11.2
183	0.395	0.323	0.43	0.424	0.389	18.28	15.94	7.07	12.6	11.33
184	0.396	0.318	0.43	0.424	0.388	18.28	16.09	7.28	12.76	11.46
185	0.395	0.315	0.406	0.424	0.388	18.23	16.19	8.3	12.92	11.61
186	0.393	0.313	0.396	0.424	0.388	18.23	16.24	7.54	13.05	11.73
187	0.392	0.31	0.388	0.424	0.388	18.27	16.31	7.7	13.17	11.86
188	0.389	0.308	0.38	0.424	0.388	18.24	16.37	8.64	13.29	11.98
189	0.387	0.306	0.376	0.424	0.388	18.18	16.4	8.33	13.39	12.09
190	0.384	0.302	0.365	0.424	0.388	18.14	16.43	10	13.5	12.2
191	0.377	0.299	0.356	0.423	0.388	18.05	16.44	11.1	13.59	12.31
192	0.369	0.297	0.346	0.423	0.388	18.06	16.45	12.59	13.68	12.42
193	0.362	0.294	0.338	0.423	0.388	18.18	16.48	12.94	13.75	12.51
194	0.356	0.292	0.332	0.422	0.388	18.34	16.56	12.66	13.82	12.59
195	0.353	0.29	0.325	0.421	0.387	18.52	16.67	11.85	13.89	12.68
196	0.352	0.288	0.318	0.421	0.387	18.63	16.78	11.39	13.97	12.76
197	0.351	0.285	0.312	0.421	0.387	18.66	16.87	13.01	14.05	12.84
198	0.351	0.283	0.308	0.419	0.386	18.69	16.94	13.41	14.14	12.93
199	0.35	0.281	0.305	0.419	0.386	18.7	17.01	14.26	14.24	13.03
200	0.348	0.279	0.301	0.417	0.386	18.68	17.04	14.39	14.32	13.11
201	0.345	0.276	0.294	0.411	0.386	18.65	17.07	14.49	14.39	13.2
202	0.341	0.273	0.288	0.406	0.385	18.59	17.09	14.58	14.47	13.29
203	0.338	0.27	0.283	0.402	0.384	18.57	17.09	14.64	14.53	13.36
204	0.333	0.266	0.277	0.392	0.384	18.58	17.09	14.68	14.59	13.43
205	0.33	0.263	0.272	0.383	0.384	18.54	17.1	14.71	14.63	13.49
206	0.328	0.261	0.269	0.377	0.382	18.48	17.12	14.79	14.7	13.58
207	0.327	0.258	0.266	0.371	0.382	18.41	17.09	14.77	14.74	13.63
208	0.327	0.256	0.263	0.361	0.382	18.4	17.08	14.79	14.78	13.68
209	0.326	0.254	0.259	0.337	0.382	18.33	17.08	14.83	14.82	13.74
210	0.324	0.252	0.256	0.323	0.382	18.15	17.04	14.87	14.86	13.8
211	0.321	0.249	0.253	0.313	0.381	17.95	16.97	14.91	14.89	13.86
212	0.314	0.245	0.25	0.305	0.38	17.83	16.89	14.91	14.92	13.91
213	0.308	0.242	0.248	0.3	0.379	17.77	16.83	14.93	14.94	13.97
214	0.303	0.238	0.245	0.295	0.378	17.81	16.79	14.9	14.95	14.01

Day after Jan.1/05	CSI Soil Water Content Sensors					CSI Soil Temperature Sensors				
	0.95 m	1.25 m	1.65 m	2.05 m	2.45 m	0.85 m	1.25 m	1.65 m	2.05 m	2.45 m
215	0.298	0.234	0.243	0.29	0.374	17.96	16.8	14.9	14.95	14.04
216	0.294	0.231	0.24	0.285	0.369	18.15	16.86	14.93	14.96	14.06
217	0.293	0.228	0.237	0.281	0.362	18.32	16.94	14.95	14.97	14.08
218	0.292	0.226	0.234	0.276	0.35	18.39	17.03	15.02	15	14.12
219	0.29	0.223	0.232	0.272	0.341	18.3	17.09	15.1	15.05	14.17
220	0.287	0.221	0.229	0.27	0.332	18.22	17.08	15.15	15.1	14.21
221	0.283	0.217	0.226	0.267	0.324	18.21	17.08	15.2	15.14	14.27
222	0.279	0.261	0.224	0.265	0.313	18.27	17.08	15.22	15.17	14.3
223	0.28	0.242	0.224	0.263	0.299	18.38	17.12	15.24	15.2	14.34
224	0.28	0.242	0.224	0.31	0.286	18.41	17.17	15.31	15.23	14.39
225	0.281	0.231	0.224	0.33	0.277	18.37	17.21	15.36	15.27	14.44
226	0.282	0.227	0.224	0.274	0.27	18.34	17.21	15.38	15.3	14.48
227	0.282	0.226	0.224	0.261	0.262	18.31	17.22	15.44	15.34	14.53
228	0.281	0.224	0.224	0.258	0.256	18.2	17.21	15.45	15.38	14.58
229	0.281	0.223	0.223	0.257	0.251	18.07	17.17	15.45	15.41	14.62
230	0.28	0.221	0.223	0.256	0.248	17.98	17.12	15.43	15.43	14.66
231	0.28	0.22	0.222	0.256	0.246	17.93	17.08	15.41	15.44	14.7
232	0.28	0.22	0.222	0.255	0.243	17.91	17.04	15.37	15.45	14.73
233	0.279	0.219	0.221	0.254	0.24	17.9	17.03	15.37	15.46	14.76
234	0.279	0.218	0.22	0.253	0.237	17.87	17	15.34	15.45	14.77
235	0.279	0.218	0.219	0.252	0.234	17.79	16.98	15.33	15.47	14.79
236	0.278	0.217	0.218	0.251	0.232	17.61	16.94	15.33	15.48	14.82
237	0.276	0.216	0.216	0.25	0.23	17.43	16.85	15.31	15.48	14.84
238	0.276	0.215	0.215	0.249	0.229	17.34	16.78	15.29	15.49	14.87
239	0.275	0.214	0.214	0.248	0.228	17.29	16.69	15.21	15.46	14.86
240	0.275	0.213	0.213	0.247	0.227	17.34	16.68	15.21	15.47	14.89
241	0.274	0.212	0.212	0.246	0.226	17.37	16.67	15.19	15.45	14.9
242	0.273	0.211	0.211	0.244	0.224	17.44	16.66	15.15	15.43	14.89
243	0.264	0.204	0.203	0.235	0.215	17.56	16.71	15.15	15.43	14.9
244	0.274	0.211	0.209	0.243	0.222	17.6	16.74	15.15	15.44	14.9
245	0.273	0.21	0.209	0.242	0.221	17.58	16.77	15.17	15.44	14.91
246	0.273	0.209	0.208	0.241	0.219	17.52	16.76	15.19	15.45	14.92
247	0.272	0.209	0.207	0.239	0.218	17.46	16.75	15.19	15.47	14.93
248	0.272	0.208	0.206	0.238	0.217	17.4	16.72	15.19	15.48	14.95
249	0.271	0.207	0.205	0.237	0.216	17.35	16.7	15.18	15.49	14.97
250	0.271	0.206	0.204	0.236	0.215	17.32	16.68	15.17	15.5	14.99
251	0.27	0.206	0.203	0.235	0.214	17.32	16.65	15.16	15.49	14.99
252	0.271	0.205	0.202	0.234	0.213	17.36	16.64	15.13	15.48	14.99
253	0.27	0.205	0.201	0.234	0.213	17.35	16.64	15.13	15.48	14.99
254	0.27	0.204	0.2	0.233	0.212	17.31	16.64	15.14	15.49	15
255	0.27	0.204	0.199	0.232	0.211	17.31	16.64	15.16	15.5	15.02
256	0.27	0.204	0.199	0.231	0.21	17.39	16.65	15.16	15.51	15.03
257	0.271	0.204	0.198	0.231	0.209	17.54	16.68	15.15	15.5	15.03
258	0.271	0.204	0.198	0.23	0.209	17.7	16.75	15.17	15.51	15.04

Day after Jan.1/05	CSI Soil Water Content Sensors					CSI Soil Temperature Sensors				
	0.95 m	1.25 m	1.65 m	2.05 m	2.45 m	0.85 m	1.25 m	1.65 m	2.05 m	2.45 m
259	0.271	0.204	0.198	0.23	0.208	17.7	16.82	15.16	15.52	15.04
260	0.271	0.204	0.198	0.23	0.207	17.59	16.84	15.23	15.56	15.07
261	0.271	0.204	0.198	0.23	0.207	17.46	16.81	15.26	15.58	15.1
262	0.271	0.204	0.198	0.229	0.206	17.35	16.77	15.26	15.6	15.12
263	0.271	0.204	0.198	0.229	0.206	17.27	16.72	15.27	15.61	15.14
264	0.271	0.204	0.198	0.229	0.205	17.23	16.68	15.26	15.62	15.16
265	0.27	0.204	0.198	0.229	0.205	17.14	16.63	15.23	15.61	9.38
266	0.27	0.204	0.198	0.229	0.205	17.1	16.59	15.2	15.6	15.18
267	0.27	0.204	0.198	0.229	0.204	17.03	16.55	15.15	15.6	15.18
268	0.27	0.204	0.198	0.229	0.204	16.86	16.5	15.14	15.59	15.2
269	0.27	0.204	0.198	0.229	0.204	16.75	16.42	15.1	15.58	15.2
270	0.27	0.204	0.198	0.229	0.203	16.79	16.36	15.05	15.56	15.2
271	0.27	0.204	0.198	0.229	0.203	16.73	16.34	15.02	15.54	15.2
272	0.27	0.203	0.198	0.229	0.203	16.54	16.27	14.98	15.52	15.2
273	0.269	0.203	0.198	0.229	0.203	16.35	16.18	14.95	15.5	15.2
274	0.269	0.203	0.198	0.229	0.202	16.02	16.06	14.92	15.49	15.21
275	0.268	0.203	0.198	0.229	0.202	15.73	15.88	14.85	15.45	15.21
276	0.268	0.203	0.198	0.229	0.202	15.57	15.72	14.77	15.41	15.21
277	0.268	0.203	0.197	0.228	0.202	15.59	15.61	14.68	15.35	15.19
278	0.268	0.203	0.197	0.228	0.201	15.74	15.57	14.6	15.29	15.17
279	0.269	0.203	0.197	0.228	0.201	15.89	15.59	14.54	15.24	15.14
280	0.269	0.203	0.197	0.228	0.201	16	15.61	14.49	15.19	15.09
281	0.269	0.203	0.197	0.228	0.2	16.01	15.65	14.44	15.16	15.06
282	0.269	0.203	0.197	0.228	0.201	15.77	15.63	14.45	15.15	15.05
283	0.268	0.203	0.197	0.228	0.201	15.4	15.51	14.41	15.13	15.04
284	0.268	0.203	0.197	0.228	0.201	15.09	15.34	14.36	15.11	15.03
285	0.268	0.203	0.197	0.228	0.2	14.87	15.16	14.21	15.06	15.01
286	0.267	0.202	0.197	0.228	0.2	14.73	15.01	14.13	15.01	14.99
287	0.267	0.202	0.197	0.228	0.2	14.64	14.9	14.05	14.95	14.96
288	0.267	0.202	0.197	0.228	0.2	14.62	14.8	13.96	14.88	14.92
289	0.267	0.202	0.196	0.228	0.2	14.61	14.74	13.89	14.81	14.88
290	0.267	0.202	0.196	0.228	0.2	14.49	14.68	13.84	14.76	14.84
291	0.267	0.202	0.196	0.228	0.2	14.3	14.58	13.76	14.7	14.8
292	0.266	0.201	0.196	0.227	0.199	14.13	14.46	13.68	14.65	14.76
293	0.266	0.201	0.196	0.227	0.199	13.94	14.33	13.62	14.58	14.72
294	0.265	0.201	0.196	0.227	0.199	13.68	14.19	13.54	14.52	14.67
295	0.265	0.201	0.196	0.227	0.199	13.38	14.01	13.43	14.45	14.63
296	0.265	0.201	0.196	0.227	0.199	13.08	13.82	13.34	14.37	14.58
297	0.264	0.201	0.196	0.227	0.199	12.74	13.6	13.19	14.28	14.52
298	0.264	0.2	0.196	0.227	0.198	12.45	13.38	13.06	14.18	14.47
299	0.263	0.2	0.195	0.227	0.198	12.17	13.16	12.92	14.08	14.4
300	0.263	0.2	0.195	0.227	0.198	11.92	12.94	12.74	13.97	14.33
301	0.263	0.2	0.195	0.226	0.198	11.71	12.74	12.59	13.85	14.25
302	0.262	0.199	0.195	0.226	0.198	11.51	12.56	12.45	13.73	14.17

Day after Jan.1/05	CSI Soil Water Content Sensors					CSI Soil Temperature Sensors				
	0.95 m	1.25 m	1.65 m	2.05 m	2.45 m	0.85 m	1.25 m	1.65 m	2.05 m	2.45 m
303	0.262	0.199	0.195	0.226	0.197	11.28	12.38	12.29	13.61	14.08
304	0.262	0.199	0.195	0.226	0.197	11.1	12.19	12.13	13.49	14
305	0.261	0.199	0.194	0.226	0.197	11.01	12.02	11.95	13.36	13.9
306	0.262	0.199	0.194	0.226	0.197	11.02	11.91	11.83	13.24	13.81
307	0.262	0.199	0.194	0.226	0.197	11	11.85	11.73	13.14	13.73
308	0.261	0.199	0.194	0.225	0.197	10.97	11.78	11.61	13.04	13.64
309	0.262	0.199	0.194	0.225	0.196	11.01	11.71	11.5	12.94	13.55
310	0.262	0.199	0.194	0.225	0.196	11.1	11.69	11.43	12.85	13.47
311	0.262	0.199	0.194	0.225	0.196	11.21	11.7	11.39	12.77	13.39
312	0.262	0.199	0.194	0.225	0.196	11.21	11.71	11.36	12.71	13.32
313	0.326	0.199	0.194	0.318	0.196	11.1	11.68	11.36	12.65	13.26
314	0.344	0.2	0.194	0.321	0.196	10.94	11.6	11.34	12.6	13.2
315	0.322	0.201	0.195	0.243	0.196	10.76	11.51	11.29	12.55	13.15
316	0.312	0.2	0.195	0.23	0.196	10.51	11.39	11.21	12.49	13.11
317	0.306	0.2	0.195	0.23	0.196	10.31	11.24	11.09	12.43	13.06
318	0.303	0.2	0.195	0.229	0.196	10.22	11.1	10.97	12.34	12.99
319	0.341	0.235	0.235	0.253	0.218	10.03	10.95	10.33	12.25	12.93
320	0.495	0.41	0.435	0.412	0.385	9.72	10.76	7.05	12.16	12.86
321	0.495	0.41	0.434	0.412	0.385	9.71	10.66	6.812	12.06	12.78
322	0.494	0.411	0.434	0.411	0.383	9.48	10.55	6.637	11.98	12.71
323	0.489	0.41	0.433	0.409	0.38	9.11	10.37	6.776	11.9	12.65
324	0.469	0.41	0.433	0.403	0.377	8.76	10.14	8.34	11.81	12.59
325	0.441	0.409	0.432	0.381	0.366	8.5	9.9	8.24	11.7	12.5
326	0.399	0.408	0.431	0.354	0.328	8.35	9.69	7.98	11.57	12.42
327	0.362	0.387	0.43	0.309	0.286	8.19	9.52	8.28	11.44	12.32
328	0.35	0.363	0.43	0.264	0.247	7.93	9.34	8.22	11.32	12.22
329	0.34	0.304	0.43	0.25	0.223	7.67	9.15	8.5	11.19	12.13
330	0.335	0.258	0.409	0.243	0.214	7.43	8.94	8.6	11.07	12.03
331	0.332	0.241	0.393	0.242	0.212	7.26	8.76	8.54	10.94	11.93
332	0.384	0.292	0.398	0.241	0.282	6.961	8.56	6.974	10.81	11.84
333	0.483	0.407	0.421	0.286	0.378	6.791	8.34	4.763	10.67	11.73
334	0.486	0.408	0.421	0.404	0.379	6.948	8.22	4.456	10.52	11.61
335	0.486	0.408	0.421	0.408	0.378	6.982	8.2	4.277	10.39	11.49
336	0.486	0.408	0.421	0.409	0.378	6.841	8.14	4.117	10.28	11.38
337	0.488	0.409	0.421	0.41	0.378	6.659	8.04	3.956	10.17	11.28
338	0.487	0.409	0.42	0.41	0.378	6.503	7.92	3.822	10.08	11.18
339	0.487	0.409	0.421	0.41	0.378	6.361	7.79	3.609	9.98	11.09
340	0.487	0.41	0.421	0.41	0.378	6.226	7.65	3.466	9.87	10.99
341	0.487	0.41	0.421	0.41	0.378	6.094	7.52	3.351	9.77	10.9
342	0.486	0.41	0.421	0.41	0.378	5.978	7.39	3.219	9.66	10.81
343	0.484	0.41	0.42	0.409	0.381	5.861	7.28	3.16	9.56	10.72
344	0.484	0.409	0.42	0.409	0.381	5.741	7.15	3.011	9.45	10.62
345	0.485	0.409	0.419	0.408	0.381	5.631	7.03	2.883	9.35	10.53
346	0.48	0.41	0.42	0.408	0.381	5.519	6.907	2.742	9.24	10.43

Day after Jan.1/05	CSI Soil Water Content Sensors					CSI Soil Temperature Sensors				
	0.95 m	1.25 m	1.65 m	2.05 m	2.45 m	0.85 m	1.25 m	1.65 m	2.05 m	2.45 m
347	0.464	0.41	0.42	0.408	0.381	5.436	6.802	2.606	9.14	10.34
348	0.45	0.41	0.42	0.409	0.381	5.358	6.704	2.482	9.04	10.25
349	0.448	0.41	0.42	0.408	0.381	5.282	6.616	2.428	8.94	10.16
350	0.442	0.41	0.42	0.408	0.38	5.211	6.529	2.266	8.85	10.07
351	0.413	0.41	0.42	0.409	0.381	5.144	6.437	2.112	8.75	9.98
352	0.397	0.411	0.42	0.409	0.381	5.081	6.353	2.031	8.66	9.89
353	0.402	0.411	0.42	0.409	0.381	5.024	6.275	1.95	8.57	9.8
354	0.406	0.411	0.42	0.409	0.381	4.976	6.206	1.884	8.48	9.72
355	0.402	0.411	0.42	0.409	0.381	4.934	6.143	1.821	8.4	9.64
356	0.398	0.411	0.42	0.409	0.381	4.897	6.086	1.788	8.32	9.56
357	0.405	0.411	0.42	0.408	0.38	4.862	6.034	1.749	8.24	9.49
358	0.414	0.411	0.42	0.409	0.381	4.827	5.98	1.643	8.17	9.41
359	0.479	0.411	0.421	0.41	0.382	4.766	5.922	1.683	8.09	9.34
360	0.49	0.413	0.422	0.412	0.384	4.663	5.846	1.698	8.02	9.26
361	0.49	0.414	0.423	0.413	0.384	4.616	5.779	1.608	7.94	9.19
362	0.49	0.413	0.422	0.412	0.384	4.579	5.725	1.635	7.87	9.11
363	0.491	0.414	0.423	0.413	0.384	4.541	5.665	1.732	7.79	9.04
364	0.491	0.414	0.423	0.414	0.385	4.496	5.606	1.591	7.72	8.96
365	0.491	0.414	0.423	0.413	0.384	4.462	5.559	1.513	7.65	8.89
366	0.492	0.414	0.423	0.413	0.385	4.435	5.514	1.436	7.58	8.83
367	0.492	0.414	0.423	0.414	0.385	4.406	5.466	1.482	7.52	8.76
368	0.493	0.415	0.424	0.415	0.386	4.373	5.421	1.541	7.46	8.7
369	0.493	0.415	0.424	0.415	0.386	4.339	5.384	1.512	7.4	8.64
370	0.493	0.415	0.424	0.415	0.386	4.298	5.333	1.409	7.33	8.57
371	0.493	0.414	0.423	0.414	0.386	4.312	5.293	1.282	7.27	8.5
372	0.492	0.414	0.423	0.413	0.385	4.298	5.278	1.2	7.22	8.45
373	0.492	0.414	0.423	0.413	0.385	4.226	5.239	1.069	7.16	8.39
374	0.492	0.414	0.423	0.413	0.385	4.149	5.187	1.017	7.12	8.34
375	0.493	0.415	0.424	0.414	0.386	4.074	5.125	0.946	7.06	8.29
376	0.493	0.414	0.424	0.414	0.386	4.017	5.069	1.05	7.01	8.24
377	0.494	0.415	0.424	0.415	0.387	3.957	5.008	1.088	6.959	8.19
378	0.494	0.415	0.424	0.415	0.386	3.956	4.964	1.069	6.906	8.14
379	0.494	0.415	0.424	0.415	0.386	4.032	4.922	0.973	6.838	8.07
380	0.491	0.414	0.423	0.414	0.386	4.167	4.943	0.79	6.783	8.01
381	0.489	0.414	0.423	0.413	0.385	4.149	4.965	0.719	6.737	7.96
382	0.488	0.413	0.423	0.413	0.385	4.062	4.955	0.808	6.707	7.92
383	0.487	0.415	0.424	0.415	0.387	3.901	4.889	0.939	6.67	7.88
384	0.488	0.415	0.424	0.415	0.387	3.786	4.808	0.805	6.625	7.83
385	0.489	0.415	0.425	0.416	0.388	3.683	4.727	0.857	6.576	7.79
386	0.49	0.416	0.425	0.416	0.388	3.59	4.634	0.82	6.51	7.73
387	0.49	0.416	0.425	0.416	0.388	3.523	4.557	0.688	6.444	7.66
388	0.489	0.415	0.424	0.415	0.387	3.475	4.491	0.583	6.38	7.61
389	0.488	0.414	0.424	0.414	0.386	3.434	4.436	0.499	6.321	7.55
390	0.488	0.414	0.424	0.414	0.386	3.388	4.376	0.378	6.261	7.5

Day after Jan.1/05	CSI Soil Water Content Sensors					CSI Soil Temperature Sensors				
	0.95 m	1.25 m	1.65 m	2.05 m	2.45 m	0.85 m	1.25 m	1.65 m	2.05 m	2.45 m
391	0.488	0.415	0.424	0.415	0.387	3.337	4.315	0.257	6.2	7.44
392	0.489	0.414	0.424	0.415	0.387	3.323	4.286	0.139	6.155	7.4
393	0.488	0.414	0.424	0.414	0.386	3.311	4.257	0.096	6.109	7.36
394	0.488	0.414	0.424	0.415	0.387	3.27	4.216	0.325	6.061	7.31
395	0.489	0.415	0.425	0.416	0.388	3.233	4.173	0.358	6.01	7.26
396	0.489	0.415	0.425	0.416	0.388	3.238	4.124	0.273	5.949	7.2
397	0.488	0.415	0.424	0.415	0.387	3.31	4.12	0.187	5.898	7.14
398	0.489	0.415	0.424	0.415	0.387	3.319	4.125	0.127	5.856	7.1
399	0.489	0.415	0.425	0.416	0.388	3.296	4.11	0.198	5.818	7.05
400	0.489	0.415	0.425	0.416	0.388	3.336	4.097	0.19	5.779	7.01
401	0.489	0.415	0.424	0.416	0.387	3.405	4.098	0.132	5.738	6.96
402	0.489	0.415	0.425	0.416	0.388	3.417	4.105	0.088	5.7	6.915
403	0.489	0.415	0.425	0.416	0.388	3.384	4.1	0.028	5.671	6.877
404	0.489	0.415	0.424	0.416	0.387	3.33	4.073	-0.022	5.641	6.84
405	0.488	0.415	0.424	0.416	0.387	3.28	4.043	-0.037	5.614	6.809
406	0.489	0.414	0.424	0.415	0.387	3.239	4.018	-0.092	5.592	6.786
407	0.489	0.414	0.424	0.415	0.387	3.185	3.978	-0.196	5.56	6.754
408	0.489	0.414	0.424	0.415	0.387	3.139	3.939	-0.227	5.53	6.725
409	0.489	0.414	0.424	0.414	0.387	3.106	3.907	-0.253	5.501	6.698
410	0.489	0.414	0.424	0.414	0.387	3.081	3.878	-0.32	5.473	6.675
411	0.489	0.414	0.424	0.414	0.387	3.056	3.85	-0.417	5.443	6.649
412	0.489	0.414	0.424	0.415	0.387	3.022	3.814	-0.282	5.408	6.617
413	0.49	0.415	0.425	0.417	0.389	2.974	3.766	-0.056	5.367	6.578
414	0.49	0.415	0.425	0.416	0.388	2.94	3.725	-0.174	5.322	6.533
415	0.489	0.414	0.424	0.416	0.388	2.918	3.698	-0.394	5.284	6.496
416	0.489	0.414	0.424	0.415	0.387	2.897	3.676	-0.455	5.253	6.466
417	0.487	0.413	0.423	0.414	0.386	2.859	3.648	-0.446	5.224	6.44
418	0.487	0.413	0.423	0.414	0.386	2.817	3.616	-0.434	5.195	6.414
419	0.487	0.413	0.423	0.414	0.386	2.771	3.575	-0.577	5.16	6.383
420	0.487	0.414	0.424	0.414	0.387	2.72	3.526	-0.718	5.12	6.346
421	0.487	0.413	0.423	0.414	0.386	2.686	3.49	-0.713	5.086	6.317
422	0.487	0.413	0.423	0.414	0.386	2.639	3.44	-0.777	5.044	6.278
423	0.486	0.413	0.423	0.413	0.386	2.608	3.406	-0.743	5.009	6.248
424	0.482	0.413	0.423	0.413	0.385	2.572	3.371	-0.76	4.973	6.216
425	0.459	0.412	0.422	0.413	0.385	2.537	3.339	-0.797	4.94	6.188
426	0.443	0.412	0.422	0.412	0.385	2.492	3.298	-0.718	4.904	6.157
427	0.407	0.412	0.422	0.412	0.385	2.452	3.252	-0.987	4.865	6.122
428	0.383	0.412	0.422	0.413	0.385	2.425	3.22	-1.003	4.833	6.095
429	0.37	0.412	0.422	0.413	0.385	2.396	3.185	-1.071	4.796	6.065
430	0.366	0.412	0.422	0.412	0.385	2.369	3.151	-1.017	4.76	6.034
431	0.334	0.381	0.391	0.382	0.356	2.343	3.115	-1.143	4.718	5.997
432	0.36	0.411	0.422	0.412	0.385	2.325	3.09	-0.903	4.689	5.973
433	0.456	0.413	0.424	0.414	0.386	2.211	3.064	-0.648	4.663	5.956
434	0.488	0.415	0.425	0.417	0.389	2.211	3.02	-0.554	4.624	5.924

Day after Jan.1/05	CSI Soil Water Content Sensors					CSI Soil Temperature Sensors				
	0.95 m	1.25 m	1.65 m	2.05 m	2.45 m	0.85 m	1.25 m	1.65 m	2.05 m	2.45 m
435	0.489	0.415	0.426	0.418	0.389	2.199	2.987	-0.585	4.584	5.906
436	0.489	0.416	0.426	0.418	0.389	2.183	2.967	-0.618	4.557	5.906
437	0.489	0.415	0.425	0.417	0.389	2.177	2.947	-0.613	4.522	5.897
438	0.489	0.415	0.425	0.417	0.389	2.186	2.9	-0.813	4.468	5.857
439	0.489	0.415	0.425	0.417	0.389	2.339	2.923	-0.851	4.434	5.839
440	0.49	0.415	0.425	0.417	0.388	2.442	2.982	-0.869	4.408	5.822
441	0.49	0.415	0.425	0.417	0.388	2.488	3.024	-0.908	4.391	5.808
442	0.489	0.414	0.425	0.416	0.388	2.515	3.054	-0.936	4.383	5.802
443	0.49	0.414	0.424	0.416	0.388	2.509	3.069	-0.966	4.377	5.799
444	0.49	0.414	0.424	0.415	0.388	2.482	3.065	-1.043	4.371	5.798
445	0.49	0.413	0.424	0.415	0.387	2.451	3.051	-1.001	4.363	5.798
446	0.49	0.413	0.423	0.414	0.387	2.42	3.035	-1.116	4.354	5.801
447	0.49	0.413	0.423	0.414	0.387	2.387	3.011	-1.146	4.339	5.8
448	0.49	0.413	0.423	0.414	0.387	2.359	2.987	-1.02	4.322	5.799
449	0.49	0.413	0.423	0.414	0.387	2.332	2.961	-1.091	4.303	5.795
450	0.49	0.413	0.424	0.414	0.387	2.309	2.937	-1.286	4.284	5.792
451	0.491	0.414	0.424	0.415	0.388	2.29	2.912	-1.359	4.264	5.788
452	0.491	0.413	0.424	0.415	0.388	2.339	2.905	-1.346	4.246	5.786
453	0.491	0.413	0.424	0.415	0.388	2.507	2.936	-1.343	4.227	5.781
454	0.492	0.413	0.424	0.415	0.388	2.779	3.029	-1.311	4.218	5.782
455	0.49	0.413	0.423	0.414	0.387	3.12	3.179	-1.129	4.224	5.79
456	0.489	0.413	0.423	0.414	0.387	3.492	3.345	-1.369	4.223	5.776
457	0.49	0.413	0.423	0.414	0.387	3.898	3.574	-1.308	4.251	5.788
458	0.488	0.412	0.423	0.414	0.386	4.141	3.804	-0.988	4.304	5.817
459	0.488	0.412	0.423	0.414	0.386	4.313	3.966	-1.139	4.353	5.837
460	0.477	0.412	0.423	0.414	0.386	4.392	4.116	-1.031	4.42	5.885
461	0.472	0.412	0.423	0.414	0.386	4.322	4.219	-0.876	4.505	5.957
462	0.481	0.412	0.423	0.414	0.386	4.247	4.228	-0.759	4.566	6.012
463	0.492	0.413	0.424	0.415	0.387	4.316	4.247	-0.793	4.611	6.064
464	0.492	0.413	0.424	0.415	0.387	4.333	4.302	-0.746	4.66	6.131
465	0.492	0.413	0.424	0.415	0.387	4.33	4.339	-0.688	4.708	6.199
466	0.492	0.413	0.424	0.414	0.387	4.42	4.384	-0.638	4.755	6.271
467	0.491	0.412	0.423	0.414	0.387	4.59	4.443	-0.603	4.783	6.318
468	0.493	0.413	0.423	0.414	0.387	4.878	4.565	-0.653	4.821	6.374
469	0.493	0.412	0.423	0.414	0.386	5.227	4.728	-0.516	4.858	6.42
470	0.493	0.412	0.423	0.414	0.386	5.641	4.942	-0.539	4.907	6.467
471	0.494	0.412	0.423	0.414	0.387	6.012	5.187	-0.414	4.971	6.521
472	0.492	0.412	0.423	0.414	0.387	6.27	5.428	-0.291	5.056	6.591
473	0.47	0.412	0.423	0.414	0.386	6.437	5.643	-0.066	5.164	6.685
474	0.45	0.412	0.423	0.414	0.386	6.567	5.812	0.173	5.275	6.787
475	0.421	0.412	0.423	0.414	0.386	6.773	5.969	0.283	5.383	6.893
476	0.399	0.411	0.423	0.414	0.385	7.04	6.129	0.256	5.476	6.978
477	0.384	0.411	0.423	0.414	0.385	7.32	6.329	0.514	5.571	7.07
478	0.379	0.411	0.423	0.413	0.385	7.54	6.52	0.534	5.661	7.17

Day after Jan.1/05	CSI Soil Water Content Sensors					CSI Soil Temperature Sensors				
	0.95 m	1.25 m	1.65 m	2.05 m	2.45 m	0.85 m	1.25 m	1.65 m	2.05 m	2.45 m
479	0.41	0.411	0.423	0.414	0.385	7.71	6.711	0.577	5.771	7.28
480	0.454	0.411	0.423	0.414	0.385	7.74	6.846	0.696	5.88	7.39
481	0.455	0.411	0.423	0.414	0.385	7.69	6.938	0.834	5.994	7.51
482	0.434	0.411	0.423	0.414	0.385	7.54	6.966	0.967	6.099	7.63
483	0.394	0.411	0.424	0.414	0.386	7.45	6.952	1.008	6.184	7.75
484	0.377	0.411	0.424	0.414	0.386	7.42	6.948	1.026	6.257	7.86
485	0.373	0.411	0.423	0.414	0.386	7.46	6.975	1.106	6.331	7.98
486	0.371	0.411	0.423	0.414	0.385	7.53	7.01	1.202	6.381	8.08
487	0.369	0.411	0.423	0.413	0.385	7.67	7.07	1.414	6.432	8.17
488	0.368	0.41	0.423	0.413	0.385	7.87	7.17	1.426	6.484	8.25
489	0.366	0.41	0.423	0.413	0.384	8.15	7.3	1.371	6.532	8.33
490	0.365	0.41	0.423	0.413	0.384	8.47	7.47	1.356	6.586	8.4
491	0.363	0.408	0.423	0.413	0.384	8.7	7.65	1.35	6.649	8.47
492	0.361	0.396	0.423	0.413	0.384	8.86	7.84	1.555	6.744	8.58
493	0.36	0.382	0.423	0.413	0.384	8.9	7.98	1.828	6.851	8.7
494	0.358	0.374	0.423	0.413	0.384	8.98	8.08	1.908	6.944	8.81
495	0.358	0.37	0.422	0.413	0.384	9.19	8.2	2.069	7.04	8.93
496	0.359	0.373	0.422	0.412	0.383	9.43	8.33	1.899	7.11	9.01
497	0.359	0.376	0.422	0.412	0.383	9.69	8.51	1.921	7.19	9.11
498	0.358	0.363	0.422	0.412	0.383	9.79	8.69	2.08	7.3	9.23
499	0.357	0.357	0.422	0.412	0.383	9.8	8.79	2.19	7.4	9.35
500	0.356	0.356	0.422	0.412	0.383	9.86	8.87	2.28	7.5	9.47
501	0.386	0.384	0.422	0.413	0.383	9.96	8.96	2.346	7.6	9.58
502	0.462	0.417	0.423	0.414	0.384	10.08	9.07	2.399	7.69	9.7
503	0.478	0.417	0.423	0.414	0.384	10.19	9.15	2.458	7.77	9.8
504	0.487	0.418	0.423	0.414	0.384	10.32	9.26	2.53	7.85	9.9
505	0.474	0.419	0.423	0.414	0.384	10.33	9.37	2.652	7.94	10.02
506	0.45	0.419	0.423	0.414	0.384	10.27	9.39	2.671	8.01	10.11
507	0.404	0.419	0.423	0.415	0.385	10.2	9.42	2.729	8.09	10.21
508	0.38	0.419	0.423	0.415	0.385	10.03	9.42	2.821	8.17	10.32
509	0.375	0.419	0.423	0.415	0.384	9.86	9.37	2.939	8.24	10.44
510	0.372	0.419	0.422	0.414	0.384	9.91	9.34	2.941	8.29	10.54
511	0.37	0.418	0.422	0.413	0.384	10.13	9	5.862	8.32	10.6
512	0.367	0.412	0.422	0.414	0.384	10.49	8.88	8.66	8.38	10.7
513	0.365	0.391	0.423	0.414	0.384	10.79	8.96	8.83	8.43	10.78
514	0.364	0.377	0.423	0.414	0.384	11.18	9.1	9.12	8.54	10.9
515	0.364	0.368	0.422	0.414	0.384	11.58	9.21	9.33	8.61	10.97
516	0.363	0.362	0.422	0.414	0.384	12.1	9.33	9.58	8.67	11.03
517	0.364	0.358	0.422	0.414	0.384	12.63	9.5	9.87	8.77	11.11

Appendix F

Soil and Water Quality Laboratory Data

Table F.1. Soil bromide, nitrate, volumetric water content (VWC) and gravimetric water content (GWC). GWC measured in the laboratory. VWC determined when sample volume could be reliably measured. Notes: a) Manually extrapolated bromide concentrations; b) Manually interpolated sample depths; c) Non-detectable results presented as the detection limit.

Station (Borehole)	Depth (m)	Soil Bromide Conc. (mg/kg)	Soil Nitrate Conc. (mg/kg)	VWC (g water/ m^3 soil)	GWC (g water/ g soil)
FEBRUARY 2005					
Station 2	0.15		1.15		0.31
(AT2)	0.45		1.50		0.18
	0.76		1.70		0.12
	1.32		2.00		0.09
	1.58		1.55		0.10
	1.88		1.55		0.10
	2.10		1.60		0.10
	2.33		1.75		0.13
	2.64		1.80		0.10
	3.20		1.80		0.10
	3.51		2.60		0.10
	3.81		2.35		0.11
	4.11		2.20		0.11
Station 3	0.15		5.45		0.23
(AT4)	0.74		3.40		0.20
	1.58		2.00		0.15
	1.85		1.70		0.08
	3.20		1.40		0.05
	3.51		1.80		0.05
	4.11		2.30		0.05
	4.65		1.65		0.05
	5.01		1.50		0.05
	5.32		2.35		0.09
Station 4	0.10		4.35		0.32
(AT5)	0.41		2.50		0.20
	0.61		1.95		0.18
	0.97		1.55		0.18
	1.32		1.40		0.20
	1.50		1.55		0.10
	1.80		1.70		0.09
	2.29		1.90		0.10
	2.62		2.30		0.09
	2.90		2.15		0.09
	3.20		1.70		0.08
	3.51		1.80		0.05
	3.81		1.70		0.05

Station (Borehole)	Depth (m)	Soil Bromide Conc. (mg/kg)	Soil Nitrate Conc. (mg/kg)	VWC (g water/ m^3 soil)	GWC (g water/ g soil)
Station 5	0.15		2.70		0.28
(AT3)	0.48		1.75		0.17
	0.74		1.45		0.14
	1.47		0.80		0.10
	1.69		0.70		0.10
	1.98		0.70		0.12
	2.39		0.80		0.06
	2.60		0.80		0.07
	2.90		0.75		0.07
	3.13		0.75		0.06
	3.37		0.75		0.08
	3.66		0.80		0.17
	4.12		0.80		0.11
	4.33		0.95		0.10
Station 6	0.15		2.95		0.22
(AT7)	0.67		1.90		0.13
	1.34		6.80		0.04
	1.51		2.35		0.05
	1.75		2.95		0.05
	0.00		4.25		0.07
	0.00		2.40		0.03
Station 8	0.15		5.70		0.29
(AT6)	0.50		2.55		0.16
	0.80		2.95		0.18
	1.68		3.00		0.08
	1.98		4.25		0.11
	2.41		4.25		0.10
	2.59		5.30		0.10
	2.90		13.10		0.10
	3.35		14.70		0.10
	3.66		8.30		0.09
AT8	0.15		1.15		0.37
	0.76		1.80		0.19
	1.07		0.95		0.10
	1.47		1.10		0.09
	1.68		1.20		0.09
	1.98		1.10		0.09
	2.29		1.15		0.10
	2.67		1.10		0.10
	2.90		1.15		0.09
	3.20		1.15		0.08
	3.51		1.10		0.09
	3.81		1.10		0.08
	4.24		1.10		0.08
	4.42		1.15		0.08
	4.75		2.00		0.07
AT1	0.43		7.55		0.20
	0.66		5.2		0.10

Station (Borehole)	Depth (m)	Soil Bromide Conc. (mg/kg)	Soil Nitrate Conc. (mg/kg)	VWC (g water/ m^3 soil)	GWC (g water/ g soil)
	1.30		2.45		0.10
	1.96		2.2		0.09
	2.39		2.95		0.13
	2.64		2.2		0.10
	2.90		2.05		0.10
	3.20		1.85		0.10
	3.51		0.55		0.08
	3.81		0.6		0.11
	4.11		0.8		0.14
	4.42		0.6		0.10
	4.62		1.5		0.15
MARCH 2005					
Station 2	0.29		14.5	0.33	0.24
(WO60)	0.38		9.12	0.39	0.24
	0.53		3.91	0.32	0.23
	0.69		3.47	0.33	0.19
	0.84		1.72	0.29	0.18
	1.60		0.4[c]	0.24	0.13
	1.79		0.955	0.28	0.14
	1.88		0.4[c]	0.28	0.14
	2.06		2.49	0.24	0.12
	2.21		1.98	0.25	0.11
	2.36		2.6	0.19	0.10
	2.51		2.37	0.22	0.11
	2.65		2.34	0.23	0.10
	2.82		2.21	0.22	0.10
	2.97		2.06	0.22	0.10
	3.16		0.4[c]	0.27	0.12
	3.31		0.4[c]	0.20	0.11
	3.46		1.5	0.22	0.12
	3.62		1.75	0.23	0.11
	3.77		1.92	0.25	0.10
	3.92		1.83	0.22	0.10
	4.07		3.13	0.21	0.10
	4.23		1.66	0.18	0.07
Station 3	0.05		1.12	0.38	0.28
(WO56)	0.17		1.49	0.35	0.25
	0.32		0.4[c]	0.31	0.21
	0.47		1.41	0.35	0.23
	0.62		0.92	0.33	0.23
	0.78		3	0.40	0.26
	0.93		5.27	0.32	0.19
	1.65		1.01	0.33	0.18
	1.81		1.08	0.33	0.18
	1.96		1.57	0.31	0.17
	2.14		1.35	0.25	0.15
	3.12		0.4[c]	0.15	0.08

Station (Borehole)	Depth (m)	Soil Bromide Conc. (mg/kg)	Soil Nitrate Conc. (mg/kg)	VWC (g water/ m^3 soil)	GWC (g water/ g soil)
	3.30		0.4[c]	0.12	0.05
	3.43		0.925	0.13	0.04
	3.64		0.4[c]	0.13	0.05
	3.73		0.4[c]	0.13	0.05
	3.89		0.67	0.11	0.05
	4.04		0.545	0.17	0.06
	4.24		1.12	0.12	0.05
	4.37		0.78	0.15	0.06
	4.50		1.52	0.15	0.06
	4.65		2.1	0.16	0.07
	4.80		0.4[c]	0.15	0.05
	4.95		0.63	0.10	0.05
	5.11		1.09	0.14	0.05
	5.26		1.1	0.14	0.06
	5.41		0.83	0.17	0.07
	5.56		1.01	0.16	0.07
	5.72		1.27	0.14	0.07
	5.87		0.775	0.24	0.11
	6.02		1.03	0.17	0.08
	6.20		0.645	0.13	0.07
	6.32		0.66	0.13	0.05
	6.48		1.14	0.11	0.05
	6.63		1.55	0.09	0.05
	6.78		0.84	0.07	0.04
	6.97		2.75	0.10	0.04
	7.09		0.88	0.09	0.04
	7.25		1.25	0.10	0.04
	7.39		0.95	0.09	0.04
	7.54		1	0.11	0.04
	8.47		0.4[c]	0.11	0.04
	8.66		0.475	0.13	0.06
	8.81		0.4[c]	0.16	0.06
	8.97		0.465	0.13	0.07
	9.12		0.4[c]	0.16	0.08
	9.22		0.77	0.11	0.04
	9.37		0.83	0.06	0.02
	9.53		1.23	0.09	0.04
	9.68		1.35	0.10	0.05
	9.83		0.96	0.08	0.03
	9.98		1.22	0.08	0.04
	10.13		1.17	0.07	0.03
	10.29		1.41	0.11	0.05
	10.44		0.845	0.06	0.03
	10.59		1.22	0.09	0.05
	10.90		0.715	0.26	0.12
	11.05		1.15	0.25	0.10
	11.20		0.825	0.23	0.09

Station (Borehole)	Depth (m)	Soil Bromide Conc. (mg/kg)	Soil Nitrate Conc. (mg/kg)	VWC (g water/ m^3 soil)	GWC (g water/ g soil)
	11.35		1.01	0.18	0.08
	11.51		0.835	0.12	0.06
	11.66		1.88	0.10	0.06
	11.81		0.88	0.12	0.06
	11.96		1.45	0.14	0.06
	12.12		0.77	0.16	0.07
	12.47		0.57	0.14	0.07
	12.62		0.555	0.12	0.05
	12.78		0.985	0.13	0.06
	12.93		1.49	0.12	0.05
	13.08		1.14	0.12	0.06
	13.23		1.11	0.12	0.05
	13.39		0.91	0.17	0.08
	13.54		1.29	0.18	0.08
	13.69		1.51	0.15	0.07
	14.86		0.4[c]	0.16	0.13
	15.01		0.685	0.22	0.13
	15.16		0.555	0.23	0.12
	15.32		1.2	0.25	0.13
	15.47		0.465	0.27	0.12
	15.62		0.5	0.21	0.09
	15.77		1.24	0.23	0.10
	15.93		1.27	0.18	0.09
	16.08		1.49	0.22	0.10
	16.23		2.1	0.18	0.08
	16.80		0.85	0.27	0.14
	16.99		2.82	0.27	0.15
	17.15		1.8	0.23	0.11
	17.30		1.79	0.23	0.10
	17.41		0.455	0.17	0.07
	17.55		1.03	0.13	0.05
	17.79		0.46	0.18	0.06
	17.93		0.64	0.15	0.04
	18.06		0.89	0.27	0.09
	18.21		1.02	0.19	0.09
	18.58		1.12	0.14	0.08
	18.67		0.4[c]	0.15	0.09
	18.82		0.54	0.25	0.11
	18.97		1.57	0.29	0.13
	19.13		2.01	0.23	0.11
	19.28		0.935	0.23	0.10
	19.43		0.685	0.22	0.09
	19.56		0.615	0.24	0.10
	19.74		0.73	0.18	0.07
Station 4	0.21		8.21	0.34	0.23
(WO61)	0.33		1.66	0.34	0.22
	0.48		2.48	0.32	0.20

Station (Borehole)	Depth (m)	Soil Bromide Conc. (mg/kg)	Soil Nitrate Conc. (mg/kg)	VWC (g water/ m^3 soil)	GWC (g water/ g soil)
	0.63		2.28	0.33	0.22
	0.78		3.25	0.38	0.21
	0.94		2.38	0.32	0.21
	1.09		1.35	0.24	0.15
	1.60		0.4[c]	0.33	0.19
	1.75		1.18	0.29	0.13
	1.91		0.985	0.23	0.11
	2.06		1.06	0.21	0.11
	2.21		1.12	0.23	0.12
	2.34		1.19	0.18	0.12
	2.51		1.17	0.23	0.10
	2.67		1.04	0.21	0.10
	2.82		1.11	0.20	0.09
	2.97		1.24	0.16	0.10
	3.12		2.08	0.30	0.15
	3.28		0.955	0.27	0.14
	3.43		0.4[c]	0.18	0.08
	3.58		1.5	0.10	0.07
	3.73		1.53	0.10	0.06
	3.89		1.02	0.11	0.06
	4.04		1.2	0.09	0.05
	4.19		1.16	0.08	0.05
	4.34		1.19	0.10	0.05
	4.50		1.23	0.11	0.07
Station 5	0.10		4.46	0.37	0.27
(WO58)	0.25		2.33	0.36	0.21
	0.40		2.32	0.36	0.21
	0.55		1.9	0.30	0.18
	0.71		2.05	0.33	0.17
	0.86		1.13	0.24	0.13
	1.79		0.98	0.26	0.15
	1.94		1.34	0.30	0.15
	2.10		1.09	0.23	0.12
	2.25		2.19	0.21	0.11
	2.40		0.745	0.20	0.10
	3.12		0.825	0.22	0.10
	3.28		0.4[c]	0.27	0.13
	3.43		1.11	0.33	0.16
	3.58		0.775	0.33	0.17
	3.73		0.89	0.32	0.17
	3.89		1.22	0.36	0.17
	4.04		0.89	0.32	0.15
	4.19		2.51	0.29	0.14
	4.37		0.695	0.28	0.13
	4.50		1.91	0.18	0.10
	5.11		1.67	0.21	0.12
	5.26		0.81	0.23	0.12

Station (Borehole)	Depth (m)	Soil Bromide Conc. (mg/kg)	Soil Nitrate Conc. (mg/kg)	VWC (g water/ m^3 soil)	GWC (g water/ g soil)
	5.41		1.37	0.28	0.14
	5.56		1.45	0.23	0.12
	5.72		0.715	0.17	0.07
	5.87		0.96	0.18	0.09
	5.98		1.96	0.22	0.10
	6.17		1.4	0.26	0.16
	6.32		1.37	0.31	0.16
	6.48		1.5	0.30	0.19
	6.63		1.46	0.27	0.14
	6.78		1.93	0.29	0.16
	6.93		1.63	0.29	0.15
	7.09		1.06	0.08	0.04
	7.24		0.73	0.13	0.06
	7.39		1.8	0.13	0.06
	7.54		1.19	0.13	0.06
	7.70		0.855	0.04	0.03
	7.85		0.4[c]	0.02	0.02
	8.00		1.28	0.03	0.02
	8.15		2.17	0.02	0.02
	8.31		1.08	0.02	0.02
	8.46		0.955	0.02	0.02
	8.76		1.67	0.02	0.02
	8.92		1.85	0.03	0.02
	9.07		0.4[c]	0.02	0.02
	9.22		0.785	0.22	0.12
	9.37		0.4[c]	0.23	0.12
	9.53		0.4[c]	0.21	0.13
	9.68		0.895	0.24	0.12
	9.83		1.22	0.20	0.11
	9.98		0.4[c]	0.17	0.08
	10.13		0.535	0.19	0.09
	10.29		0.62	0.18	0.09
	10.44		0.93	0.16	0.07
	10.59		1.65	0.12	0.06
	10.78		0.4[c]	0.08	0.03
	10.90		0.755	0.16	0.06
	11.05		0.4[c]	0.14	0.05
	11.20		0.905	0.14	0.05
	11.35		0.91	0.10	0.04
	11.51		0.82	0.13	0.05
	11.66		0.96	0.11	0.05
	11.81		0.87	0.11	0.04
	11.96		0.92	0.08	0.04
	12.10		1.12	0.11	0.05
	13.09		1.27	0.28	0.15
	13.18		0.865	0.26	0.12
	13.34		0.7	0.26	0.11

Station (Borehole)	Depth (m)	Soil Bromide Conc. (mg/kg)	Soil Nitrate Conc. (mg/kg)	VWC (g water/ m^3 soil)	GWC (g water/ g soil)
	13.49		1.3	0.22	0.10
	13.64		2.47	0.27	0.14
	14.31		1.79	0.19	0.12
	14.40		0.87	0.14	0.07
	14.55		0.965	0.12	0.05
	14.71		1.02	0.15	0.07
	14.86		1.59	0.18	0.09
	15.01		1.26	0.15	0.08
Station 6	0.88		7.38	0.33	0.21
(WO62)	0.97		3.94	0.35	0.21
	1.14		1.98	0.42	0.21
	1.30		4.46	0.44	0.23
	1.45		6.16	0.18	0.07
	1.62		1.13	0.07	0.06
	1.78		1.34	0.12	0.05
	1.95		3.19	0.07	0.04
	3.53		2.23	0.10	0.05
	3.58		2.05	0.10	0.05
	3.73		3.54	0.13	0.04
	3.89		3.05	0.09	0.03
Station 7	0.08		7.41	0.37	0.24
(WO65)	0.23		6.76	0.29	0.23
	0.41		5.71	0.28	0.23
	0.50		5.67	0.27	0.23
	0.90		4.49	0.92	0.67
	1.05		1.8	0.19	0.11
	1.35		2.22	0.23	0.11
	1.44		2.01	0.29	0.12
	1.60		2.89	0.13	0.07
	1.75		1.73	0.18	0.08
	2.24		2.5	0.13	0.07
	2.37		1.89	0.16	0.08
	2.52		1.53	0.21	0.09
	2.67		1.58	0.19	0.11
	3.18		1.67	0.15	0.09
	3.31		1.7	0.20	0.09
	3.46		1.78	0.18	0.09
	3.61		1.58	0.15	0.09
	3.77		2.96	0.28	0.15
	4.15		2.42	0.27	0.16
	4.34		2.83	0.23	0.13
	4.50		1.81	0.16	0.08
	4.65		1.72	0.16	0.08
	4.80		1.97	0.14	0.08
	5.26		1.63	0.20	0.10
	5.41		1.7	0.25	0.11
	5.56		1.58	0.22	0.10

Station (Borehole)	Depth (m)	Soil Bromide Conc. (mg/kg)	Soil Nitrate Conc. (mg/kg)	VWC (g water/ m^3 soil)	GWC (g water/ g soil)
	5.72		1.59	0.27	0.12
	6.24		1.47	0.09	0.06
	6.32		2.26	0.17	0.08
	6.50		2.4	0.20	0.09
	6.63		2.31	0.25	0.10
WO64	0.69		14.8	0.22	0.19
	0.84		2.72	0.37	0.19
	0.99		2.71	0.38	0.20
	1.14		0.88	0.28	0.15
	1.30		1.01	0.31	0.14
	1.45		0.84	0.26	0.12
	1.60		2.18	0.27	0.13
	1.75		0.98	0.27	0.13
	1.91		0.4[c]	0.21	0.11
	2.06		2.89	0.21	0.11
	2.21		0.4[c]	0.22	0.10
	2.35		0.86	0.20	0.09
	2.51		2.03	0.23	0.10
	2.71		0.845	0.18	0.09
	2.82		1.91	0.22	0.09
	3.02		3.28	0.18	0.08
	3.73		0.925	0.29	0.14
	3.89		0.4[c]	0.27	0.12
	4.04		0.4[c]	0.23	0.10
	4.17		1.65	0.12	0.06
	4.32		2.7	0.09	0.06
	4.53		2.49	0.12	0.06
NOVEMBER 2005					
Station 1	0.1	142	7.17	0.35	0.29
(TH10)	0.2	630	4.02	0.38	0.26
	0.3	2140	2.11	0.20	0.27
	0.51	413	1.48	0.26	0.15
	0.61		3.71	0.26	0.12
	0.71	41	4.73	0.20	0.10
	0.81		1.09	0.13	0.08
	0.91		0.477	0.07	0.04
	1.01		0.526	0.06	0.03
	1.1	1	0.02	0.05	0.04
	1.3		0.173	0.05	0.03
	1.4		0.309	0.06	0.04
	1.48		0.378	0.08	0.03
	1.6		0.349	0.09	0.04
	1.7		0.299	0.11	0.05
	1.8	1	0.053	0.09	0.04
	2.66		0.636	0.07	0.03
	2.86		0.566	0.06	0.04
	3.04		0.818	0.04	0.04

Station (Borehole)	Depth (m)	Soil Bromide Conc. (mg/kg)	Soil Nitrate Conc. (mg/kg)	VWC (g water/ m^3 soil)	GWC (g water/ g soil)
	3.1		0.835	0.07	0.05
Station 2	0.1	23	5.41	0.38	0.25
(TH4)	0.2	69	6.5	0.37	0.25
	0.27	90	4.7	0.39	0.27
	0.4	76	0.956	0.33	0.19
	0.5	12	0.854	0.31	0.18
	0.61		1.86	0.27	0.14
	0.7		2.47	0.26	0.13
	0.8		2.01	0.20	0.10
	0.89		1.54	0.19	0.10
	1.3	1	1.53	0.21	0.09
	1.4		1.2	0.19	0.09
	1.5		1.73	0.20	0.09
	1.59		1.45	0.20	0.10
	1.7		1.24	0.21	0.09
	1.78		1.31	0.22	0.09
	1.88	1	1.33	0.22	0.10
	2.2		1.11	0.19	0.09
	2.4		1.41	0.20	0.09
	2.61		1.41	0.20	0.09
	2.8		1.7	0.23	0.10
	2.98		1.59	0.22	0.10
	3.2		1.27	0.24	0.10
	3.4		1.7	0.22	0.10
	3.6		1.25	0.23	0.10
	3.8		1.83	0.25	0.11
	4		1.73	0.22	0.11
	4.2		1.59	0.26	0.13
	4.4		0.255	0.07	0.05
	4.6		0.351	0.05	0.03
	4.78		0.485	0.07	0.04
Station 3	0.1	23	2.37	0.30	0.21
(TH1)	0.2	45	3.48	0.29	0.19
	0.4	246	2.93	0.29	0.20
	0.5	9	1.48	0.16	0.10
	0.6		1.08	0.31	0.17
	0.7		1.02	0.28	0.17
	0.8		0.625	0.32	0.19
	0.9		0.582	0.32	0.22
	0.97	2	0.564	0.37	0.25
	1.3		0.758	0.37	0.26
	1.4		0.547	0.34	0.24
	1.5		0.469	0.22	0.10
	1.58		0.652	0.12	0.06
	1.7	1	0.266	0.10	0.06
	2.2		0.641	0.12	0.08
	2.5		0.986	0.22	0.11

Station (Borehole)	Depth (m)	Soil Bromide Conc. (mg/kg)	Soil Nitrate Conc. (mg/kg)	VWC (g water/ m^3 soil)	GWC (g water/ g soil)
	2.7		0.904	0.37	0.18
	3.2		0.173	0.06	0.03
	3.41		0.23	0.06	0.04
	3.6		0.115	0.07	0.03
	3.8		0.334	0.05	0.04
	4		0.646	0.04	0.03
	4.2		0.39	0.07	0.04
	4.5		0.214	0.05	0.03
	4.7		0.704	0.06	0.03
	5		0.59	0.04	0.02
	5.2		0.552	0.05	0.03
	5.4		0.308	0.03	0.02
Station 4	0.2	10	2.49	0.19	0.16
(TH6)	0.27	11	1.58	0.19	0.16
	0.4	123	4.35	0.32	0.19
	0.5	86	4.36	0.30	0.17
	0.6		10.8	0.34	0.21
	0.7		3.31	0.20	0.09
	0.8		0.497	0.08	0.05
	0.88		0.133	0.04	0.03
	1.3	1	0.79	0.25	0.12
	1.4		0.967	0.25	0.13
	1.5		1.03	0.27	0.14
	1.6		0.865	0.23	0.13
	1.7		0.999	0.19	0.10
	1.8		0.806	0.21	0.10
	1.9	1	0.623	0.20	0.09
	2.22		0.961	0.15	0.08
	2.41		1.06	0.16	0.09
	2.6		0.58	0.12	0.07
	2.8		0.596	0.03	0.02
	3.2		0.72	0.04	0.03
	3.4		0.301	0.05	0.03
	3.6		0.282	0.04	0.02
	3.8		0.525	0.05	0.03
	4		0.197	0.04	0.03
	4.2		0.235	0.06	0.04
	4.4		0.256	0.05	0.03
	4.6		0.346	0.05	0.03
Station 5	0.1	19	3.58	0.31	0.20
(TH2)	0.2	94	4.26	0.34	0.20
	0.4	710	8.68	0.22	0.15
	0.5	59	5.33	0.19	0.15
	0.6	5	2.76	0.13	0.09
	0.7		1.12	0.08	0.05
	0.8		0.789	0.08	0.05
	0.9		0.672	0.07	0.05

Station (Borehole)	Depth (m)	Soil Bromide Conc. (mg/kg)	Soil Nitrate Conc. (mg/kg)	VWC (g water/ m^3 soil)	GWC (g water/ g soil)
	1.3		0.894	0.10	0.07
	1.4	1	0.707	0.13	0.08
	1.5		0.588	0.13	0.08
	1.6		0.651	0.12	0.08
	1.75		0.418	0.07	0.05
	2	1	0.179	0.05	0.05
	2.2		0.346	0.11	0.07
	2.4		0.478	0.12	0.07
	2.6		0.884	0.23	0.13
	2.8		0.742	0.17	0.10
	3.2		0.77	0.18	0.11
	3.5		0.326	0.09	0.05
	3.7		0.171	0.13	0.09
	4		0.238	0.12	0.08
	4.2		0.227	0.16	0.11
	4.4		0.114	0.15	0.09
	4.6		0.115	0.10	0.06
	4.8		0.145	0.13	0.07
Station 6	0.08	23	4.61	0.30	0.19
(TH9)	0.19	48	4.24	0.16	0.18
	0.4	706	6.89	0.11	0.10
	0.5	546	9.71	0.14	0.10
	0.83	117	5.86	0.08	0.06
	1.3	1	1.03	0.06	0.04
	1.4		0.971	0.05	0.03
	1.5	1	1.03	0.05	0.03
	1.6		1.33	0.08	0.05
	1.7		0.928	0.06	0.04
	1.8		0.941	0.07	0.04
	1.9	1	1.05	0.04	0.03
	2.35		0.471	0.04	0.03
	2.55		0.641	0.05	0.03
	2.74		1.5	0.09	0.06
	2.96		1.04	0.06	0.03
	3.2		0.307	0.06	0.03
	3.4		0.161	0.04	0.03
	3.6		0.413	0.02	0.02
Station 7	0.1	55	7.03	0.36	0.28
(TH12)	0.2	443	11.7	0.36	0.25
	0.3	1200	27.7	0.35	0.23
	0.39	937	13.8	0.29	0.19
	0.65	438	8.58	0.16	0.10
	1.36	15	1.38	0.23	0.12
	1.46		1.47	0.24	0.12
	1.54		1.19	0.10	0.06
	1.66		0.915	0.10	0.05
	1.76		1.01	0.10	0.05

Station (Borehole)	Depth (m)	Soil Bromide Conc. (mg/kg)	Soil Nitrate Conc. (mg/kg)	VWC (g water/ m^3 soil)	GWC (g water/ g soil)
	1.86		1.19	0.10	0.05
	1.96	1	0.189	0.07	0.05
	2.2		0.908	0.09	0.06
	2.4		0.993	0.11	0.07
	2.6		1	0.10	0.06
	2.78		0.587	0.09	0.05
	3.22		1.57	0.15	0.09
	3.4		1.52	0.11	0.06
	3.6		0.93	0.10	0.06
	3.8		3.55	0.23	0.13
	4		3.04	0.20	0.14
	4.29		1.32	0.13	0.06
	4.49		1.09	0.25	0.12
	5		0.39	0.10	0.06
	5.21		0.356	0.10	0.05
Station 8	0.1	175	18.6	0.27	0.28
(TH8)	0.2	1110	38.8	0.31	0.24
	0.4	484	14.5	0.27	0.15
	0.5	137	0.814	0.24	0.12
	0.61	52	7.08	0.28	0.15
	0.93		4.5	0.18	0.09
	1.3		1.62	0.08	0.05
	1.57	1	3.43	0.15	0.09
	1.67	1	4.87	0.17	0.09
	1.77		7.39	0.20	0.09
	1.87		7.25	0.19	0.09
	1.97		8.07	0.52	0.22
	2.07	1	6.61	0.20	0.10
	2.2		8.23	0.17	0.08
	2.4		7.93	0.21	0.10
	2.6		7.46	0.19	0.09
	2.8		7.35	0.22	0.10
	3.2		4.6	0.20	0.10
TH13	0.1		9.85	0.36	0.26
	0.4		30.3	0.38	0.32
	0.5		9.4	0.28	0.15
	0.6		5.3	0.24	0.13
	0.7		5.3	0.36	0.24
	1.3		1.61	0.22	0.11
	1.4		2.08	0.22	0.11
	1.51		0.88	0.25	0.13
	1.61		0.525	0.21	0.12
	1.7		1.48	0.22	0.10
	1.8		1.47	0.08	0.09
	2.2		0.95	0.05	0.06
	3.2		0.865	0.07	0.04
WO66	0.1		2.72	0.32	0.23

Station (Borehole)	Depth (m)	Soil Bromide Conc. (mg/kg)	Soil Nitrate Conc. (mg/kg)	VWC (g water/ m^3 soil)	GWC (g water/ g soil)
	0.19		1.73	0.20	0.16
	0.3		0.402	0.35	0.23
	0.42		0.398	0.13	0.11
	0.5		0.118	0.08	0.05
	0.6		0.38	0.09	0.06
	0.7		0.075	0.19	0.10
	1.3		0.294	0.21	0.10
	1.4		0.468	0.21	0.09
	1.5		0.336	0.26	0.10
	1.6		0.481	0.21	0.10
	1.7		0.453	0.24	0.10
	1.8		0.48	0.21	0.10
	1.9		0.479	0.21	0.10
	2		0.965	0.21	0.10
	2.2		0.388	0.04	0.03
	2.4		0.41	0.08	0.04
	2.6		0.505	0.07	0.03
	2.8		0.223	0.06	0.04
	3.1		0.189	0.05	0.03
	3.2		0.195	0.05	0.03
	3.4		0.075	0.06	0.03
	3.6		0.0975	0.06	0.03
	3.8		0.232	0.05	0.03
	4		0.128	0.08	0.06
	4.21		0.134	0.06	0.04
	4.4		0.269	0.09	0.04
	4.6		0.276	0.06	0.03
	5		0.69	0.16	0.08
	5.8		1.35	0.12	0.09
	6		1.43	0.25	0.13
	6.8		1.15	0.21	0.08
MAY 2006					
Station 1	0.08	2.220	4.540		0.21
(TH19)	0.18	2.510	5.060		0.21
	0.38	1.135	1.720		0.17
	0.55	1.790	0.556		0.05
	0.70	7.090	0.489		0.04
	1.39	8.995	0.647		0.05
	1.54	11.785	0.835		0.05
	1.69	13.085	0.856		0.08
	2.16	32.805	0.763		0.05
	2.31	27.370	0.505		0.04
	2.46	2.000	0.465		0.08
	3.22	0.220	1.480		0.08
	3.37	0.230	1.510		0.08
	3.57	0.230	0.722		0.08
Station 2	0.11	76.400	6.070		0.19

Station (Borehole)	Depth (m)	Soil Bromide Conc. (mg/kg)	Soil Nitrate Conc. (mg/kg)	VWC (g water/ m^3 soil)	GWC (g water/ g soil)
(TH16)	0.26	205.600	6.290		0.24
	0.38	17.625	1.760		0.24
	0.53	12.060	2.440		0.15
	0.68	22.935	2.540		0.17
	0.83	23.085	2.830		0.11
	1.24	11.165	2.110		0.11
	1.39	8.505	2.970		0.10
	1.54	5.810	2.700		0.11
	1.69	1.970	2.780		0.08
	1.84	1.525	2.010		0.10
	2.16	8.190	1.480		0.09
	2.31	0.530	1.710		0.10
	2.46	0.360	1.650		0.10
	2.61	0.340	2.040		0.10
	2.76	0.430	2.040		0.10
	2.91	0.000	1.980		0.10
Station 3	0.18	2.860	5.320		0.12
(TH14)	0.33	2.470	2.070		0.18
	0.48	1.865	1.830		0.25
	0.63	6.800	1.310		0.18
	1.81	56.810	0.706		0.09
	1.96	235.500	1.340		0.16
	2.11	51.500	0.683		0.19
	2.31	66.600	0.907		0.12
	2.41	20.000[a]			
	2.45	1.000[a]			
Station 4	0.08	0.735	11.700		0.17
(TH17)	0.23	5.655	5.310		0.17
	0.33	46.925	4.070		0.18
	0.48	8.895	3.110		0.16
	0.63	21.375	2.510		0.11
	0.78	16.530	1.140		0.05
	1.24	14.340	2.580		0.15
	1.39	18.500	2.710		0.14
	1.54	24.840	2.940		0.17
	1.69	15.620	2.230		0.10
	1.84	17.595	2.680		0.12
	2.16	21.325	2.110		0.10
	2.31	21.135	2.380		0.12
	2.46	14.285	1.950		0.10
	2.61	9.410	1.460		0.09
	2.72	5.000[a]			
	2.82	1.000[a]			
Station 5	0.06	1.570	4.020		0.10
(TH15)	0.21	2.150	4.060		0.15
	0.33	1.136	1.880		0.17
	0.49	1.950	2.150		0.17

Station (Borehole)	Depth (m)	Soil Bromide Conc. (mg/kg)	Soil Nitrate Conc. (mg/kg)	VWC (g water/ m^3 soil)	GWC (g water/ g soil)
	0.63	1.598	1.110		0.13
	0.79	2.005	0.704		0.13
	0.91	1.248	0.924		0.15
	1.52[b]	10.600	0.938		0.11
	1.98[b]	17.850	1.010		0.14
	2.22	1.870	0.787		0.10
	2.36	2.903	0.618		0.09
	2.52	8.665	0.905		0.10
	2.66	8.983	0.774		0.08
	2.82	6.360	0.761		0.08
	3.00	3.500[a]			
	3.15	1.000[a]			
Station 6	0.18	0.980	9.940		0.17
(TH20)	0.33	0.750	4.070		0.15
	0.48	1.380	2.840		0.20
	0.61	4.605	1.190		0.07
	0.78	6.095	0.817		0.04
	1.29	7.375	0.679		0.06
	1.44	7.620	0.463		0.05
	1.59	34.060	1.270		0.04
	1.74	14.675	0.652		0.03
	1.89	56.355	1.200		0.13
	2.26	16.755	0.504		0.04
	2.41	5.080	0.206		0.04
	2.56	4.250	0.176		0.05
	2.71	1.195	0.369		0.06
	2.86	1.155	0.899		0.04
Station 7	0.08	0.865	14.100		0.15
(TH21)	0.23	0.785	8.470		0.18
	0.38	0.620	2.260		0.14
	0.53	0.620	2.650		0.08
	1.39	52.300	3.040		0.09
	1.54	38.050	1.540		0.05
	1.69	27.840	1.140		0.05
	1.84	40.820	1.590		0.06
	2.37	4.245	1.140		0.06
	2.52	2.850	1.420		0.07
	2.67	4.775	1.060		0.07
	2.82	23.545	0.790		0.07
	2.97	23.945	1.160		0.07
	3.07	15.325	0.468		0.07
	3.22	13.540	0.995		0.06
	3.37	7.890	0.599		0.07
	3.52	25.790	0.494		0.05
	3.67	19.895	0.377		0.06
	3.82	14.870	0.717		0.15
	4.09	6[a]			

Station (Borehole)	Depth (m)	Soil Bromide Conc. (mg/kg)	Soil Nitrate Conc. (mg/kg)	VWC (g water/ m^3 soil)	GWC (g water/ g soil)
	4.24	1[a]			
Station 8	0.13	2.205	47.900		0.22
(TH18)	0.28	7.305	10.200		0.22
	0.33	33.590	6.810		0.20
	0.48	159.000	9.700		0.16
	0.66	111.400	7.480		0.13
	0.78	94.300	6.800		0.11
	0.91	66.995	4.860		0.15
	1.24	29.445	3.200		0.07
	1.39	27.110	4.060		0.12
	1.54	3.680	5.190		0.10
	1.69	16.200	7.580		0.10
	2.16	0.67	8.43		0.10
	2.31	0.375	9.06		0.10
	2.46	0.475	7.77		0.07
	2.61	0.38	7.44		0.10

Appendix G

Supplementary Soil Water Content, Groundwater and Soil Bromide Data

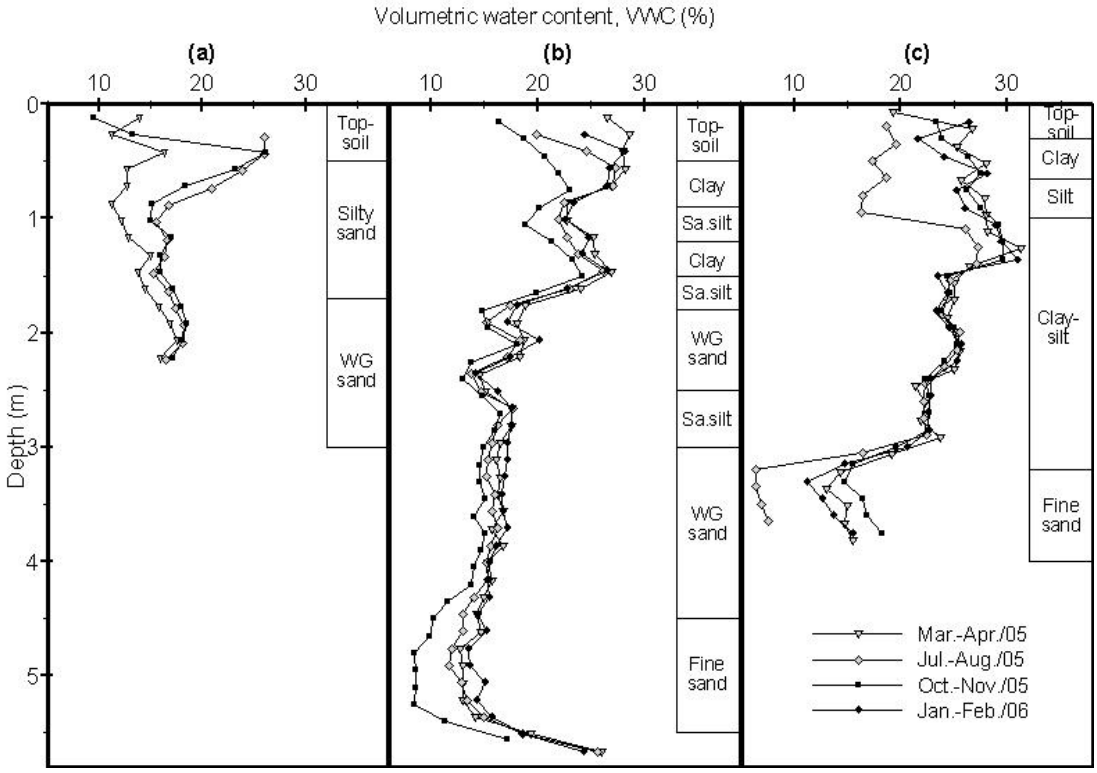

Figure G.1. Seasonal variation in volumetric soil water content (as measured with the neutron probe) at Stations a) 1; b) 3; c)

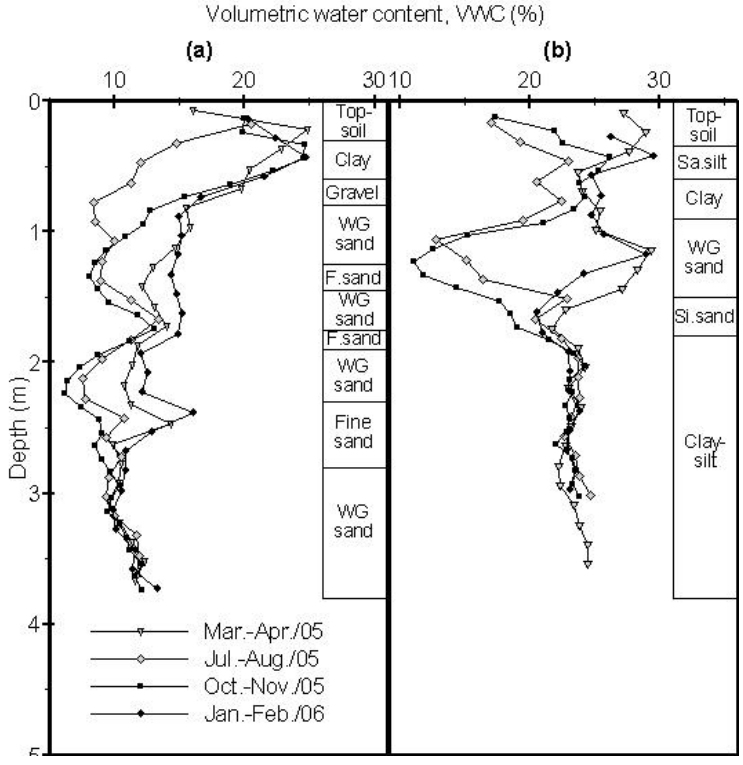

4.

Figure G.2. Seasonal variation in volumetric soil water content (as measured with the neutron probe and in core samples) at Stations a) 6; and b) 8.

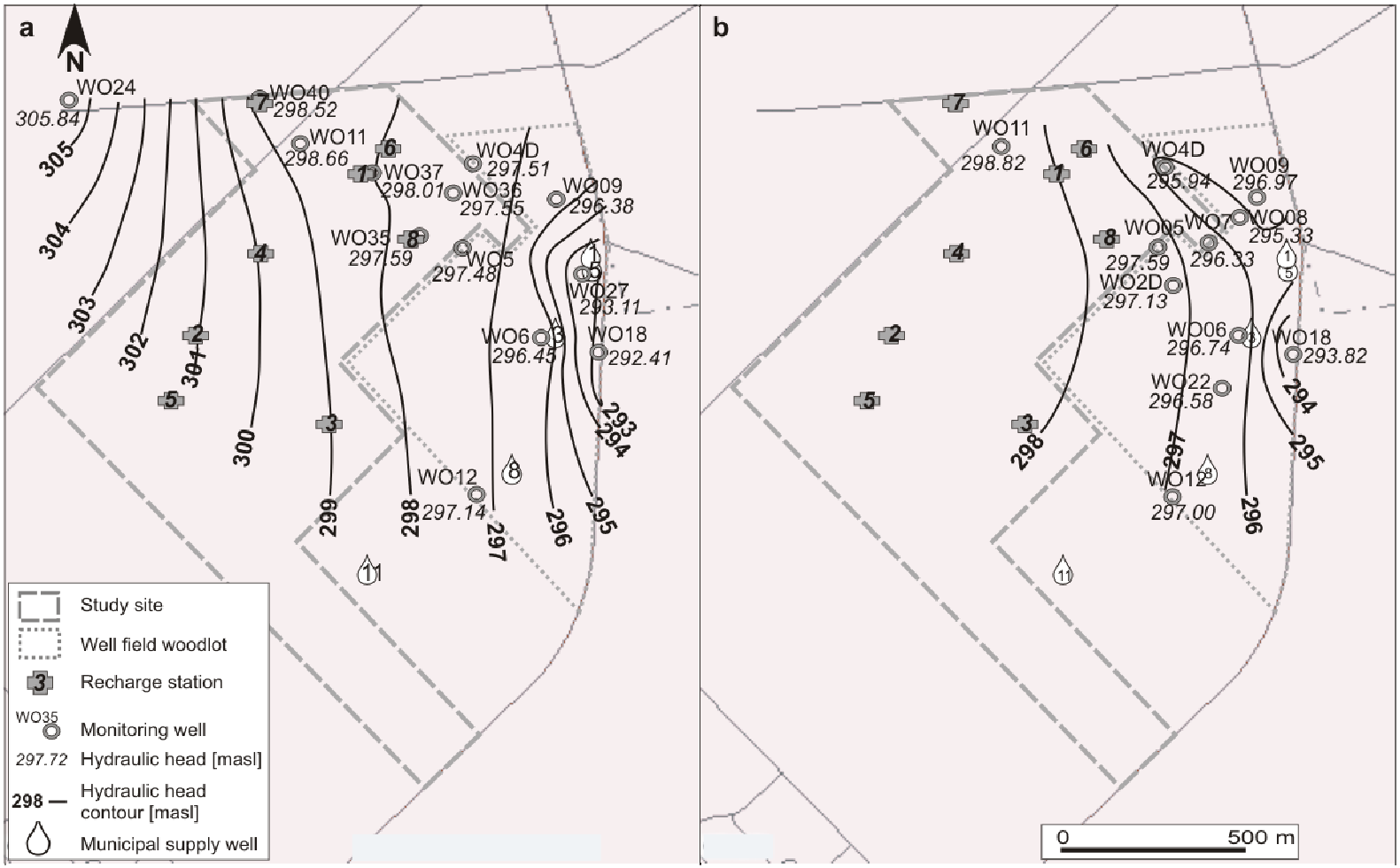

Figure G.3. January 2005 hydraulic head contours as estimated from wells across the study site and well field screened in a) Aquifer 2 and b) Aquifer 3. Contains data from The Corporation of the County of Oxford (2003b, 2003c).

Figure G.4. January 2006 hydraulic head contours as estimated from wells across the study site and well field screened in a) Aquifer 2 and b) Aquifer 3. Contains data from The Corporation of the County of Oxford (2003b, 2003c).

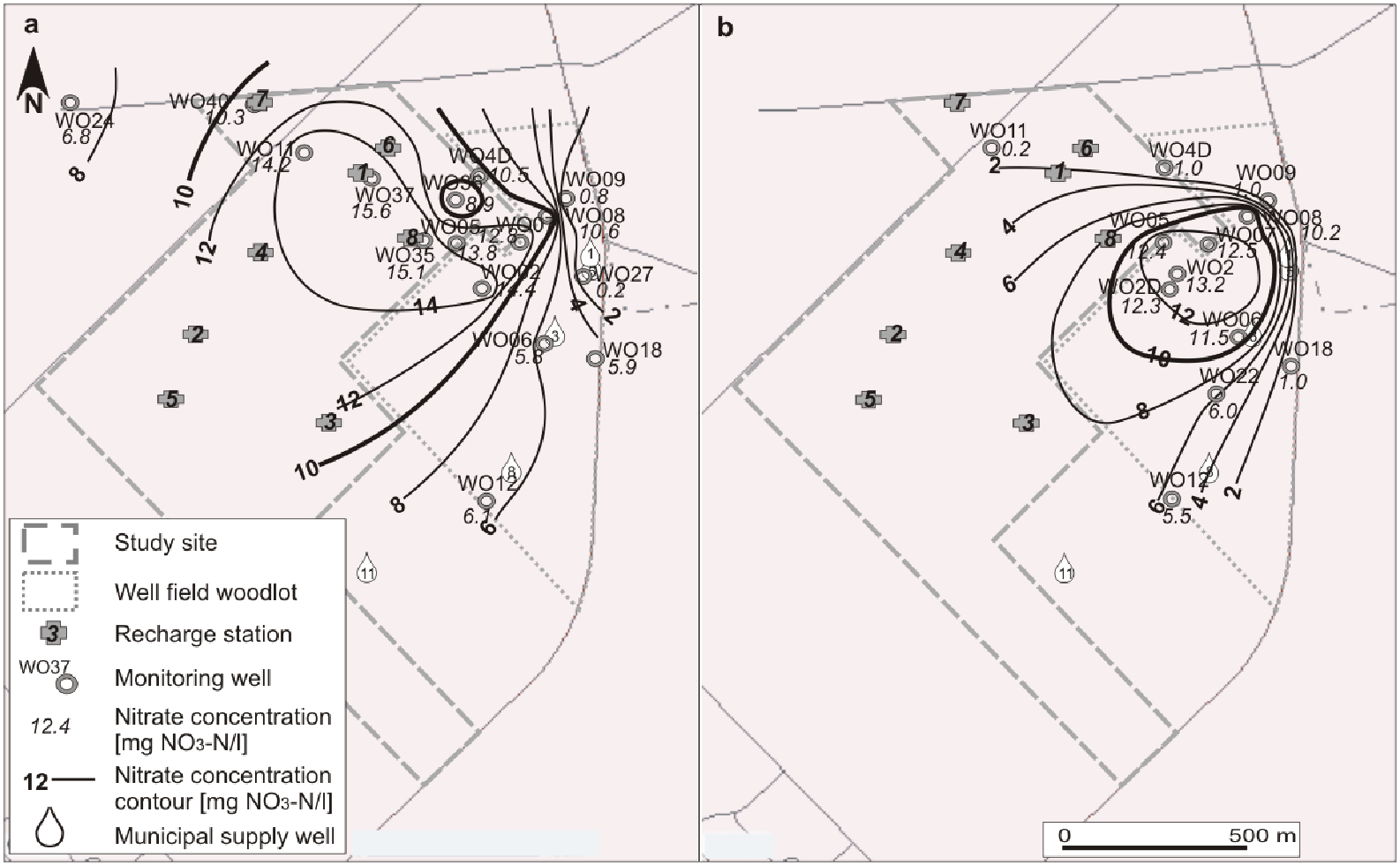

Figure G.5. January 2005 groundwater nitrate concentration contours as estimated from wells across the study site and well field screened in a) Aquifer 2 and b) Aquifer 3. Contains data from The Corporation of the County of Oxford (2003b, 2003c).

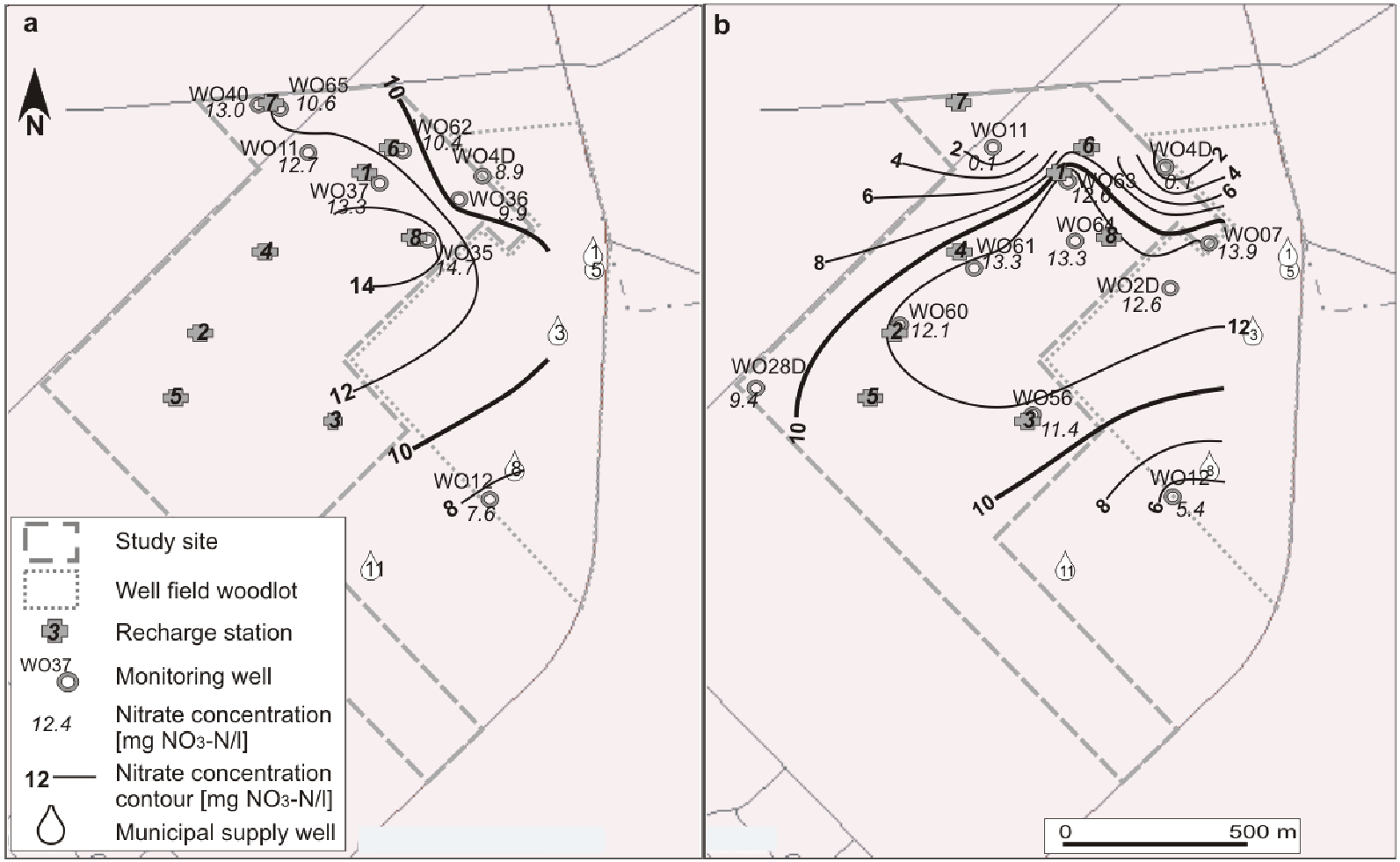

Figure G.6. January 2006 groundwater nitrate concentration contours as estimated from wells across the study site and well field screened in a) Aquifer 2 and b) Aquifer 3. Contains data from The Corporation of the County of Oxford (2003b, 2003c).

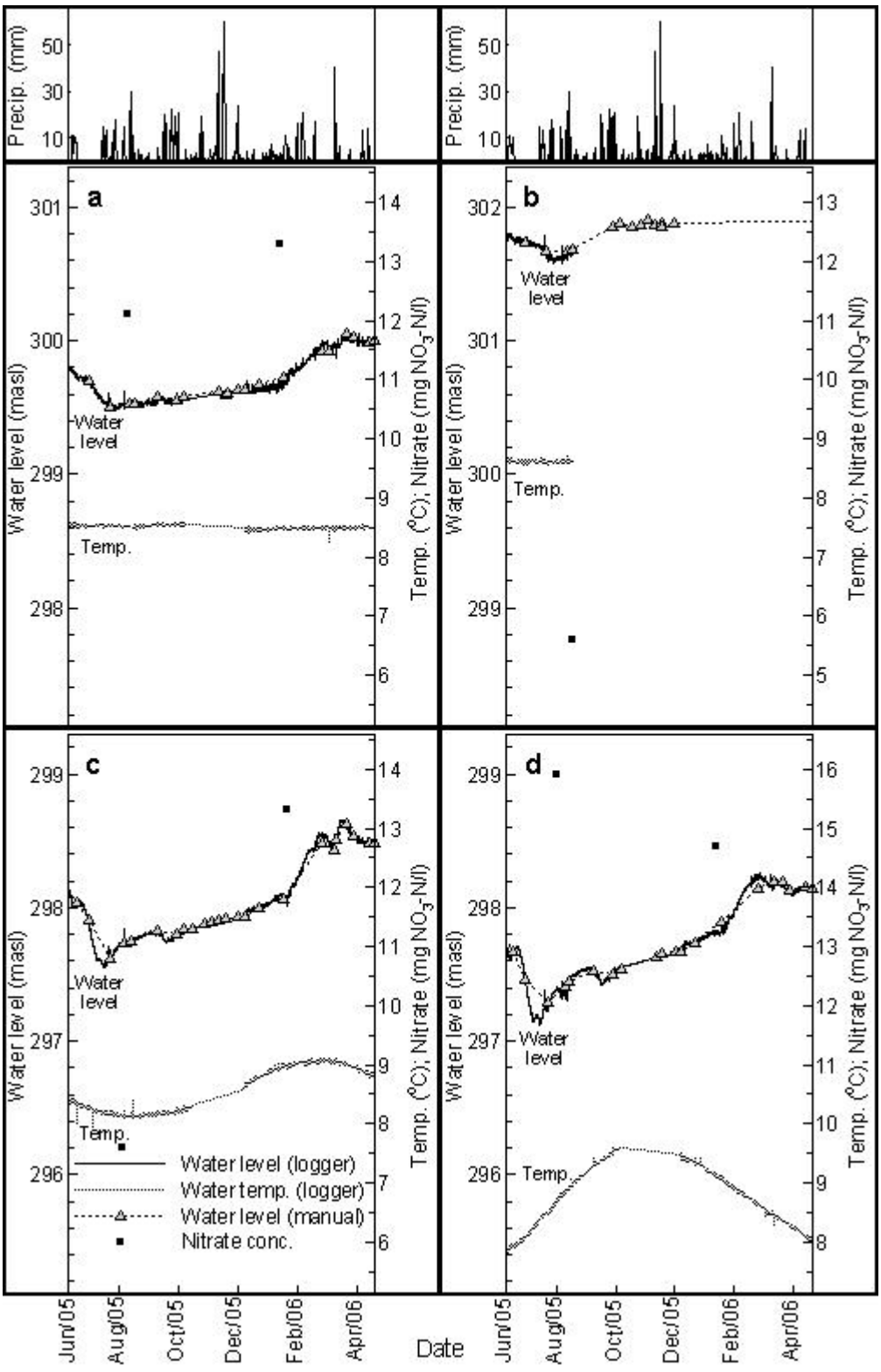

Figure G.7. Groundwater data including automated water level and temperature measurements, manual water level measurements and nitrate concentration at Stations a) 4; b) 5; c) 6; and d) 8.

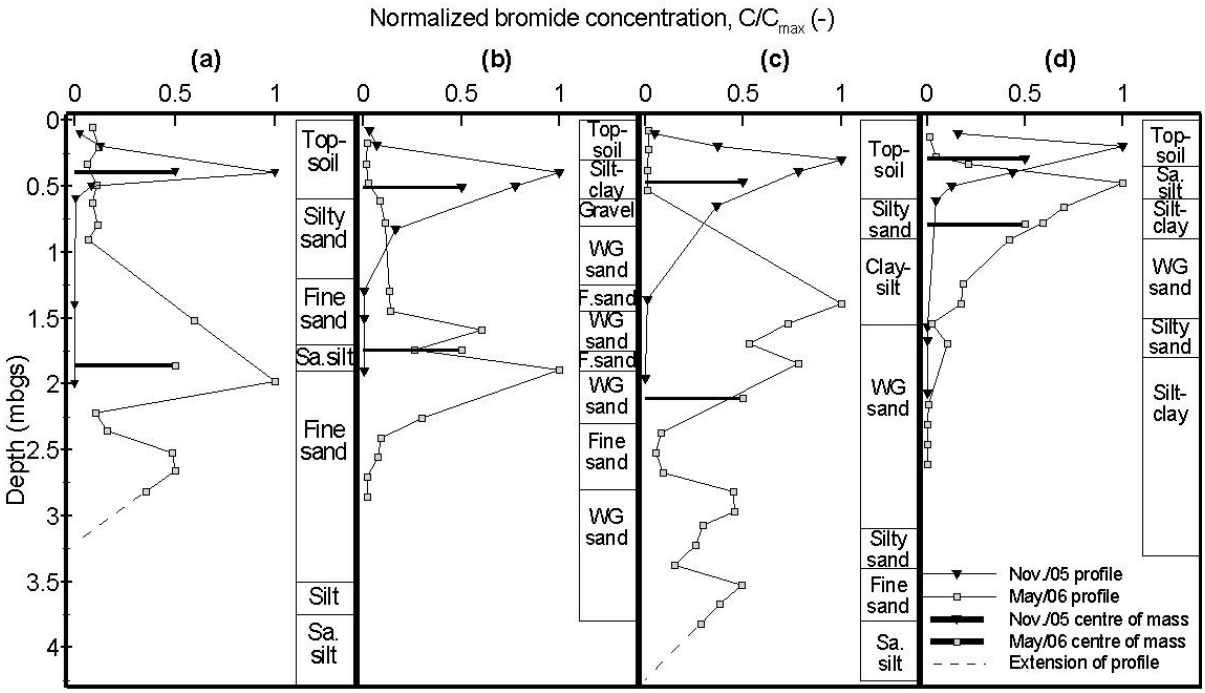

Figure G.8, Profiles of bromide concentration (normalized by dividing by the maximum concentration) from cores extracted in November 2005 and May 2006 at Stations a) 5; b) 6; c) 7; and d) 8.

Appendix H

Soil Hydraulic Parameter Background Data

Table H.1. Data used in selection of soil hydraulic parameters. Literature data is based on Campbell (undated) and Leij et al. (1996). Superscripts 1 and 2 indicate undisturbed and repacked laboratory samples, respectively.

Unit	Data source	B	ψ (m)	K_s (cm/s)	ρ_b (kg/m^2)	n	sand	silt	clay	org
Clay-silt till	Lab. Sample 64-2-1	5[2]	-0.1[2]			0.25[1]				0
	Lab. Sample 64-2-2	6[2]	-0.1[2]			0.13[1]				0
	SPAW	5	-0.5	7E-7	1740	0.34	35	45	20	0.23
	Literature	5.5	-0.3	1E-6 - 1E-4		0.10-0.20				0
	Model input	5	-0.4	7E-6	1980	0.23	35	45	20	0
Sandy silt	Lab. Sample 61-2-2	12[2]	-0.02[2]	2E-4[2]		0.29[1]				0
	SPAW	5	-0.45	1E-6	1700	0.33	35	50	15	0.22
	Literature	5	-0.5	1E-6 - 1E-4		0.35-0.50				0.20
	Model input	4	-0.3	4E-5	1700	0.34	35	50	15	0
Fine sand	Lab. Sample 58-6	1.6[2]	-0.15[2]	3E-3[2]		0.37[2]				0
	Lab. Sample 60-5	1[2]	-0.3[2]			0.36[2]				0
	SPAW	3	-0.15	6E-4	1860	0.30	95	0	5	0.10
	Literature	1.6	-0.06	1E-5 - 1E-3		0.25-0.50				0
	Model input	1.5	-0.1	7E-4	1860	0.30	95	0	5	0
Silty sand	Lab. Sample 60-6	2.6[2]	-0.2[2]	3E-4[2]		0.31[2]				0
	Lab. Sample 63-1	3[2]	-0.06[2]			0.32[2]				0
	SPAW	4.5	-0.25	5E-5	1690	0.36	55	30	15	0.20
	Literature	3.7	-0.1	1E-5 - 1E-3		0.35-0.50				0
	Model input	3.5	-0.1	5E-5	1690	0.36	55	30	15	0
WG sand	Lab. Sample 61-6	3.3[2]	-0.06[2]	3E-4[2]		0.35[2]				0
	SPAW	3.5	-0.15	8E-4	1740	0.34	90	0	10	0.14
	Literature	2.7	-0.08			0.20-0.35				0
	Model input	3	-0.1	7E-4	1740	0.34	90	0	10	0
Silt	SPAW/ Model input	3.4	-0.3	0.1	1723	0.35	5	85	10	0

Appendix I

Site Survey Data

Table I.1. Site survey data. Notes: TOC = Top of casing; Grnd = Ground surface; Bromide1 = Corner of bromide application area; MET = Meteorological station; Coordinate system NAD83 and UTM Zone 17.

Station	Equipment	Description	Survey Date	North (m)	East (m)	Elevation NAD83
1	WO63	TOC	04/13/2005	4770360.172	519848.47	300.898
1	WO63	Grnd	04/13/2005	4770360.163	519848.464	300.943
1	WO63	TOC	08/08/2005	4770360.122	519848.397	301.514
1	WO63	TOC	27/04/2006	4770360.144	519848.389	301.51179
1	WO63	Grnd	27/04/2006	4770360.156	519848.447	300.90339
1	AT13	TOC	04/13/2005	4770359.346	519846.072	301.020
1	AT13	Grnd	04/13/2005	4770359.331	519846.008	300.960
1	AT13	TOC	08/08/2005	4770359.311	519846.056	301.270
1	AT13	TOC	27/04/2006	4770359.331	519846.049	301.27002
1	AT13	Grnd	27/04/2006	4770359.313	519845.996	300.97202
1	AT19	TOC	27/04/2006	4770358.99	519845.572	301.38019
1	AT19	Grnd	27/04/2006	4770358.957	519845.576	301.00914
1	Bromide1	SW	08/08/2005	4770358.780	519846.947	300.899
1	Bromide1	NW	08/08/2005	4770360.664	519844.667	300.987
1	Bromide1	NE	08/08/2005	4770362.998	519846.628	300.881
1	Bromide1	SE	08/08/2005	4770361.156	519848.798	300.903
1	TH10	Grnd	27/04/2006	4770361.145	519846.225	300.91667
2	WO60	TOC	04/13/2005	4769960.682	519406.187	328.182
2	WO60	Grnd	04/13/2005	4769960.735	519406.214	327.242
2	WO49 (AT2)	TOC	04/13/2005	4769964.95	519408.948	327.656
2	WO49 (AT2)	Grnd	04/13/2005	4769964.965	519408.949	327.284
2	AT2	TOC	08/08/2005	4769965.005	519408.972	327.598
2	AT2	TOC	27/04/2006	4769965.028	519408.953	327.65699
2	AT2	Grnd	27/04/2006	4769965.054	519408.914	327.20649
2	AT11	TOC	04/13/2005	4769965.805	519411.038	327.464
2	AT11	Grnd	04/13/2005	4769965.798	519411.058	327.245
2	AT11	TOC	08/08/2005	4769965.765	519411.038	327.646
2	AT11	TOC	27/04/2006	4769965.814	519410.953	327.6809
2	AT11	Grnd	27/04/2006	4769965.874	519411.028	327.12833
2	AT17	TOC	27/04/2006	4769966.169	519411.368	327.52564
2	AT17	Grnd	27/04/2006	4769966.139	519411.392	327.17051
2	Bromide2	NW	08/08/2005	4769965.245	519412.779	327.162
2	Bromide2	NE	08/08/2005	4769963.012	519414.736	327.107
2	Bromide2	SE	08/08/2005	4769961.098	519412.591	327.090
2	Bromide2	SW	08/08/2005	4769963.305	519410.576	327.170

Station	Equipment	Description	Survey Date	North (m)	East (m)	Elevation NAD83
2	TH4	Grnd	27/04/2006	4769964.158	519412.853	327.10014
3	WO51 (AT4)	TOC	04/13/2005	4769719.234	519759.636	315.603
3	WO51 (AT4)	Grnd	04/13/2005	4769719.226	519759.62	315.267
3	AT4	TOC	08/08/2005	4769719.264	519759.645	315.648
3	AT4	TOC	27/04/2006	4769719.295	519759.622	315.64128
3	WO56	TOC	04/13/2005	4769720.313	519757.723	315.291
3	WO56	Grnd	04/13/2005	4769720.281	519757.791	315.308
3	WO56	TOC	08/08/2005	4769720.379	519757.736	315.674
3	WO56	TOC	27/04/2006	4769720.405	519757.732	315.66484
3	WO57 (AT9)	TOC	04/13/2005	4769721.807	519758.467	315.740
3	WO57 (AT9)	Grnd	04/13/2005	4769721.811	519758.454	315.372
3	AT9	TOC	08/08/2005	4769721.828	519758.417	315.925
3	AT9	TOC	27/04/2006	4769721.826	519758.43	315.94517
3	Bromide3	NW	08/08/2005	4769718.230	519759.828	315.280
3	Bromide3	NE	08/08/2005	4769720.850	519761.139	315.364
3	Bromide3	SE	08/08/2005	4769719.653	519763.792	315.331
3	Bromide3	SW	08/08/2005	4769717.053	519762.640	315.228
3	TH1	Grnd	27/04/2006	4769718.897	519761.875	315.27049
4	WO52 (AT5)	TOC	04/13/2005	4770111.677	519585.872	321.094
4	WO52 (AT5)	Grnd	04/13/2005	4770111.687	519585.866	320.712
4	AT5	TOC	08/08/2005	4770111.755	519585.786	321.050
4	AT5	TOC	27/04/2006	4770111.688	519585.837	321.04012
4	AT5	Grnd	27/04/2006	4770111.758	519585.791	320.69048
4	WO61	TOC	04/13/2005	4770113.481	519584.084	320.593
4	WO61	Grnd	04/13/2005	4770113.471	519584.088	320.564
4	WO61	TOC	08/08/2005	4770113.506	519584.088	320.804
4	WO61	TOC	27/04/2006	4770113.507	519584.159	320.8415
4	AT14	TOC	04/13/2005	4770113.791	519586.095	320.673
4	AT14	Grnd	04/13/2005	4770113.784	519586.071	320.598
4	AT14	TOC	08/08/2005	4770113.753	519586.064	321.319
4	AT14	TOC	27/04/2006	4770113.776	519586.06	321.35169
4	AT14	Grnd	27/04/2006	4770113.779	519586.045	320.56314
4	AT18	TOC	27/04/2006	4770114.113	519586.502	320.86316
4	AT18	Grnd	27/04/2006	4770114.123	519586.443	320.46322
4	Bromide4	NW	08/08/2005	4770110.444	519585.476	320.821
4	Bromide4	NE	08/08/2005	4770108.255	519583.443	320.938
4	Bromide4	SE	08/08/2005	4770110.249	519581.393	320.732
4	Bromide4	SW	08/08/2005	4770112.502	519583.405	320.614
4	TH6	Grnd	27/04/2006	4770110.312	519583.753	320.64615
5	WO50 (AT3)	TOC	04/13/2005	4769789.999	519346.591	323.635

Station	Equipment	Description	Survey Date	North (m)	East (m)	Elevation NAD83
5	WO50 (AT3)	Grnd	04/13/2005	4769789.973	519346.569	323.258
5	AT3	TOC	08/08/2005	4769790.020	519346.591	323.661
5	AT3	TOC	27/04/2006	4769790.064	519346.557	323.66954
5	AT3	Grnd	27/04/2006	4769790.038	519346.607	323.21448
5	WO58	TOC	04/13/2005	4769789.942	519343.953	323.436
5	WO58	Grnd	04/13/2005	4769789.929	519343.941	323.290
5	WO58	TOC	08/08/2005	4769789.934	519343.981	323.582
5	WO58	TOC	27/04/2006	4769789.956	519343.981	323.72596
5	WO58	Grnd	27/04/2006	4769789.998	519343.988	323.25344
5	WO59 (AT10)	TOC	04/13/2005	4769792.04	519345.057	323.387
5	WO59 (AT10)	Grnd	04/13/2005	4769792.02	519345.064	323.245
5	AT10	TOC	08/08/2005	4769792.041	519345.048	323.556
5	AT10	TOC	27/04/2006	4769792.027	519345.071	323.56002
5	AT10	Grnd	27/04/2006	4769792.08	519345.112	323.20281
5	AT16	TOC	27/04/2006	4769792.243	519344.699	323.56199
5	AT16	Grnd	27/04/2006	4769792.287	519344.629	323.12729
5	Bromide5	NW	08/08/2005	4769792.131	519345.305	323.196
5	Bromide5	NE	08/08/2005	4769794.066	519347.500	323.218
5	Bromide5	SE	08/08/2005	4769791.936	519349.506	323.202
5	Bromide5	SW	08/08/2005	4769789.918	519347.368	323.254
5	TH2	Grnd	27/04/2006	4769792.282	519347.577	323.19557
6	WO54 (AT7)	TOC	04/13/2005	4770429.987	519921.26	308.280
6	WO54 (AT7)	Grnd	04/13/2005	4770429.99	519921.291	307.900
6	AT7	TOC	08/08/2005	4770429.890	519921.311	308.261
6	AT7	TOC	27/04/2006	4770429.93	519921.258	308.23555
6	AT7	Grnd	27/04/2006	4770429.931	519921.216	307.88806
6	WO62	TOC	04/13/2005	4770427.858	519920.735	307.611
6	WO62	Grnd	04/13/2005	4770427.821	519920.735	307.562
6	WO62	TOC	08/08/2005	4770427.854	519920.725	307.877
6	WO62	TOC	27/04/2006	4770427.866	519920.684	307.85649
6	WO62	Grnd	27/04/2006	4770427.918	519920.734	307.54012
6	AT12	TOC	04/13/2005	4770428.769	519922.849	308.245
6	AT12	Grnd	04/13/2005	4770428.765	519922.859	307.947
6	AT12	TOC	08/08/2005	4770428.782	519922.967	308.352
6	AT12	TOC	27/04/2006	4770428.86	519922.943	308.32869
6	AT12	Grnd	27/04/2006	4770428.825	519923.004	307.88675
6	Bromide6	NW	08/08/2005	4770430.772	519920.222	307.967
6	Bromide6	NE	08/08/2005	4770432.769	519922.429	308.477
6	Bromide6	SE	08/08/2005	4770430.611	519924.436	308.377
6	Bromide6	SW	08/08/2005	4770428.654	519922.214	307.876
6	TH9	Grnd	27/04/2006	4770430.704	519922.774	308.1369
7	AT15	TOC	05/12/2005	4770549.898	519576.219	304.52609
7	AT15	Grnd	05/12/2005	4770549.9	519576.243	304.14821

Station	Equipment	Description	Survey Date	North (m)	East (m)	Elevation NAD83
7	AT15	TOC	08/08/2005	4770549.924	519576.215	304.514
7	AT15	TOC	27/04/2006	4770549.888	519576.196	304.50813
7	AT15	Grnd	27/04/2006	4770549.859	519576.183	304.121
7	WO65	TOC	05/12/2005	4770550.061	519577.393	304.79011
7	WO65	Grnd	05/12/2005	4770550.074	519577.41	304.10499
7	WO65	TOC	08/08/2005	4770550.039	519577.336	304.611
7	WO65	TOC	27/04/2006	4770550.101	519577.469	304.60435
7	WO65	Grnd	27/04/2006	4770550.034	519577.455	304.06721
7	Bromide7	NE	08/08/2005	4770552.742	519575.675	304.158
7	Bromide7	SE	08/08/2005	4770552.745	519578.441	304.149
7	Bromide7	SW	08/08/2005	4770549.776	519578.653	304.149
7	Bromide7	NW	08/08/2005	4770549.660	519575.632	304.146
7	TH12	Grnd	27/04/2006	4770551.481	519577.256	304.14869
8	WO53 (AT6)	TOC	04/13/2005	4770189.879	519978.375	303.021
8	WO53 (AT6)	Grnd	04/13/2005	4770189.852	519978.402	302.662
8	AT6	TOC	08/08/2005	4770189.872	519978.283	303.033
8	AT6	TOC	27/04/2006	4770189.899	519978.383	303.03722
8	AT6	Grnd	27/04/2006	4770189.867	519978.32	302.60904
8	Bromide8	SW	08/08/2005	4770189.721	519978.208	302.673
8	Bromide8	SE	08/08/2005	4770191.828	519980.407	302.593
8	Bromide8	NE	08/08/2005	4770193.936	519978.330	302.689
8	Bromide8	NW	08/08/2005	4770191.933	519976.315	302.678
8	TH8	Grnd	27/04/2006	4770191.976	519978.358	302.59655
	WO48 (AT1)	TOC	04/13/2005	4770408.069	519721.553	302.626
	WO48 (AT1)	Grnd	04/13/2005	4770408.048	519721.519	302.227
	AT1	TOC	08/08/2005	4770408.066	519721.554	302.724
	AT1	TOC	27/04/2006	4770408.09	519721.532	302.6932
	TH13	Grnd	27/04/2006	4770155.717	519938.608	305.13385
	WO55	Grnd	05/12/2005	4770068.141	520130.617	301.035
	WO64	TOC	27/04/2006	4770192.976	519882.206	307.17732
	WO64	Grnd	27/04/2006	4770192.988	519882.226	306.67263
	WO64	TOC	04/13/2005	4770192.991	519882.245	307.175
	WO64	Grnd	04/13/2005	4770192.995	519882.244	306.694
	WO66	TOC	27/04/2006	4770485.676	519682.852	304.4215
	WO66	Grnd	27/04/2006	4770485.649	519682.844	303.46555
	MET		04/13/2005	4769958.049	519401.224	327.339